State of the Physical, Biological and Selected Fishery Resources of Pacific Canadian Marine Ecosystems in 2018

Jennifer L. Boldt, Jillian Leonard and Peter C. Chandler (Editors)

Fisheries and Oceans Canada
Institute of Ocean Sciences
9860 West Saanich Road
Sidney, B.C. V8L 4B2

2019

Canadian Technical Report of Fisheries and Aquatic Sciences 3314

Fisheries and Oceans Canada Pêches et Océans Canada

Canada

Canadian Technical Report of Fisheries and Aquatic Sciences

Technical reports contain scientific and technical information that contributes to existing knowledge but which is not normally appropriate for primary literature. Technical reports are directed primarily toward a worldwide audience and have an international distribution. No restriction is placed on subject matter and the series reflects the broad interests and policies of Fisheries and Oceans Canada, namely, fisheries and aquatic sciences.

Technical reports may be cited as full publications. The correct citation appears above the abstract of each report. Each report is abstracted in the data base *Aquatic Sciences and Fisheries Abstracts*.

Technical reports are produced regionally but are numbered nationally. Requests for individual reports will be filled by the issuing establishment listed on the front cover and title page.

Numbers 1-456 in this series were issued as Technical Reports of the Fisheries Research Board of Canada. Numbers 457-714 were issued as Department of the Environment, Fisheries and Marine Service, Research and Development Directorate Technical Reports. Numbers 715-924 were issued as Department of Fisheries and Environment, Fisheries and Marine Service Technical Reports. The current series name was changed with report number 925.

Rapport technique canadien des sciences halieutiques et aquatiques

Les rapports techniques contiennent des renseignements scientifiques et techniques qui constituent une contribution aux connaissances actuelles, mais qui ne sont pas normalement appropriés pour la publication dans un journal scientifique. Les rapports techniques sont destinés essentiellement à un public international et ils sont distribués à cet échelon. II n'y a aucune restriction quant au sujet; de fait, la série reflète la vaste gamme des intérêts et des politiques de Pêches et Océans Canada, c'est-à-dire les sciences halieutiques et aquatiques.

Les rapports techniques peuvent être cités comme des publications à part entière. Le titre exact figure au-dessus du résumé de chaque rapport. Les rapports techniques sont résumés dans la base de données *Résumés des sciences aquatiques et halieutiques.*

Les rapports techniques sont produits à l'échelon régional, mais numérotés à l'échelon national. Les demandes de rapports seront satisfaites par l'établissement auteur dont le nom figure sur la couverture et la page du titre.

Les numéros 1 à 456 de cette série ont été publiés à titre de Rapports techniques de l'Office des recherches sur les pêcheries du Canada. Les numéros 457 à 714 sont parus à titre de Rapports techniques de la Direction générale de la recherche et du développement, Service des pêches et de la mer, ministère de l'Environnement. Les numéros 715 à 924 ont été publiés à titre de Rapports techniques du Service des pêches et de la mer, ministère des Pêches et de l'Environnement. Le nom actuel de la série a été établi lors de la parution du numéro 925.

Canadian Technical Report of Fisheries and Aquatic Sciences 3314

2019

STATE OF THE PHYSICAL, BIOLOGICAL AND SELECTED FISHERY RESOURCES OF PACIFIC CANADIAN MARINE ECOSYSTEMS IN 2018

By

Jennifer L. Boldt[1], Jillian Leonard[2] and Peter C. Chandler[3] (Editors)

[1]Fisheries & Oceans Canada
Pacific Biological Station
3190 Hammond Bay Road
Nanaimo, B.C. V9T 6N7
Canada
Jennifer.Boldt@dfo-mpo.gc.ca

[2]University of Victoria
3800 Finnerty Road
Victoria, B.C. V8P 5C2
Canada
jleo@uvic.ca

[3]Fisheries & Oceans Canada
Institute of Ocean Sciences
9860 West Saanich Road
Sidney, B.C. V8L 4B2
Canada
Peter.Chandler@dfo-mpo.gc.ca

Cat. No. Fs97-6/3314E-PDF ISBN 978-0-660-31074-9 ISSN 1488-5379

Correct citation for this publication:
Boldt, J.L., Leonard, J., and Chandler, P.C. (Eds.). 2019. State of the physical, biological and selected fishery resources of Pacific Canadian marine ecosystems in 2018. Can. Tech. Rep. Fish. Aquat. Sci. 3314: vii + 248 p.

Table of Contents

Abstract

Boldt, J.L., Leonard, J., and Chandler, P.C. (Eds.). 2019. State of the physical, biological and selected fishery resources of Pacific Canadian marine ecosystems in 2018. Can. Tech. Rep. Fish. Aquat. Sci. 3314: vii + 248 p.

Fisheries and Oceans Canada is responsible for the management and protection of marine resources on the Pacific coast of Canada. Oceanographically this area is a transition zone between coastal upwelling (California Current) and downwelling (Alaskan Coastal Current) regions. There is strong seasonality and considerable freshwater influence, and an added variability from coupling with events and conditions in the tropical and North Pacific Ocean. The region supports ecologically and economically important resident and migratory populations of invertebrates, groundfish, pelagic fishes, marine mammals and seabirds.

Since 1999 an annual State of the Pacific Ocean meeting has been held by DFO scientists in the Pacific Region to present the results of the most recent year's monitoring in the context of previous observations and expected future conditions. The workshop to review ecosystem conditions in 2018 was held March 18-19, 2019 at the Mary Winspear Centre in Sidney, BC. This technical report includes submissions based on presentations given at the meeting.

The marine heat wave of 2014-2016 continues to affect lower trophic levels and new heat waves were observed in the fall of 2018, attributed to atmospheric patterns that reduced the typical winter cooling of the ocean surface. The upwelling of cool nutrient-rich waters along the west coast of Vancouver Island in 2018 started earlier than usual, but was not as intense as previous years, implying mixed conditions for productivity and fish growth. After a three-year absence from the Strait of Georgia, a harmful algal bloom (*Heterosigma akashiwo*) occurred in early June, resulting in high aquaculture fish mortality in Jervis Inlet. This bloom was linked to a heavy snowpack in the BC interior combined with hot weather in May and June causing the snowmelt discharge from the Fraser River to be early and rapid. Warming of offshore and coastal waters has led to changes in the food web and responses by Pacific salmon on latitudinal gradients, with slightly better conditions in the north. There has been a coast wide decrease in Chinook Salmon and low returns of Fraser River Sockeye Salmon.

A special session focused on DFO's State of the Salmon and State of the Freshwater initiatives. Sue Grant is leading these efforts and gave an introduction to the initiatives. This was followed by ten presentations on salmon research in BC.

Résumé

Boldt, J.L., Leonard, J., and Chandler, P.C. (Eds.). 2019. State of the physical, biological and selected fishery resources of Pacific Canadian marine ecosystems in 2018. Can. Tech. Rep. Fish. Aquat. Sci. 3314: vii + 248 p.

Pêches et Océans Canada est responsable de la gestion et de la protection des ressources marines sur la côte ouest du Canada. L'océanographie de cette région est une zone de transition entre les remontées d’eaux profondes côtières (courant de la Californie) et les régions de plongée d'eaux (courant côtier de l'Alaska). Il existe une saisonnalité importante, une forte influence des eaux douces, et une variabilité coupleé aux événements et conditions dans tout le Pacifique, des tropiques aux régions sous Arctic. La région nourrit des populations résidentes et migratoires importantes d’invertébrés, de poissons de fond et pélagiques, et de mammifères et d’oiseaux marins.

Depuis 1999, les scientifiques du MPO ont organisé une rencontre annuelle de l'état de l'océan Pacifique pour présenter les résultats de la surveillance de la dernière année dans le contexte des observations précédentes et des conditions futures. L'atelier pour réviser les conditions de 2018 a eu lieu les 18 et 19 mars 2019 au Centre Mary Winspear près de l'Institute des sciences de la mer, Sidney, C.-B. Ce rapport technique inclut des rapports basées sur des présentations donnés lors de la rencontre.

La vague de chaleur marine de 2014-2016 continue d'influencer sur les niveaux trophiques inférieurs, et de nouvelles vagues de chaleur ont été observées à l'automne 2018, en raison de la configuration atmosphérique ayant réduit le refroidissement hivernal typique de la surface de l'océan. Les remontées d'eau riches en nutriments le long de la côte ouest de l'île de Vancouver ont débutés plus tôt que d'habitude en 2018 et n'étaient pas aussi intense que les années précédentes, impliquant des conditions mixtes à la productivité et à la croissance des poissons. Après une absence de trois ans dans le détroit de Georgia, une prolifération d'algues nuisibles (*Heterosigma akashiwo*) s'est produite en début juin, avec mortalité des poissons d'aquaculture dans le Grau de Jervis. Cette prolifération était liée à un important manteau neigeux dans l'intérieur de la Colombie-Britannique, combiné à un temps chaud en mai et juin, ce qui a provoqué un écoulement rapide et un accelération de la fonte des neiges du fleuve Fraser. Le réchauffement des eaux côtières a entraîné des changements dans la chaîne alimentaire et des réactions du saumon du Pacifique sur les gradients latitudinaux, avec des conditions légèrement meilleures dans le nord. Il y a eu un déclin synchrone des populations de saumon quinnat sur toute la côte et de faibles retours de saumon sockeye du fleuve Fraser.

Une session spéciale a porté aux initiatives du MPO sur l’état du saumon et de l’état des eaux douces. Sue Grant dirige ces efforts et a présenté les initiatives. Viennent ensuite dix exposés sur la recherche sur le saumon en Colombie-Britannique.

Highlights, Introduction, and Overview
1. HIGHLIGHTS

- Land and ocean temperatures in 2018 continued to be warmer than the average temperatures over the past 30 years. Globally, 2018 was the fourth warmest year since 1880.

- The NE Pacific marine heat wave of 2014-2016 diminished; however, in 2018 the effects on lower trophic levels remained and new heat waves were observed in the fall of 2018 due to delayed and reduced winter cooling.

- In 2018, there was a transition from a weak La Niña to a weak El Niño.

- The upwelling of cool nutrient rich waters along the west coast of Vancouver Island (WCVI) in 2018 started earlier than usual but was not as intense as previous years, implying mixed conditions for productivity and fish growth.

- Zooplankton distribution off the WCVI still reflects the effects of the 2014-2016 marine heatwave. The abundance of southern copepod species was high and subarctic copepods low; southern species were still present, consistent with reduced winter cooling.

- Multi-species small-mesh bottom trawl surveys conducted annually in May off the WCVI indicate pink shrimp biomass in 2018 continued to decline from its peak in 2014, with anomalies now below the average biomass levels observed since the survey began in 1973.

- Pacific Herring Spawning biomass was high in the Strait of Georgia (SoG) but not in other areas. Natural mortality for some stocks has increased. The relative abundance of SoG juvenile herring was the fourth lowest in the 27-year time series and may be an indicator of diminished future recruitment strength.

- An index of Eulachon spawning stock biomass in the Fraser River was estimated to be at a moderately high level (similar to 2015), compared to most other years from 2004-2017.

- In the SoG, the spring bloom timing and duration was consistent with average conditions over the past 20 years – which implies good feeding conditions for juvenile fish.

- In the SoG, juvenile salmon survey catches were average or better than average.

- On the continental shelf of Vancouver Island, however, catch rates of juvenile salmon were below average in the summer of 2018, likely due to size-selective mortality.

- Total Fraser River Sockeye Salmon (*Oncorhynchus nerka*) productivity and returns have declined since the mid-1990s. Although most populations in the Fraser River, such as Chilko and Stellako, have exhibited declining trends since the 1990s, some populations, such as Late Shuswap, have not exhibited any persistent trends, and the Harrison River population has increased in productivity.

- Unusual events occur in Canada's Pacific marine waters every year but are often not reported on or related to the broader environmental context. Some unusual events in 2018 that were reported include:
    - A later than usual onset of fall/winter cooling, which led to marine heat waves;
    - Blooms of algal species such as *Noctilua scintillans* and *Heterosigma akashiwo* were again observed in the SoG after a 3-year absence;
    - The continued effect of the 2014-2016 marine heat wave on lower trophic level community composition;
    - The continued presence of pyrosomes in BC waters (but lower abundance compared to 2017).

2. INTRODUCTION

Fisheries and Oceans Canada (DFO), Pacific Region, conducts annual reviews of physical, chemical and biological conditions in the ocean, to develop a picture of how the ocean is changing and to help provide advance identification of important changes which may potentially impact human uses, activities, and benefits from the ocean. These reviews take the form of a two day meeting, usually held in February or March of the year following the year under review. The first meeting was held in 2000 to assess conditions in 1999; reports from these reviews are available at (see bottom of web page):

http://www.dfo-mpo.gc.ca/oceans/publications/index-eng.html

Reviews and reports from 2007 to 2013 were conducted under the direction of the Fisheries & Oceans Canadian Science Advice Secretariat (CSAS). In 2014, these State of the Pacific Ocean reviews were moved to a separate process and are now presented as Fisheries & Oceans Canada Technical Reports. The report from 2018 (for conditions in 2017) is available at

http://www.dfo-mpo.gc.ca/oceans/publications/soto-rceo/2017/index-eng.html

In 2019, the meeting on conditions observed on the west coast of Canada (Figure 2-1) in 2018 took place on March 18 and 19 at the Mary Winspear Centre, Sidney, B.C. Over 150 people participated in person or by web-conference. The majority of participants were scientists from federal and provincial government, academia, non-profits, industry and private companies. A trend over the past few years has been the increased participation and presentations by non-DFO scientists. This has provided a broader perspective of the science being done on Canada's Pacific coast, and the audiences who are interested in this science.

Tseycum Chief Tanya Jimmy provided an opening prayer and a welcome to participants; she also shared stories about her Nation. Kim Houston (acting for Carmel Lowe) provided a welcome and introduction to the SOPO meeting. The main session included 44 oral presentations and 19 posters covering a range of observations from 2018. At each annual SOPO meeting there is a special session and at this year's meeting the focus was Pacific salmon – in particular to introduce the State of the Salmon and State of the Freshwater initiatives lead by Sue Grant.

Figure 2-1. Map of regions described in this report.

At the end of the first day a poster session and mixer was held with support from Ocean Networks Canada. Nineteen posters were presented in the Mary Winspear Centre while participants enjoyed snacks and refreshments (Appendix 1). A poster on unusual marine events in 2018 provided space for participants to add their own observations. The agenda for the meeting is presented in Appendix 2, and the participants are listed in Appendix 3. The meeting was co-chaired by Peter Chandler and Jennifer Boldt, and organized by Jillian Leonard.

This technical report presents the highlights and summaries of the presentations and discussions at the workshop. These summary reports are not peer reviewed, and present the status of data, interpretation, and knowledge as of the date of this meeting. For use of, or reference to, these individual presentations, please contact the individual authors.

3. OVERVIEW AND SUMMARY

During 2014 to 2016, the waters off the B.C. coast were characterized by surface and/or subsurface temperatures well above normal (compared to average conditions over the 30 years from 1981-2010), which were unfavourable for the productivity and growth of species that typically inhabit these waters. While the surface temperatures were close to average in 2017, subsurface temperatures (>100 m) remained anomalously warm throughout most of that year (Ross and Robert, section 6; Figure 3-1). Both surface and subsurface temperatures were near normal until the fall, when marine heat waves were observed offshore and on the shelf with varying spatial and temporal scales (Hannah et al., section 9). The multivariate El Niño/Southern Oscillation (ENSO) Index (Figure 3-2) was negative during the first half of 2018, associated with cooler temperatures of a La Niña. Late in 2018, the ENSO index became weakly positive associated with a weak El Niño (Ross and Robert, section 6).

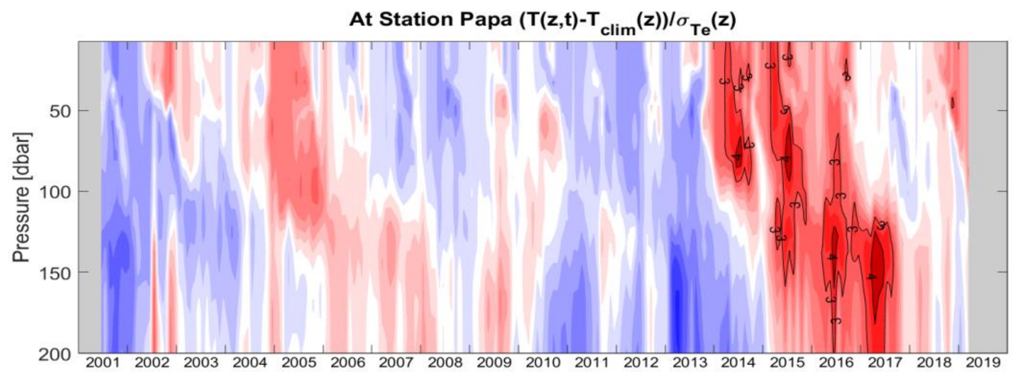

Figure 3-1. False colour plot of temperature anomalies relative to the 1956-2012 seasonally-corrected mean and standard deviation (from the Line P time series), as observed by Argo floats near Station Papa (P26: 50° N, 145° W).The cool colours indicate cooler than average temperatures and warm colours indicate warmer that average temperatures. Dark colours indicate anomalies were large compared with the 1956-2012 standard deviations. The black lines highlight regions with anomalies that were 3 and 4 standard deviations above the mean. Source: Ross and Robert, section 6.

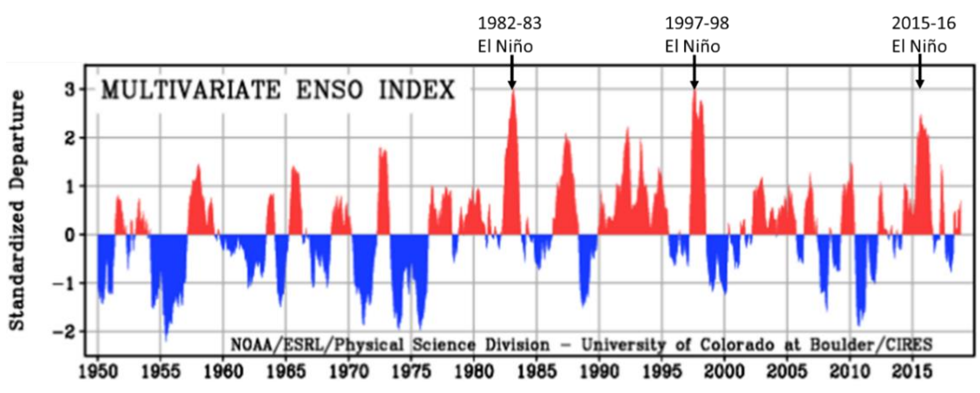

Figure 3-2. The multivariate ENSO Index. Data source: NOAA/ESRL/Physical Sciences Division – University of Colorado at Boulder/CIRES.

The long term record of surface temperatures collected at lighthouses along the B.C. coast shows that 2018 was a continuation of the warm period that started in 2014 (Chandler, section

11). Overlying the multi-year oscillations in the annual sea surface temperature there remains a long-term trend towards rising ocean temperatures (Figure 3-3; Chandler, section 11).

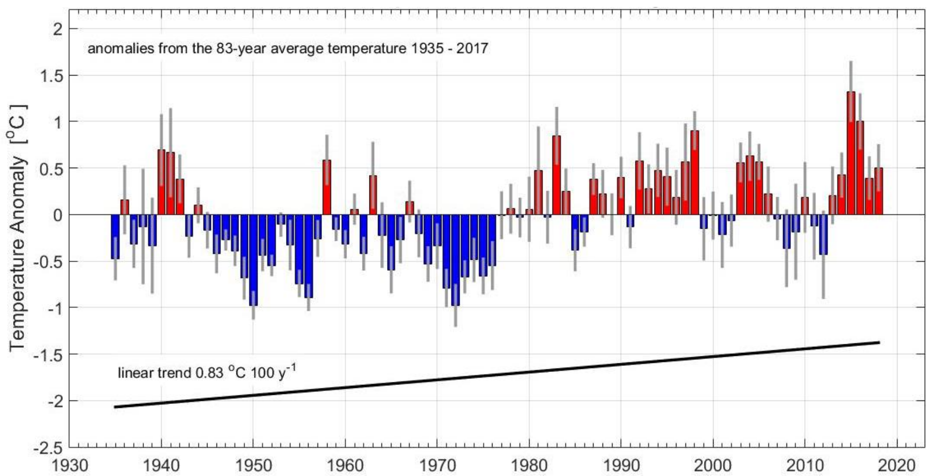

Figure 3-3. The trend in the annual temperature based on the observations of all lighthouses contributing to the British Columbia Shore Station Program. The data shown are the anomalies from the long-term average temperature (1935-2017). The bars represent the anomalies averaged over all stations (a coast wide indicator), (red – above average, blue – below average), the vertical grey lines show the variability in the lighthouse data for each year. Source: Chandler, section 11.

The marine heat wave ("the Blob") that was first observed in the Northeast Pacific in late 2013 was associated with reduced vertical mixing causing increased winter stratification. The strength of winter stratification in Figure 3-4 is represented by the minimum depth of the 1025.7 kgm^{-3} isopycnal. For three winters (2013/14, 2014/15 and 2015/16 this isopycnal remained deeper than 50 m. In 2016/17, similar to pre-marine heat wave years, there was sufficient mixing for this isopycnal to reach the surface but in 2017/18 weaker mixing was again evident (Figure 3-4; Ross and Robert, section 6). The marine heat wave in the fall 2018 suggests that there will again be decreased vertical mixing and a consequent reduced nutrient supply from deep waters (Ross and Robert, section 6).

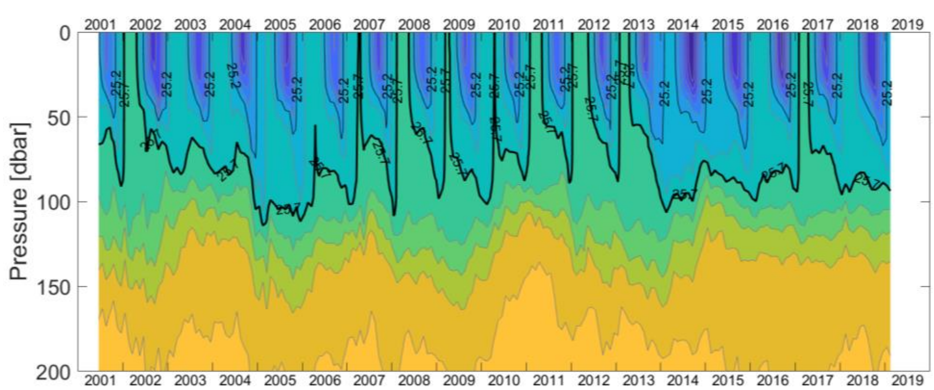

Figure 3-4. Coloured contour plot of density as observed by Argo floats near Station Papa (P26: 50° N, 145° W).The colours indicate potential density (yellow is denser and blue lighter). The black lines highlight the $sigma_{theta}$=25.2 kg/m3 (thin) and 25.7 kg/ m3 (thick) isopycnals. Source: Ross and Robert, section 6.

The upwelling of nutrient rich water off the west coast of Vancouver Island is an indicator of marine coastal productivity across trophic levels from plankton to fish to birds. Variability in the upwelling index corresponds to the strength and longitudinal position of the Aleutian low-pressure system in the Gulf of Alaska. In 2018, the timing and magnitude of upwelling showed mixed conditions for productivity (Hourston and Thomson, section 7). The intensity of the upwelling in 2018 was weak, associated with low productivity; however, the timing of the transition to upwelling was early, associated with high productivity (Hourston and Thomson, section 7; Figure 3-5).

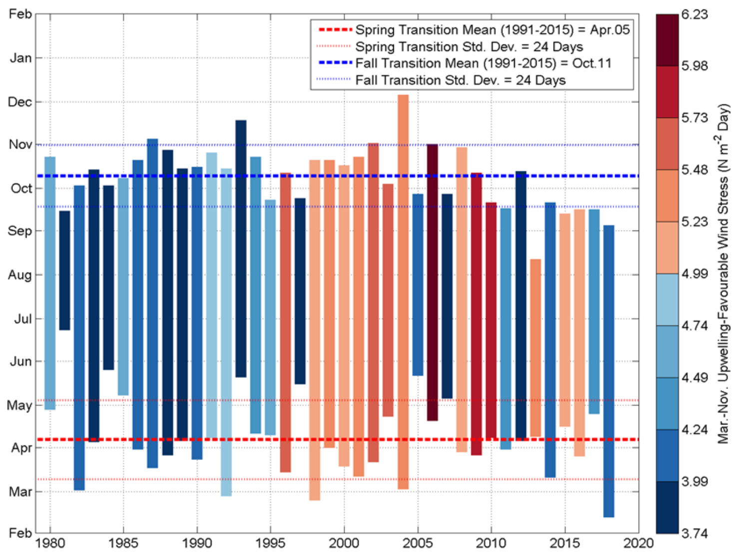

Figure 3-5. The upwelling index for the west coast of British Columbia. Bar plot showing Spring and Fall Transitions and upwelling-favourable wind stress magnitude. The length of the bar corresponds to the duration of the upwelling season, coloured by the intensity of the upwelling (red indicates intense upwelling, blue indicates weak upwelling). Bold dashed lines indicates the average spring (red) and fall (blue) transition dates. Light-dashed lines indicate standard deviations of the spring (red) and fall (blue) transition dates. Source: Hourston and Thomas, section 7.

In the spring and summer 2018, nutrient concentrations were among the lowest on record along central Line P stations, but within the range of past values for other areas off the WCVI (Pena and Nemcek, section 14). On the west coast of B.C., the phytoplankton biomass and community composition were generally within the range of past values, except there was an unusual increase in phytoplankton biomass and relative abundance of diatoms at most stations along Line P in spring (Peña and Nina Nemcek, section 14; Batten, section 15).

The zooplankton community off the west coast of Vancouver Island continues to reflect warm water conditions, with higher abundances of gelatinous and lower abundances of crustacean taxa (Galbraith and Young, section 16; Batten, section 15; Figure 3-6). Subarctic and boreal copepods are favourable for fish growth and abundances of these species have been below average in recent warm years. In 2018, the trend of decreasing subarctic copepod biomass slowed (trends vary by area); whereas, boreal copepod biomass increased (except in Hecate Strait) (Galbraith and Young, section 16). The biomass of southern copepods continued to be above average in 2018. The colonial tunicate, *Pyrosoma atlanticum*, that first appeared in BC waters in 2017, declined in abundance but was still present along the shelf break in 2018 (Galbraith and Young, section 16).

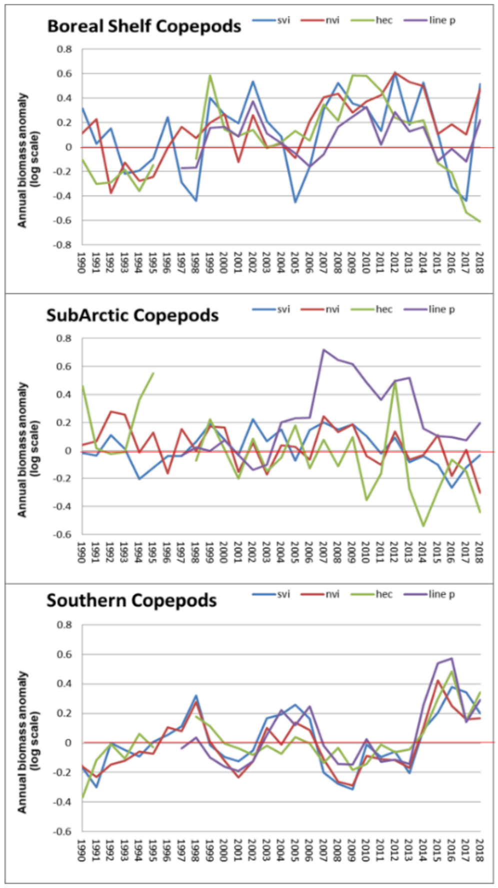

Figure 3-6. Zooplankton species-group anomaly time series for the regions shown in Figure 2-1. Line graphs are annual log scale anomalies. Southern Vancouver Island (SVI) blue; Northern Vancouver Island (NVI) red; Hecate Strait (HEC) green; Line P – purple for all graphs. Note the y-axis changes with each taxonomic group. Source: Galbraith and Young, section 16.

The growth rate of Cassin's Auklets is linked to the abundance of their primary prey: *Neocalanus cristatus* copepods, which are more abundant during relatively cold years (Hipfner 2009). In 2018, growth rates of Cassin's auklet nestlings on Triangle Island were similar to the long term average (Hipfner, section 22). Off the west coast of Vancouver Island Pink Shrimp biomass in 2018 continued to decline from the peak in 2014, with anomalies below the climatological mean (Perry et al., section 20). The community composition sampled in 2018 was similar to that sampled in 2017, but different from 2009-2015 (Perry et al., section 20). Trends observed in multiple groundfish surveys include the return of North Pacific Spiny Dogfish to the west coast of Vancouver Island after an absence of about four years, and increases in the abundance indices for Boccacio Rockfish, Sablefish, Petrale Sole, Flathead Sole, and Longspine Thornyhead (Anderson and Workman, section 21).

During 2018 in the Strait of Georgia (SoG), spring and summer temperature and salinity conditions were near-normal, but as the year progressed temperatures at all depths became warmer than normal (Chandler, section 26). During the fall and winter, lower than normal oxygen levels were widespread with the exception of the deep SoG. There was an early, rapid and high volume Fraser River freshet (Figure 3-7). In 2018, depth averaged temperatures in the central Strait of Georgia were similar to conditions in 2017 with three periods of warm water anomalies extending to 40 m depth; however the previously observed long-term freshening trend did not continue in 2018 (Chandler, section 26).

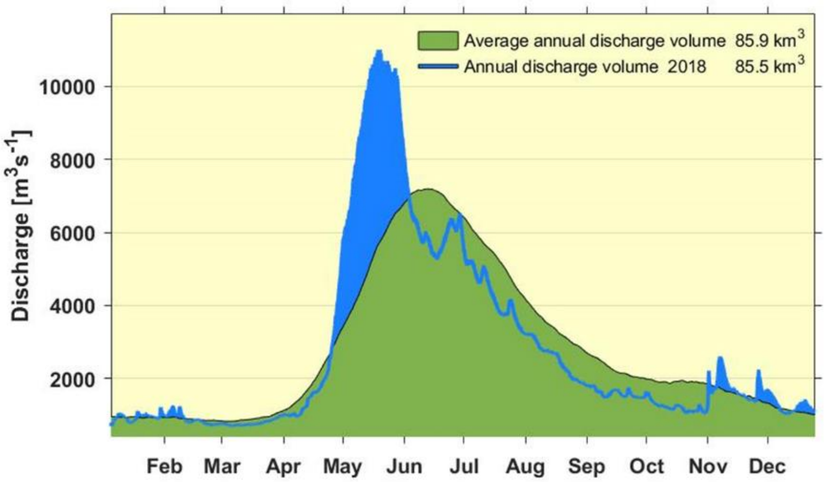

Figure 3-7. Fraser River discharge at Hope B.C.; 2017 (blue), 105 year average (green). Data source: The Water Survey of Canada.

After a three-year absence from the Strait of Georgia, a harmful algal bloom (*Heterosigma akashiwo*) occurred in early June, resulting in high aquaculture fish mortality in Jervis Inlet (Esenkulova and Pearsall, section 35, Haigh and Johnson, section 34, Nemcek et al., section 31). This bloom was linked to the early and high Fraser River freshet and hot weather in May-June (Esenkulova and Pearsall, section 35, Haigh and Johnson, section 34, Nemcek et al., section 31).

SoG zooplankton biomass was near the long-term average in 2017 and 2018 with peaks in May and June for the North and Central SoG, respectively (Young et al., section 32). In 2018, euphausiid abundance (preferred food for juvenile salmon) peaked in spring, but not in the fall as it did in 2017 (Young et al., section 32).

In the SOG, the spring bloom timing and duration was comparable to the long-term average (Gower and King, section 13; Costa, section 29; Allen et al., section 30; Sastri et al., section 27) – which implies good feeding conditions for juvenile fish. For example, the timing of the spring phytoplankton and subsequent zooplankton blooms in the Strait of Georgia are linked to the survival of herring (Boldt et al., section 33). Over the last 8 years, Pacific Herring biomass estimates increased in the Strait of Georgia; however, over the last 2 to 5 years, the biomass of other stocks was either stable (West Coast of Vancouver Island) or decreased (Central Coast, Haida Gwaii, Prince Rupert) (Cleary et al., section 19; Figure 3-8). Other forage fish show varied trends. For example, Northern Anchovy consumes zooplankton and has been abundant in SoG survey catches during the last three years (Neville, section 43, Boldt et al., section 33). An index of Eulachon spawning stock biomass in the Fraser River was estimated to be at a moderately high level (similar to 2015), compared with most other years from 2004-2017 which were relatively low (Flostrand, section 18).

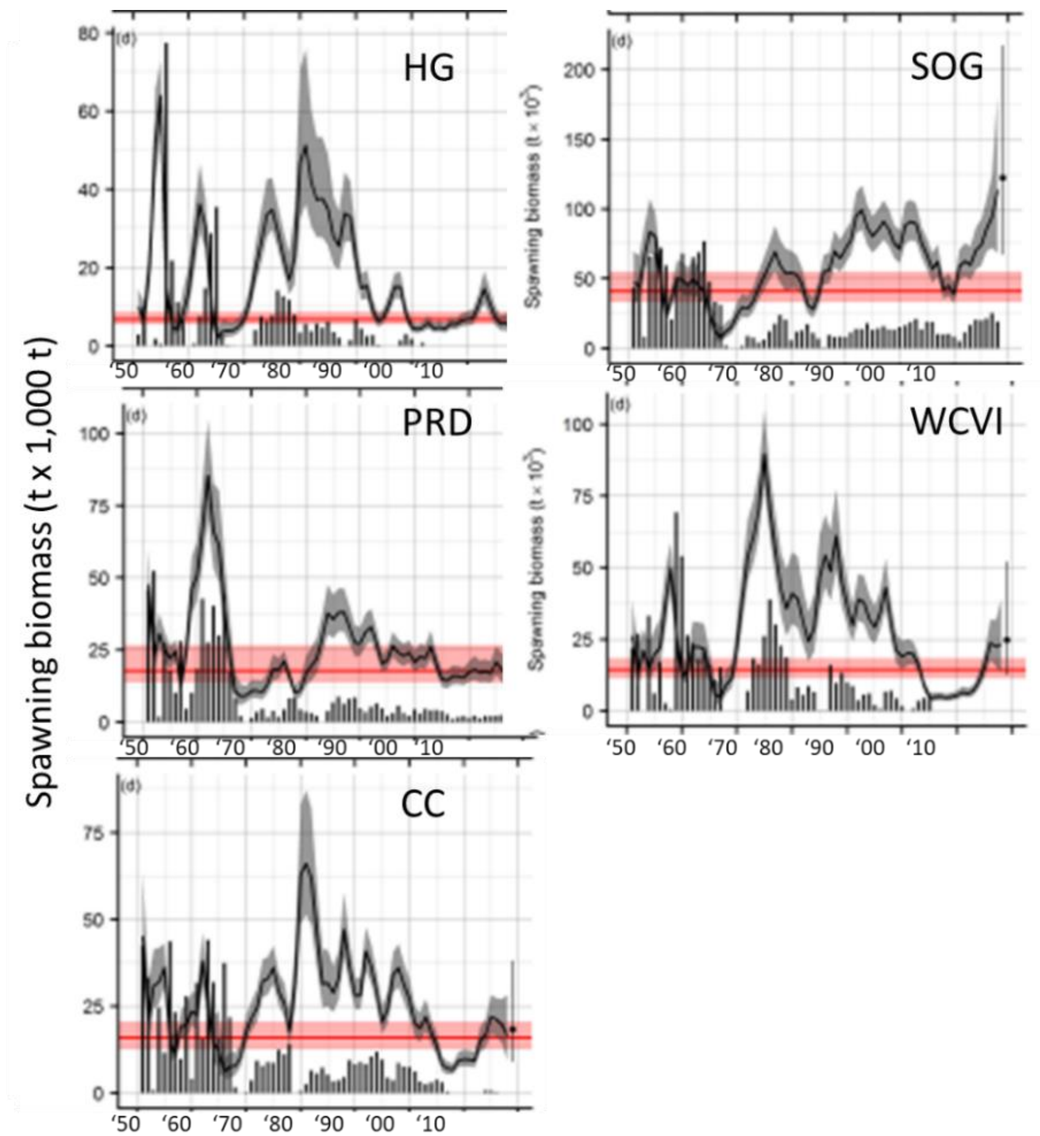

Figure 3-8. Spawning biomass of Pacific Herring from 1951 to 2018, where solid lines with surrounding grey envelopes represent medians and 5-95% credible intervals. Also shown is the reconstruction of spawning biomass (SBt) for each year t, with unfished values shown at far left (solid circle and vertical lines) and the projected spawning biomass given zero catch (SB2019) shown at the far right (solid circle and vertical lines). Time series of thin vertical lines denote commercial catch (excluding commercial spawn-on-kelp). The horizontal red line indicates the LRP= limit reference point. Figure adapted from DFO (2019). Source: Cleary et al., section 19.

In the SOG, juvenile salmon species survey catches were average or better than average SOG (Neville et al., section 43). Off the WCVI, however, there were fewer juvenile salmon than normal likely due to size-selective mortality (King et al., section 42). Recent warming in the ocean and freshwater, early river freshets, and summer drought have led to changes in the food web and low survival and productivity of Sockeye Salmon coastwide (Grant et al., section 39; Hyatt et al., section 41, Xu et al., section 44; Figure 3-9).

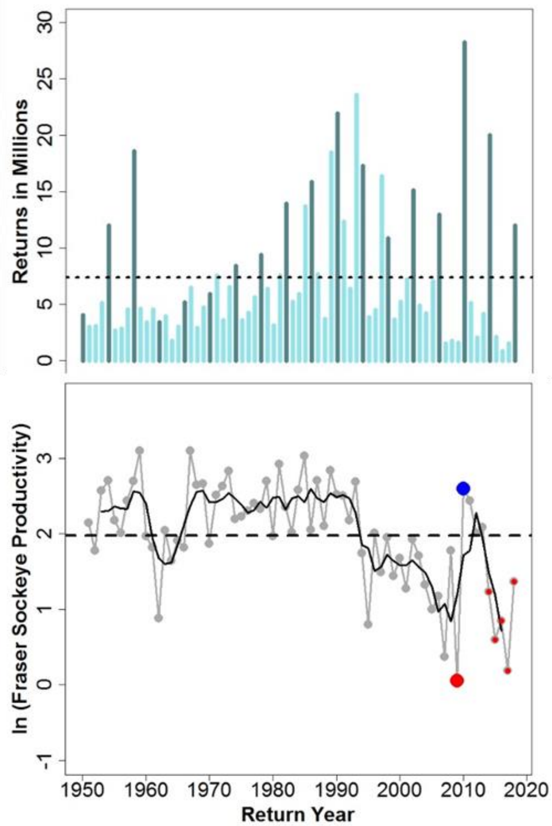

Figure 3-9. Total Fraser Sockeye annual returns (dark blue vertical bars for the 2018 cycle and light blue vertical bars for the three other cycles) (top panel). Recent returns from 2016 to 2018 are preliminary, and 2018 (the last data point) is an in-season estimate only. Total Fraser Sockeye productivity (log_e (returns/total spawner)) up to the 2018 return year (bottom panel). The grey dots and lines represent annual productivity estimates and the black line represents the smoothed four year running average. For both figures, the dashed line is the time series average. Source: Grant et al., section 39.

4. REFERENCES

Hipfner, J.M., 2009. Euphausiids in the diet of a North Pacific seabird: annual and seasonal variation and the role of ocean climate. Mar. Ecol. Progr. Ser. 390: 277-289.

5. ACKNOWLEDGMENTS

The authors and contributors to this Technical Report wish to thank all the officers and crew of the many vessels that have been involved in collecting data and maintaining monitoring stations for these studies. Without their assistance many of the reports in this document would not be possible.

Individual reports on conditions in the Northeast Pacific and British Columbia’s outer coast

6. ANOTHER WARM, BUT ALMOST NORMAL, YEAR FOR THE NORTHEAST PACIFIC OCEAN

Tetjana Ross and Marie Robert, Fisheries and Oceans Canada, Institute of Ocean Sciences, Sidney, British Columbia, Tetjana.Ross@dfo-mpo.gc.ca, Marie.Robert@dfo-mpo.gc.ca

6.1. Highlights

- For most of 2018 temperatures were slightly warm, but near-normal in the Northeast Pacific (NEP), likely due to La Niña conditions that persisted throughout the first half of the year.
- The exception was a strong sea surface temperature (SST) anomaly (a marine heatwave sometimes called 'Son of the Blob' due to its location) from October-November in the NEP.
- El Niño conditions are now present and climate indices suggest warm conditions in B.C. waters, so 2019 will likely be another very warm year.

6.2. Summary

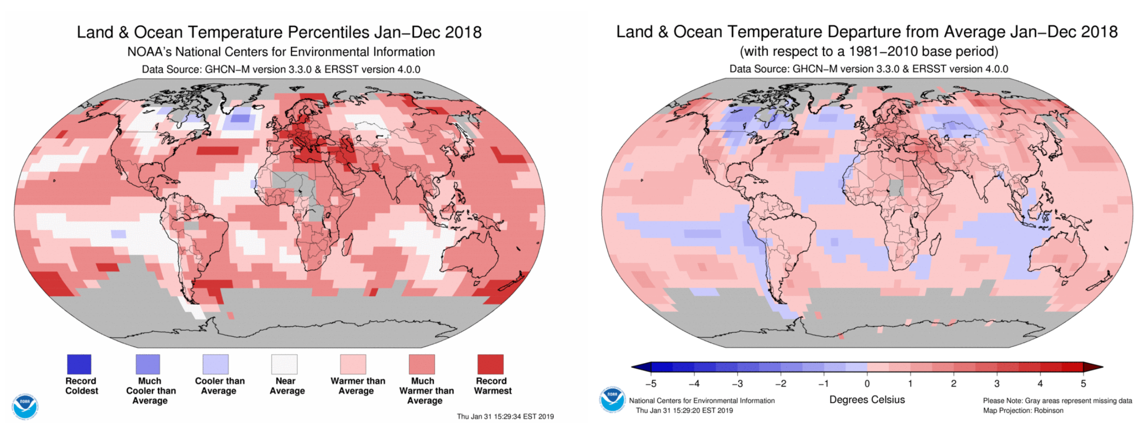

Figure 6-1. Maps of the globe show surface temperature percentiles (panel a) and anomalies (panel b) in the year 2018. ***Panel a****: Colours indicate percentiles, with "warmer than average", "near average" and "cooler than average" indicating, respectively, the top, middle and bottom terciles of the 139 year record. Source: https://www.ncdc.noaa.gov/sotc/service/global/map-percentile-mntp/201801-201812.gif* ***Panel b****: Colour bar shows the magnitude of the temperature anomaly scale, with warm colours for relatively warm regions and cool colours for relatively cool regions. Source: https://www.ncdc.noaa.gov/sotc/service/global/map-blended-mntp/201801-201812.gif* ***Both panels****: Grey areas represent missing data.*

Based on NOAA land and sea surface data dating back to 1880, 2018 was the fourth warmest year on record globally (NOAA State of the Climate). This is consistent with the recent trend, wherein eight of the ten warmest years are in the last decade. In ranked order, the ten warmest years are 2016, 2015, 2017, 2018, 2014, 2010, 2013, 2005, 2009, and 1998. Sea surface temperatures (SSTs) in the Northeast Pacific (NEP) were a little more than 1^{o}C above the average for the 1981-2010 base period (Figure 6-1b).

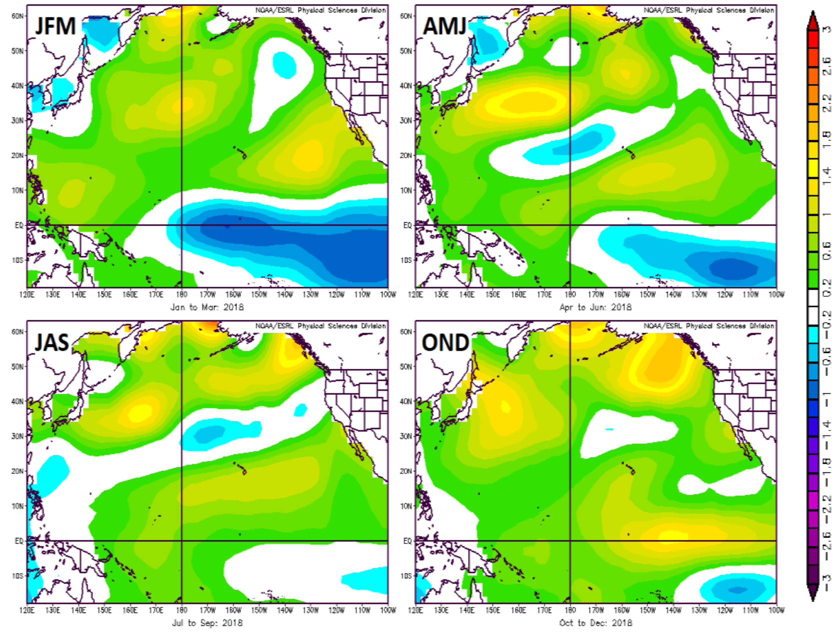

Figure 6-2. Seasonal maps of temperature anomalies in the Pacific Ocean for 2018.The colour bar on the right, showing the temperature anomaly in ºC, applies to all panels. Source: NOAA Extended SST v4

La Niña conditions were present for the first half of the year, switching to El Niño conditions near the end of the year (Figure 6-2). This La Niña was likely responsible for the slightly lower than average temperatures in the NEP in the winter (Jan-Feb-Mar), but the subsequent El Niño was quite weak, so unlikely to be responsible for the magnitude of the temperature anomalies seen in the NEP in the Fall (Oct-Nov-Dec). These temperature anomalies were due to a strong, but short-lived marine heat wave that some have called the "Son of the Blob" (Britten 2018). This marine heatwave (Hannah et al., section 9) was so strong that, while SSTs in the NEP were near average throughout most of the year (Figure 6-2), it brought the yearly anomaly into the "much warmer than average" tercile (Figure 6-1a).

Near normal temperatures (i.e. near both the 1981-2010 (Figure 6-1b and Figure 6-2) and 1956-2012 (Figure 6-3) means) were observed subsurface as well. The record of temperature anomalies at Station Papa (based on the interpolation of Argo float data onto the location of Station Papa; Figure 6-3, showed near-normal subsurface temperatures at Station Papa throughout 2018. This is in contrast to 2017, where subsurface temperatures had remained anomalously warm beneath 100 m throughout most of the year. Note that the Fall marine heatwave shows up as most intense at ~45 m depth in November (over 3 standard deviations in Figure 6-3); this is because the historical variability was smaller in that depth range and the temperature deviation (~2ºC) was of the same magnitude throughout the upper 50 m.

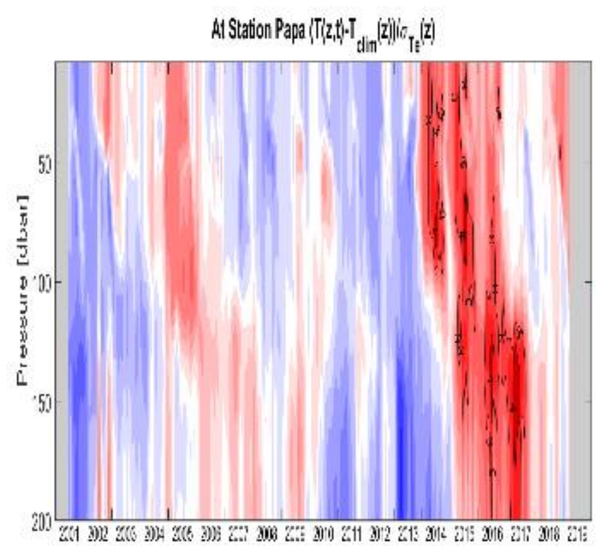

Figure 6-3. False colour plot of temperature anomalies relative to the 1956-2012 seasonally-corrected mean and standard deviation (from the Line P time series), as observed by Argo floats near Station Papa (P26: 50º N, 145 º W).The cool colours indicate cooler than average temperatures and warm colours indicate warmer that average temperatures. Dark colours indicate anomalies large compared with the 1956-2012 standard deviations. The black lines highlight regions with anomalies that are 3 and 4 standard deviations above the mean.

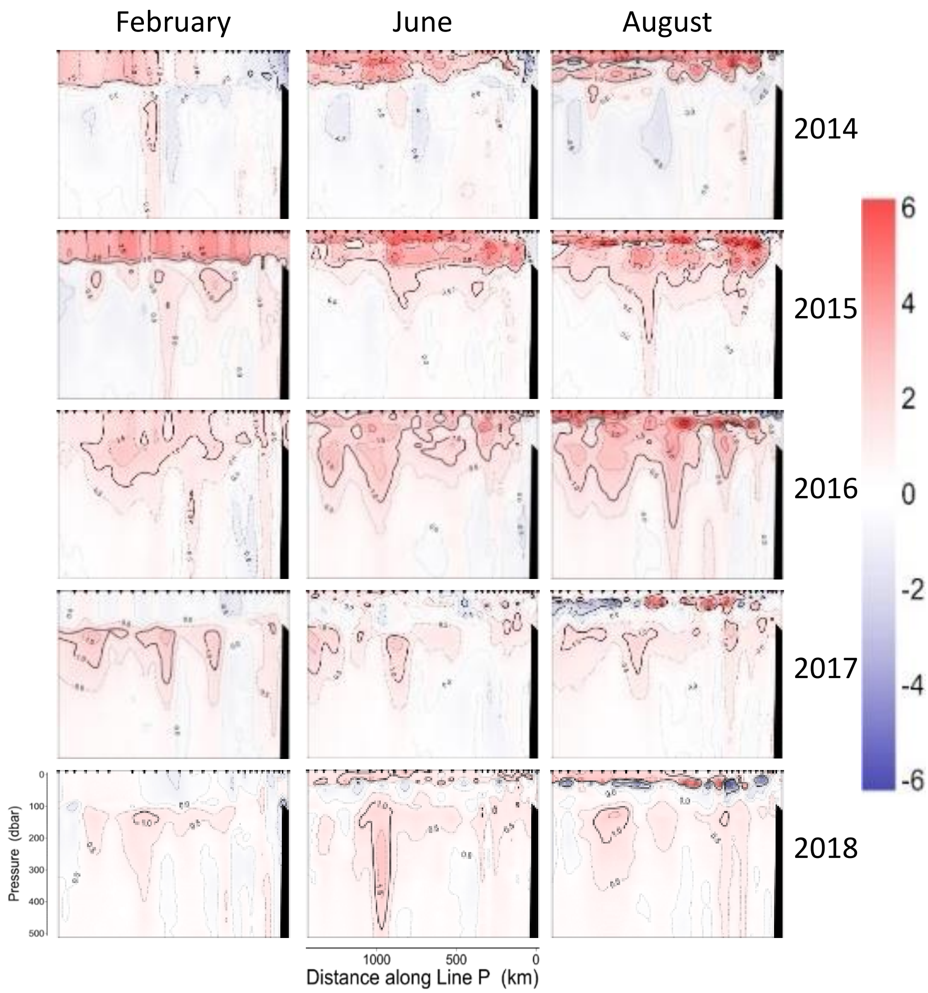

Figure 6-4. Temperature anomalies (°C) along Line P from 2014 to 2018 with respect to the 1981-2010 average.

Due to its short duration and onset in October (Hannah et al., section 9), the marine heatwave was not observed in the 2018 Line P data (Figure 6-4). These high resolution temperature anomaly sections show that the subsurface data followed the same trend as the SST across the NEP: slightly warm but mostly normal subsurface temperatures.

The winter stratification was stronger in 2017/18 than 2016/17, similar to 2015/16. After several years of stronger than usual winter stratification caused by reduced mixing due to warmer surface waters, i.e. the winters of 2013/14, 2014/15 (Freeland 2015), and even 2015/16, it seemed that winter mixing had returned to normal in the winter of 2016/17. The history of the 1025.7 kg/m^3 isopycnal (highlighted with a thick black line in Figure 6-5) illustrates this. It remained very deep throughout the 2013-2015 marine heatwave, deeper even than much of the 2003-2005 warm period, and shoaled in the winter of 2015/16 to levels last experienced during 2003-2005, while in 2016/17 stratification returned to a level similar to the winters of 2010/11 and 2011/12. This return to weaker mixing – surprising given the normal SST conditions during 2017/18 — suggests that nutrient supply from deep waters should have been weaker and therefore early spring nutrient levels lower in the spring of 2018. With the marine heatwave in the fall of 2018 it is likely that 2018/19 will also have weaker than normal winter mixing.

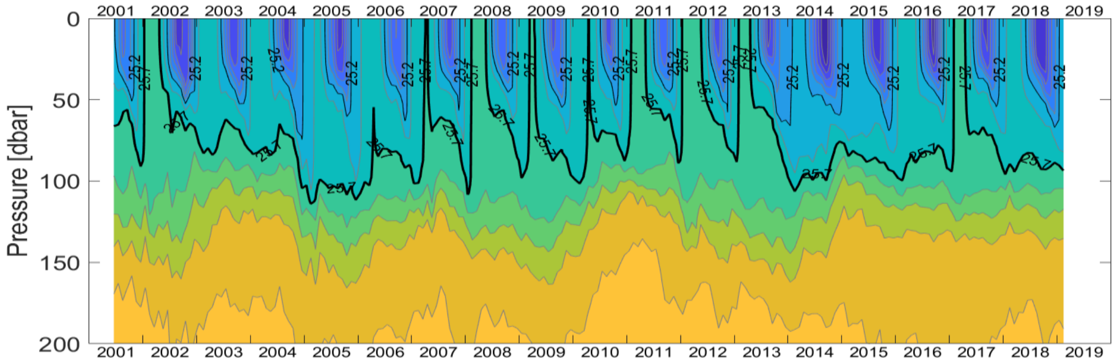

Figure 6-5. Coloured contour plot of density as observed by Argo floats near Station Papa (P26: 50º N, 145º W).The colours indicate potential density (yellow is denser and blue lighter). The black lines highlight the σ_θ=25.2 kg/m^3 (thin) and 25.7 kg/ m^3 (thick) isopycnals.

As mentioned above, La Niña generally leads to cooler than average winters in western North America. The combination of this negative anomaly with global temperature rise led to normal temperature conditions in the NEP throughout much of 2018. Near the end of 2018, the NEP experienced a short-lived marine heatwave and the onset of a weak El Niño. The El Niño-La Niña is represented by the Oceanic Niño Index (ONI; Figure 6-6)

Looking at the climate indices collectively (Figure 6-6) there were mixed indications for 2018; not surprising given the near-normal observation for most of the year. Looking ahead, most of the indices (only ONI shown for 2018/19) are trending toward indicating a warm year for 2019.

6.3. Climate Indices

The **North Pacific Index (NPI)** is the area-weighted sea level pressure over the North Pacific Ocean from 30°N to 65°N and 160°E to 140°W. This index, like the Aleutian Low Pressure Index (ALPI; Surry and King 2015) reported last year, is a useful indicator of the intensity and areal extent of the Aleutian Low Pressure system. The NPI was generally positive (blue) from 1950 to 1976, and generally negative (red) from 1977 to 2008; a change than can be attributed to the strengthening of the Aleutian Low Pressure system after 1977. From 2008 to present, the NPI was mostly positive, due to weaker Aleutian Lows. The NPI anomaly (Figure 6-6) was calculated from the NPI by removing the 1950-2018 mean. Monthly time series of the NPI are provided by the Climate Analysis Section, NCAR at Boulder, Colorado and based on Trenberth and Hurrell (1994):
https://climatedataguide.ucar.edu/sites/default/files/cas_data_files/asphilli/npindex_monthly.txt.

The **Southern Oscillation Index (SOI)** is the anomaly in the sea level pressure difference between Tahiti (17°40′ S 149°25′ W) and Darwin, Australia (12°27′0″ S 130°50′0″ E). It is a measure of the large-scale fluctuations in air pressure occurring between the western and eastern tropical Pacific (i.e. the state of the Southern Oscillation) and, as it represents the changes in winds that set up El Niño/La Niña events, the ONI follows it quite closely. SOI is provided by the NOAA's National Weather Service National Centers for Environmental Prediction CPC and is available from: www.cpc.ncep.noaa.gov/data/indices/soi.

The **Oceanic Niño Index (ONI)** is a monthly index which is a 3-month running mean of sea surface temperature (SST) anomalies in the Niño 3.4 region (5° N-5° S, 120°-170° W) plotted on the center month. The SST anomalies are calculated based on 30-year base periods that are updated every 5 years, which accounts for global warming and some of the decadal-scale SST variability (as seen in the PDO index). The ONI is provided by the NOAA's National Weather Service National Centers for Environmental Prediction CPC and is available from: http://www.cpc.ncep.noaa.gov/products/analysis_monitoring/ensostuff/ensoyears.shtml.

The **Pacific Decadal Oscillation (PDO) Index** is defined as the leading mode of monthly sea surface temperature variability (1^{st} principal component [PC] of SST) in the North Pacific (Mantua et al. 1997, Zhang et al. 1997). It represents a long-lived El Niño-like pattern of Pacific climate variability, generally indicating warm/cool patterns that persist for a decade or more. The PDO is provided by the Joint Institute for Studies of Atmosphere and Ocean of NOAA and is available from: http://research.jisao.washington.edu/pdo/.

The **North Pacific Gyre Oscillation (NPGO)** is a climate pattern that emerges as the second dominant mode of sea surface height (SSH) variability (2^{nd} PC of SSH) in the Northeast Pacific. The NPGO has been shown to be significantly correlated with fluctuations of salinity, nutrients and chlorophyll-a from long-term observations in the California Current (CalCOFI) and Gulf of Alaska (Line P) (Di Lorenzo et al. 2008). Monthly values of NPGO are available from: http://www.o3d.org/npgo/.

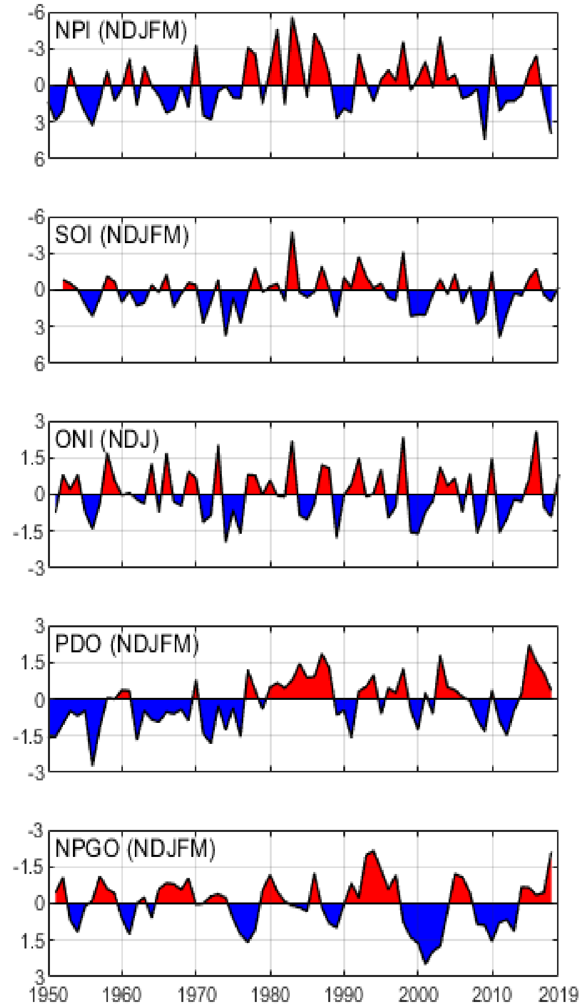

Figure 6-6. Time series of Pacific Ocean climate indices. Except for the ONI, each of the monthly indices were averaged over the months of Nov, Dec, Jan, Feb, and Mar and plotted for the year in Jan. Some series are inverted (negative values are above the axes) so that all series are red when coastal B.C. temperatures are anomalously warm. See text for a description and the source of each index.

6.4. References

Britten, L. 2018. 'Son of the blob': Unseasonably warm weather creating new anomaly off B.C. coast [online]. Available from https://www.cbc.ca/news/canada/british-columbia/blob-pacific-ocean-bc-1.4867674 [accessed 5 April 2019].

Di Lorenzo, E., Schneider, N., Cobb, K. M., Chhak, K., Franks, P. J. S., Miller, A. J., McWilliams, J. C., Bograd, S. J., Arango, H., Curchister, E., Powell, T. M., and Rivere, P. 2008. North Pacific Gyre Oscillation links ocean climate and ecosystem change. Geophys. Res. Lett. 35: L08607, doi: 10.1029/2007GL032838.

Freeland, H. 2015. The "Blob" or Argo and other views of a large anomaly in the Gulf of Alaska in 2014/15. In: Chandler, P.C., King, S.A., and Perry, R.I. (Eds.). 2015. State of the physical, biological and selected fishery resources of Pacific Canadian marine ecosystems in 2014. Can. Tech. Rep. Fish. Aquat. Sci. 3131: vi + 211 p. Available online: http://www.dfo-mpo.gc.ca/Library/358018.pdf.

Mantua, N.J., Hare, S.R., Zhang, Y., Wallace, J.M., and Francis, R.C. 1997. A Pacific interdecadal climate oscillation with impacts on production. Bulletin of the American Meteorological Society 78: 1069-1079.

NOAA National Centers for Environmental Information, State of the Climate: Global Climate Report for Annual 2018, published online January 2019, retrieved on March 17, 2019 from https://www.ncdc.noaa.gov/sotc/global/201813.

Surry, A.M., and King, J.R. 2015. A New Method for Calculating ALPI: the Aleutian Low Pressure Index. Can. Tech. Rep. Fish. Aquat. Sci. 3135: 31 + v p.

Trenberth, K.E. and Hurrell, J.W. 1994. Decadal atmosphere-ocean variations in the Pacific. Climate Dynamics, 9:303-319.

Zhang, Y., Wallace, J.M., and Battisti, D.S. 1997. ENSO-like interdecadal variability: 1900-93. J. Climate 10: 1004-1020.

7. WIND-DRIVEN UPWELLING/DOWNWELLING ALONG THE NORTHWEST COAST OF NORTH AMERICA: TIMING AND MAGNITUDE

Roy A.S. Hourston and Richard E. Thomson, Fisheries & Oceans Canada, Institute of Ocean Sciences, Sidney, B.C., Roy.Hourston@dfo-mpo.gc.ca, Richard.Thomson@dfo-mpo.gc.ca

7.1. Highlights

- Based on the timing of upwelling-favourable winds and alongshore currents, the 2018 Spring Transition timing was early relative to the historical (1991-2015) mean. This favoured above-average upwelling-based coastal productivity in 2018.
- The magnitude of the upwelling-favourable winds between 45°-50° N, during 2018 was below the 1991-2015 mean which favoured below average large-scale upwelling-based productivity. Between 50°-60° N, above average upwelling-favourable winds favoured above average productivity.

7.2. Upwelling Timing: The Spring Transition Index

7.2.1. The time series

The shift in spring from predominantly downwelling-favourable poleward winds in winter to predominantly upwelling-favourable equatorward winds in summer is referred to as the Spring Transition. The reverse process in fall is called the Fall Transition. The alongshore winds drive a seasonal cycle in the alongshore surface currents over the continental slope, from poleward in winter to equatorward in summer. The Spring and Fall Transitions for the Pacific coast are derived using along-shore wind stress time series from NCEP/NCAR Reanalysis-1 (Kistler et al. 2001), along-shore wind velocity from the Environment and Climate Change Canada meteorological buoy 46206, and the along-shore current velocity at 35 and 100 m depth at mooring A1 (Figure 7-1; Folkes et al. 2017, Thomson et al. 2013).

The onset of seasonal upwelling that accompanies the Spring Transition varies from year to year (Thomson et al. 2014). In years such as 2005 and 2010, when the Spring Transition was relatively late, marine coastal productivity across trophic levels from plankton to fish to birds was generally average to below-average, and was particularly poor in 2005 (DFO 2006). In years when the spring transition timing was average to early, such as 1999 and 2014, productivity was generally average to above-average (e.g. see Chandler et al. 2015, reports on outer British Columbia).

7.2.2. Status, trends, and implications

In 2018, the Spring Transition timing was early compared to the 1991-2015 mean (Figure -1), suggesting that upwelling-based spring productivity near the west coast of Vancouver Island during the 2018 summer was likely to be above average. From 2008 to 2016, the Spring Transition timing had generally been average to early, which favoured average to above-average summer productivity. The Spring Transition has exhibited marked variability since 1980 but there is no apparent linear trend over this period. Interannual variability in the winds, currents and other indices is sufficiently high to continue to mask any possible long-term trend due to the changing climate.

Since 2005, however, there appears to be a trend to earlier Fall Transition timing, and perhaps earlier Spring Transition timing as well (Figure 7-1). This decreases the length of the upwelling season. Whether these trends continue or what their implications are is uncertain.

7.3. Upwelling Magnitude: The Upwelling Index

7.3.1 The time series

Because they drive offshore surface Ekman transport and compensating onshore transport at depth, the strength (duration and intensity) of upwelling-favourable (northwesterly) winds are considered indicators of coastal productivity (e.g., Xu et al., section 44). To gauge low-frequency variability in coastal productivity, we have summed upwelling-favourable-only wind stresses by month along the west coast of North America from 45°-60° N latitude (Figure 7-2) using the NCEP/NCAR Reanalysis-1 analyses (Kistler et al. 2001) and subtracted the 1991-2015 mean to derive the Upwelling Index.

7.3.2 Status, trends, and implications

The Upwelling Index time series (Figure 7-2) indicates that upwelling-favourable wind stress was both below and above average over the 45°-60° N latitude range in 2018. As a consequence, conditions favoured below average large-scale upwelling-based productivity over the summer of 2018 south of 50° N, and above average productivity north of 50° N. No recent trends in upwelling-favourable winds were evident (Figure 7-3).

7.4. The Spring Transition and Upwelling Indices Together

Upwelling conditions are summarized by combining the Spring Transition Timing and Upwelling magnitude indices into a simple “stoplight” graphical format (Figure 7-3a). Favourable coastal upwelling conditions are in green and unfavourable conditions in red. Annual upwelling timing and magnitude values appear in three equal terciles (relative to 1991-2015): early timing/high magnitude years are green; late timing/low magnitude years are red; and the middle third of values for both are yellow. The 2018 upwelling timing was in the early one third of annual values and summer upwelling magnitude was in the lower third of annual values. Consequently, coastal upwelling-favourable conditions for productivity were a mix of good and bad in 2018. Figure 7-3a also shows that in 2005, a year noted for poor productivity (DFO 2006), upwelling timing and magnitude were both in the red category (late and small, respectively). It was also the case in 2017 during the recovery from the marine heat wave (Chandler et al. 2018), although conditions were not as dramatic as in 2005.

Another way of looking at these data is depicted in Figure 7-3b It shows that upwelling-favourable wind stress magnitude has been mostly greater than average since 1998, the upwelling season appears to be getting earlier since about 2005, and how 2017 had a stronger upwelling magnitude and later Spring Transition than 2005, even though both years are characterized as “red” in the stoplight diagram (Figure 7-3a).

7.5. Acknowledgements

NCEP/NCAR Reanalysis-1 wind stress provided by the NOAA/OAR/ESRL PSD, Boulder, Colorado, USA, from their web site at http://www.esrl.noaa.gov/psd/.

7.6. References

Chandler, P.C., King, S.A., and Perry, R.I. (Eds.). 2015. State of the physical, biological and selected fishery resources of Pacific Canadian marine ecosystems in 2014. Can. Tech. Rep. Fish. Aquat. Sci. 3131: vi + 211 p.

Chandler, P.C., King, S.A., and Boldt, J. (Eds.). 2018. State of the physical, biological and selected fishery resources of Pacific Canadian marine ecosystems in 2017. Can. Tech. Rep. Fish. Aquat. Sci. 3266: viii + 245 p.

DFO. 2006. State of the Pacific Ocean 2005. DFO Sci. Ocean Status Report. 2006/001.

Folkes, M., Thomson, R., and Hourston, R. 2017. Evaluating Models to Forecast Return Timing and Diversion Rate of Fraser Sockeye Salmon. DFO Can. Sci. Advis. Sec. Res. Doc. 2017/nnn. vi + 220 p.

Foreman, M.G.G., Pal, B., and Merryfield, W.J. 2011. Trends in upwelling and downwelling winds along the British Columbia shelf. Journal of Geophysical Research: Oceans 116(C10).

Kistler, R., Kalnay, E., Collins, W., Saha, S., White, G., Woolen, J., Chelliah, M., Ebisuzaki, W., Kanamitsu, M., Kousky, V., van del Dool, H., Jenne, R., and Fiorino, M. 2001. The NCEP–NCAR 50-year reanalysis: monthly means CD-ROM and documentation. Bulletin of the American Meteorological Society 82: 247–267.

Thomson, R.E., Hessemann, M., Davis, E.E., and Hourston, R.A.S. 2014. Continental microseismic intensity delineates oceanic upwelling timing along the west coast of North America, Geophys. Res. Lett., 10.1002/2014GL061241.

Thomson, R., Hourston, R., and Tinis, S. 2013. OSCURS for the 21st Century: Northeast Pacific Salmon Tracking and Research (NEPSTAR) Project, Year 3 Interim Report. Annual report submitted to the Pacific Salmon Commission. 37p.

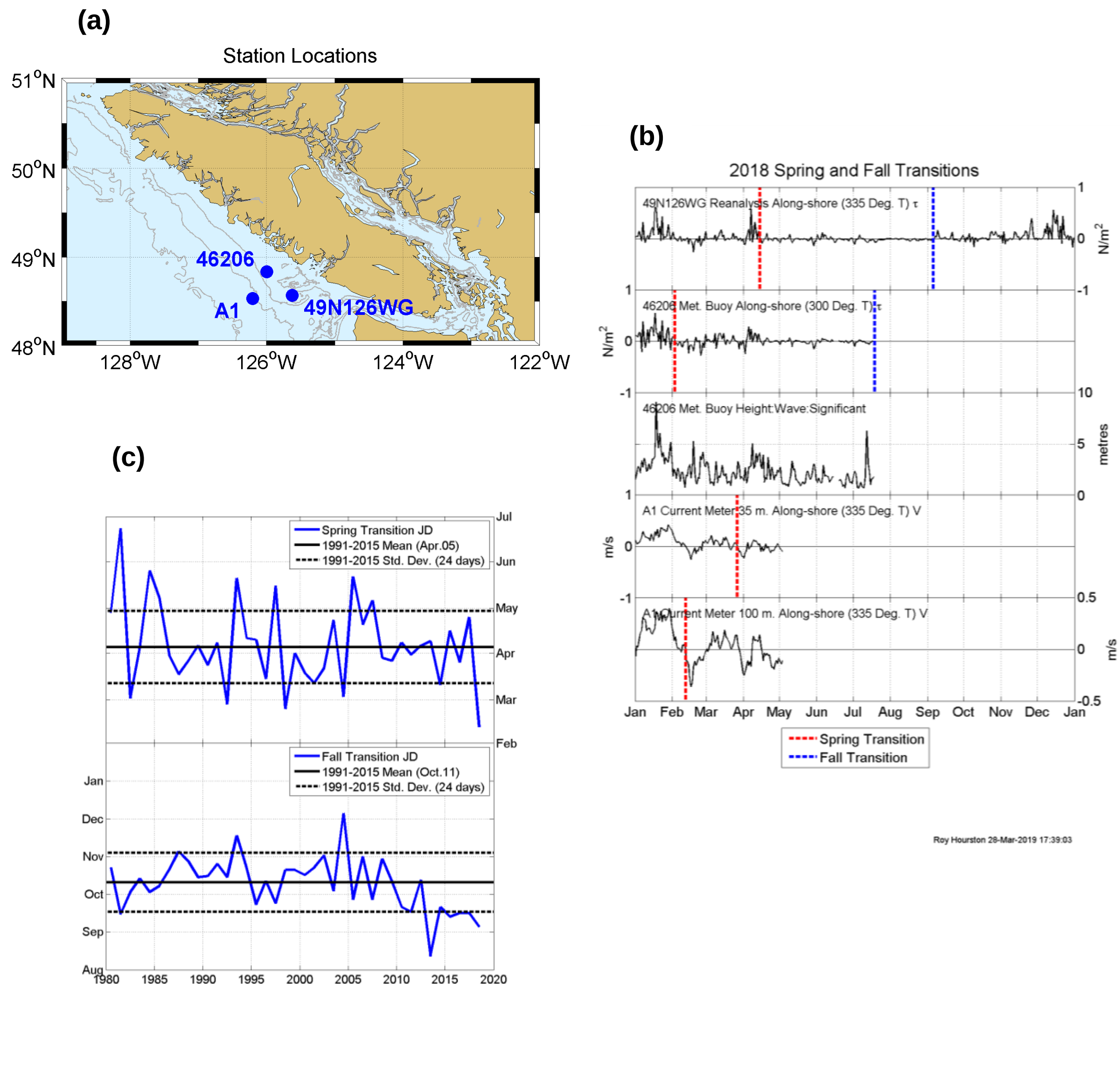

Figure 7-1. (a) Locations of observations used to delineate historical Spring and Fall Transitions. (b) Time series depicting the Spring and Fall Transitions off the west coast of Vancouver Island in 2018. Wind stress at Reanalysis-1 grid point 49N126W and meteorological buoy 46206; significant wave height at 46206; along-shore current velocity at 35 and 100 m depth at mooring A1 (Folkes et al. 2017; Thomson et al. 2013). Positive flow is poleward (downwelling-favourable) and negative flow is equatorward (upwelling-favourable). Vertical dashed lines show derived transition times using a cumulative sum approach (e.g. Foreman et al. 2011).(c) The timing of the annual Spring and Fall Transitions derived from time series in panel (b).

(a)

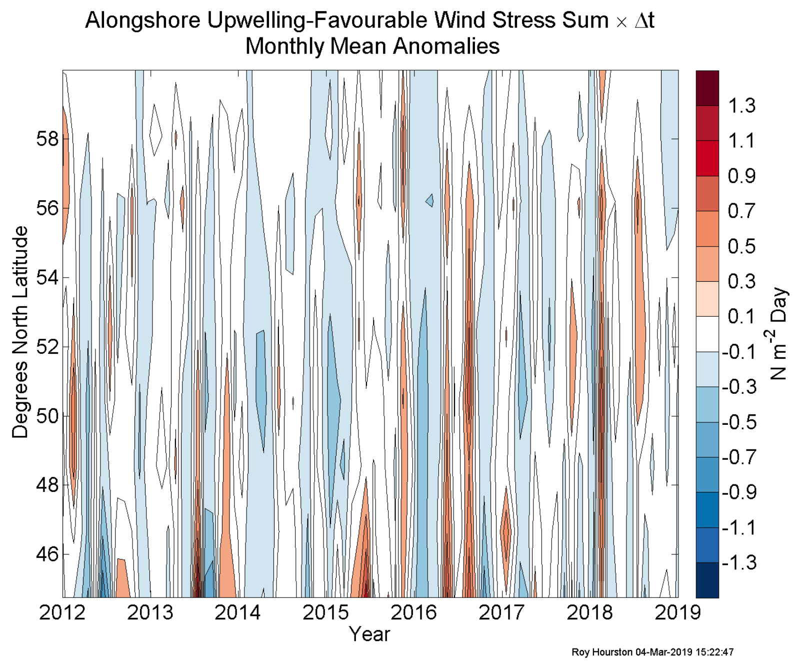

(b)

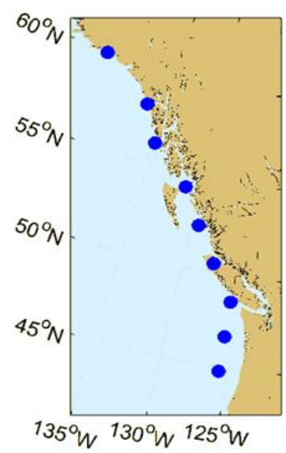

Figure 7-2. Recent (2012 to 2018) monthly mean anomalies (relative to 1991-2015) of monthly sums of alongshore upwelling-favourable (equatorward) wind stress (a) from the NCEP/NCAR Reanalysis-1 coastal surface wind stress grid locations, 45-60° N (b).

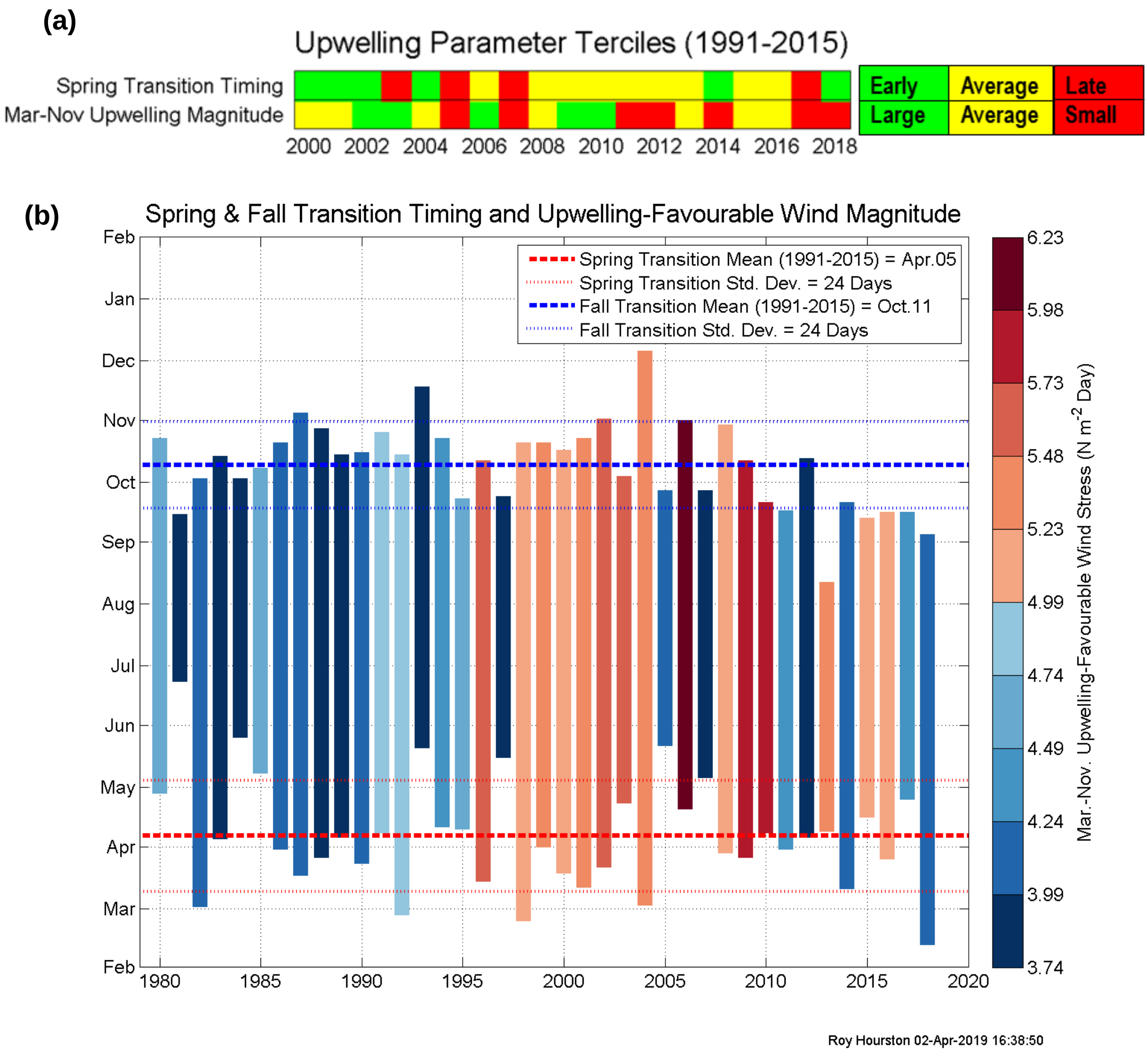

Figure 7-3. (a) Stoplight diagram depicting equal terciles of both the Spring Transition Timing Index and the Upwelling Magnitude Index for 49° N, 126° W. (b) Bar plot showing Spring and Fall Transitions and upwelling-favourable wind stress magnitude.

8. VANCOUVER ISLAND WEST COAST SHELF BREAK CURRENTS, TEMPERATURES, AND WIND STRESS

Roy A.S. Hourston and Richard E. Thomson, Fisheries & Oceans Canada, Institute of Ocean Sciences, Sidney, B.C., Roy.Hourston@dfo-mpo.gc.ca, Richard.Thomson@dfo-mpo.gc.ca

8.1. Highlights

- West coast shelf break surface and subsurface temperatures, wind stress, and currents have returned to near-average conditions after higher than average temperatures and stronger than average poleward and equatorward flow associated with the 2014-2016 El Niño. Temperatures at 100 m were still moderately higher than average at the beginning of 2018.

8.2. West Coast Shelf Break Temperatures and Currents

8.2.1. The time series

Subsurface temperature and current velocities at the shelf break have been observed at mooring A1, water depth ~500 m (Figure 8-1) since 1985. Nearby meteorological buoy 46206 has provided sea surface temperature and wind velocity time series since 1988. We have combined these series to obtain the vertical structure of temperature and flow through the water column.

8.2.2. Status, trends, and implications

At the beginning of 2018, temperatures at the surface, 35, 100, and 175 m depth continued to reflect the warm water signature of the marine heat wave and El Niño conditions that persisted over 2014-2016 (Figure 8-2a, left). Subsurface data are not available after April 2018 (mooring hit) or after July 2018 at the surface (buoy failed).

Also, at the beginning of 2018, the alongshore surface winds and subsurface currents at 35, 100, and 175 m depth indicated stronger than average poleward (downwelling-favourable) flow in January, but then reversed for even stronger equatorward (upwelling-favourable) flow for more than a month starting in February (Figure 8-2a, right). This strong anomalous upwelling signal in February was also noted off the west coast of Vancouver Island (Sastri, section 27), and in Rivers Inlet by the intrusion of offshore upwelled water (Jackson, section 25).

Figure 8-2b, shows monthly mean values, 2010-2018, and for temperature the positive anomalies associated with the marine heat wave and El Niño over 2014-2016 are most evident. For alongshore flow strong anomalies occurred in 2013 (weak poleward flow in winter preceding the marine heat wave), and enhanced equatorward flow in the summers of 2015 and 2016, and enhanced poleward flow over the winters of 2015-2016 and 2016-2017. These features are likely due to stronger large-scale surface atmospheric circulation features (Aleutian Low and North Pacific High) associated with the El Niño. The stronger poleward flow may also been due to an eastward shift of winter storm tracks to closer to the coast.

Higher temperatures and enhanced poleward flow were also observed during the previous strong El Niño in 1997-1998 (Figure 8-2c). While temperatures and flow have generally returned to long-term average conditions, at 100 m temperature anomalies are still moderately high.

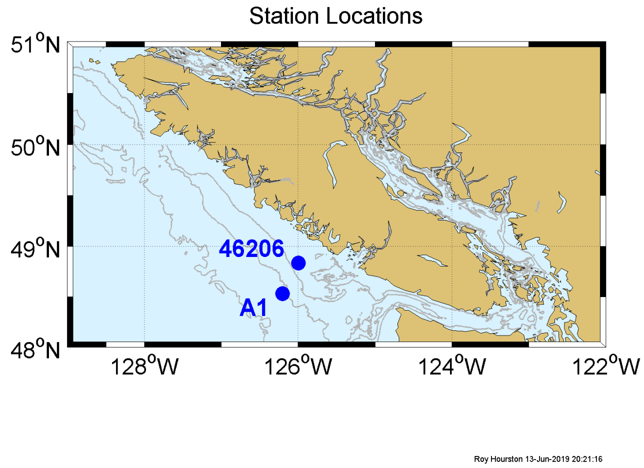

Figure 8-1. Locations of mooring A1 and meteorological buoy 46206.

(a)

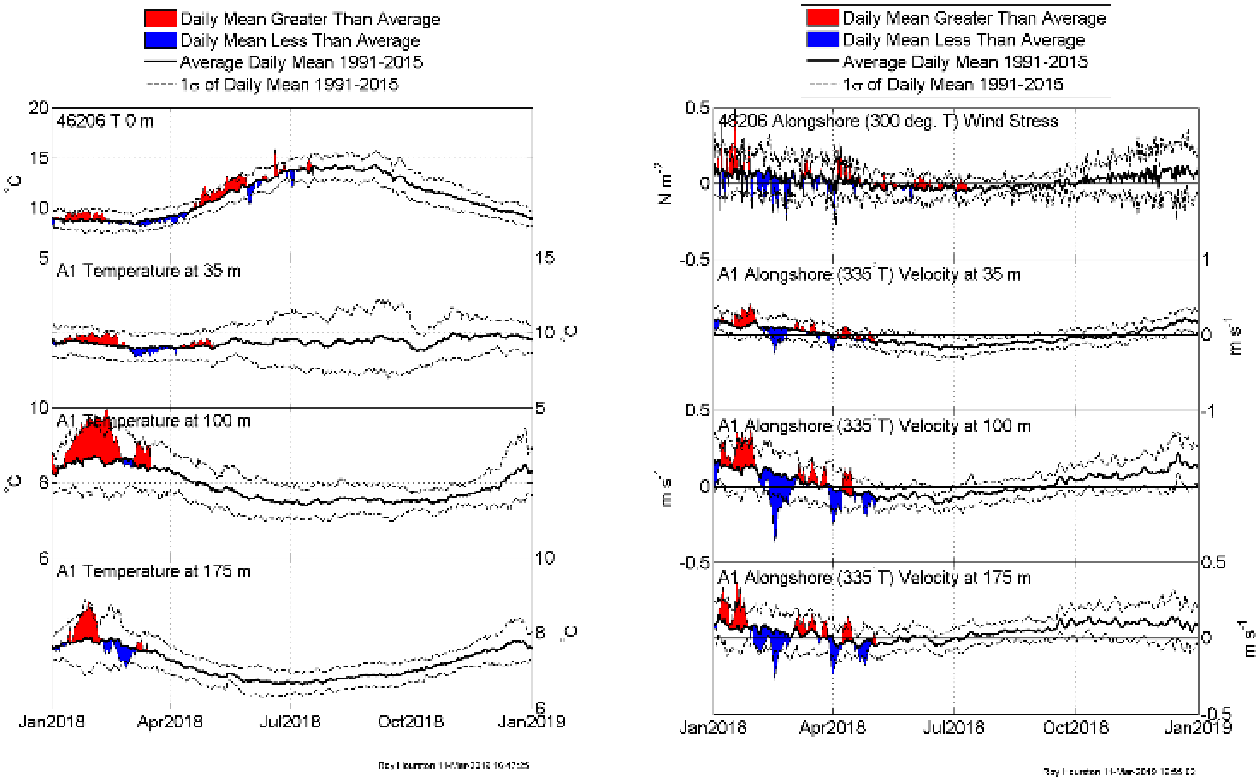
Daily Mean Greater Than Average
Daily Mean Less Than Average
Average Daily Mean 1991-2015
1σ of Daily Mean 1991-2015
46206 T 0 m
A1 Temperature at 35 m
A1 Temperature at 100 m
A1 Temperature at 175 m
°C
Jan2018
Apr2018
Jul2018
Oct2018
Jan2019
46206 Alongshore (300 deg. T) Wind Stress
A1 Alongshore (335°T) Velocity at 35 m
A1 Alongshore (335°T) Velocity at 100 m
A1 Alongshore (335°T) Velocity at 175 m
N m⁻²
m s⁻¹

(b)

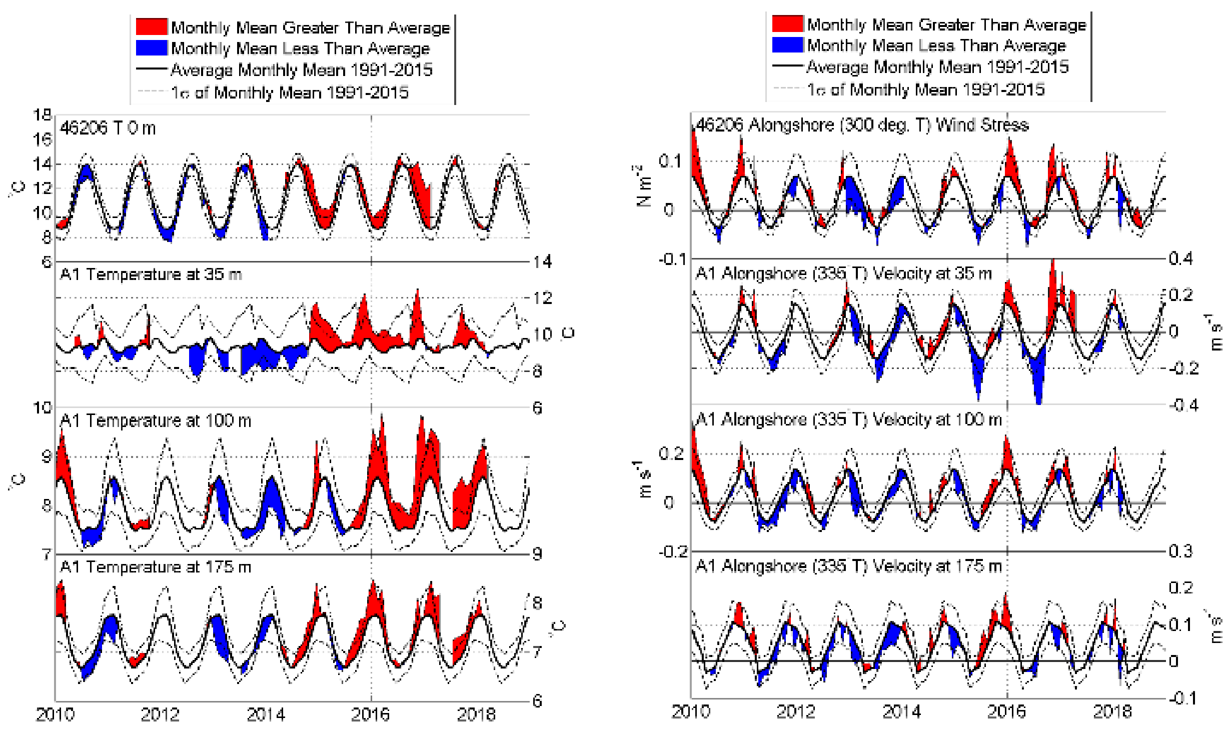
Monthly Mean Greater Than Average
Monthly Mean Less Than Average
Average Monthly Mean 1991-2015
1σ of Monthly Mean 1991-2015
46206 T 0 m
A1 Temperature at 35 m
A1 Temperature at 100 m
A1 Temperature at 175 m
°C
2010
2012
2014
2016
2018
46206 Alongshore (300 deg. T) Wind Stress
A1 Alongshore (335°T) Velocity at 35 m
A1 Alongshore (335°T) Velocity at 100 m
A1 Alongshore (335°T) Velocity at 175 m
N m⁻²
m s⁻¹

(c)

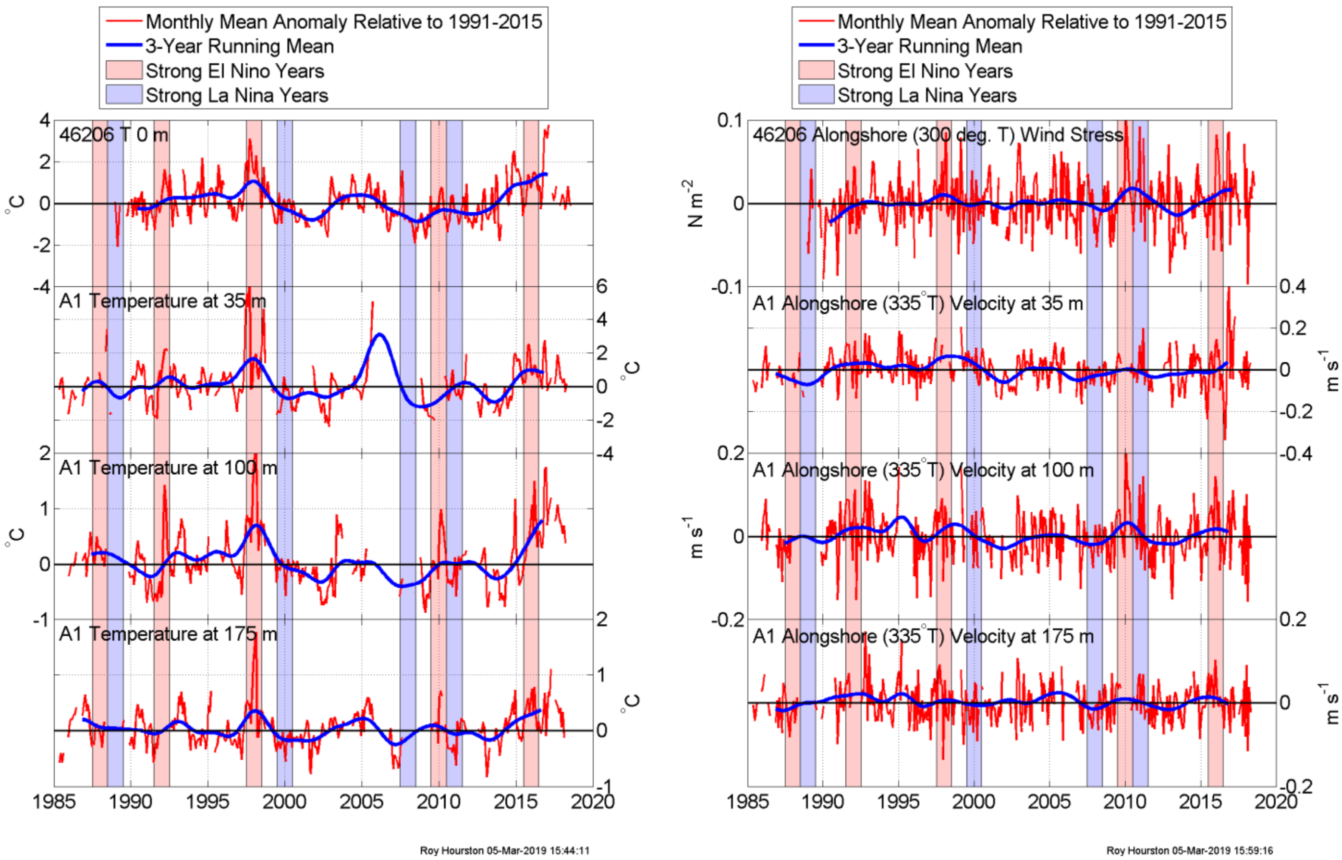

Figure 8-2.Temperature (left panels) and alongshore wind stress/ocean current (right panels) at the surface, 35 m, 100 m, and 175 m from meteorological buoy 46206 and mooring A1. Angle in brackets (°T) is the principal direction of the wind or current vector in degrees true compass bearing. (a) Daily means (b) Monthly means (c) Monthly anomalies.

9. OCEAN SURFACE TEMPERATURES IN 2018: ANOTHER MARINE HEAT WAVE?

Charles Hannah, Stephen Page and Tetjana Ross, Fisheries and Oceans Canada, Sidney, B.C., Charles.Hannah@dfo-mpo.gc.ca, Stephen.Page@dfo-mpo.gc.ca, Tetjana.Ross@dfo-mpo.gc.ca

9.1. Highlights

- There was a widespread positive sea surface temperature (SST) anomaly in the Northeast Pacific during the fall of 2018. The magnitude of the temperature anomalies (with respect to the 1971-2000 baseline) in the Gulf of Alaska was 2-3°C.
- At three offshore weather buoys the fall of 2018 qualified as a category 1 marine heat wave.
- On the shelf there was substantial spatial and temporal variability in the marine heat wave statistics. In Hecate Strait, the fall of 2018 may have been a major marine heat wave (Category 2 and 3) for two months, whereas Dixon Entrance only experienced a Category 1 marine heat wave for 1 or 2 weeks and in the southern Queen Charlotte Sound there was no marine heat wave.
- The SST anomalies arose because the ocean cooled less quickly than normal. This was the result of fewer fall storms in October and early November and then normal cooling in November and December. As a result the anomalies persisted even though the ocean surface was cooling.
- In early 2019, the SST conditions have largely returned to normal.
- It is likely that the ridging events and associated marine heat waves are predictable on seasonal time scales. Environment and Climate Change Canada (ECCC) produces seasonal forecasts with lead time up to 12 months. The forecast for the summer of 2019 produced on Dec 31, 2018 is for warmer than normal air temperatures off the BC coast and normal precipitation.

9.2. Description of the time series

Hobday et al (2016, 2018) define a marine heatwave (MHW) event ‘if it lasts for 5 or more days, with temperatures warmer than the 90th percentile based on a 30 year historical period. Categories of MHW are defined based on the difference between the 90th percentile and the mean, where both resolve the annual cycle call the difference curve the ‘increment’. A category 1 MHW has sea surface temperatures in excess of the 90th percentile for 5 consecutive days. A category 2 MHV is in excess of the 90th percentile plus 1 increment for 5 consecutive days, a category 3 MHV is excess of the 90th percentile plus 2 increments, and so on.

The SST anomaly maps (Figure 9-1) were obtained from the National Centre for Environmental Prediction website http://www.emc.ncep.noaa.gov/research/cmb/sst_analysis/ under the weekly anomaly archive.

The time series used are the SSTs measured by the British Columbia weather buoy network maintained by Environment and Climate Change Canada. The data are available from DFO at http://www.meds-sdmm.dfo-mpo.gc.ca/isdm-gdsi/waves-vagues/data-donnees/index-eng.asp. For this analysis we used the 3 offshore NOMAD buoys plus central Dixon, north and south Hecate, and west Sea Otter (Figure 9-2).

Table 9-1 shows when the various weather buoys started delivering data. The 3 NOMAD buoys have been in existence for more than 30 years. North Hecate and West Sea Otter do not quite have the 30 years of data required for the Hobday et al (2016, 2018) definition of a MHW. For the preliminary analysis presented here we used the entire record to define the annual cycle and the 90th percentile.

Table 9-1: The start dates for the weather buoys.

Station	Start date
North Nomad	20-Sep 1987
Middle Nomad	20-Sep 1987
South Nomad	22-Sep 1987
North Hecate	15-May 1991
West Sea Otter	07-Sep 1989
Central Dixon	16-April 1991

9.3. Status and trends

In the fall of 2018 the sea surface temperatures (SST) in the northeast Pacific were 2-3°C above normal. These anomalous temperatures caused some to wonder whether this situation represented a return to 'blob' conditions (Britten 2018) which persisted in the northeast Pacific from 2014-2016 (Bond et al. 2015, Peterson et al. 2016). The Washington Post published an excellent article on the conditions which led to the development of the anomalous temperatures though mid October 2018 (Livingston 2018).

The SST anomalies (with respect to the 1971-2000 baseline) in mid October and late November are shown in Figure 9-1. In October a large area of the Gulf of Alaska (the northeast Pacific) had temperature anomalies of 1.5 to 3.5°C. In November the amplitude of the anomalies was reduced to 1.5-2.5°C but the spatial extent was broader. The typical SST values in mid-October at the south Nomad weather buoy (Figure 9-2) are close to 14°C (Figure 9-3; black line) and they are about 12°C at North Nomad. Thus SST anomalies of 2°C are roughly equivalent to moving the SSTs at the latitude of Victoria (48.4 N) to the latitude of Prince Rupert (54.3 N). The elevated SST anomalies persisted over most of the Gulf of Alaska into December.

The 2018 SST anomalies originated in the late spring, when SSTs started to increase faster than normal in May or June and were about 1°C higher than normal through the summer (Figure 9-3), but they never reached Category 1 MHW status. Under normal conditions (the black line, Figure 9-3), the SSTs started to decline in late September at south NOMAD and declined at about 2°C per month into December. In 2018 the cooling slowed (or stopped) in mid-October which led to the 2-3°C anomalies (relative to normal conditions). In late October the cooling started again at the normal rate and as a result the temperature anomalies persisted into December. The result was a Cat 1 MHW at south NOMAD from mid-October to early December. Similar conditions prevailed at the middle and north NOMAD buoys. The temperatures started to decline more rapidly in December and by early January the anomalies at the 3 weather buoys were reduced to about 1°C.

At the North Hecate buoy (Figure 9-4) the picture is much more complicated. 2015 and 2016 show as important in the winter and spring. 2018 shows two Category 2 MHW events in the summer and category 2 and 3 MHW events through the fall and into December. There was still a category 1 MHW at the end of December. There are insufficient data at south Hecate to confirm this event and these extreme conditions were not seen at south Sea Otter or central Dixon.

In 2015 there was a Category 2 MHW at south NOMAD from mid-May through the end of August and Category 1 conditions prevailed at various times through to late November. Notice also that there was no data from the winter and spring of 2015.

We did not do a heat wave analysis for Station Papa in the NE Pacific, however, Ross and Robert (section 6) show that the fall of 2018 now defines the maximum temperatures observed there from mid-October through early December. Vertical sections of temperature created by projecting Argo float data onto Line P (upper 500 m) also show temperature anomalies of 2-3°C in the surface mixed layer in the fall of 2018 (Howard Freeland, DFO, pers. comm.). The mixed layer depths were about 30 m in mid-October, and increased to 50 m in mid-November and 70 m in early December. During this time the anomalies were in the 1-3°C range as seen in the satellite SST and at the weather buoys.

9.4. Factors influencing trends

The proximate cause of the heat wave in the fall of 2018 was the presence of a high pressure atmospheric ridge (at 500 mbar height) that diverted the usual fall storms into the Arctic. The ridge is the same phenomenon that gave rise to the 2014-2016 Blob (Bond et al. 2015, Peterson et al. 2016) and the persistent drought in California (Wang et al. 2014). The generation of future marine heat waves will depend on the formation of the atmospheric ridge, its location and intensity. Conceptually one can think of the 2018 warm event as a combination of summer conditions extending further into fall, and California conditions extending further north.

This anomalous pressure ridge and its consequences have been widely studied in the California context. The link between drought conditions and the occurrence of these atmospheric ridging events has been established, it has been shown that the creation of these ridges is linked to atmospheric conditions in the western tropical Pacific, and that the occurrence of ridging events are likely to increase due to climate change (Swain et al. 2014, Swain 2015, Swain et al. 2017, Wang et al. 2014). This work has not been done for British Columbia.

It is likely that the ridging events and associated marine heat waves are predictable on seasonal time scales. At the PICES meeting in October 2018, Antonietta Capotondi (NOAA) gave a talk entitled ‘Optimal tropical precursors of US West Coast marine warming’. She found that the optimal metric was based on conditions in the central and western equatorial Pacific and that the tropical conditions lead the west coast temperatures by 9 months. Environment and Climate Change Canada (ECCC) produces seasonal forecasts with lead time up to 12 months (https://weather.gc.ca/saisons/index_e.html). The forecast for the summer of 2019 produced on Dec 31, 2018 is for warmer than normal air temperatures off the BC coast and normal precipitation. These forecasts should be evaluated for their skill in forecasting the strength and northward extent of the anomalous pressure ridge and the associated elevated sea surface temperatures.

9.5. References

Bond, N.A., Cronin, M.F., Freeland, H. and Mantua, N. 2015. Causes and impacts of the 2014 warm anomaly in the NE Pacific. *Geophysical Research Letters*, *42*(9), pp.3414-3420.

Britten, L. 2018. 'Son of the blob': Unseasonably warm weather creating new anomaly off B.C. coast. Canadian Broadcasting Corporation. October 18, 2018. https://www.cbc.ca/news/canada/british-columbia/blob-pacific-ocean-bc-1.4867674

Hobday, A.J., Alexander, L.V., Perkins, S.E., Smale, D.A., Straub, S.C., Oliver, E.C.J., Benthuysen, J., Burrows, M.T., Donat, M.G., Feng, M. and others. 2016. A hierarchical approach to defining marine heatwaves. Progress in Oceanography 141:227–238, https://doi.org/10.1016/j.pocean. 2015.12.014.

Hobday, A.J., Oliver, E.C.J., Sen Gupta, S., Benthuysen, J.A., Burrows, M.T., Donat, M.G., Holbrook, N.J., Moore, P.J., Thomsen, M.S., Wernberg, T. and Smale, D.A. 2018. Categorizing and naming marine heatwaves. Oceanography 31(2):162–173, https://doi.org/10.5670/oceanog.2018.205.

Livingston, I. 2018. Persistent Alaska warmth this fall has brought back 'the blob.' If it lasts, it could mean a wild winter in the Lower 48. Washington Post, October 18, 2018. https://www.washingtonpost.com/weather/2018/10/18/persistent-alaska-warmth-this-fall-has-brought-back-blob-if-it-lasts-it-could-mean-wild-winter-lower/

Peterson, W., Bond, N. and Robert, M. 2016. The blob (part three): Going, going, gone?. *PICES Press*, *24*(1), p.46.

Swain, D.L., Tsiang, M., Haugen, M., Singh, D., Charland, A., Rajaratnam, B. and Diffenbaugh, N.S. 2014. The extraordinary California drought of 2013/2014: Character, context, and the role of climate change. *Bull. Am. Meteorol. Soc*, *95*(9), pp.S3-S7.

Swain, D.L. 2015. A tale of two California droughts: Lessons amidst record warmth and dryness in a region of complex physical and human geography. *Geophysical Research Letters*, *42*(22), pp.9999-10.

Swain, D.L., Singh, D., Horton, D.E., Mankin, J.S., Ballard, T.C. and Diffenbaugh, N.S. 2017. Remote linkages to anomalous winter atmospheric ridging over the northeastern Pacific. *Journal of Geophysical Research: Atmospheres*, *122*(22).

Wang, S.Y., Hipps, L., Gillies, R.R. and Yoon, J.H. 2014. Probable causes of the abnormal ridge accompanying the 2013–2014 California drought: ENSO precursor and anthropogenic warming footprint. *Geophysical Research Letters*, *41*(9), pp.3220-3226.

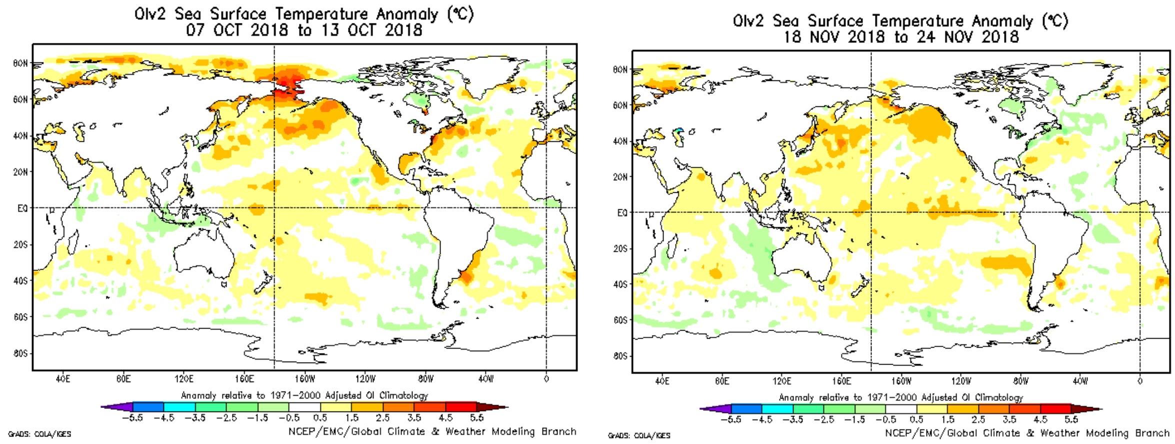

Figure 9-1. Global SST anomalies for the periods 7-13 October, 2018 and 18-24 November 2018. The peak anomalies in the northeast Pacific in October are in the 2.5-3.5°C range. The anomalies are relative to the mean conditions from 1971-2000 for the appropriate dates. The figure was obtained from the National Centre for Environmental Prediction website http://www.emc.ncep.noaa.gov/research/cmb/sst_analysis/ under the weekly anomaly archive.

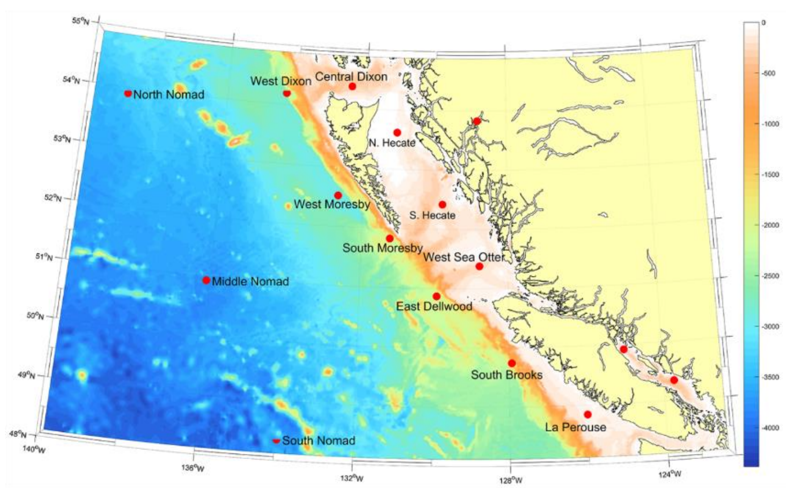

Figure 9-2. Map showing the locations of the weather buoys.

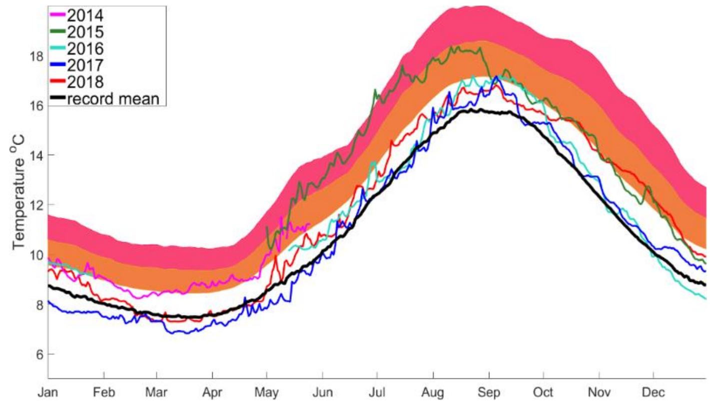

Figure 9-3. The sea surface temperature observed at the south NOMAD weather buoy. The salmon colour represents a Category 1 Marine Heatwave and the pink a Category 2.

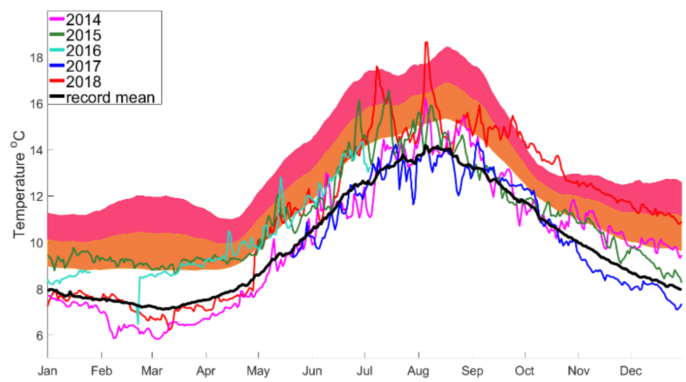

Figure 9-4. The sea surface temperature observed at the north Hecate weather buoy. The salmon colour represents a Category 1 Marine Heatwave and the pink a Category 2.

10. SEA LEVEL IN BRITISH COLUMBIA, 1910 TO 2018

Anne Ballantyne, Canadian Hydrographic Service, Fisheries & Oceans Canada, Institute of Ocean Sciences, Sidney, B.C., Anne.Ballantyne@dfo-mpo.gc.ca

10.1. Highlights

- In 2018, the annual mean water levels at Victoria and Tofino were above the long term trend line while the annual mean was below the trend line for Prince Rupert.
- Removing the vertical uplift changes the long term trend at the three locations.

10.2. Summary

The Canadian Hydrographic Service monitors sea levels along the B.C. coast. At three locations (Victoria, Tofino and Prince Rupert) the annual deviations from the long-term average are shown in Figure 10-1. Both Tofino and Victoria have records that began in 1910, while the record at Prince Rupert began in 1912.

A linear trend line was fitted to the data and the average sea level in 2018 was above the trend at Victoria and Tofino (for the fifth year in a row), while the 2018 average at Prince Rupert was below the trend line (for the second year in a row).

The linear sea level rise trend at each port (in cm/century):

Prince Rupert	+11.5
Victoria	+6.9
Tofino	-12.0

Tectonic motion is lifting the land at Tofino faster than sea level is rising, so that local sea level (measured relative to the land) is dropping at an average rate of 12 cm per 100 years. Removing the tectonic motion from the sea level values using a 1.9 mm annual uplift (Thomas James pers. comm. 2018) results in a linear trend at Tofino of 6.9 cm per 100 years (Figure 10-2).

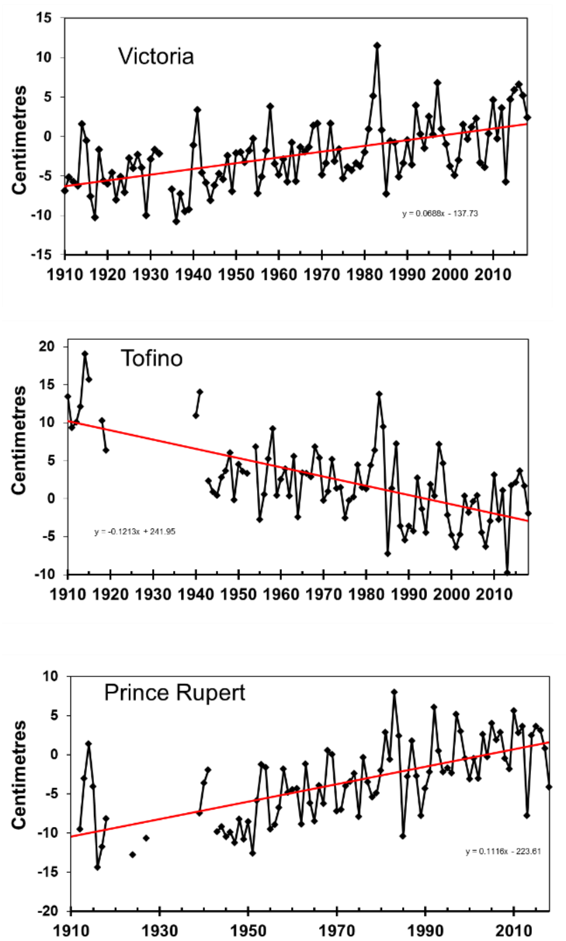

Figure 10-1.Annual-average sea level anomalies at three British Columbia ports. Reference years are 1981 to 2010. Average linear trends are plotted as red lines

The land is also rising at Victoria and Prince Rupert although not at the same rate as at Tofino. When this movement is removed at Victoria the linear trend becomes 12 cm per 100 years and at Prince Rupert the linear trend becomes 15 cm per 100 years.

The linear sea level rise trend at each port corrected for vertical land movement (in cm/century):

Prince Rupert	+15.0
Victoria	+12.0
Tofino	+6.9

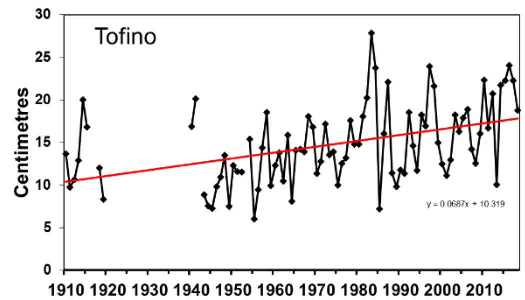

Figure 10-2. Annual-average sea level anomalies at Tofino with vertical land movement removed. Reference years are 1981 to 2010.

Global sea levels rose by 17± 5 cm in the 20th century (Church et al. 2011). The Intergovernmental Panel on Climate Change (IPCC 2014) predicts sea level to rise from 26 to 55 cm to 45 to 82 cm toward the end of the 21st century, depending on levels of mitigation of CO_2 emissions, but recent observations of ice melt in Greenland and Antarctica suggest these projections might be too low. Therefore, we can expect to observe greater rates of sea level rise in British Columbia in the future than we saw in the 20th century.

10.3. References

Church, J.A. and White N.J. 2011. Sea-level rise from the late 19th to the early 21st Century. Surveys in Geophysics.

IPCC. 2014: Climate Change 2014: Synthesis Report. Contribution of Working Groups I, II and III to the Fifth Assessment Report of the Intergovernmental Panel on Climate Change. Core Writing Team, R.K. Pachauri and L.A. Meyer (eds.). IPCC, Geneva, Switzerland, 151 p.

11. SEA SURFACE TEMPERATURE AND SALINITY OBSERVED AT LIGHTHOUSES AND WEATHER BUOYS IN BRITISH COLUMBIA, 2018

Peter Chandler, Fisheries & Oceans Canada, Institute of Ocean Sciences, Sidney, B.C., Peter.Chandler@dfo-mpo.gc.ca

11.1. Highlights

- The average annual sea surface temperature (SST) in 2018 (10.89°C) was generally warmer than in 2017 with a coast-wide average annual increase in SST of 0.14°C. Cooler conditions were observed at seven of the stations with an average decrease of 0.13°C, while the other 16 stations experienced a 0.25°C warming.
- Anomalies from the 30 year (1981-2010) sea surface temperature record show periodic warm and cold periods with durations of several years; 2018 is a continuation of a warm period starting in 2014, with a coast wide SST 0.46°C above the 30 year average.
- The long-term data from the light stations shows a linear trend to warmer coastal sea surface temperatures of 0.83°C over 100 years.
- Marine heat waves (using the Hobday et al. 2016 criteria) were evident in the SST records at several stations.
- Annual salinity observations showed an increase at eight of 11 stations with an average coast wide increase of 0.56 PSU (standard deviation of 0.80).

11.2. Description of the time series

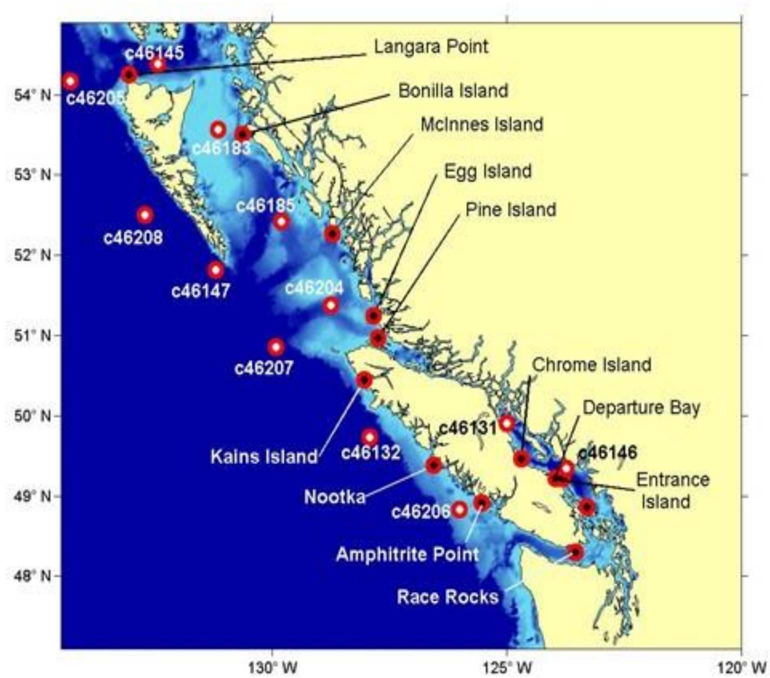

Figure 11-1. Red dots with black centers show the locations of 12 stations in the present shore station network. Red dots with white centers show the locations of 12 weather buoys in the Canadian weather buoy network. See table below for details.

Station	Years of data
Departure Bay	105
Race Rocks	98
Nootka	85
Amphitrite	85
Kains I	84
Langara	83
Entrance I	83
Pine Island	82
McInnes	65
Bonilla	59
Chrome I	58
Egg Island	49

Buoy ID	Buoy Location	Years of data
c46146	Halibut Bank	27
c46131	Sentry Shoal	27
c46206	La Perouse	31
c46132	South Brooks	25
c46207	East Dellwood	30
c46147	South Moresby	26
c46208	West Moresby	29
c46205	West Dixon	29
c46145	Central Dixon	28
c46204	West Sea Otter	30
c46185	South Hecate	28
c46183	North Hecate	28

Two sources of data are used to describe changes in sea surface conditions in the coastal waters of B.C. in 2018. As part of the DFO Shore Station Oceanographic Program sea surface temperature (SST) and salinity are measured daily at 12 shore stations, at the first daylight high tide. Most stations are at lighthouses (Figure 11-1), with observations taken by lighthouse keepers using a handheld electronic instrument (YSI Pro 30). The buoy data are provided by Environment and Climate Change Canada from a network of ODAS (Offshore Data Acquisition Systems) buoys that collect sea surface temperature hourly.

11.3. Status and trends

The lighthouse observations show that the annual average daily SST (Figure 11-2, upper panel) at all stations was generally warmer in 2018 than in 2017 (mean increase of 0.12°C, standard deviation of 0.12°C). The weather buoys data show an annual average daily increase of 0.15°C, standard deviation of 0.46°C). The coast wide SST is lower by 0.72°C compared to conditions in 2015 during the marine heat wave known as “the Blob”, but still warmer than the 30 year climatology (1981-2010) for the lighthouse data and (1991-2018) for the weather buoy data.

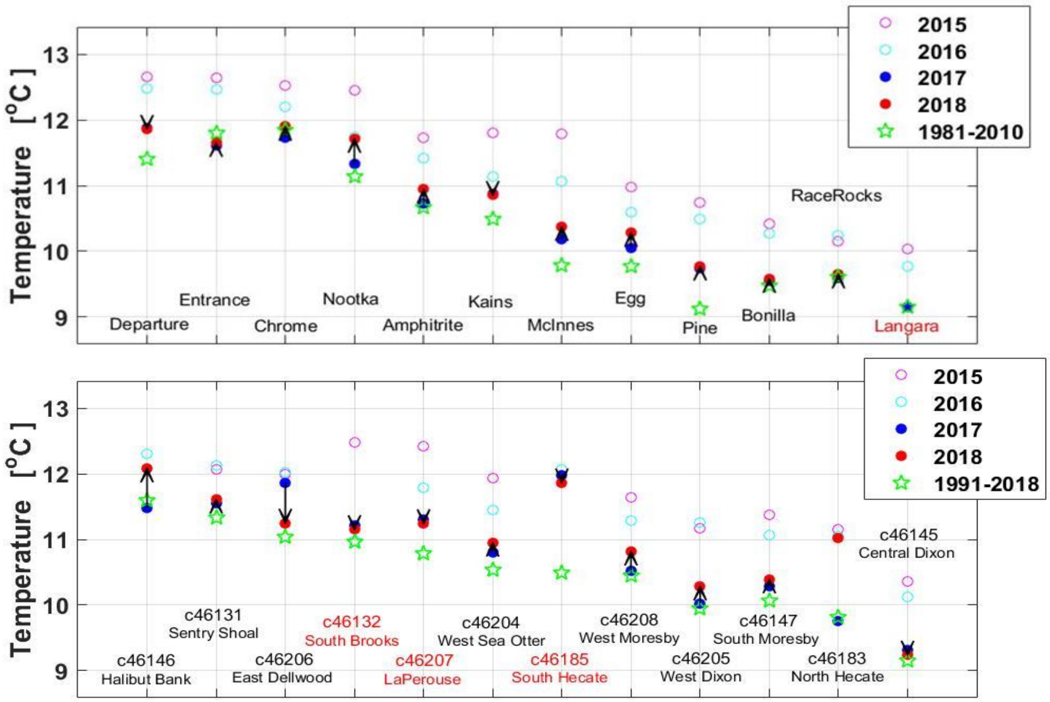

Figure 11-2. Upper pane: The average sea surface temperature in 2017 (dark blue dots), and 2018 (red dots) from daily observations at shore stations along the west coast of Canada. Lower panel: The average sea surface temperature from hourly observations at weather buoys along the west coast of Canada. The open circles show conditions in 2015 and 2016 when SST was significantly higher than normal, the stars represent the climatological mean annual temperature. Stations in red indicate uncertainty due to missing data in 2018.

Assuming a linear change over the entire data record, the time series of temperature at all of the shore stations show a warming trend at a 95% confidence level. Figure 11-3 shows a coast wide warming trend (using data from all light stations) as 0.83°C over 100 years. Figure 11-4 shows this warming at representative stations for each of three regions (North Coast, West Coast Vancouver Island, and the Strait of Georgia). A similar trend analysis applied to the salinity data (Figure 11-5) shows a continuing long-term trend toward less saline conditions.

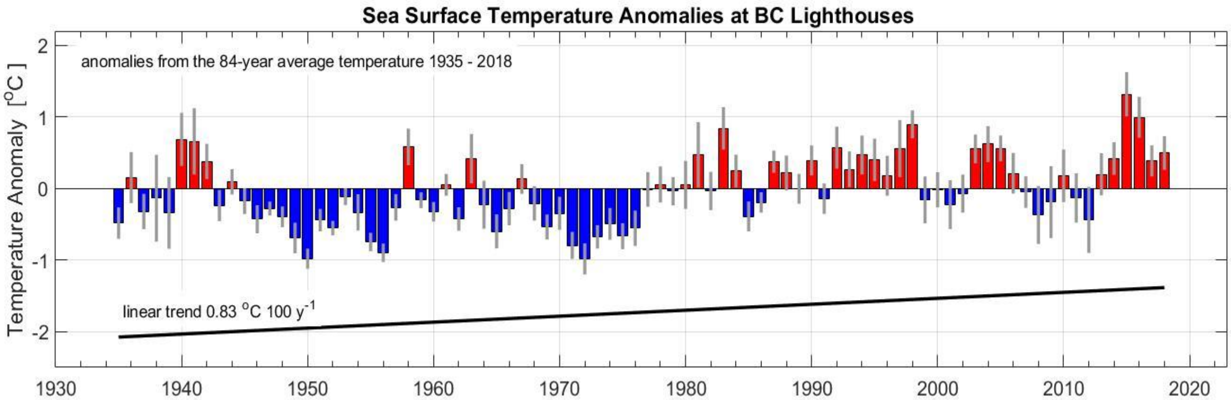

Figure 11-3. The trend in the annual temperature based on the observations of all lighthouses. The data shown are the anomalies from the long-term average temperature (1935-2018). The bars represent the anomalies averaged over all stations (a coast wide indicator), (red – above average, blue – below average.) and the vertical grey lines show the variability in the lighthouse data for each year.

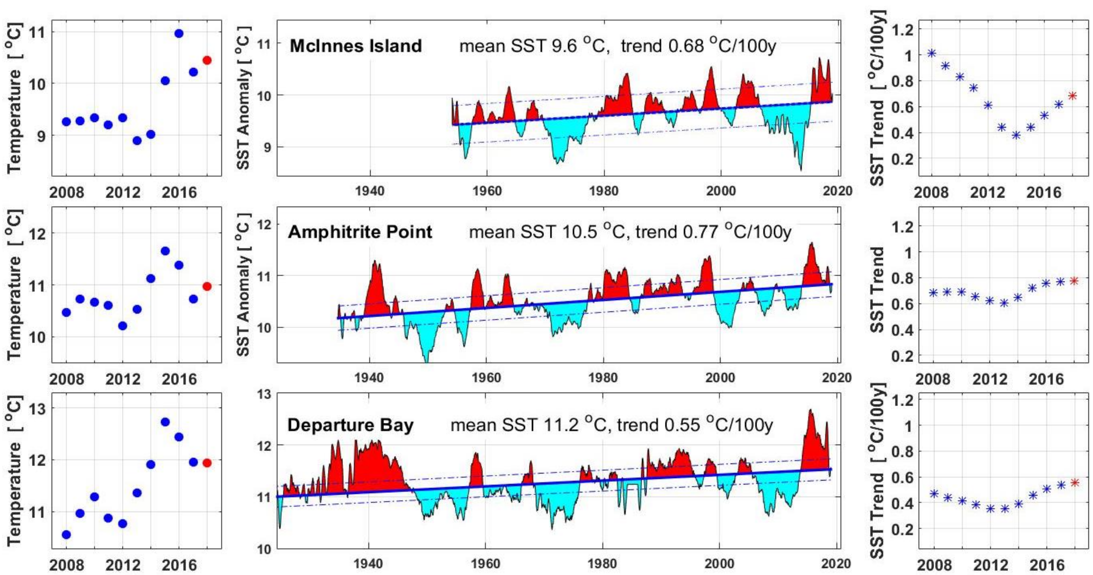

Figure 11-4. Time series of daily temperature observations, averaged over 12 months, at stations representing the North Coast, West Coast Vancouver Island and Strait of Georgia. Positive anomalies from the average temperature of the entire record are shown in red, negative in blue. The panel to the left shows the annual mean SST for the year shown on the x-axis. The panel to the right shows the slope of the trend lines calculated using only data up to the year shown on the x-axis.

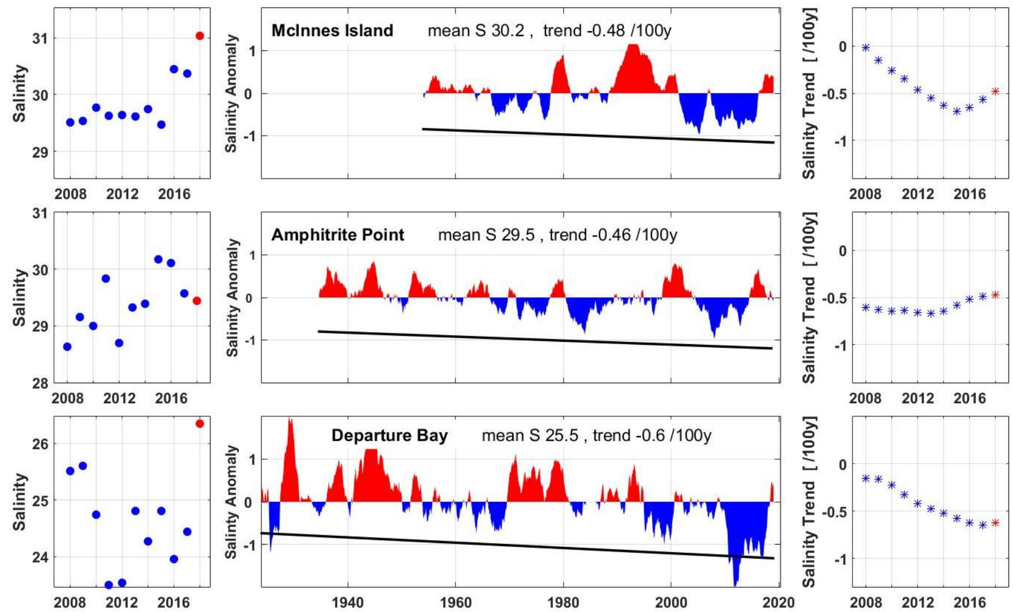

Figure11-5. As in Figure 11-4 for long-term time series of daily salinity observations.

11.4. Factors influencing trends

The sea surface temperatures in 2018 continue the period of warmer than normal water, similar to 2017 but not as warm as 2015-16. The transition from weak La Niña conditions to a weak El Niño during 2018 is reflected more so in the wave buoy data than in the near shore observed at the light stations.

The long-term temperature record shows that overlying the multi-year oscillations in the annual SST there remains a long-term trend towards rising ocean temperatures, and it is more pronounced in the semi-enclosed Strait of Georgia than along the outer coasts.

The long-term salinity observations show a trend to less saline conditions at most stations along the B.C. Coast. Variability in the salinity signal along the Pacific coast is governed by a combination of the integrated effects of atmospheric forcing and coastal precipitations; the Strait of Georgia data is strongly influenced by the discharge from the Fraser River (Cummins and Masson 2014).

11.5. Implications of these trends

The sea surface temperature and salinity are fundamental water properties defining the habitat of organisms that live in the upper waters of the ocean. The impacts of these changes to the water properties will depend on the time and space scales relevant to organisms of interest and are described for various trophic levels in B.C. waters in Galbraith and Young (section 16), and Hyatt et al. (section 41).

11.6. References

Cummins, P.F., and Masson, D. 2014. Climatic variability and trends in the surface waters of coastal British Columbia. Progress in Oceanography, 120: 279–290.

Hobday, A.J., Alexander, L.V., Perkins, S.E., Smale, D.A., Straub, S.C., Oliver, E.C.J., Benthuysen, J. A., Burrows, M.T., Donat, M.G., Feng, M., Holbrook, N.J., Moore, P.J., Scannell, H. A., Gupta, A.S., Wernberg, T. 2016. A hierarchical approach to defining marine heatwaves. Progress in Oceanography, 141: 227–238.

12. OXYGEN CONCENTRATION IN SUBSURFACE WATERS

Bill Crawford and Angelica Peña, Fisheries & Oceans Canada, Institute of Ocean Sciences, Sidney, B.C., Bill.Crawford@dfo-mpo.gc.ca, Angelica.Pena@dfo-mpo.gc.ca

12.1. Highlights

- Low concentrations of subsurface oxygen are normally observed on the continental shelf of southwest Vancouver Island in late summer. O_2 has been monitored regularly at Station LB08 in this region since 1979.
- O_2 at LB08 decreased from typical values of 65 µmol/kg in 1979 to very low values of 35 to 50 µmol/kg in 2006 to 2014. Higher concentrations were observed in 2016, attributed to warm, buoyant waters. However, with the intrusion of saltier, denser water in 2018, O_2 decreased to a very low concentration of about 35 to 40 µmol/kg.
- On the continental margin to about 700 km offshore, O_2 on constant density surfaces in the thermocline increased between the decades of 1950s to 1980s. O_2 has declined since then except for higher O_2 in 2014 to 2017 attributed to cooler fresher water. Farther offshore there has been a linear decrease since the 1950s, accompanied by an oscillation similar in period to the lunar nodal cycle of 18.6 years.

12.2. O_2 on the continental shelf

12.2.1. Continental Shelf

A plot of historical near-bottom O_2 in summer is presented in Figure 12-1. Symbols reveal locations where hypoxia was observed. Hypoxia is defined as O_2 less than 1.4 ml/L or 60 µmol/kg.) Many of these symbols are in inlets where deep seawater is naturally hypoxic due to low rates of inflow from outside waters.

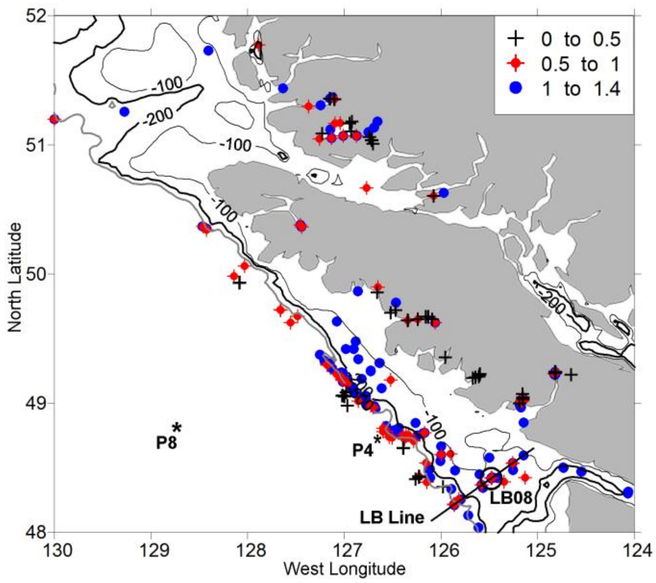

*Figure 12-1. Oxygen concentration (O_2, ml/L) in summer within 20 metres of the ocean bottom for regions of the continental shelf and slope where bottom depth is less than 1000 metres (1 ml/L = 43 μmol/kg). Each symbol represents a measurement by DFO research programs. Only observations with O_2 less than1.4 ml/L (60μmol/kg) are plotted. A black **O** denotes the location of Station LB08, where O_2 has been monitored for 40 years. LB Line is indicated by a black line through LB08. Stations P4 and P8 along Line P are also shown.*

On the continental shelf and slope, lowest O_2 values are found in deeper waters because O_2 decreases with increasing depth and increasing water density. Lowest O_2 on the shelf is off southwest Vancouver Island near sampling Line LB, the region of the B.C. coast where summer upwelling is strongest. Sampling programs have monitored oxygen concentration off SW Vancouver Island since 1979 and LB Line has been sampled regularly since the 1980s. Decreasing O_2 in subsurface waters is normally accompanied by increasing acidity. Both trends are of great concern to marine life.

The annual cycle of O_2 in near-bottom waters off SW Vancouver Island at Station LB08 in 145 metres of water is presented in Figure 12-2. This graph shows that O_2 is usually lowest between late August and early October (days 230 to 280). Although there is considerable year-to-year variability in O_2 for this season, one can see a decrease from higher O_2 in 1979 - 2005 to lower concentration in 2006 to 2018, excluding 2015. The highest ever late summer O_2 was 2.14 ml/L (92 μmol/kg) measured in early September 2015, attributed to “the blob” as mentioned in previous year’s reports. O_2 concentrations in late summer 2017 and 2018 were 0.80 and 0.86 ml/L (35 and 37 μmol/kg), respectively, very close to the record low of the entire 40-year series.

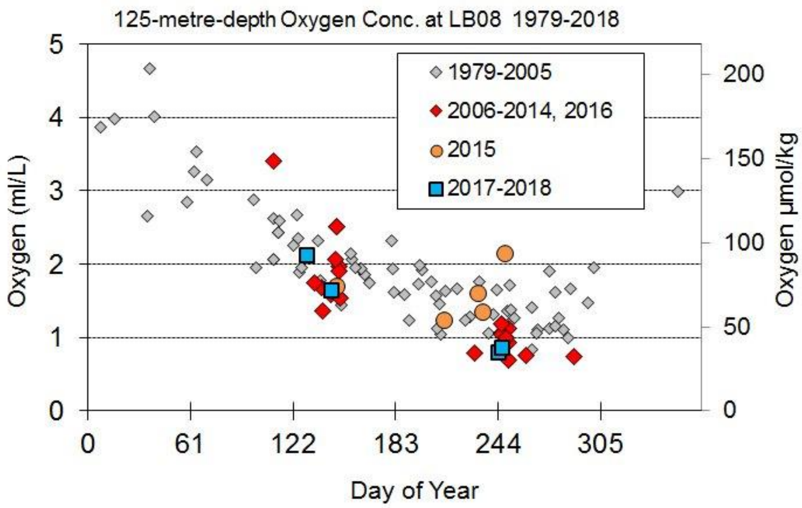

Figure 12-2. Oxygen concentration (O_2) at 125 m below ocean surface at Station LB08. Symbols represent observations, plotted on the day of the year the sample was collected. Day 244 is 1 Sept. Figure is based on Crawford and Peña (2013). See Figure 12-1 for location of LB08.

Over the period of 1991 to 2018 there was a tendency for lowest O_2 at LB08 in late summer to be in denser, saltier water, indicating that the low O_2 is possibly due to an increase in northward flow of Pacific Equatorial water along the continental slope from the south. Highest O_2 is usually found in fresher water that flows in from the west, so much of the variability in these years was due to different blends of these two water types. However, in years between 1979 and 1991 O_2 concentrations did not follow this pattern, and the overall decline in O_2 from 1979 to 2018 was due to a changing concentration of oxygen within these water masses.

Figure 12-3a shows cross-shelf contours of O_2 along LB Line averaged for the period of 2006 to 2018 (excluding 2015), corresponding to the recent era of low O_2 at LB08 shown in Figure 12-2. Lowest O_2 near bottom in Figure 12-3a is at LB07 and LB08, at about 40 km from Station LB01, which itself is very close to Vancouver Island. O_2 near bottom at these two stations was below 50µmol/kg. O_2 was higher at stations shoreward of about 40 km due to the oxygen-rich Vancouver Island Coastal Current that flows to the northwest here. The doming of O_2 contours near 40 km was due to the Juan de Fuca Eddy, centred at 40 km from LB01, and a southeastward flowing current centred over the outer end of the continental shelf at 80 km from LB01. Figure 12-3b shows O_2 in late summer 2018, when near-bottom O_2 was below the 2006-2018 average. Lower-than-average O_2 in near-bottom waters in 2018 extended from 20 to 80 km from LB01.

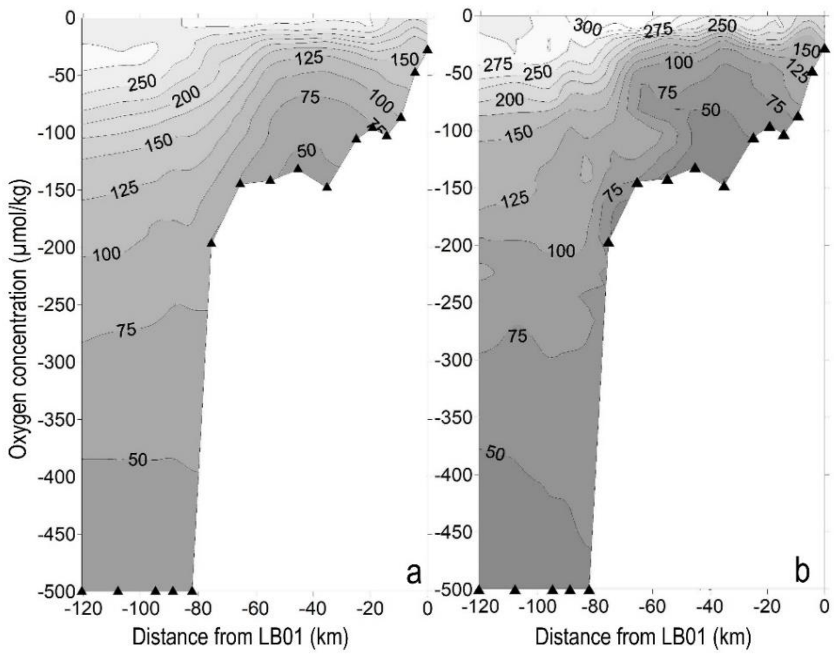

Figure 12-3. Oxygen concentration (O_2) on the continental shelf and slope along LB Line of sampling stations of southwest Vancouver Island. Contours show concentration in late summer for (a) average of years 2006 to 2018 (excluding 2015), and (b) 2018. LB01 is at the shoreward end of LB Line. See Figure 12-1 for location of LB Line.

12.3. Oxygen concentration in continental slope and offshore waters

There are few stations in offshore waters with regular sampling before 1980. To evaluate trends prior to 1980, we composited observations in areas around each of the intensive sampling stations along Line P and included all observations in archives. Details of this process and results to 2011 are described by Crawford and Peña (2016). Of the six main Line P stations that are intensively sampled, we present updates for Ocean Station P (OSP, also named P26) and for Station P8 in Figure 12-4 below. Station P8 lies on the outer continental slope in 2400 metres of water.

O_2 was calculated on constant density surfaces rather than at constant depths below surface, to allow inclusion of observations in all months of the year. The time series at OSP (Figure 12-4a) are updates of results presented by Whitney, Freeland and Robert (2007). Time series at P8 (Figure 12-4b) are an update of Crawford and Peña (2016).

Briefly, there is a general decrease in O_2 at OSP since 1956, modulated by an oscillation that fits to the 18.6-year lunar nodal cycle, a feature first noted by Whitney, Freeland and Robert (2007), who note that this variability might be due to advection of seawater from the western Pacific near Japan, where similar variability has been observed. O_2 at P8 was highest in about 1980 with lower concentration in the 1950s and 2000s, as defined by the solid curves for 26.7 and 27.9 density surfaces. O_2 changes over these six decades at OSP are similar to those at P20; O_2 changes in time at P8 are similar to those at P4 and P12. The transition region between these two types of variability lies near P16, which is also transited more often by Haida Eddies than other Line P stations, although a Haida Eddy hit P20 in June 2018.

Although O_2 in 2018 on all density surfaces at OSP and P8 was close to the fitted line and curves in Figure 12-4, oxygen concentrations in the two to five previous years were somewhat higher at OSP, and at P8 were much higher. These increases are attributed to colder fresher water advecting along the density surfaces, carrying more oxygen.

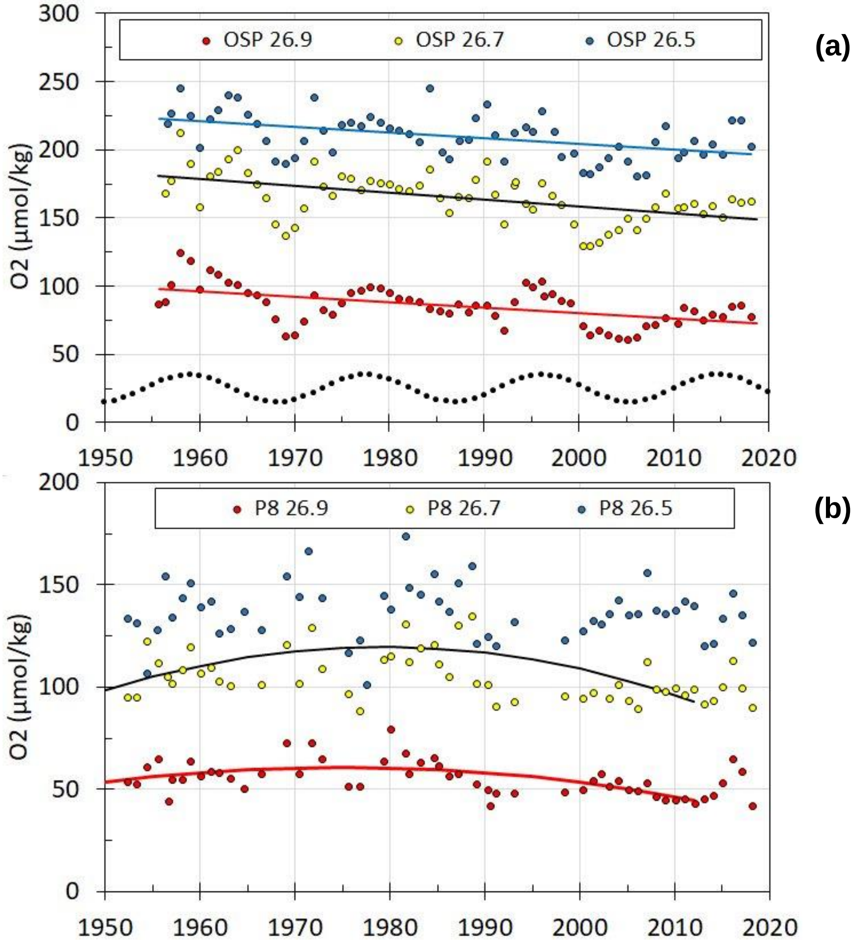

Figure 12-4. Annual average oxygen concentration (O_2) at (a) Ocean Station P (OSP) in offshore region, and (b) Station P8 near the continental slope. O_2 has been interpolated onto the constant density surfaces 26.5, 26.7, and 26.9, representing potential densities of 1026.5 to 1026.9 kg/m^3. Typical depths of these density surfaces are 140, 170 and 280 m at OSP, and 160, 250 and 410 at P8. Trends at OSP are -0.4 µmol kg^{-1} y^{-1} *on the 26.5 and 26.9 surfaces, and -0.5 µmol kg^{-1} y^{-1} on the 26.7 surface.*

12.4. References

Crawford, W.R. and Peña, M.A. 2016. Decadal trends in oxygen concentration in subsurface waters of the Northeast Pacific Ocean. *Atmosphere-Ocean* 54(1), 171-192 doi.org/10.1080/07055900.2016.1158145.

Crawford, W.R. and Peña, M.A. 2013. Declining oxygen on the British Columbia continental shelf. *Atmosphere Ocean* 51(1), 88–103. doi:10.1080/07055900.2012.753028.

Whitney, F.A., Freeland, H.J. and Robert, M. 2007. Persistently declining oxygen levels in the interior waters of the eastern subarctic Pacific. *Progress in Oceanography* 75, 179–199, doi:10.1016/j.pocean.2007.08.007.

12.5. Acknowledgements

Analysis of O_2 on constant density surfaces was undertaken by Nick Bolingbroke. We are also grateful for the Line P and La Perouse Programs of DFO, managed respectively by Marie Robert and Doug Yelland, as well as data quality and archiving by Germaine Gatien and Di Wan of DFO. The Marine Environmental Data Service of DFO Ottawa, and NOAA National Centers for Environmental Information (formerly NODC) also provided data for observations on constant density surfaces.

13. SATELLITE OBSERVATIONS OF B.C. WATERS

Jim Gower[1] and Stephanie King[2]

[1]Institute of Ocean Sciences, Fisheries and Oceans Canada, North Saanich, B.C., Jim.Gower@dfo-mpo.gc.ca

[2]Sea This Consulting, Nanaimo, B.C., currently with Pentair Aquatic Ecosystems King, Stephanie.King@Pentair.com

13.1. Highlights

- Global indicators show accelerating climate change with an increased rate of carbon emissions in 2018.
- A major *Heterosigma* bloom was observed in the Strait of Georgia, Juan de Fuca Strait and off Barkley Sound in June and July 2018.
- Bright blooms, assumed to be Coccolithophores, were observed off the west coast (14 to 24 May), and in Nitinat Lake and in higher concentrations in SE Alaska (inlets of Prince of Wales Island) and in Washington State (Hood Canal), all in the same period (20 July to 5 August 2018).
- Spring bloom in the Strait of Georgia occurred on 8 March 2018 in the central Strait, preceded by a strong bloom in Sechelt Inlet. Spring bloom occurred 10 March 2018 in the northern Strait.

13.2. Description of the time series

The "Keeling curve" (ftp://aftp.cmdl.noaa.gov/products/trends/co2/co2_mm_mlo.txt) shows carbon dioxide concentrations in the earth's atmosphere since measurements began in 1957. These have grown at an accelerating rate expressed by CO_2(ppmv)=301.4+0.0123(Year-1925.7)^2. As one response, the global average sea level measured by satellite altimetry from 1993 to 2018 (https://www.aviso.altimetry.fr/en/data/products/ocean-indicators-products/mean-sea-level.html), has risen according to: Level (cm) = exp(0.0285(Year-1920)).

The *Heterosigma* bloom was detected using global composite images provided to us by the European Space Agency (Gower et al. 2008) from image data collected by the MERIS imager (2002 to 2012) and the follow-on OLCI imager since 2016. These two instruments are the only global systems providing measurements in the 709nm spectral band where surface slicks of Heterosigma give a characteristic peak signal, measured by the MCI (Maximum Chlorophyll Index).

Bright Coccolithophore blooms give a strong signal measured by many satellite imaging systems. NASA's Worldview (https://worldview.earthdata.nasa.gov/) provides a convenient display.

Spring bloom timing has been measured with MODIS and Sentinel 3A satellite imagery, with in-situ fluorometers mounted on BC ferries along ferry routes from Nanaimo to Tsawwassen and Horseshoe Bay by Oceans Networks Canada, and on surface weather buoys 46131 (northern Strait) and 46146 (central Strait).

13.3. Status and trends

In 2018, Keeling measurements of carbon dioxide concentration moved above the long-term average curve, indicating an even faster increase in emissions (Figure 13-1), in spite of global plans for reductions. As one response, the sea level measured by global satellite altimetry from 1993 to 2018 (https://www.aviso.altimetry.fr/en/data/products/ocean-indicators-products/mean-sea-level.html) fits the exponential relation.

The *Heterosigma* bloom in 2018 was first observed in Sentinel 3a satellite imagery using the MCI index, spreading from the waters of the Fraser River plume on 29 May 2018 and covering larger areas of the Strait of Georgia on 4, 9, 10 June. In the next cloud-free period, images showed the bloom off Barkley Sound and no longer in the Strait of Georgia on June 16, 17, (Figure 13-2), then no bloom on July 2,3, then bloom again off Barkley Sound on July 10, 14, 21, 22, 25 in a pattern similar to Figure 13-2.

Bright Coccolithophore blooms were visible in the inlets of Prince of Wales Island and of the mainland, north of Dixon Entrance, from 20 July to 5 August 2018. Nitinat Lake in BC and the Hood Canal in Washington State were bright for this same period. Figure 13-3 shows a Sentinel 3 image of 560nm – 865nm radiance difference from Prince of Wales Island in pseudocolour on 28 July. Patches of bright water occurred west of Vancouver Island from 14 to 24 May 2018.

Near-surface chlorophyll concentrations in the Strait of Georgia were monitored in 2018 by satellites and fluorometers on ferries and weather buoys. Images and instruments gave consistent start dates for the spring bloom, 8 March 2018 in the central Strait preceded by a strong bloom in Sechelt Inlet, 10 March 2018 in the northern Strait.

13.4. Factors influencing trends

Emissions from burning fossil fuels have raised carbon dioxide levels in the atmosphere from 280ppmv in pre-industrial times (before about the year 1850) to 410 today, with doubling expected by about the year 2070. The resulting sea level rise will soon have dramatic effects in many parts of the world, especially if the exponential rise rate continues. This may finally result in determined global action to reduce emissions. Associated warming will also cause significant changes. Harmful and other blooms are expected to become more common as ocean temperatures warm and nutrient flow into coastal waters continues to increase.

The spring bloom in the Strait of Georgia was again relatively early, with a bloom in Sechelt Inlet that may have seeded the start of the bloom in the Strait.

13.5. Implications of these trends

Climate change is a global problem which is accelerating in the absence of concerted action to reduce carbon emissions. The change affects almost all aspects of the present SOPO report. Sea level rise is resulting in increased coastal erosion in many areas locally, a trend which is expected to increase.

Heterosigma blooms in 2018 caused significant harm to farmed salmon in 2018. An increase in the frequency of such blooms would affect the economics of aquaculture, perhaps leading to a shift towards farms on land.

Coccolithophore blooms do not themselves cause harm, but they provide an indication of bloom activity in ocean and coastal waters. Any change implies a change in water properties, perhaps associated with global climate change, which needs to be understood.

Timing of the spring bloom in the Strait of Georgia is known to be important for migrating juvenile salmon. The importance of seeding from blooms in inlets in affecting this date is still undetermined and requires modelling with high spatial resolution.

13.6. References

Gower, J.F.R., King, S.A., and Goncalves, P. 2008. Global Monitoring of Plankton Blooms Using MERIS MCI. Int. J. Remote Sensing 29: 6209–6216. doi:10.1080/01431160802178110.

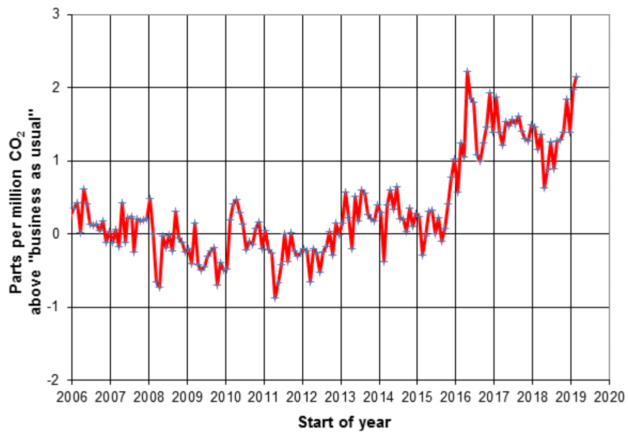

Figure 13-1. Concentration of carbon dioxide in the earth's atmosphere after removing the annual cycle and the constantly accelerating "business as usual" trend. The residual (shown) is less than 1ppm except for a brief period near the eruption of Mt Pinatubo in 1991 and years since 2016. In 2018 the residual climbed again, and is now over 2ppm.

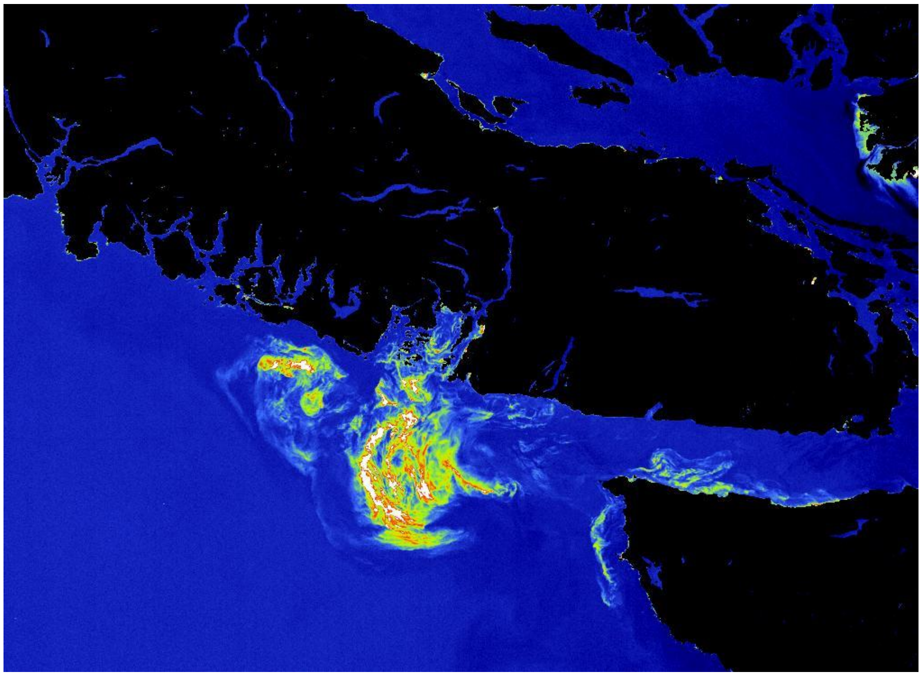

Figure 13-2. Water with high MCI signal off the mouth of Juan de Fuca Strait on June 16 2018. This was confirmed as due to Heterosigma based on water samples collected in the Strait of Georgia, the Strait of Juan de Fuca and off Barkley Sound in June, July and September.

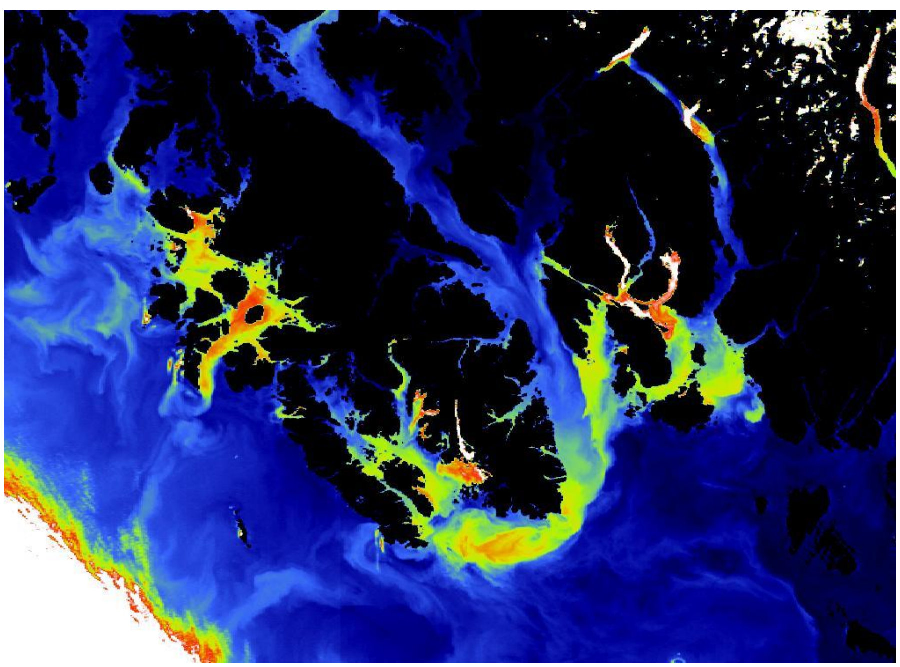

Figure 13-3. Sentinel 3 OLCI image of 560nm - 865 nm radiance difference showing bright water in inlets of Prince of Wales Island and the mainland, on 28 July 2018. Cloud gives a high difference signal at lower left.

14. PHYTOPLANKTON IN SURFACE WATERS ALONG LINE P AND OFF THE WEST COAST OF VANCOUVER ISLAND

Angelica Peña and Nina Nemcek, Fisheries & Oceans Canada, Institute of Ocean Sciences, Sidney, B.C., Angelica.Pena@dfo-mpo.gc.ca, Nina.Nemcek@dfo-mpo.gc.ca

14.1. Highlights

- There was an unusual increase in phytoplankton biomass and diatom abundance in the transition region of Line P in the spring of 2018.
- Surface nutrient concentrations in spring and summer of 2018 were among the lowest on record along the transition region of Line P. In particular, spring silicate values were lower than those observed during "the Blob" and consistent with the increase in diatoms.
- On the continental shelf of the west coast of Vancouver Island nitrate concentrations, phytoplankton biomass and community composition in May and September 2018 were within the range of values from previous years.

14.2. Description of the time series

Monitoring changes in phytoplankton biomass and community composition is important for the evaluation of ecosystem function and status, as well as for the study of biogeochemical cycles. Phytoplankton community composition, chlorophyll-a ("chl-a", an indicator of phytoplankton biomass) and nutrients are measured on DFO cruises three times a year in February, June, and August/September along Line P in the northeast subarctic Pacific, and twice a year in May/June and early September on the La Perouse cruise off the west coast of Vancouver Island. Sampling for phytoplankton composition has been carried out at most of the stations along Line P (Figure 14-1a) since June 2010. Phytoplankton sampling along a series of transects on the west coast of Vancouver Island (Figure 14-1b) has been carried out since 2011. Sampling along the west coast was extended farther north in 2017.

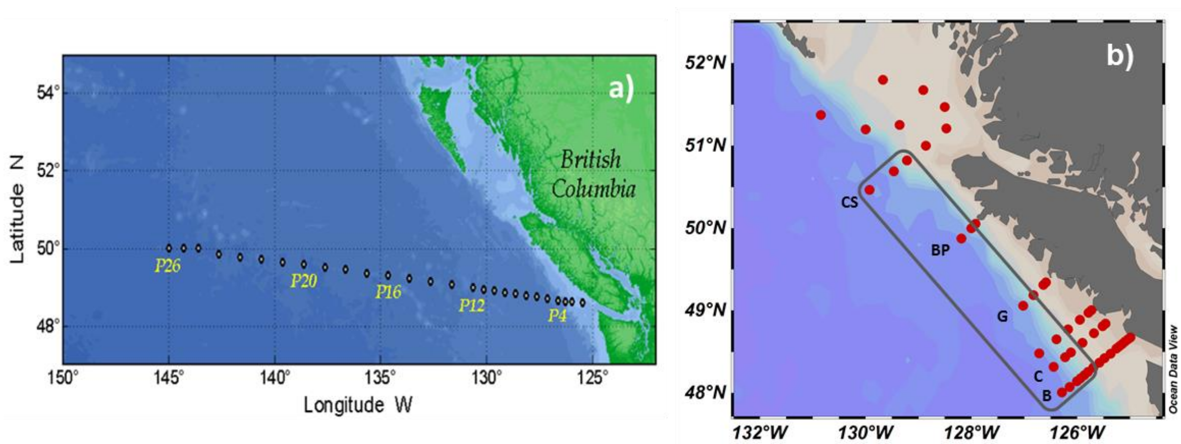

Figure 14-1. Location of sampling stations: a) along Line P, and b) on the west coast of Vancouver Island showing the outer coast stations (inside the grey rectangle) and continental shelf stations.

The abundance and composition of phytoplankton are determined from phytoplankton pigments (chlorophylls and carotenoids) analyzed by high performance liquid chromatography (HPLC) as described in Nemcek and Peña (2014). The HPLC pigment data are processed using a factorization matrix program (CHEMTAX) to estimate the contribution of the main taxonomic groups of phytoplankton to total chl-a (Mackey et al. 1996).

14.3. Status and trends

Nutrient concentrations in surface waters are usually high (>5 mmol m^{-3}) and chlorophyll concentrations low (<0.5 mg m^{-3}) year-round in the Fe-poor haptophyte-dominated offshore waters, whereas high seasonal variability in nutrient concentrations and phytoplankton biomass occurs towards shore. In 2018, spring and summer surface nutrient values were among the lowest on record in the central portion of Line P (Figure 14-2) with silicate values in spring being lower than those observed during the Blob that restricted winter nutrient renewal in 2014/15 due to increased stratification. Similarly, there was an increase in chlorophyll concentrations in the spring of 2018 in the transition region of Line P (Figure 14-2) but summer concentrations were within the range of values from previous years.

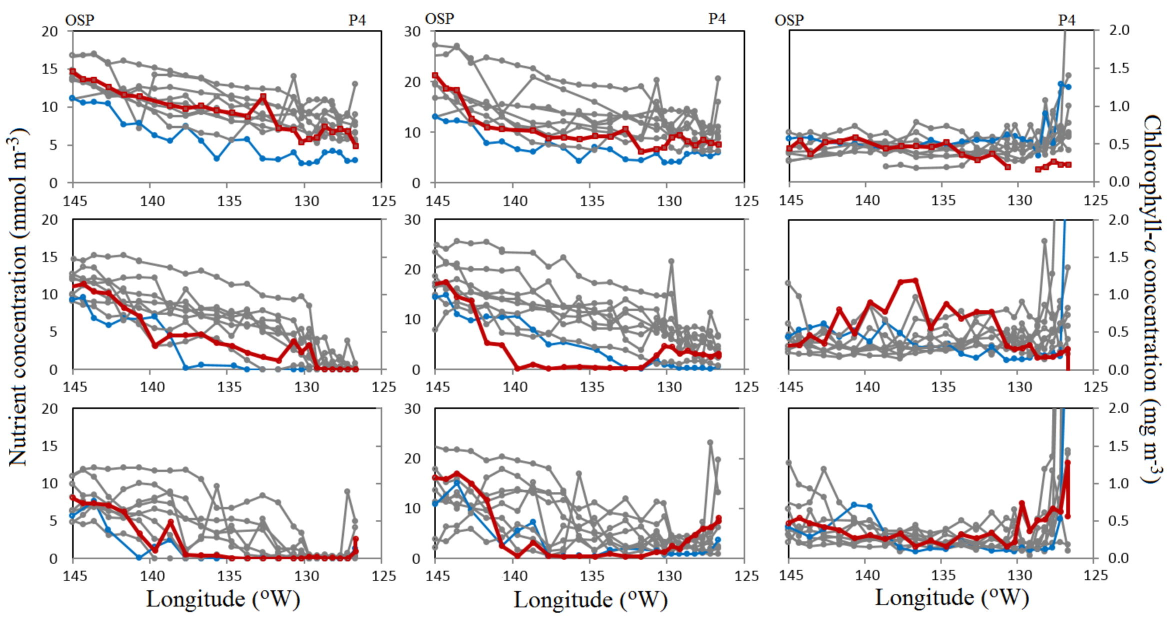

Figure 14-2. Nitrate (left panels, mmol m^{-3}), silicate (center panels, mmol m^{-3}), and chlorophyll-a (right panels, mg m^{-3}) in surface waters along Line P from P4 to OSP in winter (top panels), spring (middle panels) and summer (bottom panels) of 2009 to 2018. Data for 2018 are shown in red and for 2015 in blue.

Phytoplankton assemblage composition showed an unusual increase in the relative abundance of diatoms at most stations along Line P in June 2018, consistent with the decrease in silicate concentration. By August 2018, phytoplankton composition was in general similar to the composition observed in previous years, with haptophytes dominating phytoplankton biomass at most stations (Figure 14-3).

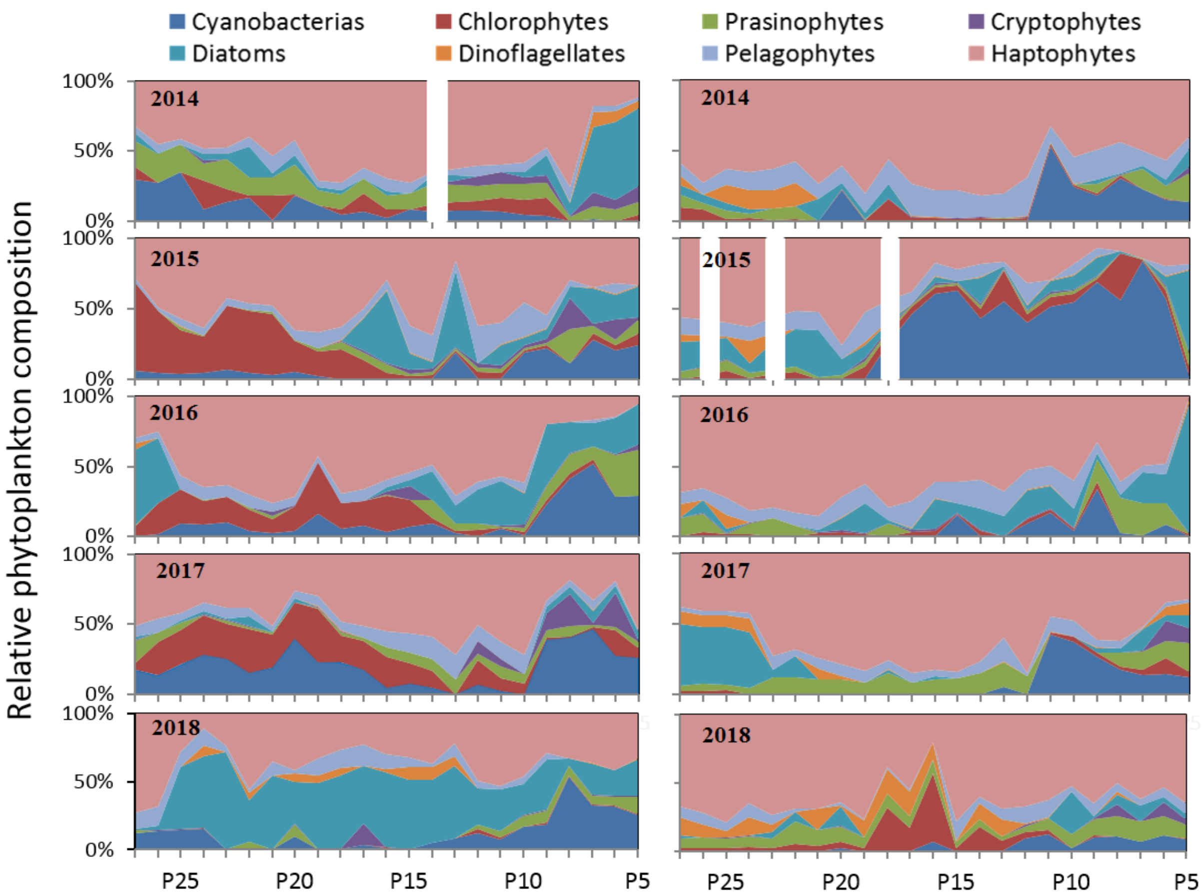

Figure 14-3. Relative phytoplankton composition in the upper layer at stations along Line P (see Figure 14-1) in June (left panels) and Aug./Sept. (right panels) of 2014 to 2018.

Nutrient and chl-a concentrations are highly variable in surface waters off the west coast of Vancouver Island. On the continental shelf, surface nutrient concentrations are usually lower in May compared to September. Chl-a is usually high (>5 mg m^{-3}) on the continental shelf off southern Vancouver Island where blooms of phytoplankton (>20 mg m^{-3} chl-a) are often observed in May and/or September. At stations beyond the continental shelf (outer coast), chl-a and nutrient concentrations are usually lower than on the continental shelf. In 2018, nitrate concentrations in May and September were within the range of values observed in previous years (Figure 14-4). Chl-a concentrations in May and September of 2018 were within the range of values observed in previous years, and show a bloom of phytoplankton off Juan de Fuca Strait in May and an off Brook Peninsula in September (Figure 14-4).

Diatoms usually dominate phytoplankton biomass at the ocean surface along the continental shelf although dinoflagellates are found to occasionally dominate in September (Figure 14-5). At the outer coast stations beyond the continental shelf phytoplankton community composition is more diverse and variable than on the continental shelf, with dinoflagellates, diatoms, haptophytes and cryptophytes dominating at times and far fewer diatoms than seen on the coast.

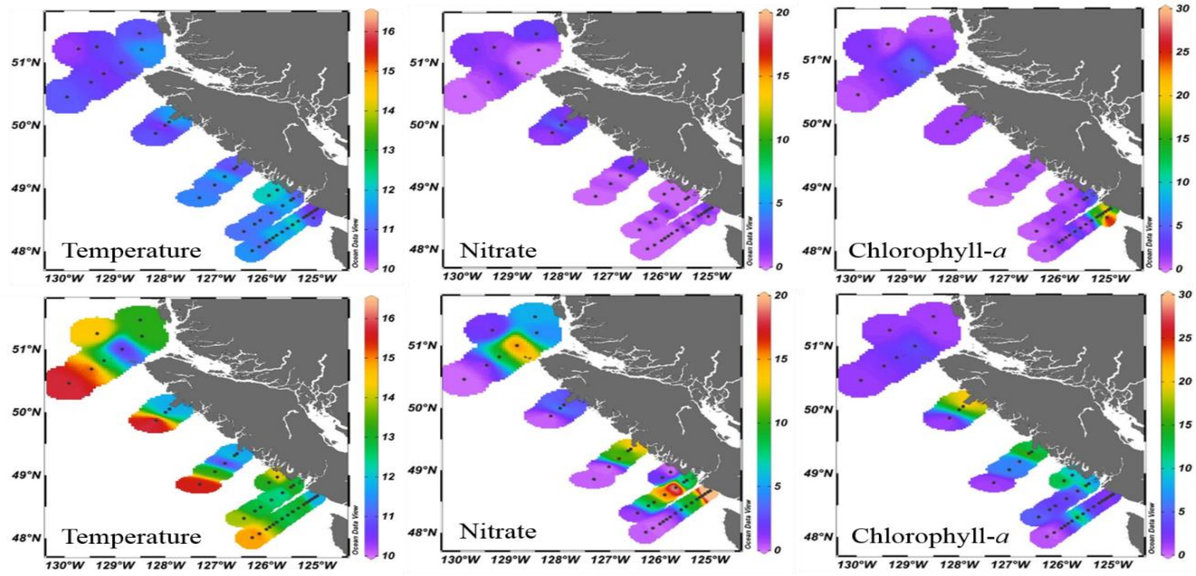

Figure 14-4. Temperature (°C), nitrate (mmol m^{-3}) and chlorophyll-a (mg m^{-3}) at 5 m depth over the study area in May (top row) and Sept. (bottom row) of 2018.

In May 2018, as in previous years, diatoms dominated the phytoplankton biomass on the continental shelf. In the outer coast, phytoplankton biomass was in the lowest range and a mixed population was observed similar to most previous years. In September 2018, phytoplankton biomass and community composition in the continental shelf and outer coast were similar to previous years.

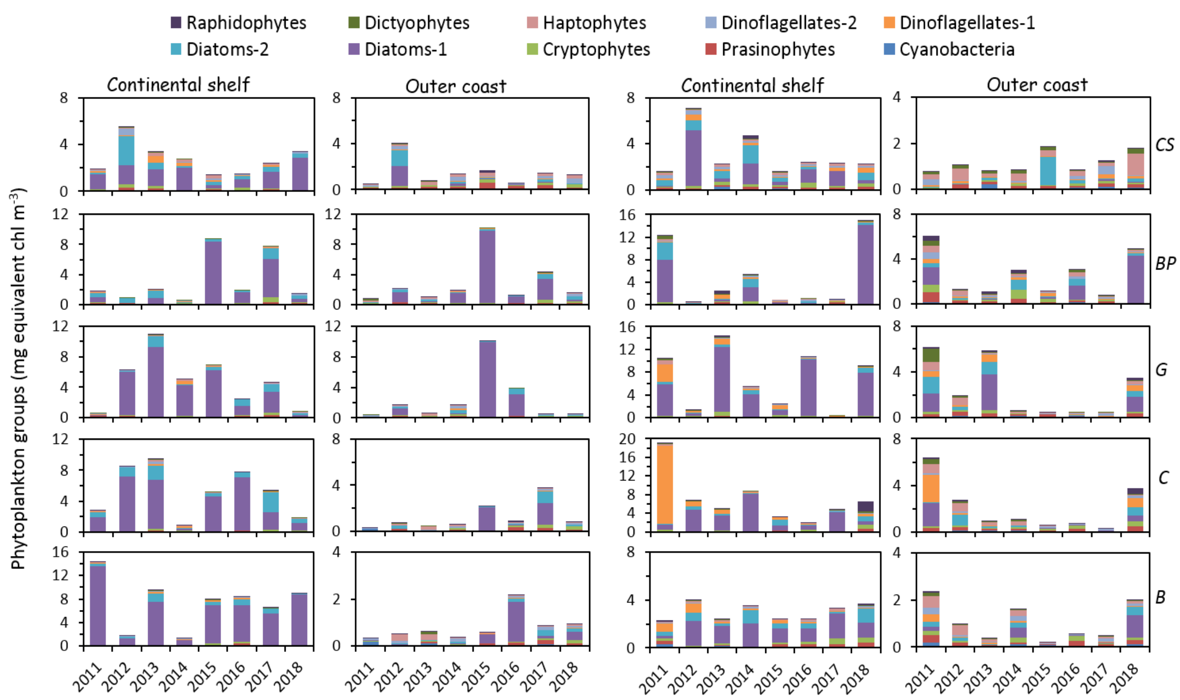

Figure 14-5. Time-series of mean phytoplankton composition at the surface at stations on the continental shelf and outer coast for Line B, C, G, BP and CS (see Figure 14-1) in May (left panels) and September (right panels).

14.4. Factors influencing trends

Several environmental factors including temperature, irradiance and nutrient availability, as well as grazing pressure determine phytoplankton abundance and community composition. The observed changes in phytoplankton abundance and composition along Line P during the Blob years were likely in response to the increase in surface temperature and changes in nutrient availability (Peña et al. 2019). The observed sporadic increases in phytoplankton biomass and diatoms at the most offshore stations of Line P in the last two years and in the transition region of Line P in June 2018 are likely related to changes in subsurface nutrient remineralization as well as grazing pressure after the Blob. In coastal regions, such as the west coast of Vancouver Island where environmental conditions fluctuate rapidly, our sampling frequency (twice a year) is not adequate to study year-to-year variability in phytoplankton since the observed differences in chl-a concentrations and phytoplankton composition could be as much due to intra-seasonal as to inter-annual variability. To be able to compare among years, frequent (daily to bi-weekly) observations would be necessary depending on the time of the year.

14.5. Implications of trends

Phytoplankton abundance and community composition are key factors influencing trophic processes and biogeochemical cycles in the ocean. Organic matter produced by phytoplankton is continuously transferred from lower to higher trophic levels, so the abundance, composition and distribution patterns of phytoplankton ultimately affect the sustainability of all marine life. The observed changes at the base of the food web could have ecosystem-wide implications. It is unclear, however, how fast phytoplankton can adapt to environmental conditions and how reversible these responses are.

14.6. References

Mackey, M.D., Mackey, D.J., Higgins, H.W., and Wright, S.W. 1996. CHEMTAX-a program for estimating class abundance from chemical markers: application to HPLC measurements of phytoplankton. Mar. Ecol. Prog. Ser. 144: 265-283.

Nemcek, N., and Peña, M.A. 2014. Institute of Ocean Sciences Protocols for Phytoplankton Pigment Analysis by HPLC. Can. Tech. Rep. Fish. Aquat. Sci. 3117: x + 80 p.

Peña, M.A., Nemcek, N. and Robert, M. 2019. Phytoplankton responses to the 2014–2016 warming anomaly in the Northeast Subarctic Pacific Ocean, Limnology and Oceanography, 64, 515-525, doi: 10.1002/lno.11056.

15. LOWER TROPHIC LEVELS IN THE NORTHEAST PACIFIC

Sonia Batten, Marine Biological Association, UK, c/o 4737 Vista View Cr, Nanaimo, BC, V9V 1N8, Sonia.Batten@mba.ac.uk

15.1. Highlights

- Abundance anomalies of diatoms and zooplankton were not unusual in 2018, but this overlooks changes in community composition that may be of note.
- Phytoplankton community composition was consistent with low nutrient conditions offshore.
- Shelf zooplankton contained high numbers of larval life stages of benthic invertebrates.
- Large copepods were observed in low numbers offshore and on the shelf.
- There was still a bias towards warm-water taxa in both phytoplankton and zooplankton.

15.2. Sampling

Sampling from commercial ships towing a Continuous Plankton Recorder (CPR) occurred approximately monthly 6-9 times per year between March and October in the NE Pacific (Figure 15-1) continuing a time series begun in 2000. Each CPR sample contained the near-surface (about 7 m depth) plankton from an 18.5 km length of transect, filtered using 270 µm mesh, and afterwards analysed microscopically to give taxonomically resolved abundance data. Data to July 2018 have been finalised at the time of writing and are included here.

15.3. Description of the Plankton Time Series

15.3.1. Phytoplankton

The CPR effectively retains larger phytoplankton cells, especially chain forming diatoms and hard-shelled dinoflagellates, and several time series are generated which reflect abundance and community composition changes: i) Time series of seasonal (spring, summer and autumn) diatom abundance anomalies are calculated for each region. ii) Broad community composition in spring (March to June) is also calculated for each region and each year as the proportion of the cells comprising centric diatoms, rod-like diatoms (includes pennate taxa and long, narrow centric taxa), dinoflagellates and “others”. iii) Detailed community composition, including all taxa recorded from the samples, as the mean annual (in this case March to July) Community Temperature Index (CTI) is calculated for each region using each taxon’s mean abundance and Species Temperature Index (STI; calculated as the mean temperature the taxon was found at in all CPR samples with in situ temperature recorded so that taxa found in warmer waters have a higher STI than taxa found in colder waters).

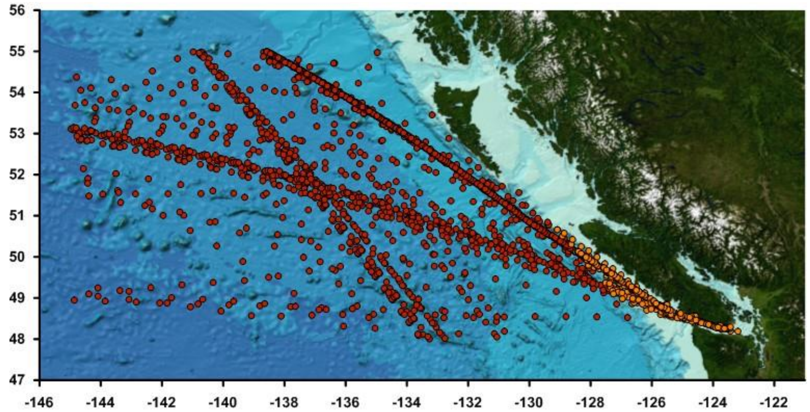

Figure 15-1. Map showing the location of the samples (2000 - 2018) averaged for the two regions described in this report. Red samples (n=2,045) are offshore, orange samples are from the shelf and slope (n=557). Note that for the shelf region only June was sampled in 2000-2003.

15.3.2. Zooplankton

Mesozooplankton, especially crustacea, are well sampled by the CPR and several zooplankton time series are generated: i) seasonal anomalies of total zooplankton abundance (spring, summer and autumn). ii) Broad community composition in spring (March to June) of major zooplankton groups. iii) Annual mean CTI for all the zooplankton taxa (again, March to July) for each region (calculated as described above for the phytoplankton CTI).

15.4. Status and Trends

15.4.1. Phytoplankton

The seasonal diatom anomalies revealed that in 2018 spring diatoms were quite low in the offshore but positive in the shelf region, but the reverse was true for the summer with mild anomalies in both regions. When combined they show that diatoms in 2018 were near neutral in terms of abundance.

The broad community composition shown in Figure 15-2 however, suggests that in the offshore the relative abundance of the rod-like diatoms was relatively high in 2018, second only to 2015. Their high surface area relative to their volume makes these cells efficient at taking up nutrients and they tend to do better than centric diatoms in low nutrient conditions. Winter mixing was quite low in 2018 (Ross and Robert, section 6) and nutrients along Line P were also low (Peña and Nemcek, section 14) so that the 2018 spring conditions were almost as challenging for lower trophic levels as in 2015. The shelf phytoplankton were also still showing a “warm” community composition in 2018, though not as dramatically as in 2014-15 with a similar broad composition to 2016-17.

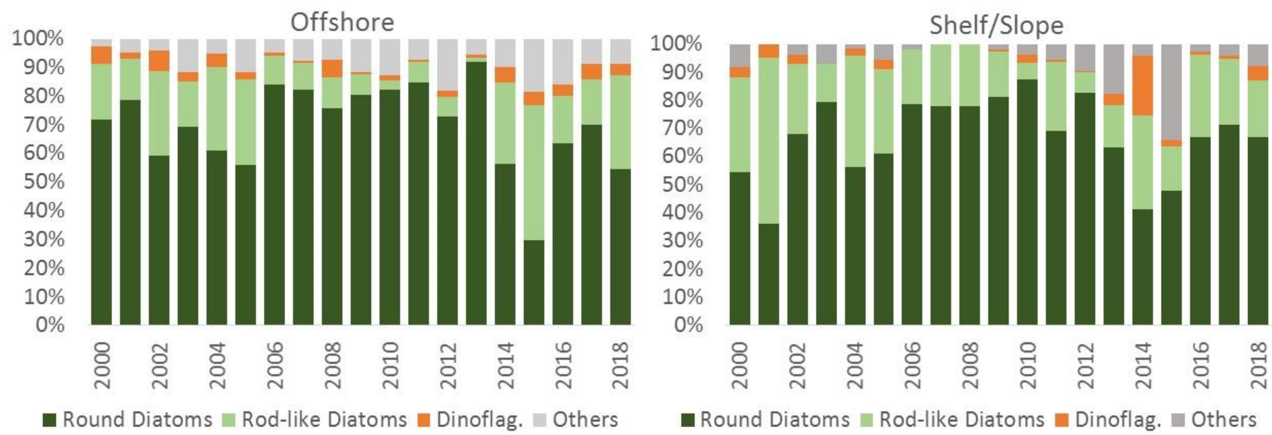

Figure 15-2. Contribution of each group to the mean March-June phytoplankton community.

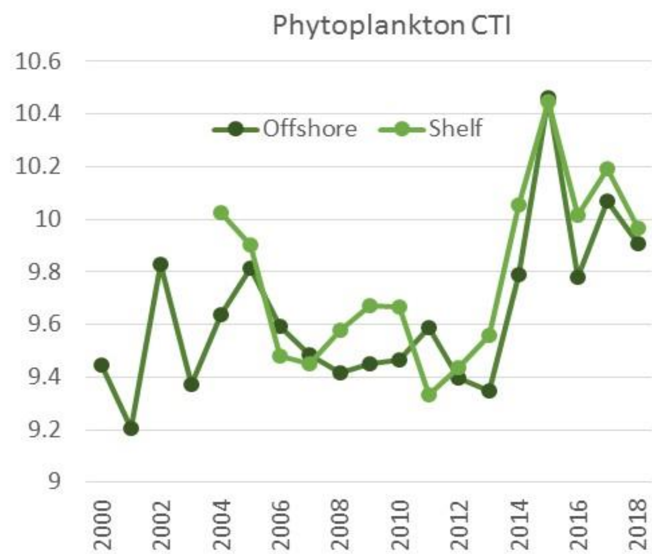

Figure 15-3. The mean annual phytoplankton Community Temperature Index (Mar-July) for each region.

This is also evident in Figure 15-3 where the Community Temperature Indices are shown. Both offshore and shelf regions show similar trends in CTI; warmer communities in 2004 and 2005, cooler communities in the 2007 to 2012 period before reaching a maximum in 2015. The values for 2018 are not as high as 2015, but in both regions are still higher than the pre-heat wave period.

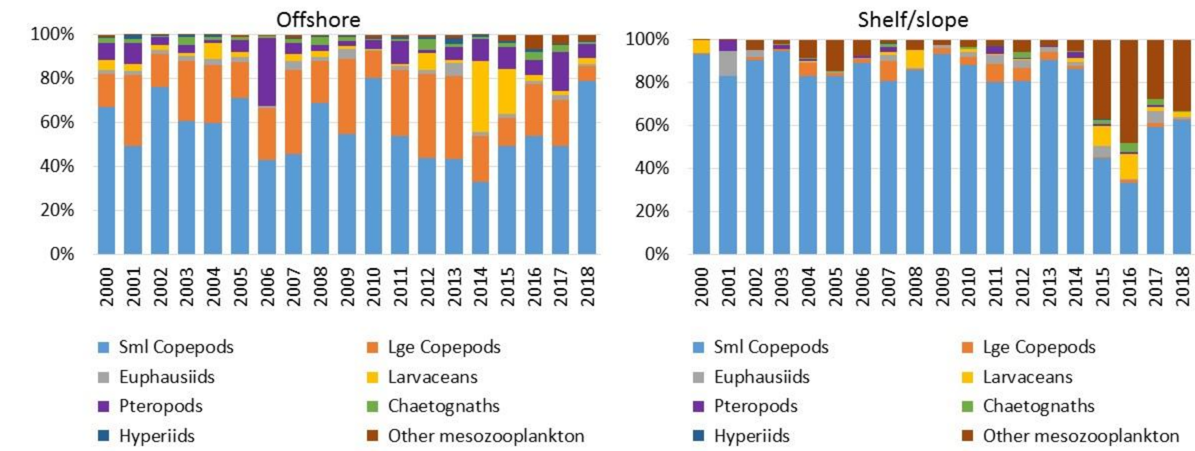

Figure 15-4.Spring (Mar-June) zooplankton broad community composition for each region.

15.4.2. Zooplankton

The seasonal anomalies of total zooplankton abundance were slightly positive for both regions in 2018 (not shown) but not unusual. Broad community composition shown in Figure 15-4 reveals that spring 2018 offshore had the lowest proportion (and number) of large copepods and the highest of small copepods in the time series. Other groups were at average abundances.

In the shelf/slope region, 2018 saw a continuation begun in 2015, of a greater contribution by “other” mesozooplankton which are principally the larval forms of benthic invertebrate species (i.e. meroplankton) such as barnacle, echinoderm and decapod larvae. The seasonal cycle of when their larvae appear in the plankton is on average high from spring through summer so it is possible that their greater abundance in spring is due to a shift in timing and spawning events happened earlier in the warmer ‘heat wave’ years. It is also possible that more larvae are being released. Whatever the reason, the community composition has certainly changed in spring since 2015. Large copepods were also very low on the shelf in 2018 and small copepods were higher than in 2015-2017.

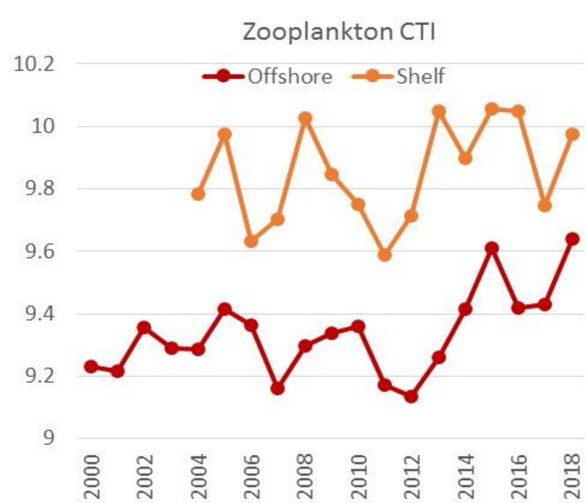

Figure 15-5. The mean annual Zooplankton Community Temperature Index (Mar-July) for each region.

The CTI for zooplankton (Figure 15-5) shows that shelf communities were comprised of taxa with a warmer bias than the offshore, however although 2018 was warmer than average there was no long-term trend. In contrast, the offshore region did show an increasing trend with the 2018 value the highest of the time series. While 2016 and 2017 were lower than 2015 and 2018 (i.e. a higher contribution of cooler biased taxa) all four years were higher than the pre-heat-wave period.

15.5. Factors influencing the trends and implications

Although the marine heat wave of 2014-2016 (DiLorenzo and Mantua 2016) has ended, ocean temperatures are still relatively warm and the lower trophic levels are still impacted. Increased stratification and lower nutrients affect the phytoplankton composition which in turn will impact the zooplankton that feed on them. Warmer water also favours certain taxa over others, as seen by the fact that warmer water taxa are more prevalent and increasing the CTI. This may persist for several years after a heat-wave event, especially in zooplankton taxa that have a longer, annual life cycle, such as the large sub-arctic copepods. The reduction in large copepod abundance will influence the food web functioning and likely have nutritional impacts on their predators (e.g. fish and some seabirds). While we cannot be certain how changing taxonomic composition of the prey affects predators via nutritional contributions to their diet there is likely to be some impact.

15.6. References

DiLorenzo, E., and Mantua, N. 2016. Multi-year persistence of the 2014/15 North Pacific marine heatwave. Nature Climate Change, published online: 11 July 2016 DOI:10.1038/nclimate3082

.

16. WEST COAST BRITISH COLUMBIA ZOOPLANKTON BIOMASS ANOMALIES 2018

Moira Galbraith and Kelly Young, Institute of Ocean Sciences, Sidney, B.C., Moira.Galbraith@dfo-mpo.gc.ca, Kelly.Young@dfo-mpo.gc.ca

16.1. Highlights

- Consecutive years of warm water intrusions from the south are effectively making the west coast of Vancouver Island like the nearshore California Current: high in gelatinous taxa and low in crustaceans.
- *Pyrosoma atlanticum* declined in abundance but is still present along the shelf break and Hecate Strait in small numbers.
- The downward trend of the past 4 years of the sub-Arctic copepod biomass has slowed, and the southern copepod and chaetognath species have started to decrease in biomass.
- 2018 was very much like 2017 but it is still not an “average” boreal/subarctic zooplankton community.

16.2. Description of the time series

Zooplankton time-series are available for southern Vancouver Island (SVI; 1979 - present), northern Vancouver Island (NVI; 1990 - present), Line P (1980-present) and Hecate Strait (HEC; 1998 - present), although with lower density and/or taxonomic resolution for NVI and Hecate Strait earlier in the time series. For this report, we present data from 1990 onwards; except Line P 1997 to present. The ‘standard’ sampling locations are averaged within the SVI, NVI, Line P and Hecate regions shown in Figure 16-1. Additional locations are included in averages when they are available. Samples were collected during DFO research surveys using vertical net hauls from near-bottom to sea surface on the continental shelf and upper slope, and from 250 m to surface at deeper locations (for methods see Mackas 1992 and Mackas et al. 2001). Abundance and biomass are estimated for all zooplankton species in these areas (>50 species).

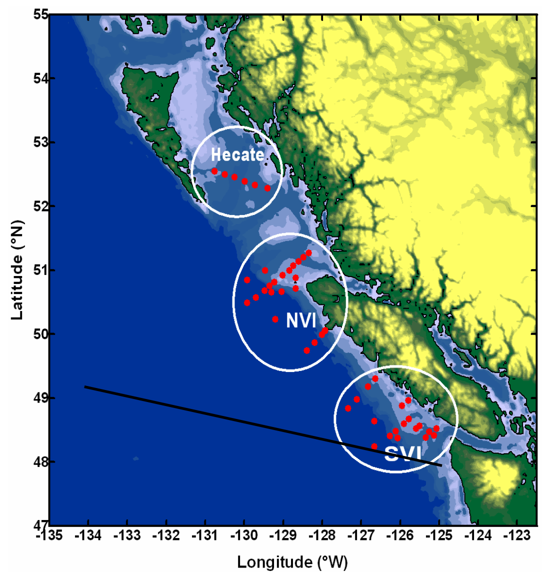

Figure *16-1. Zooplankton time series sampling locations (red dots) in B.C. marine waters. Data are averaged for samples within each area. There are more samples included in the analysis than shown in figure.*

To avoid confounding seasonal and interannual variability, climatology was estimated for each region, using the data from the start of each time series through to 2008, and compared to monthly conditions during any single year. To describe the interannual variability, our approach has been to calculate within each year a regional, logarithmic scale biomass anomaly for each species and for each month that was sampled in a given year. We then average the monthly anomalies in each year to give an annual anomaly (see Mackas 1992 & Mackas et al. 2001 for mathematical details). Zooplankton species on the west coast with similar zoogeographic ranges and ecological niches usually have very similar anomaly time series (Mackas et al. 2006). Therefore multiple species are averaged within species groups (and size classes within major taxa) to show interannual variability (Table 16-1; Mackas et al. 2013, Irvine and Crawford 2013). All data presented here are very preliminary as analysis is on-going; numbers will change but directions of trends usually don't.

Table 16-1. Zooplankton groups described in the time series in Figure 16-2.

Zooplankton group	**Species**	**Comments**
Southern copepods	*Acartia danae, A. tonsa, Clausocalanus spp., Calocalanus spp., Ctenocalanus vanus, Eucalanus californicus, Mesocalanus tenuicornis*, *Paracalanus spp.*	Centered about 1000 kilometers south of our study areas (either in the California Current and/or further offshore in the North Pacific Central Gyre)
Boreal shelf copepods	*Calanus marshallae, Pseudocalanus mimus, Acartia longiremis*	Southern Oregon to the Bering Sea
Subarctic oceanic copepods	*Neocalanus plumchrus*, *N. cristatus*, *N. flemingeri*, *Eucalanus bungii*	Inhabit deeper areas of the subarctic Pacific and Bering Sea from North America to Asia
Euphausiids	*Euphausia pacifica, Thysanoessa spinifera*	Centered off west coast of N. America; euphausiid biomass corrected for day/night tows.
Southern chaetognaths	*Mesosagitta minima, Serratosagitta bierii, Parasagitta euneritica*	Centered off California/Mexico
Northern chaetognath	*Parasagitta elegans*	Boreal Pacific into the Arctic
Cnidarians	*Aglantha digitale, Pleurobrachia bachei, Nanomia bijuga*	Hydromedusae, ctenophores, siphonophores ; boreal Pacific to Arctic

16.3. Status and trends

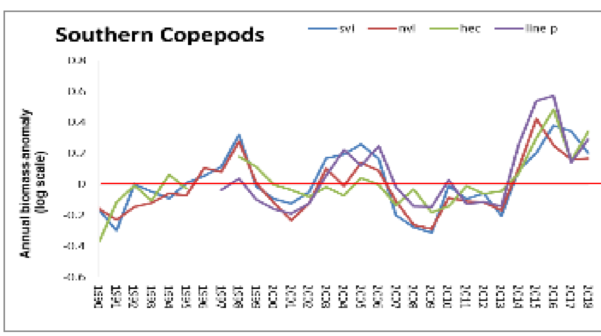

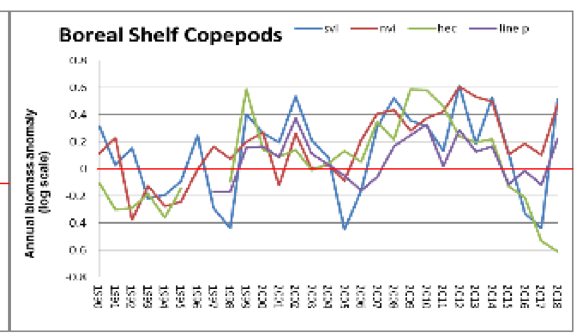

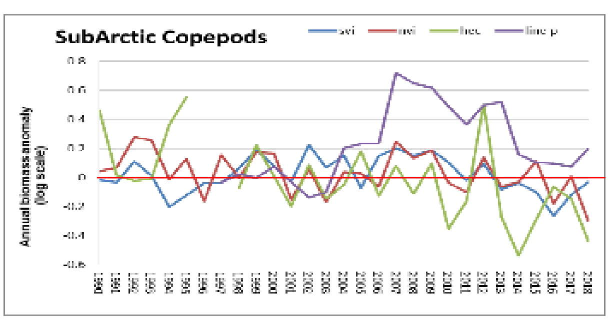

Figure 16-2. Zooplankton species-group anomaly time series for the regions shown in Figure 16-1. Line graphs are annual log scale anomalies. Southern Vancouver Island (SVI) blue; Northern Vancouver Island (NVI) red; Hecate Strait (HEC) green; Line P – purple for all graphs. Note the y-axis changes with each taxonomic group.

The biomass anomaly time series for copepod species groups and representative chaetognaths and euphausiids in the SVI, NVI, Line P and Hecate statistical areas are shown in Figures 16-2 and 16-3. Cool years tend to favor endemic ‘northern’ taxa; whereas warm years favor colonization by ‘southern’ taxa. See earlier State of the Ocean reports for pre-1990 anomalies. It is important to note that the anomalies are log scale and therefore multiplicative on a linear scale: an anomaly of +1 for a given taxon means that taxon had 10X higher biomass than in the climatology; an anomaly of -1 means the biomass was 1/10th the climatology. The range of interannual biomass variability within a species or species group is about one log unit (i.e. factor of 10). This is 2-3 times greater than the interannual variability of total biomass in our regions. Anomalies often persist for several years and, in addition to the covariation within species groups mentioned above, results in strong covariation between some species groups. The clearest covariation has been in the three copepod groups and in the chaetognaths.

In both the near shore and offshore regions of Vancouver Island, there were strongly positive anomalies for southern zooplankton. This increased throughout the years as warm nearshore water with higher abundances of southern oceanic zooplankton species moved poleward but 2018 was not as strong as 2016. By June the whole continental margin of B.C. was inundated with large masses of gelatinous animals, mainly pyrosomes on the shelf to shelf break (Brodeur et al. 2017), doliolids in Hecate Strait and hydromedusae and ctenophores across all shelf areas. Boreal copepods continued an upward trend along the shelf, except for Hecate region, whereas subarctic copepods were up along Line P and SVI but down for NVI and Hecate. Southern copepods were positive in all regions, but not as strong as in 2015-16 and appeared to be leveling off in 2018 (Figure 16-2).

(a) **(b)**

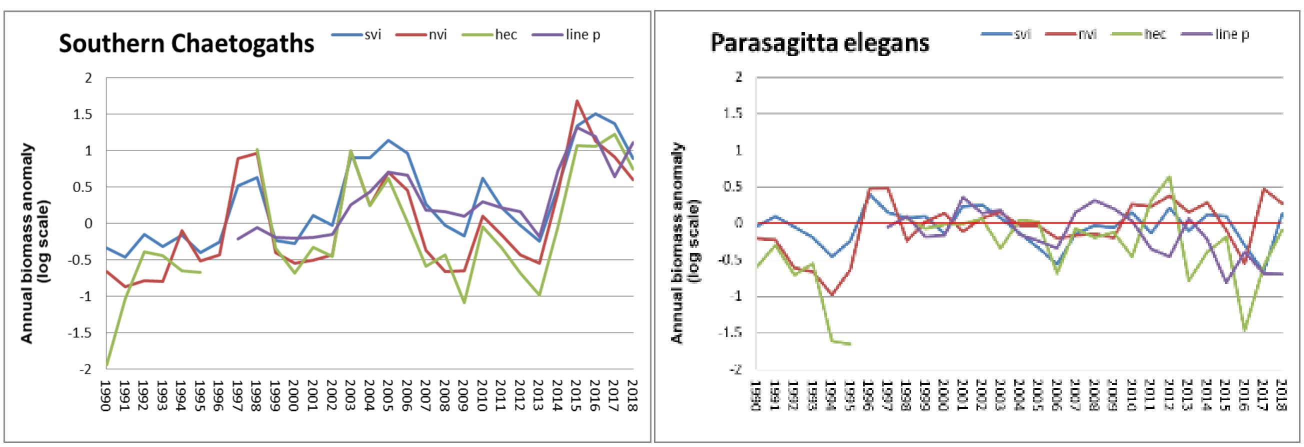

Figure 16-3. Chaetognath anomaly time series (vs climatological baseline) for all regions. Chaetognaths divided into southern species groups (a) and northern species groups (b); blank years mean no samples.

Southern chaetognaths are prevalent in all areas, and the biomass anomaly has not returned to average but also has not increased in abundance as in the past couple of years (Figure 16-3a). *Parasagitta elegans* biomass had a slight rebound to average values in all areas except for Line P where the species has been decreasing in numbers since 2013 (Figure 16-3b). Euphausiids continue to trend fairly positive over the last five years off the west coast of Vancouver Island (WCVI; Figure 16-4). Off California, both *Euphausia pacifica* and *Thysanoessa spinifera* are the dominant species suggesting that warmer waters may enhance their reproductive success along Vancouver Island. However, the warming events since 2015 tended to favour *E. pacifica* over *T. spinifera* off the BC coast. A recovery to average biomass appears to be in the works but it is a mixed signal across the regions. In Hecate Strait, NVI and

SVI shelf, there was a decrease in *T. spinifera* biomass since 2015 but all areas have seen an increase in 2018, Hecate Strait most noticeably so. *E. pacifica* had average biomass in all areas except for Hecate Strait where the biomass jumped, similar to *T. spinifera*. The euphausiid biomass anomaly along Line P showed no trend which may be a result of averaging nearshore with oceanic stations. Euphausiid species whose distribution centres off Oregon orCalifornia and south (*Thysanoessa gregaria* and *Nematocelis difficilis*) continue to be found along the Vancouver Island shelf edge and at Line P nearshore stations (data not shown).

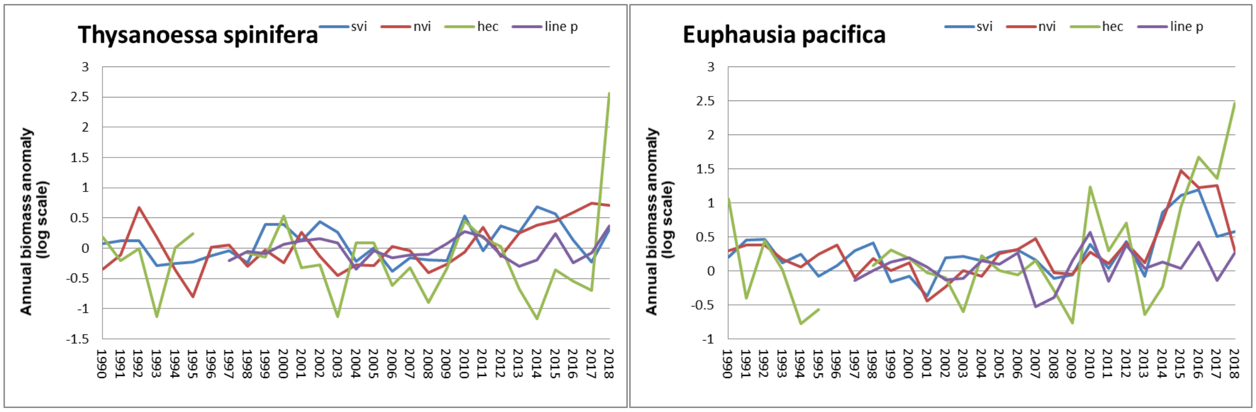

Figure 16- 4. Euphausiid biomass anomaly time series (vs climatological baseline) for all regions shown in Figure 16-1. Euphausiid biomass corrected for day/night sampling; blank years mean no samples.

Ctenophores, siphonophores and hydromedusae biomass anomalies were all positive for 2018; more in SVI shelf area and shelf break of NVI and throughout Hecate Strait. For Line P, the cnidarian community did not show much change from average. Doliolids were found at the inner line stations (P4-P12) and the influxes of salps were at the outer stations (P20 and P26). Doliolids and salps also added to the gelatinous community in Hecate Strait which has continued as a positive trend since 2014 (Figure 16-5). In an attempt to summarize and simplify, all the material presented here has been condensed into a CSIndex, or “Crunchie: Squishy” Index:

- Crunchies: all zooplankton having a hard, chitinous exoskeleton; mainly crustaceans with high protein and lipid material – copepods, euphausiids, amphipods, decapods, etc.
- Squishies: all zooplankton with a hydrostatic skeleton; mainly gelatinous animals with high water content and low nutritional value – hydromedusae, salps, doliolids, ctenophores, etc.

Several higher-order zooplankton taxa (with widely differing ecological niches) are classified as “gelatinous zooplankton”. However, all have high to very high peak reproductive rates compared to the crustaceans and chaetognaths, and all tend to have a “boom and bust” population time series. The most important gelatinous zooplankton groups considered here are:

- Salps, doliolids and pyrosomes. These are planktonic tunicates, and are primarily herbivorous (broad spectrum filter feeders).
- Thecosomatous pteropods (e.g. *Limacina helicina*). These are planktonic snails. Unlike the previous two groups, their bodies are not gelatinous, but they use a large external gelatinous feeding web to capture their food.

- Hydromedusae and siphonophores (“jellyfish”) and ctenophores (“comb jellies”). These are predatory on other zooplankton, sometimes on larval fishes but are mainly competitors with larval and juvenile fish.

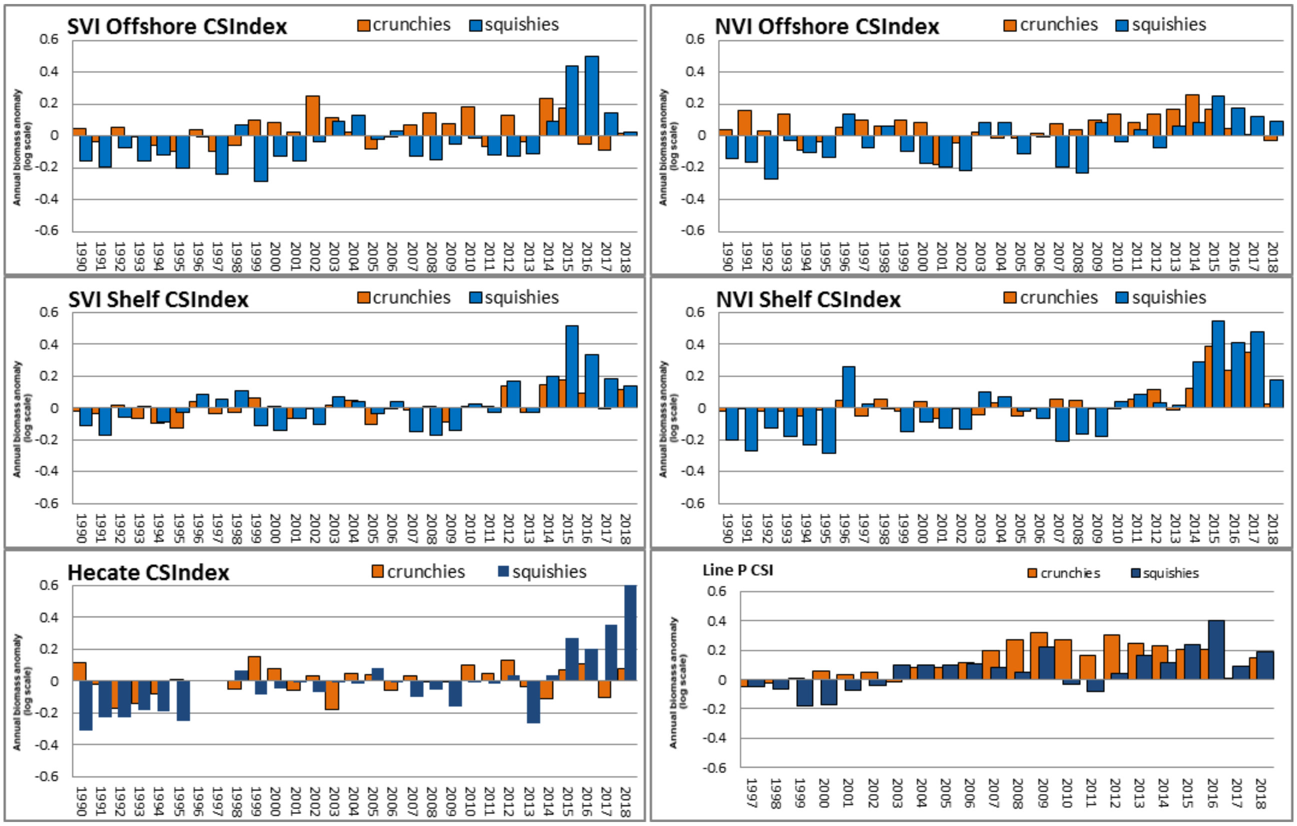

Figure 16-5. CS-Index: Comparing the gelatinous zooplankton (i.e. squishies) versus arthropod taxa (i.e. crunchies, ignoring meroplankton and removing southern crustacean species) biomass anomalies.

16.4. Implications of these trends

The Hecate region had a negative anomaly for subarctic copepods. This, coupled with the decline in boreal copepods and the inundation of southern species and combined with the huge increase in gelatinous taxa into the strait up to Dixon Entrance, becomes of some concern for the larval fish, juvenile fish (especially the seagoing salmonid component migrating through the area) and planktivorous sea birds. This concern is somewhat offset by the tenfold increase in euphausiid biomass in the area, the caveat there being the match/mismatch in seasonal timing. The low and/or sporadic sampling effort in Hecate Strait made it difficult to summarize those data but the pattern is similar for the most part as that of NVI shelf. The 2018 pattern showed that something unusual is still going in Hecate Strait; the amount of gelatinous biomass far out-strips the crustacean contribution. Temperature was elevated in 2015/16 for the whole west coast of British Columbia (Yelland and Robert 2017) and this continued into 2018 but not as high (Chandler, section 11; Ross and Robert, section 6). In times of warming events (1997/98, 2003/04, 2015/16; Ross 2017) the SVI shelf and offshore area were inundated with low nutrient gelatinous animals (Figure 16-5). This makes foraging for food a more arduous (calorie consuming travel) and risky (more exposure to predators) for the animals that rely on the spring and summer bonanza of crustaceans in the nearshore areas. Expectations are that the years when gelatinous zooplankton are more abundant equates to poor survival prospects for juvenile fish and seabirds. As with the long term trend in the copepod species groups, the net effect has been to make the zooplankton community off BC more like the community found in nearshore parts of the California Current System to the south of BC: high in gelatinous content and low in lipid rich large copepods.

16.5. References

Brodeur, R., Perry, I., Boldt, J., Flostrand, L., Galbraith, M., King, J., Murphy, J., Sakuma, K. and Thompson, A. 2018. An unusual gelatinous plankton event in the NE Pacific: The great pyrosome bloom of 2017. PICES Press Vol. 26, No. 1.

Irvine, J.R. and Crawford, W.R. 2013. State of physical, biological, and selected fishery resources of Pacific Canadian marine ecosystems in 2012. DFO Can. Sci. Advis. Sec. Res. Doc. 2013/032. viii + 140 p.

Mackas, D.L. 1992. The seasonal cycle of zooplankton off southwestern British Columbia: 1979-89. *Can. J. Fish. Aquat. Sci*. 49: 903-921.

Mackas, D.L., Thomson, R.E., and Galbraith, M. 2001. Changes in the zooplankton community of the British Columbia continental margin, and covariation with oceanographic conditions, 1985-1998. *Can. J. Fish. Aquat*. Sci. 58: 685-702.

Mackas, D. L., Peterson, W.T., Ohman, M.D., and Lavaniegos, B.E. 2006. Zooplankton anomalies in the California Current system before and during the warm ocean conditions of 2005, *Geophys. Res. Lett*., 33, L22S07, doi: 10.1029/2006GL027930.

Mackas, D.L., Batten, S., and Trudel, M. 2007. Effects on zooplankton of a warming ocean: recent evidence from the North Pacific. *Progr. Oceanogr*. 75: 223-252.

Mackas, D.L, Galbraith, M., Faust, D., Masson, D., Young, K., Shaw, W., Romaine, S., Trudel, M., Dower, J., Campbell, R., Sastri, A., Bornhold Pechter, E.A., Pakhomov, E., and El-Sabaawi, R. 2013. Zooplankton time series from the Strait of Georgia: Results from year-round sampling at deep water locations, 1990–2010. *Progr. Oceanogr*. 115:129-159.

Ross, T. 2017. La Niña, the Blob and another warmest year. In: Chandler, P.C., King, S.A., and Boldt, J. (Eds.). 2017. State of the physical, biological and selected fishery resources of Pacific Canadian marine ecosystems in 2016. Can. Tech. Rep. Fish. Aquat. Sci. 3225: vi + 243 p.

Yelland, D. and Robert, M. 2017. 2016 oceanographic conditions along Line P and the coast of Vancouver Island. In: Chandler, P.C., King, S.A., and Boldt, J. (Eds.). 2017. State of the physical, biological and selected fishery resources of Pacific Canadian marine ecosystems in 2016. Can. Tech. Rep. Fish. Aquat. Sci. 3225:vi + 243 p.

17. PACIFIC HERRING SUMMER DISTRIBUTION AND ABUNDANCE OFF THE VANCOUVER ISLAND CONTINENTAL SHELF

Jennifer Boldt[1], Hilari Dennis-Bohm[1], Jackie King[1], Chelsea Stanley[2], Erika Anderson[1], Tyler Zubkowski[1], Stéphane Gauthier[2]
[1] Fisheries & Oceans Canada, Pacific Biological Station, Nanaimo, B.C.; contact: Jennifer.Boldt@dfo-mpo.gc.ca
[2] Fisheries & Oceans Canada, Institute of Ocean Sciences, Sidney, B.C.

17.1. Highlights

- Pacific Herring are broadly distributed on the Vancouver Island continental shelf in the upper ~45 m of the water column during night time hours.
- Pacific Herring were more broadly distributed in 2018 compared to 2017.
- Pacific Herring were absent from areas with high densities of Pacific Hake during daylight hours.

17.2. Description of the time series

The Integrated Pelagic Ecosystem survey is part of an integrated project designed to study the structure and function of the pelagic ecosystem on the Vancouver Island Continental Shelf (< 200 m bottom depth; Figure 17-1) during summer. The main goal of the survey is to understand factors affecting the distribution, abundance, and food web linkages of pelagic fish species, such as Pacific Herring and juvenile Pacific Salmon. Survey objectives are to: 1) examine species distribution, composition, and abundance; 2) collect morphometric data, diet data, and biological samples; and 3) examine the prey environment by sampling zooplankton (vertical bongo net hauls) and conducting oceanographic monitoring (temperature, salinity, fluorescence). This is a random stratified trawl survey with 8 strata defined by depth and biological communities. Each stratum was divided into 4 x 4 km blocks, and a subset of blocks was randomly selected; the number of blocks was allocated by strata sizes.

Midwater trawl nets were used to sample fish (2017: CanTrawl 250; 2018: LFS 7742; see King et al., section 42). Depths of trawl tows were assigned randomly for selected blocks (surface or 15 m head rope depth). Each selected block was sampled both in the day and night. Pacific Herring exhibit diel vertical migration, ascending at night into upper waters sampled by the trawl gear; therefore, night time catches are reported. All catches were sorted to species and weighed. Catch per unit effort (CPUE) was calculated by dividing catch weights by the swept volume (product of net mouth opening height, width, and distance towed). Morphometric measurements and biological samples were collected from subsampled fish.

Oceanographic and zooplankton data were also collected at each block. The survey was conducted during July 6-August 2, 2017 and July 5-29, 2018. In 2018, acoustic data were collected along standardized transects during daylight hours. Acoustic data were collected with a SIMRAD EK60 scientific echo sounder operating at 38 kHz and 120 kHz. Although there were no trawl tows conducted to verify species composition of the echosign, the echosign patterns and trawl catches from the randomized survey were used to determine the spatial distribution of euphausiids, coastal pelagic fish (primarily Pacific Herring), and Pacific Hake. Previous surveys have validated echosigns for these three taxonomic groupings.

17.3. Status and trends

In the summer, Pacific Herring are broadly distributed on the Vancouver Island continental shelf in the upper ~45 m of the water column during night time hours (Figure 17-1). Areas of higher CPUE were located off of the north, northwest, and southwest coasts of Vancouver Island. Pacific Herring were more broadly distributed in 2018 compared to 2017.

In 2018, during daylight hours, acoustic backscatter, attributed to coastal pelagic species (primarily Pacific Herring), was observed in areas where Pacific Hake were absent (Figure 17-2). Areas of higher coastal pelagics backscatter were located off the north, central and southwest coasts of Vancouver Island. Echosign attributed to Pacific Hake tended to be distributed in the offshore portions of the survey area. The spatial distribution of the Euphausiid-like echosign was similar to that attributed to Pacific Hake (Figure 17-2).

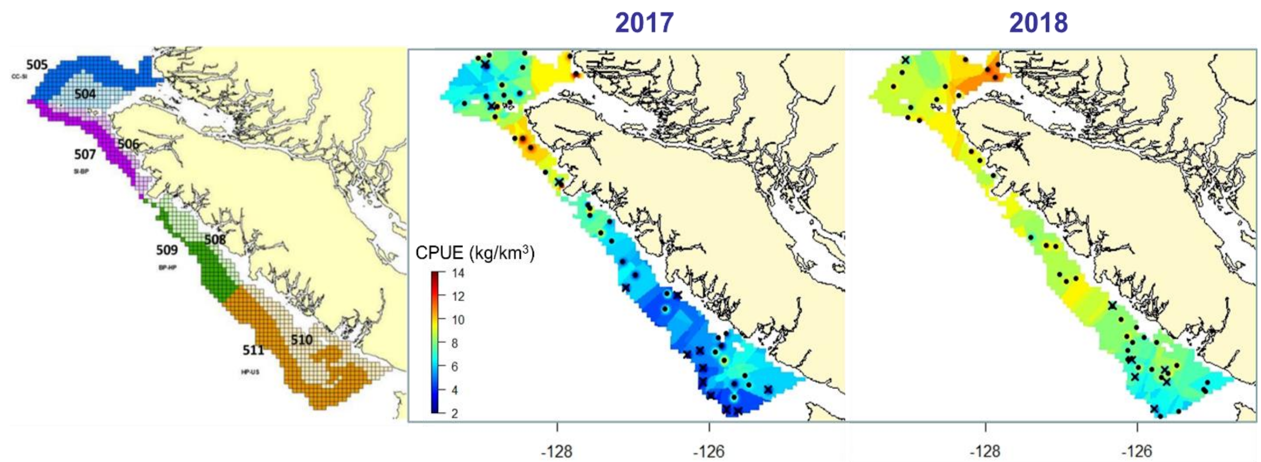

Figure 17-1. Integrated Pelagic Ecosystem Survey on the Vancouver Island Continental shelf (<200 m bottom depth), with 8 strata based on bottom depth and biological communities (left panel). Catch per unit effort (kg/km^3) of Pacific Herring in night time trawl hauls of the Integrated Pelagic Ecosystem Survey, 2017-2018 (middle and right panels). Catch per unit effort values were spatially interpolated using kriging. Black dots indicate stations where herring were caught; black 'x''s indicate stations where a trawl haul was conducted but no herring were caught. These are preliminary results and may change with additional analyses.

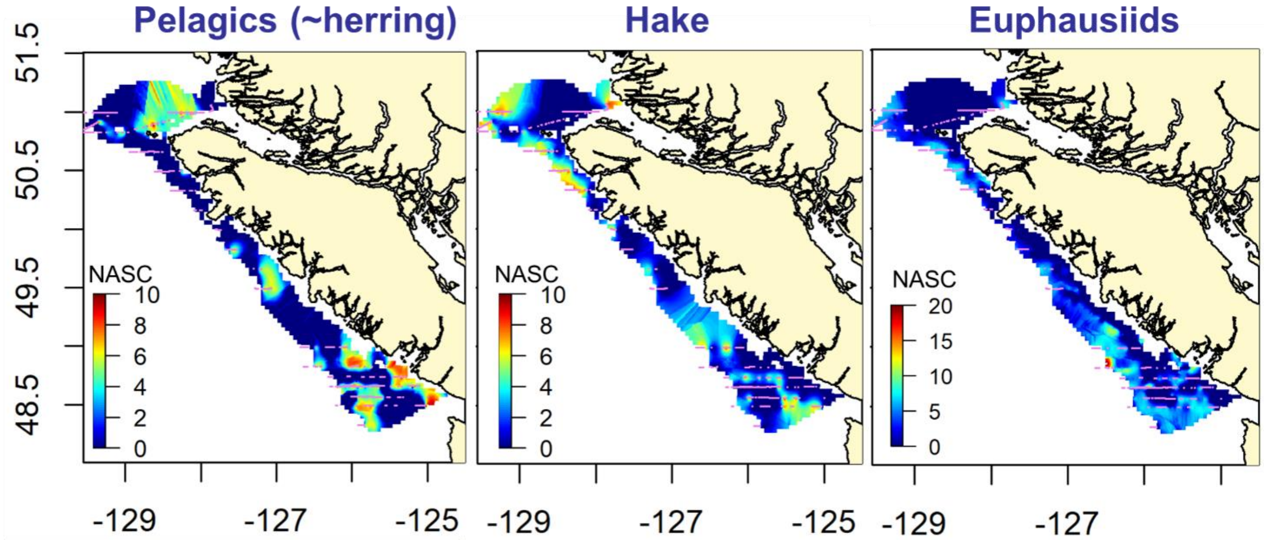

Figure 17-2. Acoustic backscatter observed along standard transects during day light hours on the Integrated Pelagic Ecosystem Survey, 2018. Backscatter was attributed to 3 general taxonomic groupings based on patterns of previously observed echograms and trawl survey catches conducted during the survey. The taxonomic groupings are coastal pelagics (primarily Pacific Herring, based on trawl survey catches), Pacific Hake, and Euphausiids. Backscatter was summed for all depths and spatially interpolated using kriging. These are preliminary results and may change, with additional analyses. NASC = Nautical Area Scattering Coefficient, m^2/nmi^2.

17.4. Factors influencing trends

Environmental variables, such as temperature, are known to affect Pacific Herring recruitment and survival (Tester 1948, Ware 1991). Bottom-up control of production also can influence fish abundance (Ware and Thompson 2005, Perry and Schweigert 2008, Schweigert et al. 2013, Boldt et al. 2018). Pacific Herring are zooplanktivorous, consuming primarily euphausiids and some copepods (Wailes 1936). Changes in ocean conditions, such as temperature or currents, could affect the amount and types of prey available. For example, a northerly current direction could result in the presence of California Current waters off the WCVI, bringing warm-water zooplankton species that have a lower energetic value, creating poorer feeding conditions for herring (Schweigert et al. 2010, Mackas et al. 2004).

There are a wide variety of herring predators, including Pacific Hake, Lingcod, Pacific Spiny Dogfish, Pacific Cod, Sablefish, Arrowtooth Flounder, Pacific Halibut, Steller Sea Lions, Northern Fur Seals, Harbour Seals, California Sea Lions, and Humpback Whales (Schweigert et al. 2010). Off the WCVI, Pacific Herring recruitment has been correlated with piscivorous Pacific Hake biomass (i.e., Pacific Hake that are large enough to consume herring) suggesting predation may be an important factor influencing West Coast of Vancouver Island Pacific Herring recruitment (Tanasichuk 2012). At the margins of Pacific Hake and Pacific Herring distributions, consumption of Pacific Herring by Pacific Hake may be high (Ware and McFarlane 1986, 1995). Pacific Herring may have to trade off predation risk in areas of high Pacific Hake densities against finding prey (e.g., euphausiids).

17.5. Implications of those trends

One of the many types of data collected on this survey is a time series of Pacific Herring abundance and distribution during their summer foraging period. Stock assessments for Pacific Herring are driven by spring egg dive surveys to estimate spawning stock biomass; however, stock assessments indicate temporal changes in natural mortality – the causes of which are unknown. This survey examines Pacific Herring abundance and distribution in the summer, providing an improved understanding of factors affecting their mortality. Spatial data supports the hypothesis that Pacific Hake predation is an important factor to include in estimating Pacific Herring mortality. Pacific Herring aggregations along the west coast of Vancouver Island are also informative for determining variability in seabird and marine mammal distributions. Mismatch between Pacific Herring aggregations and seabird or marine mammal foraging areas could translate into decreased growth or survival of those predators. This time series provides an indicator of ecosystem productivity (Pacific Herring and euphausiid as indicators) and the availability of Pacific Herring to their predators.

17.6. References

Boldt, J.L, Thompson, M., Rooper, C.N., Hay, D.E., Schweigert, J.F., Quinn, T.J. II, Cleary, J.S., Neville, C.M. 2018. Bottom-up and top-down control of small pelagic forage fish: factors affecting age--0 herring in the Strait of Georgia, British Columbia. Mar. Ecol. Prog. Ser. https://doi.org/10.3354/meps12485.

Mackas, D.L., Peterson, W.T., and Zamon, J.E. 2004. Comparisons of interannual biomass anomalies of zooplankton communities along the continental margins of British Columbia and Oregon. Deep-Sea Research II, 51: 875-896.

Perry, R. I., and Schweigert,J. F. 2008. Primary productivity and the carrying capacity of herring in NE Pacific marine ecosystems. Progress in Oceanography 77: 241–251.

Schweigert, J.F., Boldt, J.L., Flostrand, L., and Cleary, J.S. 2010. A review of factors limiting recovery of Pacific herring stocks in Canada. ICES J. Mar. Sci. 67:1903-1913.

Schweigert, J.F., Thompson, M., Fort, C., Hay, D.E., Therriault, T.W., and Brown, L.N. 2013. Factors linking Pacific herring (*Clupea pallasi*) productivity and the spring plankton bloom in the Strait of Georgia, British Columbia, Canada. Progress in Oceanography 115: 103-110.

Tanasichuk, R. 2012. Euphausiids and west coast Vancouver Island fish production. p. 47-49 In Irvine, J.R. and Crawford, W.R. 2012. State of the physical, biological, and selected fishery resources of Pacific Canadian marine ecosystems in 2011. DFO Can. Sci. Advis. Sec. Res. Doc. 2012/072. xi +142 p.

Tester, A.L. 1948. The efficacy of catch limitation in regulating the British Columbia herring fishery. Transactions of the Royal Society of Canada, Vol. XLII: Series III: 135-163.

Wailes, G.H. 1936. Food of *Clupea pallasi* in southern British Columbia waters. Journal Biological Board of Canada, 1: 477–486.

Ware, D.M., 1991. Climate, predator and prey: behavior of a linked oscillating system, pp. 279–291. In: Kawasaki, T. (Ed.), Long-term Variability of Pelagic Fish Populations and their Environment. Pergamon Press, Tokyo.

Ware, D.M,. McFarlane, G.A. 1986. Relative impact of Pacific hake, sablefish and Pacific cod on west coast of Vancouver Island herring stocks. Int. North Pacific Fish. Comm. Bull. 47:.67–78.

Ware, D.M., McFarlane, G.A. 1995. Climate induced changes in hake abundance and pelagic community interactions in the Vancouver Island Upwelling System. Climate Change and Northern Fish Populations. Beamish, R.J. (Ed.) Can. Spec. Publ. Fish. Aquat. Sc.i 121:.509–521.

Ware, D., and Thomson, R. 2005. Bottom-up ecosystem trophic dynamics determine fish production in the northeast Pacific. Science 308: 1280-1284.

18. EULACHON STATUS AND TRENDS IN SOUTHERN B.C.

Linnea Flostrand, Fisheries and Oceans Canada, Pacific Biological Station, Nanaimo, B.C., Linnea.Flostrand@dfo-mpo.gc.ca

18.1. Highlights

- In 2011 COSEWIC assessed Eulachon in British Columbia as three designatable units, spawning stocks in the:
    - Central Coast and Fraser River were assessed as endangered, and
    - Nass/Skeena was assessed as Special Concern.
- Eulachon is an important First Nation fishery resource and in-river Eulachon Food, Social and Ceremonial fisheries have occurred in years up until and including 2018.
- Commercial fishing for Eulachon in Canada has been closed since 2004.
- In 2018, the index of Eulachon spawning stock biomass in the Fraser River was estimated to be at a moderately high level (408 tonnes) similar to in 2015 (317 tonnes), compared with most other years from 2004-2017 which were relatively low (4-120 tonnes).
- Eulachon catch per unit effort estimates from an annual spring west coast of Vancouver Island multispecies trawl survey were relatively high in 2013 to 2015 but dropped to relatively low levels in 2016 to 2018.
- In the 2018 spring multispecies trawl survey, fish lengths appeared to have a bi-modal distribution with peaks within the ranges of 8-10 cm and 14-17 cm.
- There is considerable uncertainty associated with the factors that affect trends in Eulachon stock dynamics.

18.2. Description of indices

Indices of Eulachon (*Thaleichthys pacificus)* trends used to monitor population dynamics over time are based on:

1) annual Fraser River Eulachon egg and larval surveys (1995 to 2018) used to estimate spawner abundance. For information on methods associated with the egg and larval survey index, see Hay et al. (2002) and McCarter and Hay (2003).

2) Eulachon catches and catch samples from spring small-mesh multispecies trawl surveys off the west coast of Vancouver Island (WCVI, 1973-2018) and in the Queen Charlotte Sound (QCS, 1998-2012, 2016).

3) In river catches of spawning Eulachon from a commercial fishery in the Fraser River (1900-2004); a commercial fishery in the Columbia River (1888-2010 and 2014-2015) systems; and standardized gillnet surveys in the Fraser River (1995-2004; 2017-2018). Trends from in-river commercial and survey sources are not included in this report due to not being current or not available to DFO.

18.3. Status and trends

Eulachon have experienced long-term declines in many rivers throughout their distribution from California to Alaska. The *Committee on the Status of Endangered Wildlife in Canada* (COSEWIC) assessed Eulachon in British Columbia as three designatable units (DUs): the British Columbia Central Coast and Fraser River DUs were assessed as endangered, and the Nass/Skeena DU was assessed as a species of special concern (COSEWIC 2011, 2013). Information in support of Eulachon recovery potential assessments in Canada are reported in Levesque and Therriault (2011) and Schweigert et al. (2012).

Eulachon is an important First Nation fishery resource and in-river Eulachon Food, Social and Ceremonial fisheries have occurred in years up until and including 2018 (DFO 2019). Eulachon has also been caught as part of mixed-species marine catches from trawl fisheries and research surveys. There was an active commercial fishery for Eulachon in the Fraser River for over 96 years until a closure in 1997, followed by temporary openings in 2002 and 2004. Commercial fishing for Eulachon in the Fraser River has been closed since 2004.

In 2018, the index of Eulachon spawning stock biomass in the Fraser River was estimated to be at a moderately high level (408 tonnes) similar to in 2015 (317 tonnes), compared with most other years from 2004-2017, which were relatively low (4-120 tonnes) (Figure 18-1).

In 2018, the mean Eulachon catch per unit effort (CPUE) from the spring WCVI multispecies trawl survey was again relatively low, especially compared to the relatively high levels observed in 2013-2015 (Figure 18-2).

Eulachon standard lengths measured from samples taken during the 2017 WCVI multispecies trawl survey show prominent bimodal trends with peaks within the ranges of 8-10 cm and 14-17 cm. (Figure 18-3). This length distribution also shows a lower frequency mode for smaller fish with a peak around 7-8 cm, similar to 2016 observations.

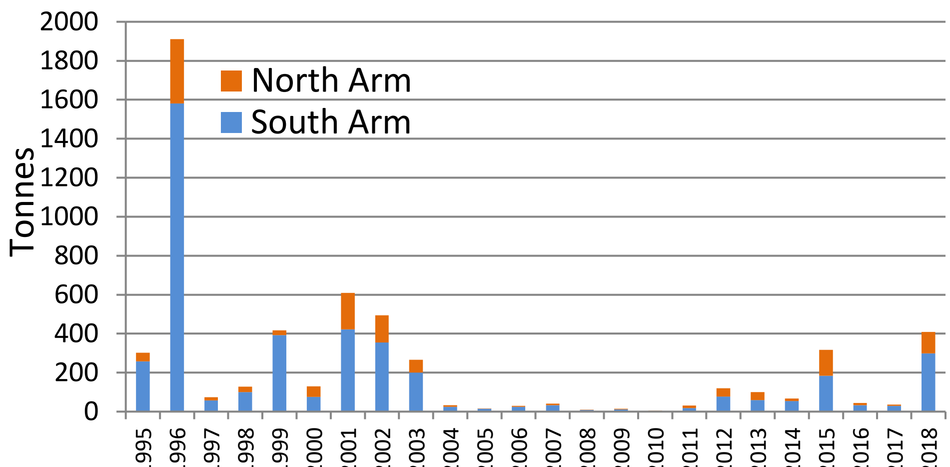

Figure 18-1. Estimated spawning stock biomass (SSB in tonnes) of Eulachon in the Fraser River, 1995-2018, comprised of sampling observations from the South and North Arms combined.

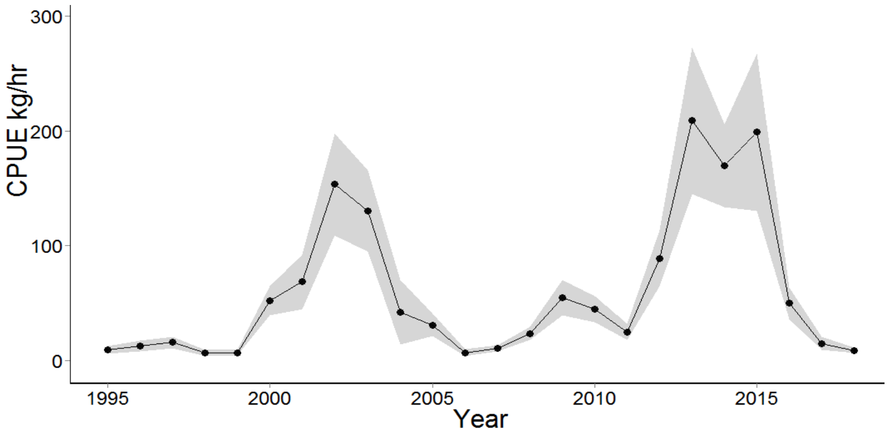

Figure 18-2. Eulachon mean catch per unit effort observations from spring WCVI multispecies trawl surveys (1987-2018). Mean 95% confidence intervals are enveloped in grey.

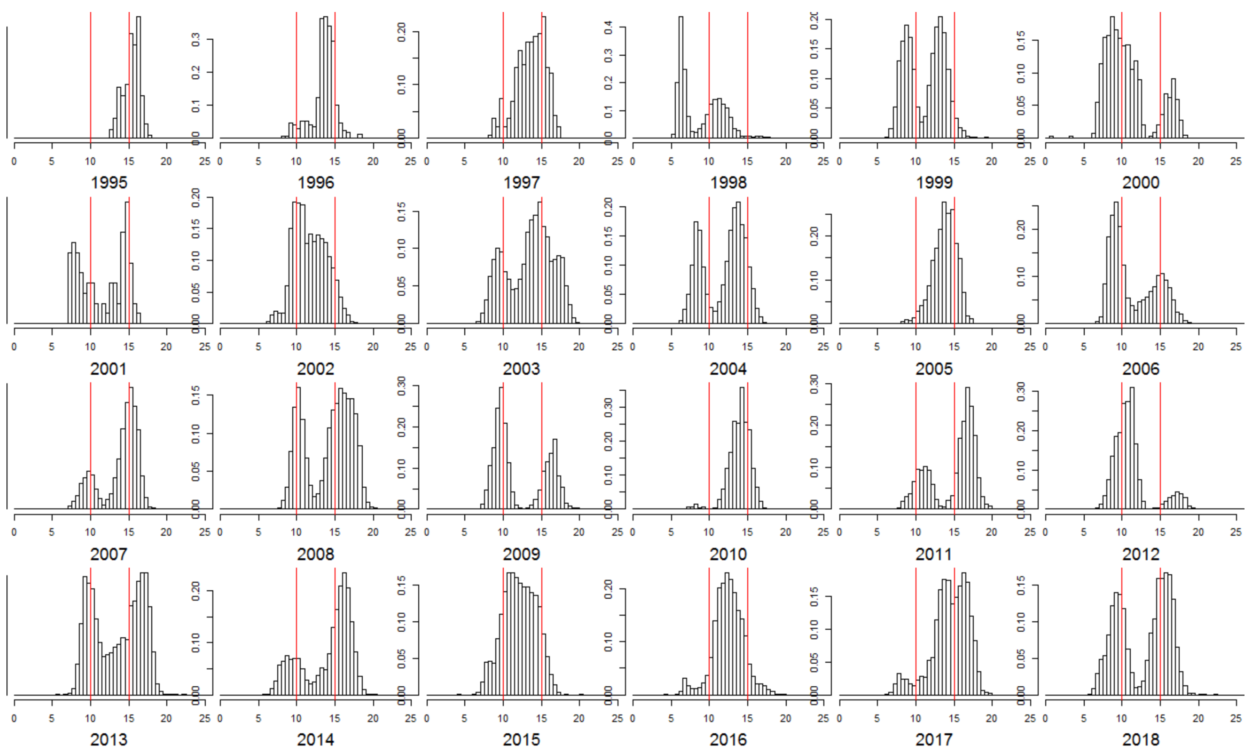

Figure 18-3. Density histograms of Eulachon standard lengths (in cm) from pooling sample data by year from WCVI survey samples 1995-2018. Red vertical lines are visual markers at 10 cm and 15 cm to assist comparisons between positions and shapes of annual length distributions.

18.4. Factors causing those trends

Eulachon are anadromous and spawning is limited to the lower reaches of rivers. Spawning typically begins in April or May on the Fraser River. Indigenous people in the area have noted that runs may begin as early as February or March. During spawning, adhesive eggs, about 20,000 to 40,000 per female, attach to sand or pebbles and hatch in three to five weeks at ambient temperatures, usually between 3 and 10° Celsius. Once hatched, larvae are rapidly flushed to estuarine or marine waters. They are believed to live at sea for approximately three to five years before returning to natal rivers for spawning. Determining the age of eulachon has proven to be difficult and there is a lot of uncertainty interpreting ages from size trends and physical structures such as otoliths and fish scales. Spawning adults typically reach a length of 15 to 20 cm and weigh between 40 and 60 grams. Large post-spawning mortalities occur and most, if not all, Eulachon are expected to die after spawning.

There are uncertainties associated with the ecology and biology of Eulachon stocks as well as the factors affecting Eulachon recruitment and survival. For example, it is uncertain what ranges in ages comprise the spawning stock each year, the composition of ages by cohort group, and to what degree spawning stocks and cohorts may mix on the spawning grounds and in different areas and seasons of the marine environment.

As for factors affecting Eulachon survival, Schweigert et al. (2012) state that:

> "No single threat could be identified as most probable for the observed decline in abundances among DUs [designatable units] or in limiting recovery. However, mortality associated with coastwide changes in climate, fishing (direct and bycatch) and marine predation were considered to be greater threats at the DU level, than changes in habitat or predation within spawning rivers".

18.5. Implications of those trends

Reduced biomass of Eulachon has negative implications for First Nations, commercial and recreational fishers (DFO 2019). Eulachon are socially and culturally significant to First Nations and are harvested by First Nations at low levels. Commercial and recreational fisheries are currently closed.

Reduced Eulachon abundance also likely has negative impacts on their predators. Important predators of Eulachon include: marine mammals (particularly seals and sea lions in the estuaries), Chinook and Coho Salmon, Spiny Dogfish, Pacific Hake, White Sturgeon, Pacific Halibut, Walleye Pollock, Sablefish, rockfish, Arrowtooth Flounder, and others (Levesque and Therriault 2011). Diet data time series of all animals in the ecosystem would improve our ability to examine temporal trends in predator-prey interactions and the implications of those trends.

18.6. References

COSEWIC. 2011. Committee on the Status of Endangered Wildlife in Canada assessment and status report on the Eulachon, Nass/Skeena Rivers population, Central Pacific Coast population and the Fraser River population *Thaleichthys pacificus* in Canada. Committee on the Status of Endangered Wildlife in Canada. Ottawa. xv + 88pp.

COSEWIC. 2013. Committee on the Status of Endangered Wildlife in Canada assessment assessment and status report on the Eulachon, Nass/Skeena population, *Thaleichthys pacificus* in Canada. Committee on the Status of Endangered Wildlife in Canada. Ottawa. xi + 18 pp.

DFO. 2015. Recovery Potential Assessment For Eulachon – Fraser River Designatable Unit. DFO Can. Sci. Advis. Sec. Sci. Advis. Rep. 2015/002.

DFO 2019. Pacific Region Integrated Fisheries Management Plan January 1-December 31, 2019, Eulachon Fraser River.

Hay, D.E., McCarter, P.B., Joy, R., Thompson, M. and West, K. 2002. Fraser River Eulachon Biomass Assessments and Spawning Distribution: 1995-2002. Canadian Stock Assessment Secretariat Research Document 2002/117.

Levesque, C. and Therriault, T. 2011. Information in support of a recovery potential assessment of (*Thaleichthys pacificus*) in Canada. CSAS Research Document 2011/101.

McCarter, P.B. and Hay, D.E. 2003. Eulachon embryonic egg and larval outdrift sampling manual for ocean and river surveys. Can. Tech Rep. Fish. Aquat. Sci. 2451: 33p.

NMFS. 2017. National Marine Fisheries Service, September 2017 Recovery Plan for the Southern Distinct Population Segment of Eulachon (*Thaleichthys pacificus*). National Marine Fisheries Service, West Coast Region, Protected Resources Division, Portland, OR, 97232.

NOAA. 2010. National Oceanic and Atmospheric Administration. U.S.A. Federal Register / Vol. 75, No. 52 / Thursday, March 18, 2010 / Rules and Regulations, p. 13012.

Schweigert, J., Wood, C., Hay, D., McAllister, M., Boldt, J. McCarter, B., Therriault, T.W., and Brekke, H. 2012. Recovery potential assessment of eulachon (*Thaleichthys pacificus*) in Canada. CSAS Research Document 2012/098.

19. PACIFIC HERRING IN BRITISH COLUMBIA, 2018

Jaclyn Cleary*, Matt Grinnell, Chris Grandin, Kristen Daniel, and Matt Thompson, Fisheries & Oceans Canada, Pacific Biological Station, Nanaimo, B.C. *Jaclyn.Cleary@dfo-mpo.gc.ca

19.1. Highlights

- Estimated spawning biomass has increased in the Strait of Georgia stock since 2010, despite declines in survey data in the past 2 years. Strait of Georgia is the largest of the 5 major herring stocks. Over the last 2 to 5 years, the biomass of the other stocks was rebuilding (West Coast of Vancouver Island stock), stable (Prince Rupert), or declining (Haida Gwaii, Central Coast).

- Factors contributing to changes in biomass and stock status include changes in recruitment, natural mortality, mean weight-at-age, and model fits to the spawn index.

- There has been a continued increase of weight-at-age in all stocks, following a declining trend during approximately 1980 to 2010.

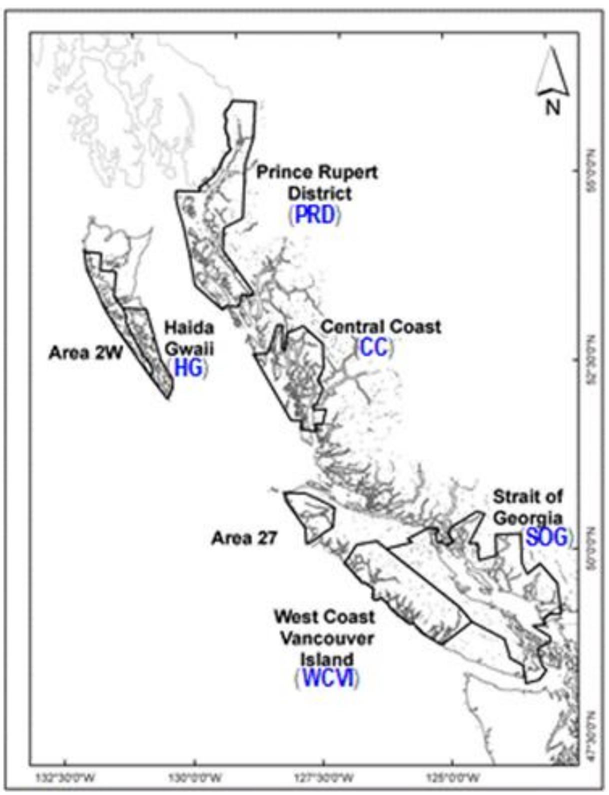

Figure 19-1. Location of the five major (Strait of Georgia, West Coast of Vancouver Island, Prince Rupert District, Haida Gwaii, and Central Coast) as well as two minor (Area 2W, and Area 27) Pacific Herring stocks in BC.

19.2. Summary

In B.C., Pacific Herring are managed as five major stocks (Strait of Georgia, SOG; West Coast of Vancouver Island, WCVI; Prince Rupert District, PRD; Haida Gwaii, HG; and Central Coast, CC), and two minor stocks (Area 2W and Area 27) (DFO 2019; Figure 19-1. For each stock, model estimates of Pacific Herring biomass reflect herring population trends. Statistical catch-at-age models are fit to time series data: commercial and test fishery biological samples (age, length, weight, sex, etc.), herring spawn survey data (spawn index), and commercial harvest data. In 2018, the model was used to provide (in part) estimates of Pacific Herring spawning biomass and age-2 recruit abundances (DFO 2019). Herring biomass, recruit abundance, and weight-at-age are important indicators of stock status; however, there are additional considerations such as distribution of spawn. Readers are referred to DFO (2019) for important additional information regarding the status of B.C. Pacific Herring stocks.

19.3. Status and trends

In all five major herring stocks, there was a declining trend in weight-at-age beginning in the 1980s through 2010, with an increase in recent years (Figure 19-2). The 2018 spawning biomass for HG, PRD, and CC stocks is estimated to be at low levels (DFO 2019; Figure 19-3). WCVI spawning biomass in 2018 was similar to that of 2016-2017 (DFO 2019). The estimated spawning biomass of SOG herring increased to historic highs in 2018, despite declines in survey data in the past 2 years (DFO 2019).

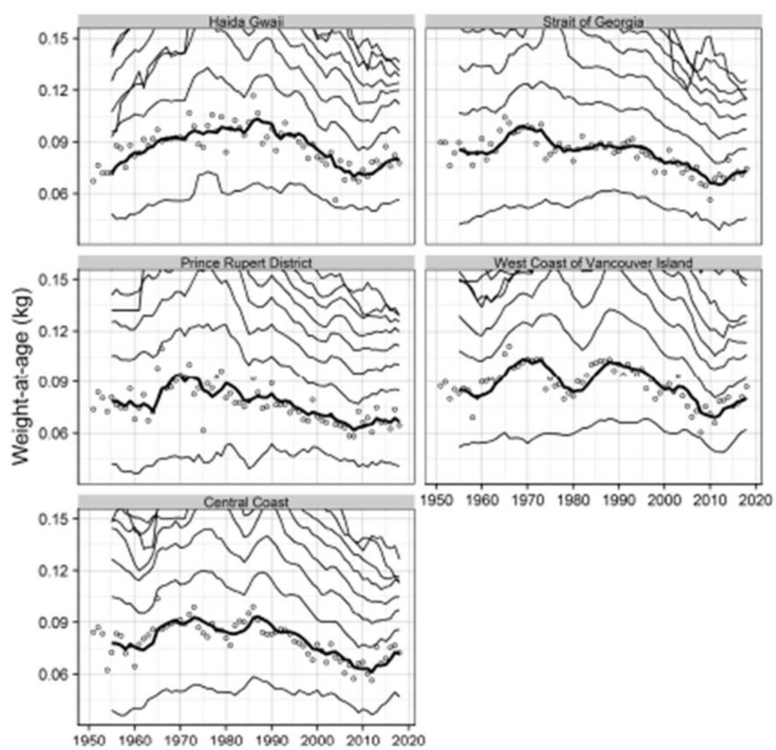

Figure 19-2. Time series of observed weight-at-age 3 (circles) and five-year running mean weight-at-age 3 (dark line) for major Pacific herring stocks, 1951 to 2018. Thinner black lines represent five-year running mean weight-at-age 2 (lowest) and ages 4-7 (incrementing higher from age 3). Figure adapted from DFO (2019).

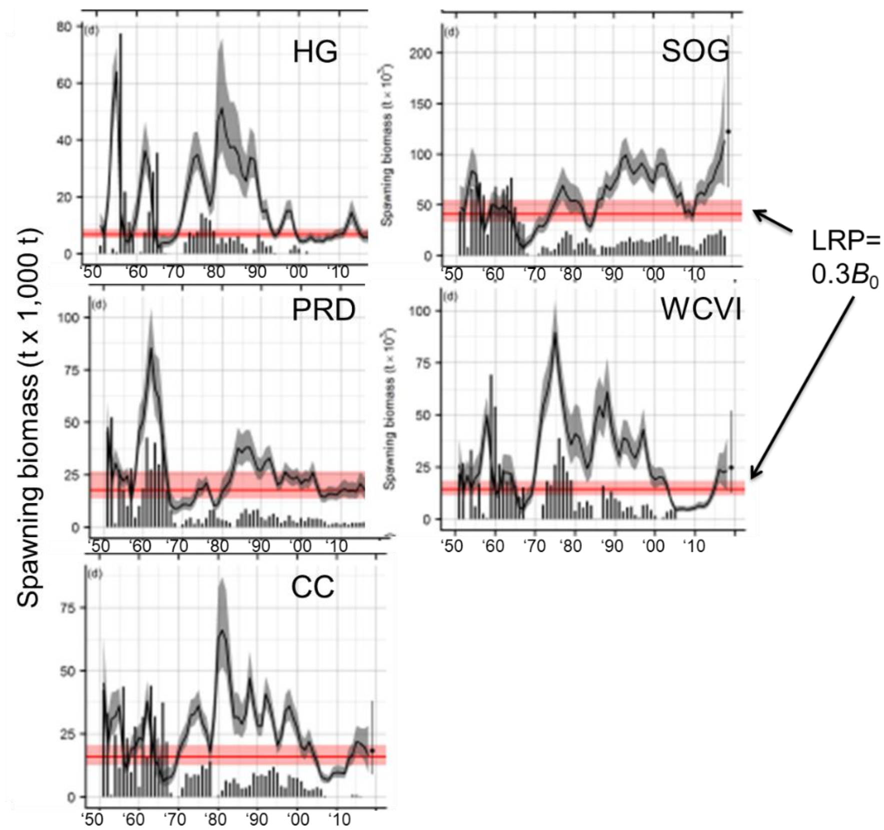

Figure 19-3. Summary of the dynamics of the five Pacific Herring stocks from 1951 to 2018, where solid lines with surrounding grey envelopes, represent medians and 5-95% credible intervals. Also shown is the reconstruction of spawning biomass (SBt) for each year t, with unfished values shown at far left (solid circle and vertical lines) and the projected spawning biomass given zero catch (SB_{2019}) shown at the far right (solid circle and vertical lines). Time series of thin vertical lines denote commercial catch (excluding commercial spawn-on-kelp). LRP= limit reference point. B_0 = unfished biomass. Figure adapted from DFO (2019).

19.4. Factors influencing trends in herring biomass

The biomass of Pacific Herring in three major stock areas (HG, CC and WCVI) experienced prolonged periods of low biomass in the absence of fishing (DFO 2019). The SOG has been open to fishing and has seen record high biomass estimates. Consideration of these biomass trends in combination with common trends in herring weight-at-age observed for all stock areas suggests that large-scale factors may also be influencing herring population trends. Changes in environment, food supply and quality, predator abundance, and competition are factors that could affect trends in herring biomass and weight-at-age (Schweigert et al. 2010, Hay et al. 2012).

Pacific Herring are zooplanktivorous, consuming primarily euphausiids (krill) and some copepods (Wailes 1936). Changes in ocean conditions, such as temperature or currents, could affect the amount and types of prey available. For example, a northerly current direction could result in the presence of California current waters off the WCVI, bringing California Current zooplankton species that have a lower energetic value, creating poorer feeding conditions for herring (Schweigert et al. 2010, Mackas et al. 2004). In addition, Tanasichuk (2012) related WCVI herring recruitment to the biomass of euphausiids.

There are a wide variety of herring predators, including Pacific Hake, Lingcod, Spiny Dogfish, Pacific Cod, Sablefish, Arrowtooth Flounder, Pacific Halibut, Steller Sea Lions, Northern Fur Seals, Harbour Seals, California Sea Lions, and Humpback Whales (Schweigert et al. 2010). Off the WCVI, fish predator abundance has decreased in recent years, while the abundance of most marine mammal predators has increased (Olesiuk 2008, Olesiuk et al. 1990). This has resulted in a relatively stable or slightly decreasing trend in the amount of WCVI herring consumed by predators since 1973 (Schweigert et al. 2010). Although a significant proportion of the herring population could be consumed annually by predation, trends in model estimates of natural mortality of WCVI herring were not found to be directly attributable to trends in estimates of predation (Schweigert et al. 2010). Herring recruitment, however, has been correlated with piscivorous hake biomass (piscivorous hake are those hake that are large enough to consume herring), suggesting that predation may be an important factor influencing WCVI herring recruitment (Tanasichuk 2012).

19.5. Implications of trends

Trends in herring biomass have implications for both fisheries and predators. Pacific Herring comprise an important component of commercial fisheries in British Columbia. Fisheries Management uses forecasts of herring biomass, in conjunction with decision tables, performance metrics (including LRPs), and harvest rates to set total allowable catches.

Trends in herring biomass have implications for herring predators, such as fish, marine mammals and seabirds. The relative importance of herring in each predator’s diet varies; however, herring may represent up to 88% of Lingcod diet (Pearsall and Fargo 2007), 40% of Pacific Cod and Pacific Halibut diets (Ware and McFarlane 1986), and 35% to 45% of pinniped diets (Olesiuk et al. 1990, Womble and Sigler 2006, Trites et al. 2007, Olesiuk 2008). Depending on the level of diet specialization and ability to switch to alternate prey, herring abundance and condition may affect predators’ growth and abundance. Time series of diets of animals in this ecosystem would improve our ability to examine temporal trends in predator-prey interactions and implications of those trends.

19.6. References

DFO. 2019. Status of Pacifc Herring (*Clupea pallasii*) in 2018 and forecast for 2019. DFO Can. Sci. Advis. Sec. Sci. Resp. 2019/001.

Hay, D., Schweigert, J., Boldt, J., Cleary, J., Greiner, T.A. and Hebert, K. 2012. Decrease in herring size-at-age: a climate change connection? Pages 66-69 In: Irvine, J.R. and Crawford, W.R. 2012. State of the physical, biological, and selected fishery resources of Pacific Canadian marine ecosystems in 2011. DFO Can. Sci. Advis. Sec. Res. Doc. 2012/072. xi +142 p.

Mackas, D.L., Peterson, W.T., and Zamon, J.E. 2004. Comparisons of interannual biomass anomalies of zooplankton communities along the continental margins of British Columbia and Oregon. Deep-Sea Research II, 51: 875-896.

Olesiuk, P.F. 2008. Abundance of Steller sea lions (*Eumatopias jubatas*) in British Columbia. DFO Can. Sci. Advis. Sec.Res. Doc. 2008/063. iv + 29 p.

Olesiuk, P. F., Bigg, M. A., Ellis, G.M., Crockford, S.J., and Wigen, R.J. 1990. An assessment of the feeding habits of harbour seals (*Phoca vitulina*) in the Strait of Georgia, British Columbia, based on scat analysis. Canadian Technical Report of. Fisheries and Aquatic Sciences, 1730. 135 p.

Pearsall, I.A., and Fargo, J.J. 2007. Diet composition and habitat fidelity for groundfish assemblages in Hecate Strait, British Columbia. Canadian Technical Report of Fisheries and Aquatic Sciences, 2692. 149 p.

Schweigert, J.F., Boldt, J.L., Flostrand, L., and Cleary, J.S. 2010. A review of factors limiting recovery of Pacific herring stocks in Canada. ICES J. Mar. Sci. 67:1903-1913.

Tanasichuk, R. 2012. Euphausiids and west coast Vancouver Island fish production. Pages 47-49 In: Irvine, J.R. and Crawford, W.R. 2012. State of the physical, biological, and selected fishery resources of Pacific Canadian marine ecosystems in 2011. DFO Can. Sci. Advis. Sec. Res. Doc. 2012/072. xi +142 p.

Trites, A. W., Calkins, D.G., and Winship, A.J. 2007. Diets of Steller sea lions (*Eumatopias jubatus*) in southeast Alaska, 1993–1999*.* Fishery Bulletin*,* 105: 234–248.

Wailes, G.H. 1936. Food of *Clupea pallasi* in southern British Columbia waters. Journal Biological Board of Canada, 1: 477–486.

Ware, D.M., and McFarlane, G.A. 1986. Relative impact of Pacific hake, sablefish and Pacific cod on west coast of Vancouver Island herring stocks. International North Pacific Fisheries Commission Bulletin, 47: 67–78.

Womble, J.N., and Sigler, M.F. 2006. Seasonal availability of abundant, energy-rich prey influences the abundance and diet of a marine predator, the Steller sea lion *Eumatopias jubatus*. Marine Ecology Progress Series, 325: 281–293.

20. WCVI SMALL-MESH MULTI-SPECIES BOTTOM TRAWL SURVEYS (TARGET SPECIES: SMOOTH PINK SHRIMP): 2018 UPDATE

R. Ian Perry[1], Ken Fong[2], Brenda Waddell[2]

[1]Fisheries & Oceans Canada, Pacific Biological Station, Nanaimo, B.C., and Institute of Ocean Sciences, Sidney, B.C. Ian.Perry@dfo-mpo.gc.ca

[2]Fisheries & Oceans Canada, Pacific Biological Station, Nanaimo, B.C. Ken.Fong@dfo-mpo.gc.ca, Brenda.Waddell@dfo-mpo.gc.ca

20.1. Highlights

- Smooth Pink Shrimp biomass in Areas 124-125 continued to decline from its peak in 2014, with anomalies in 2018 well below the climatological (1981-2010) mean.
- A statistically significant relationship exists between the sea surface temperature (SST) at Amphitrite Point in Year *i* – 2, the biomass of Pink Shrimp in Year *i* – 1, and the sampled biomass of Smooth Pink Shrimp in Year *i*.
- Using this relationship, Smooth Pink Shrimp Biomass for 2019 is forecast to increase slightly from its value in 2018.
- Among the well-sampled finfish taxa, Lingcod and Eulachon continued to have negative biomass anomalies; biomass anomalies for all other well-sampled fish taxa remained positive
- The biomass composition of "well-sampled" taxa in 2017 and 2018 was similar, but was different from 2009-2015.

20.2. Description of the time series

Fishery-independent bottom trawl surveys using a small-mesh net (targeting the Smooth Pink Shrimp *Pandalus jordani*) have been conducted annually during May since 1973 in two regions, and since 1996 in three regions, off the west coast of Vancouver Island (Figure 20-1). The survey masks for these regions, over which the total biomass of each species has been estimated, generally occur between the 100m and 200m isobaths for Areas 124 and 125. A different vessel was used for the survey in 2017 and 2018.

This small-mesh multi-species bottom trawl survey was designed to target Smooth Pink Shrimp on the shrimp fishing grounds (Figure 20-1). The interannual variability of biomass estimates of other taxa caught along with Smooth Pink Shrimp depend on whether these other taxa are highly mobile in and out of the survey area or are highly patchy in their distribution. An autocorrelation analysis was used to identify 14 "well-sampled" taxa (i.e. which have positive autocorrelations of at least a one year lag; Table 20-1) out of the 36 taxa that have been regularly sampled and identified to species on this survey. Data are calculated as the total biomass over the survey area and are presented as standardised (by the standard deviation) $\log_{10}$-scaled species anomalies from the climatological period 1981-2010.

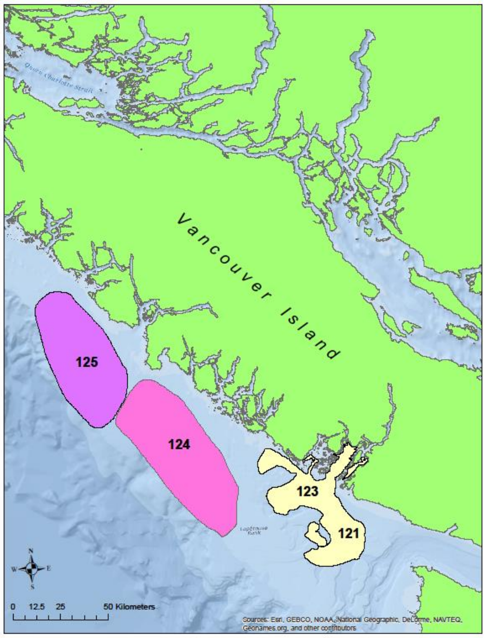

Figure 20-1. Map showing the three main shrimp (Pandalus jordani) fishing grounds and survey areas off Vancouver Island. The Nootka (Area 125) and Tofino (Area 124) Grounds have been surveyed since 1973. The area off Barkley Sound (Areas 23, 121 and 123) has been surveyed since 1996.

Table 20-1. List of 'core' species which have been sampled and identified routinely during these small mesh surveys since 1973 and for which annual biomass estimates are calculated. Taxa in blue are those with significant (p<0.05) autocorrelations and which are therefore considered to be "well-sampled" by this survey.

Pelagics	Demersals		Benthics
Pacific Hake	Silvergrey Rockfish	Pacific Cod	Sea Mouse
American Shad	Darkblotch Rockfish	Sablefish	Heart Urchin
Pacific Herring	Green Rockfish	Lingcod	Sea Urchins
Eulachon	Yellowtail Rockfish	Ratfish	Sea Cucumber
Dogfish	Boccacio	Smooth Pink Shrimp	
Walleye Pollock	Canary Rockfish	Dover Sole	
	Redstripe Rockfish	Pacific Sanddab	
	Pacific Ocean Perch	Petrale Sole	
	Arrowtooth Flounder	Rex Sole	
	English Sole	Flathead Sole	
	Pacific Halibut	Slender Sole	
	Yelloweye Rockfish	Spot Prawn	

20.3. Status and Trends

There is a significant statistical relationship (accounting for 48% of the variance) between the biomass of Smooth Pink Shrimp in a year and two variables: the biomass of Shrimp in the previous year, and the annual average of sea surface temperature two years previous (Figure 20-2). Using this relationship with Amphitrite Point sea surface temperature (SST) in 2017 and the biomass of Smooth Pink Shrimp in Areas 124+125 in 2018, the forecast indicates a slight increase in Smooth Pink Shrimp biomass in Areas 124+125 in 2019, although with very wide 95% confidence intervals (Figure 20-3).

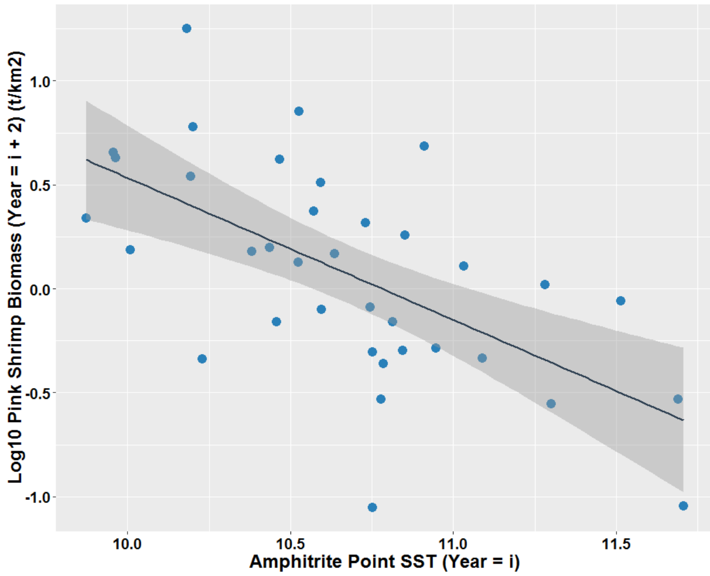

Figure 20-2. Regression relationship between Sea Surface Temperature (SST) at Amphitrite Point in year i versus the log_{10} biomass of Smooth Pink Shrimp two years later (in year i + 2). The full regression equation included the biomass of Smooth Pink Shrimp in year i +1: R^2= 0.48, P<0.001.

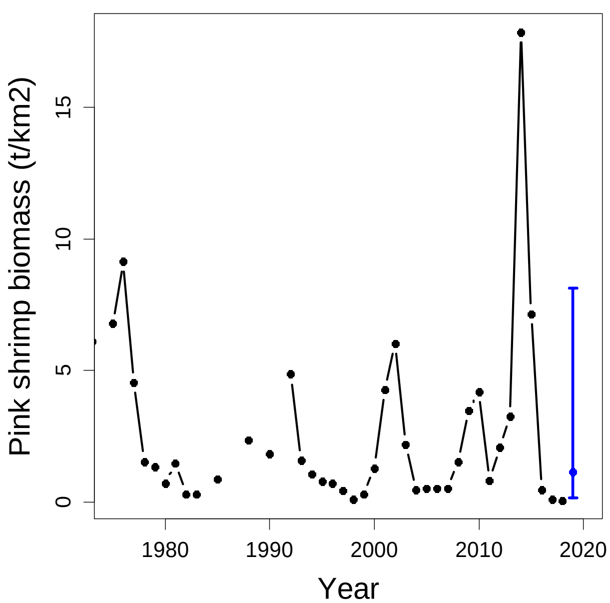

Figure 20-3. Annual biomass of Smooth Pink Shrimp in Areas 124+125 off the west coast of Vancouver Island as determined by these surveys. The blue dot and 95% confidence interval (vertical line) at 2019 represents the biomass predicted from the above multiple regression.

Surveys in May 2018 found the biomass of *Pandalus jordani* shrimp off central Vancouver Island had declined from the record high level observed in 2014, and was now a substantial negative anomaly (Figure 20-4). Only two other species had negative biomass anomalies in 2017 and 2018: Lingcod and Eulachon. The biomass anomalies of Arrowtooth Flounder declined in 2018 but have remained mostly positive since 2000. The biomass anomalies of Walleye Pollock in 2018 remained among the highest of its time series (Figure 20-4). Other finfish species with record or near-record high positive biomass anomalies in 2018 were Pacific Cod, Sablefish, Petrale Sole, Rex Sole, Dover Sole, Flathead Sole and Slender Sole. A cumulative anomaly index (calculated by stacking the anomalies for each species in each year and then adding them) illustrates that anomalies for most species were negative from 1973 to 1999, and have been mostly positive since 2000 with a slight negative period from 2006-2008 (Figure 20-5). The years 2017 and 2018 had among the highest cumulative biomass anomalies of the time series. Negative biomass anomalies occurred for Smooth Pink Shrimp, Lingcod, Eulachon and Sea Cucumber (Figure 20-5).

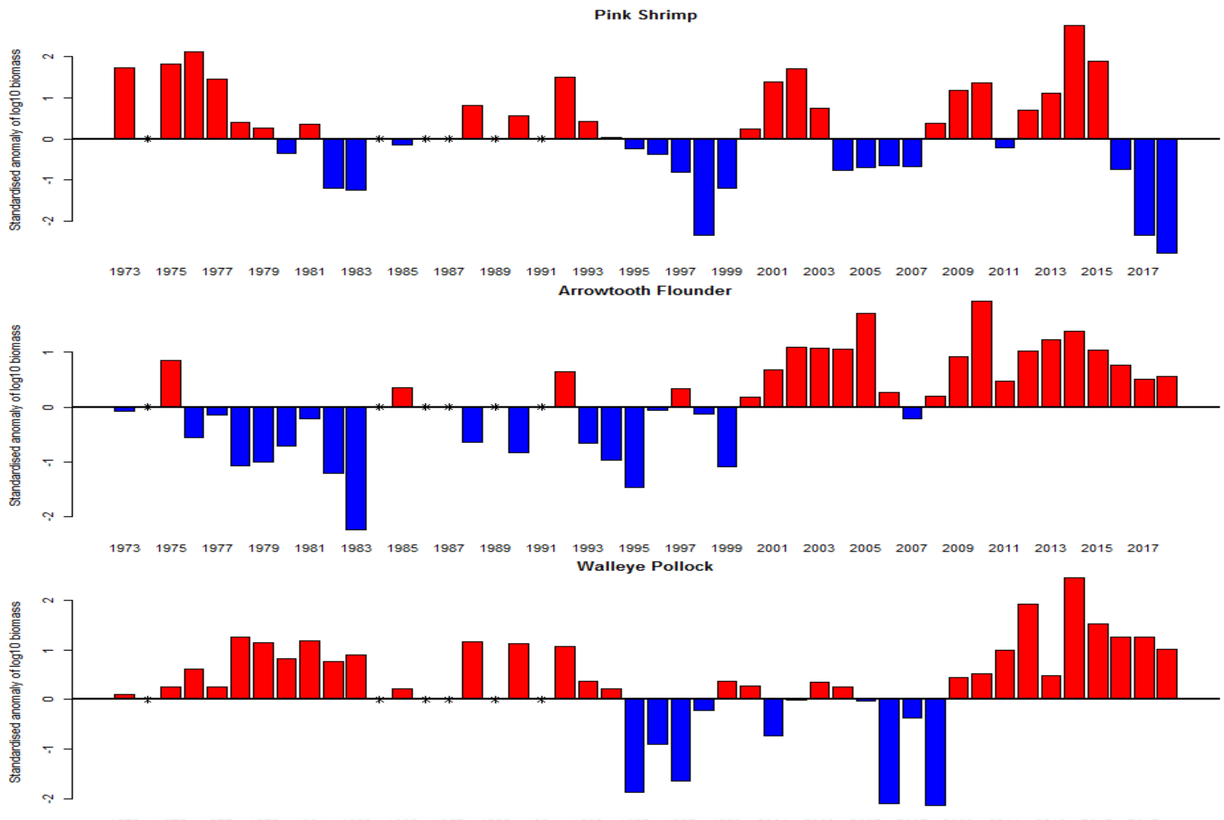

Figure 20-4. Standardised (by the standard deviation) anomalies of log$_{10}$ species biomass for three of the "well-sampled" taxa. Climatology period is 1981-2010.

20.4. Factors influencing these trends

Potential causes for the observed trends are under investigation. Climate and environmental factors are expected to be the main drivers of trends over this length of time. The negative regression relationship between Smooth Pink Shrimp biomass and Sea Surface Temperature two years previously is consistent with the life cycle of these shrimp, in which they are recruited to this survey gear mostly by age 2. Temperature may have a direct effect on the survival of larval shrimp (with cooler temperatures being favoured) and/or temperature serves as a proxy for other processes taking place (e.g. example, increased abundances of predators on larval shrimp when conditions are warmer). The additional inclusion in this regression relationship of the Smooth Pink Shrimp Biomass in the previous year represents the fact that this survey captures Smooth Pink Shrimp predominately of ages 2 and 3.

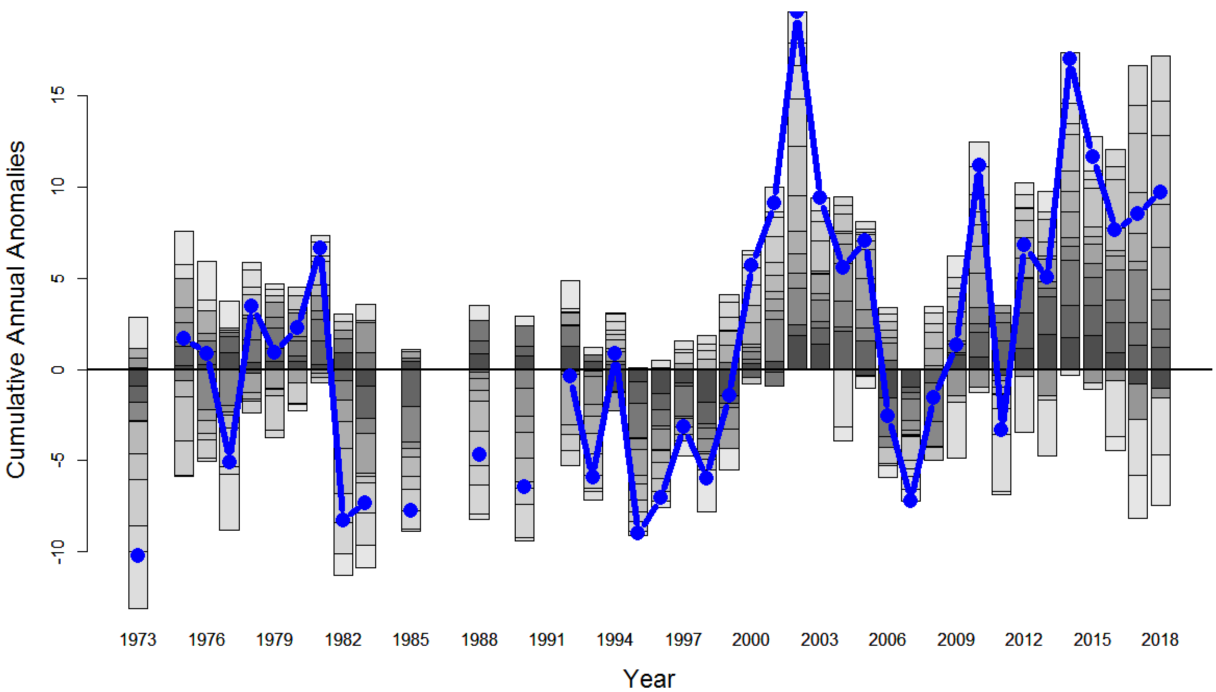

Figure 20-5. Cumulative anomaly index for the "well-sampled" taxa. The climatology period is 1981-2010. Individual shaded boxes represent the anomalies (positive or negative) for each of these "well-sampled" 16 taxa (see Table 20-1).

20.5. Implications of these trends

Many of the species considered to be "well-sampled" by this survey are of commercial interest. Considered collectively (Figure 20-5), biomass anomalies of many of these taxa have been largely positive since 2000. The implication is that groundfish biomass off the west coast of Vancouver may also have increased compared with the 1980s and 1990s, at least for these selected species in these small areas surveyed with sandy bottom types that are the preferred habitat for Smooth Pink Shrimp. This is under investigation.

21. A REVIEW OF GROUNDFISH SURVEYS IN 2018 AND AN INTRODUCTION TO THE GROUNDFISH DATA SYNOPSIS REPORT

Sean C. Anderson and Greg D. Workman, Fisheries & Oceans Canada, Pacific Biological Station, Nanaimo, B.C. Sean.Anderson@dfo-mpo.gc.ca, Greg.Workman@dfo-mpo.gc.ca

21.1. Highlights

- The dominant species from trawl surveys off the west coast of Vancouver Island were North Pacific Spiny Dogfish, Sharpchin Rockfish, Sablefish, Splitnose Rockfish and Canary Rockfish. Off the west coast of Haida Gwaii, the dominant species were Pacific Ocean Perch, Sharpchin Rockfish, Rougheye/Blackspotted Rockfish Complex, Silvergray Rockfish, and Shortspine Thornyhead.
- Notable trends in abundance included the return of North Pacific Spiny Dogfish to the west coast of Vancouver Island after an absence of about four years, and increases in the abundance indices for Boccacio Rockfish, Sablefish, Petrale Sole, Flathead Sole, and Longspine Thornyhead. We also observed decreases in abundance indices in some areas for Arrowtooth Flounder, Pacific Cod, Silvergray Rockfish, and Lingcod.
- This year, the Groundfish Section introduced a fully automated and reproducible synopsis report that gives a snapshot of population and fishing trends, growth and maturity patterns, as well as data availability, for 113 fish species (CSAS in press; draft available at https://github.com/pbs-assess/gfsynopsis).

21.2. Description of the time series

21.2.1. Fisheries-independent groundfish surveys

The Fisheries and Oceans Canada (DFO) Groundfish Section conducts a suite of randomized surveys using bottom trawl, longline hook and longline trap gear that, in aggregate, provide coverage for all offshore waters of Canada's Pacific Coast (Figure 21-1). Two multi-species synoptic bottom trawl surveys are conducted each year. Surveys in Queen Charlotte Sound (QCS) and Hecate Strait (HS) alternate with surveys on the West Coast of Vancouver Island (WCVI) and the West Coast of Haida Gwaii (WCHG) (WCHG and WCVI were conducted in 2018). In addition to the bottom trawl surveys, two Hard Bottom Longline (HBLL) surveys are conducted. One survey is conducted in "inside" waters (east of Vancouver Island) while the second is conducted in "outside" waters (everything else). Each year the surveys alternate between northern and southern areas (the southern areas were surveyed in 2018). Lastly, a coast-wide longline trap survey targeting sablefish (Sablefish Research and Assessment Survey) is conducted every year.

The randomized surveys follow depth-stratified designs and have in common full enumeration of the catches (all catch sorted to the lowest taxon possible), size and sex composition sampling for most species, and more detailed biological sampling of selected species. Most of the surveys are conducted in collaboration with the commercial fishing industry under the authorities of various collaborative agreements. In addition to the random depth-stratified surveys, the Groundfish Section conducts a hydroacoustic assessment of Pacific Hake and collects additional information from a DFO Small-Mesh Multi-species Bottom Trawl Survey (fixed-station survey of commercially important shrimp grounds off the West Coast of Vancouver Island and eastern Queen Charlotte Sound) and the International Pacific Halibut Commission (IPHC) Setline Survey.

21.2.2. **The groundfish data-synopsis report**

The above-mentioned surveys, combined with 100% at-sea and dockside monitoring of the commercial fleets, results in large quantities of data relevant to groundfish species in BC. Historically, however, the Groundfish Section has lacked the capacity to regularly report on most of these data through formal stock assessments. This year, the Groundfish Section developed a reproducible “synopsis” report that gives a snapshot of population and fishing trends, growth and maturity patterns, as well as data availability, for 113 species of relevance to the Groundfish Section.

The Groundfish Section had a number of goals in developing the synopsis report. First, the report aims to facilitate regular review by groundfish scientists and managers of trends in survey indices and stock composition. Second, through the tools developed to produce the report, the project aims to generate standardized datasets and visualizations that will help assessment scientists develop stock assessments and conduct groundfish research. Third, it aims to increase data transparency between Fisheries and Oceans Canada, the fishing industry, non-governmental organizations, and the public.

The report is structured to facilitate viewing all data for one species simultaneously and to quickly browse the data holdings for multiple species. The report starts with clickable indexes sorted by species code, common name, and scientific name. Then, following a series of figure captions, the report visualizes most available survey, fisheries, and biological sample data for each of the 113 species in the same two-page layout for each species (e.g., Figure 21-2). The first page for each species includes visualizations showing timeseries and maps of relative biomass from the surveys, commercial fisheries catch categorized by gear type and region, and standardized commercial catch per unit effort from the commercial bottom-trawl fleet. The second page for each species focuses on biological samples. The page starts with length and age distributions, shows length-age and length-weight growth model fits, and shows age- and length-at-maturity model fits. The second page concludes with graphical tables illustrating the number of fish specimens that have had their length, weight, age, or maturity assessed as well as the number of available aging structures (usually otoliths) by year across all surveys and commercial samples. The main visualizations are followed by detailed appendices explaining the data processing and model fitting approaches.

All the data extraction, data manipulation, model fitting, and visualization for the report are automated and reproducible. The Groundfish Section plans to publish an updated version of the report every one to two years. The report has been accepted as a CSAS Research Document and is currently undergoing final formatting and translation. In the meantime, a draft can be downloaded at https://github.com/pbs-assess/gfsynopsis. It is important to note that the report outputs are not a substitute for stock assessment; many important caveats to consider are listed in the report.

21.3. Status and trends

The dominant species from trawl surveys off the west coast of Vancouver Island were North Pacific Spiny Dogfish (*Squalus suckleyi*), Sharpchin Rockfish (*Sebastes zacentrus*), Sablefish

(*Anoplopoma fimbria*), Splitnose Rockfish (*Sebastes diploproa*) and Canary Rockfish (*Sebastes pinniger*) (Figure 21-3). Off the west coast of Haida Gwaii, the dominant species were Pacific Ocean Perch (*Sebastes alutus*), Sharpchin Rockfish, Rougheye/Blackspotted Rockfish Complex (*Sebastes aleutianus/melanostictus*), Silvergray Rockfish (*Sebastes brevispinis*), and Shortspine Thornyhead (*Sebastolobus alascanus*) (Figure 21-3).

Notable trends in abundance included the return of North Pacific Spiny Dogfish to the west coast of Vancouver Island after an absence of about four years and increases in the abundance indices for Bocaccio Rockfish (*Sebastes paucispinis*), Sablefish, Petrale Sole (*Eopsetta jordani*), Flathead Sole (*Hippoglossoides elassodon*), and Longspine Thornyhead (*Sebastolobus altivelis*) (Figure 21-3). We also observed decreases in abundance indices in some areas for Arrowtooth Flounder (*Atheresthes stomias*), Pacific Cod (*Gadus macrocephalus*), Silvergray Rockfish, and Lingcod (*Ophiodon elongatus*) (Figure 21-3).

21.4. Factors influencing trends

There are many potential causes for observed trends including the direct impacts from fishery removals, climate change, and increasing benthic anoxia (oxygen dead zones). A more comprehensive analysis than is presented here is required to tease apart the various influences on survey trends.

21.5. Implications of trends

While there do appear to be persistent trends for some species in several of these survey time series, they cannot be taken to represent stock status on their own. These indices must be incorporated into comprehensive stock assessment analyses before conclusions can be drawn about stock status.

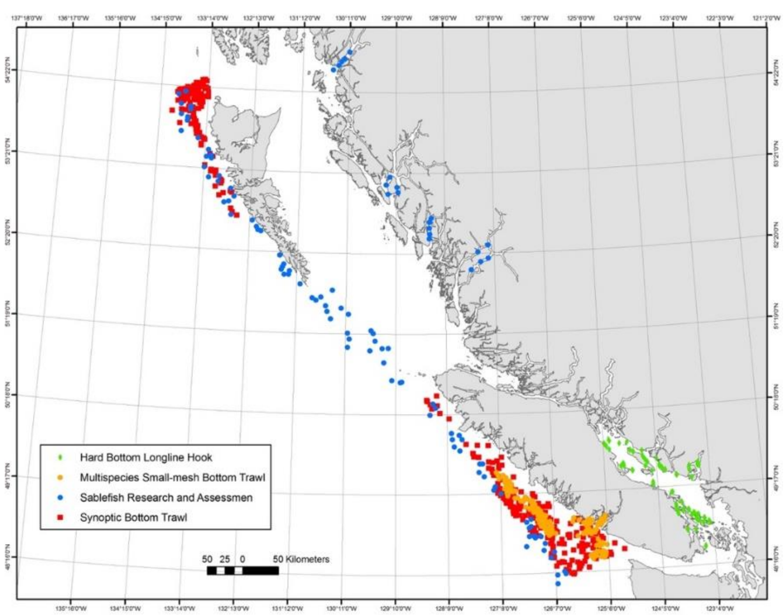

Figure 21-1. Survey set locations of the 2018 groundfish surveys. Note that the Hard Bottom Longline Survey (outside, south) and the International Pacific Halibut Commission Setline Survey are not shown here.

5.49 SILVERGRAY ROCKFISH

Sebastes brevispinis (405)
Order: Scorpaeniformes, Family: Scorpaenidae, FishBase link, WoRMS link
Last Research Document: Starr et al. (2016)
Last Science Advisory Report: Fisheries and Oceans Canada (2014b)

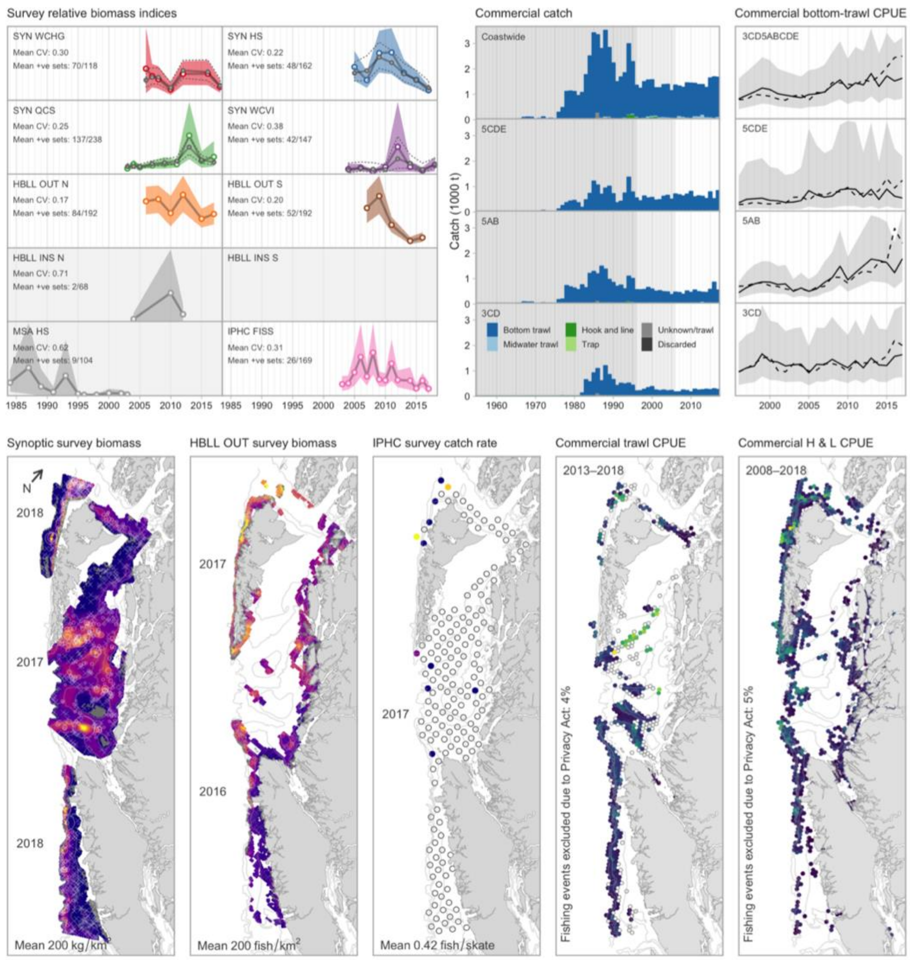

Figure 21-2. Example page (one of two per species) from the groundfish data synopsis report for Silvergray Rockfish. The first page for each species includes species-specific metadata (top), relative biomass index trends from surveys (top left), modeled survey biomass or abundance in space (lower row). A second page for each species (not shown) includes information on biological samples such as growth and maturity; see https://github.com/pbs-assess/gfsynopsis.

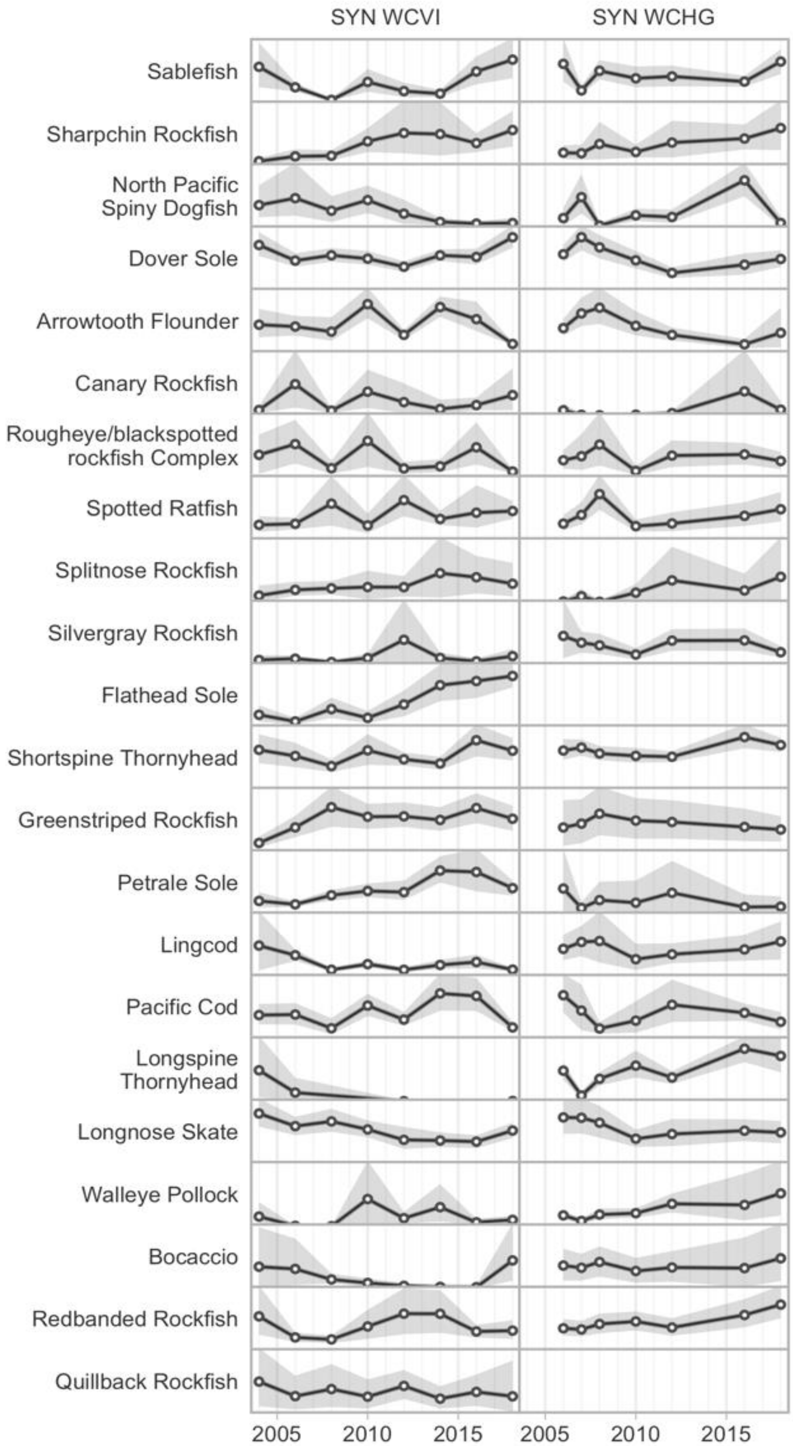

Figure 21-3. Selected annual relative biomass indices from the West Coast Vancouver Island and West Coast Haida Gwaii Synoptic Bottom Trawl surveys (SYN WCVI and SYN WCHG, respectively). Mean estimates are shown with dots and lines and 95% bootstrap confidence intervals are shown with shaded regions. Species are ordered by total relative biomass in 2018 across both surveys. Time series are scaled to have the same maximum upper confidence interval values.

22. SEABIRD OBSERVATIONS ON THE OUTER B.C. COAST IN 2018

Mark Hipfner

Environment and Climate Change Canada, Wildlife Research Division, Pacific Wildlife Research Centre, Delta, B.C., Mark.Hipfner@canada.ca

22.1. Highlights

- Cassin's Auklets had a near-average breeding season in 2018 relative to the 1996-2017 baseline on the world's largest colony on Triangle Island, as expected based on the neutral state of the Pacific Decadal Oscillation.
- Overall, there was little juvenile salmon in diets fed to nestling Rhinoceros Auklets on Pine, Triangle and Protection islands in 2018, but amounts at Lucy Island were the highest in twelve years of study.

22.2. Growth rates of Cassin's Auklet nestlings

Like other breeding parameters, growth rates of nestling Cassin's Auklets (*Ptychoramphus aleuticus*) are affected very strongly by oceanographic conditions, which have a profound influence on seasonal patterns of prey availability. In general, nestling auklets grow more quickly on Triangle Island, the world's largest breeding colony, in cold-water, PDO-negative years when the subarctic copepod *Neocalanus cristatus* persists in their diets through the bulk of the provisioning period from mid-May to late June (Hipfner 2008, Hipfner et al. ms in review). Growth rates in the 2018 season were close to the long-term (1996-2017) average in 2018, as would be expected from the neutral state of the PDO over the preceding winter and spring (Figure 22-1).

22.3. Salmon in Rhinoceros Auklet diets

Pacific salmon (*Oncorhynchus* spp.) have an anadromous life-cycle, spending a few months to 2 years in freshwater, followed by 1-4 years at sea where they fall prey to a variety of fish, mammals and birds. Mortality rates during the marine phase of the life cycle of Pacific salmon generally exceed 90%, and it is widely believed that most mortality is due to predation in the first few weeks to months following ocean entry (Beamish and Mankhen 2001). On their northerly seaward migration, the vast majority of pink salmon (*O. gorbuscha*), chum salmon (*O. keta*) and sockeye salmon (*O. nerka*) smolts from stocks in southern and central British Columbia funnel past aggregations of hundreds of thousands of Rhinoceros Auklets (*Cerorhinca monocerata*) breeding on colonies scattered along the province's Central and

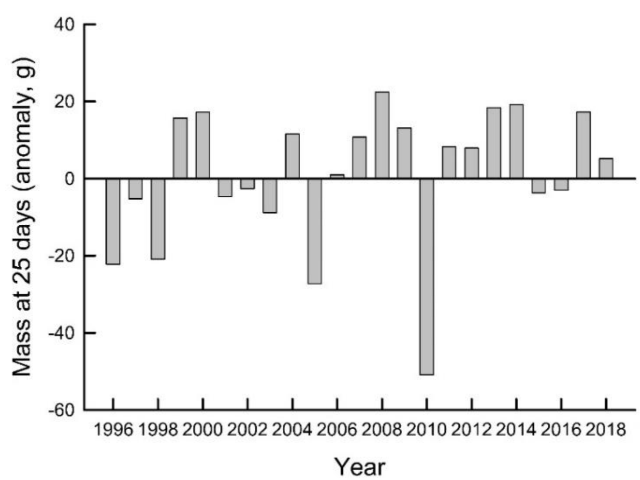

Figure 22-1. Yearly anomalies of mean 25 day mass (a proxy for growth rate) of nestling Cassin's Auklets on Triangle Island, BC, in 1996-2018.

North coasts. The auklets are wing-propelled, pursuit-diving seabirds that forage mainly in the top 5-10m of the water column and within ~90 km of their breeding colonies. The smolts' migration occurs in June and July, coinciding with the period when the auklets are delivering whole and intact fish, including salmon smolts, to their nestlings.

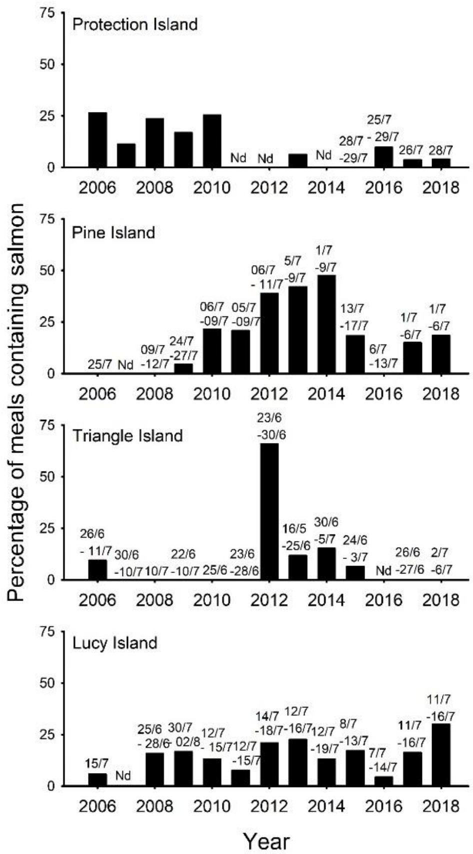

Figure 22-2. Percentage of meals delivered to nestling Rhinoceros Auklets that included one or more salmon (pink, chum, or sockeye) on 3 colonies in BC, Triangle, Pine and Lucy islands, and on Protection Island, WA, in 2006-2018. Dates of sampling (day/month) are indicated above the bars.

Scientists with Environment Canada and Fisheries and Oceans Canada have been quantifying predation by Rhinoceros Auklets on salmon smolts since 2006, and some clear patterns have emerged. First, there is marked temporal and spatial variation in the importance, and species and stock composition, of salmon in nestling diets. In general, salmon is most important at Pine Island; in 2018, the amount of salmon in diets was quite low (Figure 22-2). Salmon has been less important overall and less variable in diets at Lucy Island, but the amount present in 2018 was the highest of any year through the study period. Salmon was an important component of auklet nestling diets at Triangle Island only in 2012 (largely Fraser River sockeye), and was absent altogether in 2018 sampling. Our collaborators in Washington State have been tracking diets of Rhinoceros Auklets at Protection Island over the same time period, and salmon was uncommon in auklet nestling diets there in 2018. An analysis of the species and stock composition of the salmon component of the auklets' diet through the study period is underway.

22.4. References

Beamish, R.J. & Mahnken, C. 2001. A critical size and period hypothesis to explain natural regulation of salmon abundance and the linkage to climate and climate change. Prog. Oceanogr. 49: 423-437.

Hipfner, J.M. 2008. Matches and mismatches: ocean climate, prey phenology and breeding success in a zooplanktivorous seabird. Mar. Ecol. Progr. Ser. 368: 295-304.

Hipfner, J.M., Galbraith, M., Bertram, D.F. & Green, D.J. Ms. in review. Basin-scale oceanographic processes, zooplankton community structure, and diet and reproduction of a sentinel North Pacific seabird over a 22-year period.

23. COASTAL ICE-OCEAN PREDICTION SYSTEM (CIOPS-W): A SNAPSHOT OF NORTHEAST PACIFIC CONDITIONS IN 2018

Hauke Blanken[1], Jean-Philippe Paquin[2], Youyu Lu[1], Gregory Smith[2], Stephanne Taylor[1]

[1]Fisheries and Oceans Canada, Sidney, BC & Dartmouth, NS, Hauke.Blanken@dfo-mpo.gc.ca; Youyu.Lu@dfo-mpo.gc.ca; Stephanne.Taylor@dfo-mpo.gc.ca

[2]Environment and Climate Change Canada, Dorval, QC, Jean-Philippe.Paquin@canada.ca; Gregory.Smith2@canada.ca

23.1. Highlights

- A novel regional ocean operational forecasting system, the Coastal Ice-Ocean Prediction System for Canada's west coast (CIOPS-W), has been developed and will be put into daily operations in summer 2019.
- Comparison of CIOPS-W against temperature and salinity observed in 2018 shows that the system offers good representation of spatial and temporal variations of these water properties.
- CIOPS-W can be used to supplement and aid in interpretation of observational data for future State of the Pacific Ocean reporting.

23.2. CIOPS-W Overview

An operational oceanographic forecasting system named the Coastal Ice Ocean Prediction System for Canada's west coast (CIOPS-W) has been developed through a collaboration of Fisheries and Oceans Canada (DFO) and Environment and Climate Change Canada (ECCC) with the primary purpose of supporting enhanced maritime safety and drift prediction. After several years of development the system was subjected to a rigorous performance evaluation in the fall of 2018 prior to implementation into daily forecasting operations at the Canadian Meteorological Centre, which is scheduled for mid 2019. Results pertaining to the system's ability to forecast ocean temperature and salinity in the northeast Pacific are presented here along with a general description of these water properties during 2018. The purpose here is to introduce the CIOPS-W system and encourage use of the model results beyond the objectives listed above, as the data may be suited for a wide variety of applications.

CIOPS-W is an implementation of the Nucleus for European Modelling of the Ocean (NEMO) ocean modelling system (https://www.nemo-ocean.eu/; Madec 2016) covering the coastal and shelf seas of British Columbia and the adjacent northeast Pacific (Figure 23-1). It has a nominal horizontal resolution of 1/36-degree in longitude/latitude (about 2.5 km grid spacing) and 75 vertical levels. CIOPS-W is linked to the pan-Canadian Regional Ice Ocean Prediction System (RIOPS), with a horizontal resolution of 1/12-degree (Dupont et al. 2015) through one-way nesting. RIOPS has recently been extended to incorporate the northeast Pacific and include a complicated methodology to assimilate observational data. CIOPS-W applies a less complicated and more computationally efficient spectral nudging method (Thompson et al. 2006, Wright et al. 2006) in the deep ocean off the shelf break, to ensure that the mean state and meso-scale eddies in CIOPS-W are consistent with the RIOPS solution, and the influence of the deep ocean on the shelf is realistically captured. Over the continental shelf and coastal waters, the CIOPS-W solution is unconstrained to take advantage of its ability to resolve finer structures of ocean variability. Atmospheric forcing is generated from ECCC's High-Resolution Deterministic Prediction System (HRDPS; Milbrandt et al. 2016) where available, and the Regional Deterministic Prediction System (RDPS) over the area outside of the HRDPS domain. More detailed descriptions of the CIOPS-W system will be given in upcoming publications to accompany the commencement of daily forecasting.

23.3. 2018 Modelled Temperature and Salinity and Performance Evaluation

The observed temperature and salinity in 2018 are well reproduced by the model, as indicated by comparison of CIOPS-W results against the CTD casts collected by DFO as well as from the ARGO program. Figure 23-2 shows the profiles of bias and root-mean-square error (RMSE) of modelled temperature and salinity minus observed values derived for 7 regions within the CIOPS-W model domain. Bias and RMSE are based on all available CTD casts in the regions. Biases in the deep ocean and on the continental shelf are small, less than 0.5ºC for temperature and 0.2 psu for salinity, and in the deep ocean are generally restricted to the upper 200 – 250m. Near the shelf break a slight warm bias exists in the upper 1500m. Some larger deviations are noted near the base of the mixed layer, which appears to be too shallow in the model results (not shown). Deviations between modelled and observed water properties are slightly larger in coastal regions such as the Salish Sea, the Strait of Juan de Fuca, and Hecate Strait, with the maximum biases reaching 1ºC and 1.5 psu. These are likely due to the model resolution not being able to resolve the details in coastline and topography, or inaccuracy in the river forcing. The model does capture the primary patterns of the evolution of the water masses. For example, the salty bias at depth in the Salish Sea is reduced significantly in the Strait of Juan de Fuca, suggesting that mixing of the entire water column takes place in the Gulf Islands.

A further example of model performance is given by comparing temperature and salinity measured along Line P in February 2018 to equivalent modelled values (Figure 23-3). The modelled and observed sections are a close visual match, though the modelled section is slightly smoother than the observations. The model clearly reproduces the subsurface temperature maximum observed in early 2018, which has been attributed to the NE Pacific marine heat wave of 2014-2016. The close match between model results and observations, and the generally strong performance of the model with respect to error metrics, suggests that CIOPS-W can be a useful resource for interpretation of observations of temperature and salinity in the northeast Pacific.

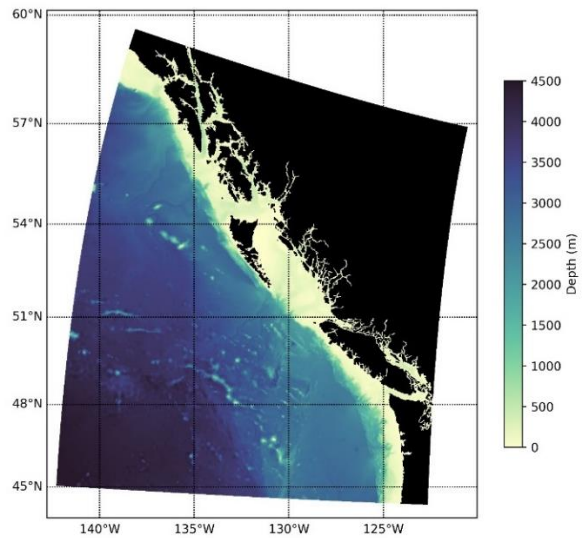

Figure 23-1. CIOPS-W model domain and bathymetry (color shading, in m).

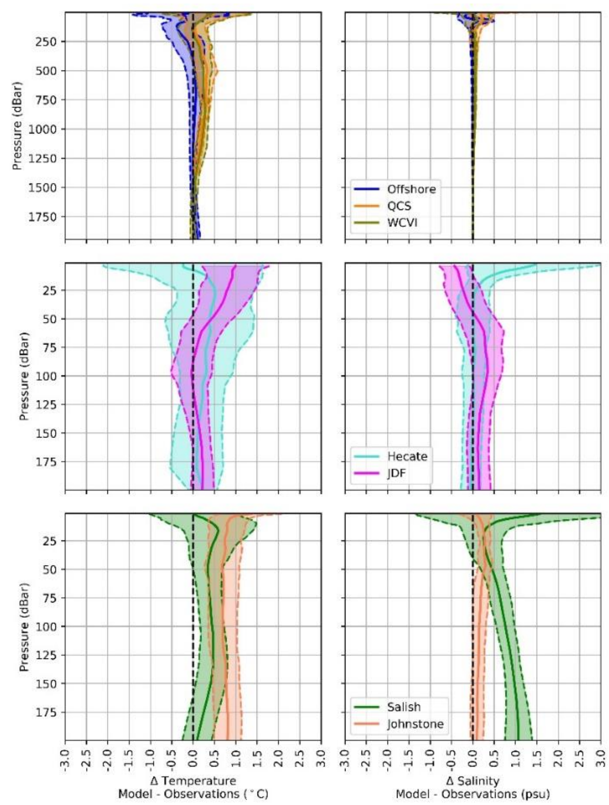

Figure 23-2. Bias (solid lines) and root-mean-square error (dashed lines) of modelled temperature (left) and salinity (right). Values are grouped for the deep ocean and continental shelf (top), coastal straits (Hecate Strait and Strait of Juan de Fuca, middle), and inshore seas (Salish Sea and Johnstone Strait, bottom).

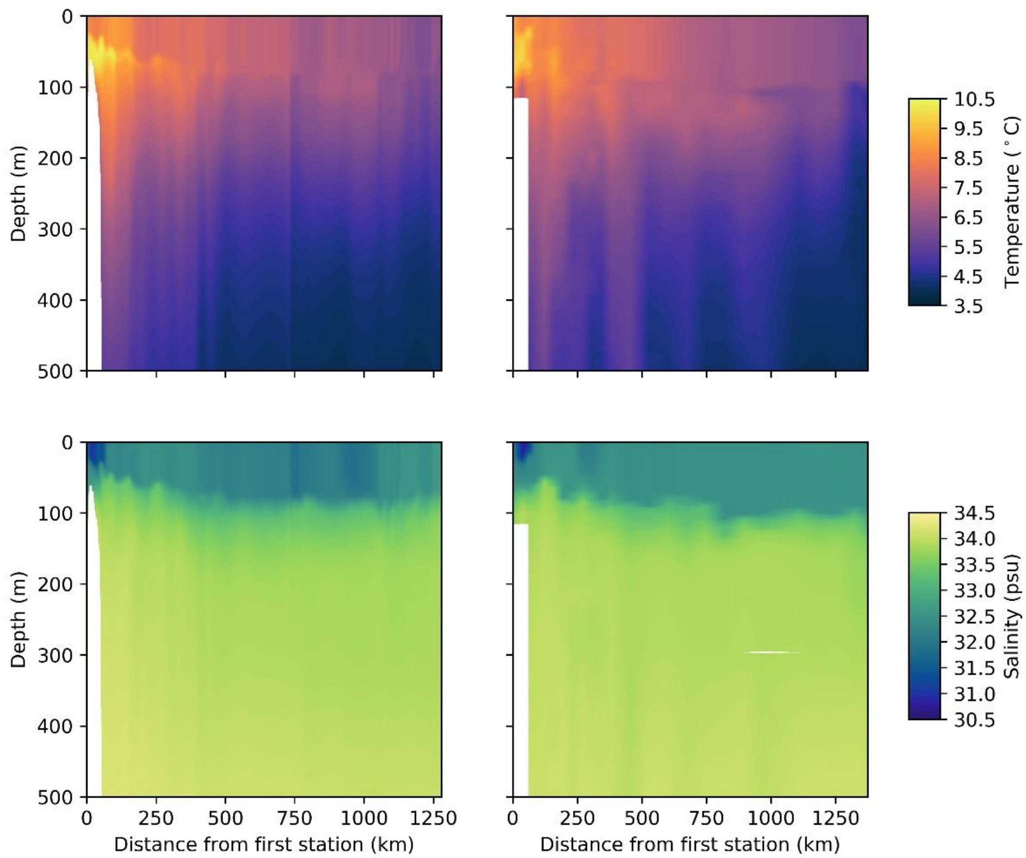

Figure 23-3. Modelled (left) and observed (right) temperature (top) and salinity (bottom) along Line P in February 2018, over the upper 500m of the water column. X-axis values are distance from station P1.

23.4. References

Madec, G. 2016. NEMO ocean engine, Note du Pole de modélisation, 27. https://zenodo.org/record/1472492#.XJ7FHSFKipo (accessed 29 March, 2019).

Dupont, F., Higginson, S., Bourdallé-Badie, R., Lu, Y., Roy, F., Smith, G.C., Lemieux, J.F., Garric, G., Davidson, F. 2015. A high-resolution ocean and sea-ice modelling system for the Arctic and North Atlantic oceans. Geosci. Model Dev. 8: 1577–1594.

Milbrandt, J.A., Bélair, S., Faucher, M., Vallée, M., Carrera, M.L., Glazer, A. 2016. The Pan-Canadian High Resolution (2.5 km) Deterministic Prediction System. Weather Forecast. 31: 1791–1816.

Thompson, K.R., Wright, D.G., Lu, Y., Demirov, E. 2006. A simple method for reducing seasonal bias and drift in eddy resolving ocean models. Ocean Modelling. 13: 109-125.

Wright, D.G., Thompson, K.R., Lu, Y. 2006. Assimilating long-term hydrographic observations in an eddy-permitting model of the North Atlantic. Journal of Geophysical Research. 111: C09022.

24. UNUSUAL EVENTS IN CANADA'S PACIFIC MARINE WATERS IN 2018

Jennifer Boldt[1], Peter Chandler[2]

[1] Fisheries & Oceans Canada, Pacific Biological Station, Nanaimo, B.C.

[2] Fisheries & Oceans Canada, Institute of Ocean Sciences, Sidney, B.C.

24.1. Highlights

- Unusual events occur in Canada's Pacific marine waters every year but are often not reported on or related to the broader environmental context.
- Some unusual events in 2018 that were reported include: late onset of fall/winter cooling, which led to marine heat waves; the blooms of algal species such as *Noctilua scintillans* and *Heterosigma akashiwo* were again observed in the Strait of Georgia (SOG) after a 3-year absence; the continued effect of the 2014-2016 marine heat wave on lower trophic level community composition; the continued presence of pyrosomes in BC waters (but lower abundance compared to 2017).

24.2. Description of the time series

Every year, unusual marine events occur in the Northeast Pacific: some are reported to DFO, many are not. These are often seen as "one-off" events, which are isolated from other events, in time, space, and by different observers. It is therefore difficult to make a complete story or a synthesis of such observations. However, if enough of these events are observed and reported, it may be possible to identify broader patterns and processes that collectively tell us how our marine ecosystems are changing and responding to diverse pressures. For example, the REDMAP (Range Extension Database and Mapping Project; http://www.redmap.org.au) program in Australia engages citizen scientists and the interested public to report their observations of unusual organisms and events to a structured network, which can subsequently be used in scientific (and other) publications (e.g. Pecl et al. 2014, Lenanton et al. 2017). The LEO network (www.leonetwork.org) is a network of local observers and topic experts who share knowledge about unusual animal, environmental and weather events.

This report presents a selection of unusual events in Canada's Pacific waters in 2018 that have been reported to DFO Science staff. Some of these events may be included in other short reports in this document, whereas other observations may not be presented in detail or at all. In addition, viewers of this poster during the State of the Ocean meeting were invited to provide their own observations of weird and wonderful unusual events, which are included in this report.

24.3. Status and trends

Observations in 2018 that were reported to DFO by participants at the 2019 State of the Pacific Ocean workshop are presented in Table 24-1.

In 2017, there was an explosion of the pyrosome *Pyrosoma altanticum* along the coast of B.C. Large masses of these gelatinous animals were first reported in October of 2016 (Galbraith and Young 2017) and were observed along the west coast of North America through 2017 (Perry et al. 2017, Perry et al. 2018, Grupe and Norgard 2018, Galbraith and Young 2018, Brodeur et al. 2018). In 2018, they were still present in BC waters (particularly along the continental shelf), but in lower abundances compared to 2017.

The community composition of zooplankton still reflects the 2014-2016 marine heat wave. In 2018, there was a late onset of fall/winter cooling leading to new marine heat waves, which will likely have additional effects on the zooplankton community.

After a 3-year absence in the Strait of Georgia there was a bloom of *Noctiluca scintillans*, which is not unusual, but had not been observed in 2015-2017. *Heterosigma akashiwo* caused a harmful algal bloom in the Strait of Georgia after also having a 3-year absence. This resulted in high finfish mortality at aquaculture sites in Jervis Inlet.

Table 24-1. 2018 Observations of weird, wonderful and/or unusual marine events reported during 2018 or reported at the 2019 State of the Pacific Ocean meeting.

Event	Where	When	Reported by	(Brief) Details
Late onset of fall/winter cooling	NE Pacific	Fall/winter 2017/2018	Tetjana Ross, DFO	Sea surface temperature remained ~14°C until mid-October at Station Papa. Ross, T., Fisher, J., Bond, N., Galbraith, M., and Whitney, F. 2019. The Northeast Pacific: Current status and recent trends. PICES Press Vol. 27, No. 1, pp. 36-39.
Bloom of *Noctiluca scintillans* after 3 year absence	SOG	April, May, and June, 2018 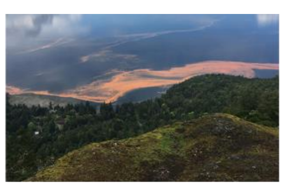 May 2, 2018, Salt spring Island	Svetlana Esenkulova, PSF	Not unusual, but not observed much in 2015-2017. Heterotrophic dinoflagellates; do not produce toxins but disrupt classic (from diatoms to zooplankton) energy transfer; produce ammonia, cause low dissolved oxygen.

Event	Where	When	Reported by	(Brief) Details
Unusual blooms of small dinoflagellate – cf *Gonyaulax* spp.	SOG	June, 2018  June 16, 2018, Pat Bay	Svetlana Esenkulova, PSF	Quite an unusual type of bloom for the SOG; not toxic.
Blooms of *Heterosigma akashiwo* after a 3-year absence	SOG	mostly June (some in May, July, August), 2018	Svetlana Esenkulova, PSF; Nina Nemcek, DFO	Toxic to fish and zooplankton; killed aquaculture salmon: 50% biomass mortality at two Grieg Seafood locations in Jervis Inlet.
Relatively early start of spring bloom	SOG	Feb-March, 2018	Jim Gower, DFO	Satellite images show bloom in Sechelt Inlet on Feb. 22 and March 1; may have seeded main bloom.
Intense spring bloom	WCVI (off Barkley Sound)	June-July, 2018 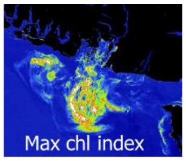	Jim Gower, DFO	Satellite image (June 16, 2018) shows patch of water off Barkley Sound, ~30km across, indicating presence of strong, near-surface plankton bloom.
Abundant young of year rockfish	WCVI	July 2017 & 2018	Jackie King & Jennifer Boldt, DFO	Juvenile rockfish unusually abundant (2017) and widely distributed (2017 and 2018), Integrated Pelagic Ecosystem survey, N & WCVI.
Northern Anchovy still abundant	SOG	Fall 2018	Jennifer Boldt, DFO	Proportion of SOG juvenile herring survey catches that contain Northern Anchovy was still high.

Event	Where	When	Reported by	(Brief) Details
Low abundance of large copepods	BC offshore	March-June, 2018	Sonia Batten, Pacific CPR survey	Lowest mean abundance of large copepods; 2nd highest of small copepods
Continued 'heat wave'-zooplankton community	BC Shelf	March-June, 2018	Sonia Batten, Pacific CPR survey	Larvae of benthic zooplankton more abundant and dominant.
Intense pCO_2 draw down in surface waters	Quadra Island field station, Northern Salish Sea	mid-late October, 2018	Wiley Evans, Hakai Institute	Broad draw down of pCO_2 was the strongest observed in the last 4 years.
Low nutrient concentrations	Western (deep) Johnstone Strait	Spring and summer, 2018	Hayley Dosser, UBC	Nitrate, silicate, phosphate were roughly 2 standard deviations below pre-2015 mean values

24.4. Factors influencing trends

Potential factors influencing these events include a changing climate, natural population changes and anthropogenic pressures. It is often difficult to establish whether these observations are part of a trend, a cycle or a singular event. Disease is a potential factor causing mortality, but is often overlooked or difficult to assess. As the climate changes, extreme weather will continue to be a factor in affecting marine biology (e.g. January 2018 storm; increasing sea-level).

It is typical of gelatinous zooplankton such as Pyrosomes to have a "boom and bust" population cycle (Galbraith and Young 2018). Brodeur et al. (2018) suggested that the Pyrosome explosion may have been a result of the ocean returning to normal temperatures after the warm "Blob" years as well as abundant food.

24.5. References

Brodeur, R., Perry, I., Boldt, J., Flostrand, L., Galbraith, M., King, J., Murphy, J., Sakuma, K. and Thompson, A. 2018. An unusual gelatinous plankton event in the NE Pacific: The great pyrosome bloom of 2017. PICES Press Vol. 26, No. 1.

Galbraith, M., and Young, K. 2017. Zooplankton along the B.C. continental margin in 2016. In: Chandler, P.C., King, S.A., and Boldt, J. (Eds.). 2017. State of the physical, biological and selected fishery resources of Pacific Canadian marine ecosystems in 2016. Can. Tech. Rep. Fish. Aquat. Sci. 3225: vi + 243 p.

Galbraith, M., and Young, K. 2018. Zooplankton along the B.C. continental margin in 2017. In: Chandler, P.C., King, S.A., and Boldt, J. (Eds.). 2018. State of the physical, biological and selected fishery resources of Pacific Canadian marine ecosystems in 2017. Can. Tech. Rep. Fish. Aquat. Sci. 3266: viii + 245 p.

Grupe, B., and Norgard, T. 2018. Offshore protected areas: Canada's oldest marine protected area and newest areas of interest. In Chandler, P.C., King, S.A., and Boldt, J. (Eds.). 2018. State of the physical, biological and selected fishery resources of Pacific Canadian marine ecosystems in 2017. Can. Tech. Rep. Fish. Aquat. Sci. 3266: viii + 245 p.

Lenanton, R., Dowling, C., Smith, K., Fairclough, D., and Jackson, G. 2017. Potential influence of a marine heatwave on range extensions of tropical fishes in the eastern Indian Ocean —Invaluable contributions from amateur observers. Regional Studies in Marine Science 13: 19–31.

Pecl, G., Barry, Y., Brown, R., Frusher, S., Gärtner, E., Pender, A., Robinson, L., Walsh, P., and Stuart-Smith, J. 2014. REDMAP: ecological monitoring and community engagement through citizen science. The Tasmanian Naturalist 136: 158:164.

Perry, R.I., Fong, K., and Waddell, B. 2017. WCVI small-mesh multi-species bottom trawl surveys (target species: Smooth Pink Shrimp): 2016 update. In: Chandler, P.C., King, S.A., and Boldt, J. (Eds.). 2017. State of the physical, biological and selected fishery resources of Pacific Canadian marine ecosystems in 2016. Can. Tech. Rep. Fish. Aquat. Sci. 3225: vi + 243 p.

Perry, R.I., Fong, K., and Waddell, B. 2018. WCVI small-mesh multi-species bottom trawl surveys (target species: Smooth Pink Shrimp): 2017 update. In Chandler, P.C., King, S.A., and Boldt, J. (Eds.). 2018. State of the physical, biological and selected fishery resources of Pacific Canadian marine ecosystems in 2017. Can. Tech. Rep. Fish. Aquat. Sci. 3266: viii + 245 p.

Individual reports on inside waters (including the Strait of Georgia)

25. RIVERS INLET WATER PROPERTIES IN 2018 COMPARED TO A 1951 TO 2018 TIME SERIES

Jennifer Jackson, Hakai Institute, Victoria, B.C., Jennifer.Jackson@hakai.org

25.1. Highlights

- Monthly oceanographic data have continued to be collected in Rivers Inlet, lengthening the time series from 1951 to 2019.
- Rivers Inlet deep water (140m to bottom) has been warmer than average since the fall of 2015 until at least March 2019 and this can be explained by the summer upwelling of offshore marine heatwave water along the 1026 kgm^{-3} isopycnal.
- Deep water upwelled into Rivers Inlet was hypoxic from August 2018 to February 2019, and this is the first time that was observed during the time series.
- Surface water was anomalously warm and the freshest water was observed in August.

25.2. Description of the time series

Temperature, salinity, and oxygen data have been collected in Rivers Inlet since 1951 (Figure 25-1). From 1951 to 1993, temperature was measured with a reversing thermometer, and salinity and oxygen were measured from water collected by a Niskin or Nansen bottle. Since 1998, temperature and salinity were measured using a Seabird or RBR CTD sensor and oxygen was measured with a Seabird or Rinko oxygen sensor.

From 1951 to 1987, the University of British Columbia collected data. From 1990 to present, Fisheries and Oceans Canada have collected data. From 2008 to present, the Hakai Institute has collected data. To date, 667 temperature and salinity profiles and 554 oxygen profiles have been collected in Rivers Inlet, with more than 90% of the data collected since 2001.

Following water type definitions in fjords (Farmer and Freeland 1983), three water types were defined. These water types were surface (potential density relative to surface pressure of less than 1022.5 kgm^{-3}), intermediate (from the base of surface water to sill depth) and deep (below sill depth). There is significant seasonal variation in all water types, which normally dwarfs interannual variation. To compare 2018 to the long-term time series, first a monthly average of temperature, salinity and oxygen using all data from 1951 to 2018 was calculated for all water types. Then the monthly average from 2018 was calculated.

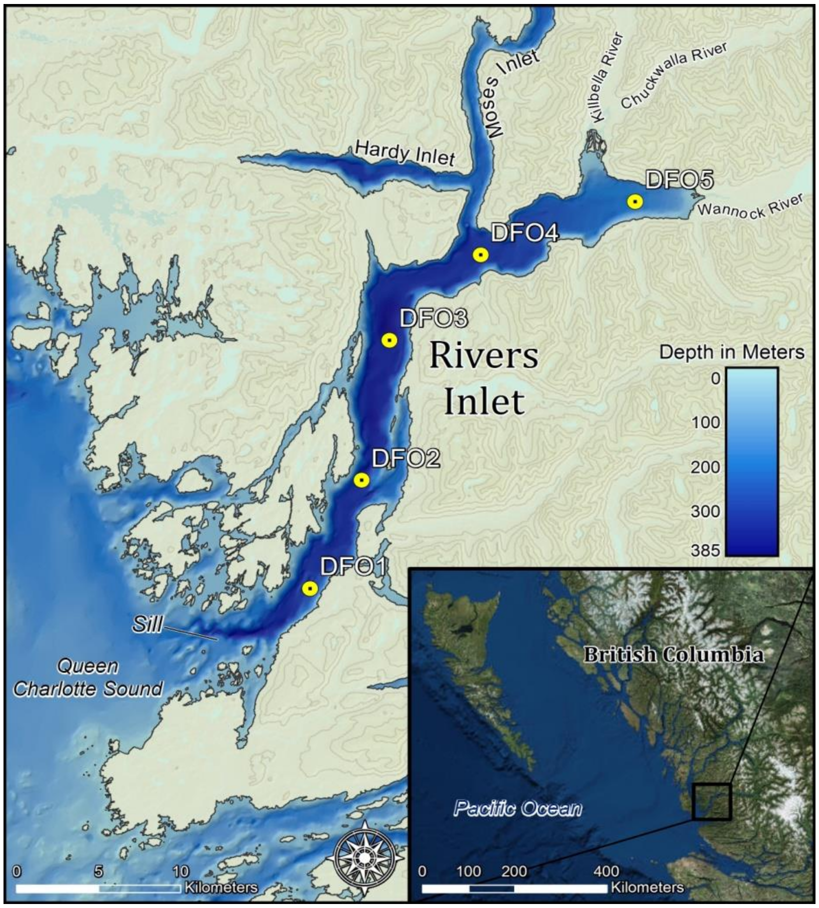

Figure 25-1. Rivers Inlet is a fjord located on British Columbia's central coast that is about 45 km long and 3 km wide. At the mouth of Rivers Inlet is a sill that is approximately 140m deep at low tide (Pickard 1961), which deepens to a basin that is about 340 m deep that shoals towards the head of the inlet. Stations DFO1, DFO2, DFO3, and DFO4 are located in the basin and station DFO5, is located on the slope near the head of the inlet.

25.3. Status and trends

Comparing the long term times series to 2018 for the surface water (Figure 25-2) shows that the surface was warmer and had less oxygen than average. The coldest surface temperature (6.5°C) was observed in February and the warmest surface water (14.4°C) was observed in August. The freshest surface water (13.8) was observed in August, approximately 2 months later than the typical June freshest (Wolfe et al. 2015) and the June salinity minimum (Tommasi et al. 2013) observed from 2006 to 2010.

In 2018, both intermediate (Figure 25-3) and deep (Figure 25-4) water were warmer, saltier, and less oxygenated in 2018 than the long-term average. Recent research has traced the warm anomaly, which originated during the northeast Pacific marine heatwave and has been advected via upwelling to Rivers Inlet along the 1026 kgm^{-3} isopycnal (Jackson et al. 2018). Deep water in Rivers Inlet has been anomalously warm since the fall of 2015. Increased salinity in intermediate and deep water suggests enhanced upwelling, and this is supported by the wind data (Hourston and Thomson, section 7). The low oxygen water was first observed in July, when deep-water renewal via upwelling was occurring. This suggests that the source of the hypoxic deep water was upwelling and this is the first time in the Rivers Inlet time series that upwelled water was hypoxic.

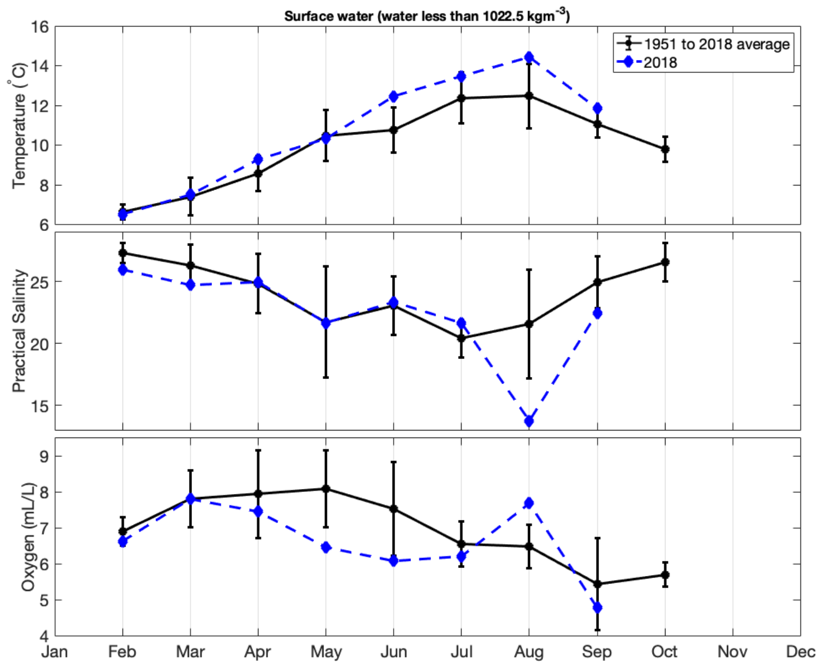

Figure 25-2. The monthly average surface (defined as water fresher than 1022.5 kgm^{-3}) conditions for (top) temperature, (middle) practical salinity, and bottom (oxygen) at station DFO2 in Rivers Inlet. The solid black line denotes the monthly average from 1951 to 2018 and the dashed blue line shows the 2018 monthly average. Error bars represent the standard deviation of the 1951 to 2018 time series. Only months that were sampled on at least 5 different years were shown.

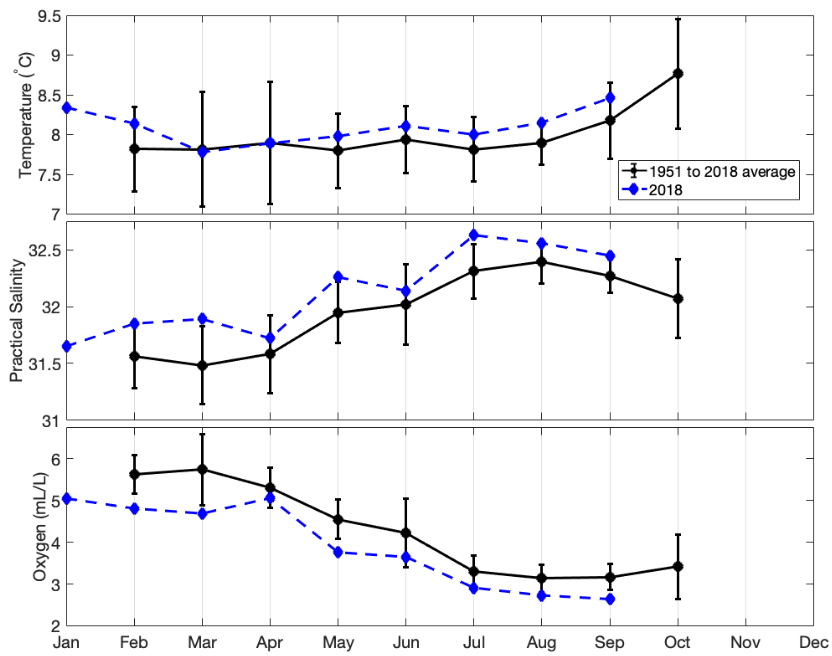

Figure 25-3. As in Figure 25-2 but for intermediate water, which was defined as water between the base of the surface layer and the 140m sill depth.

.

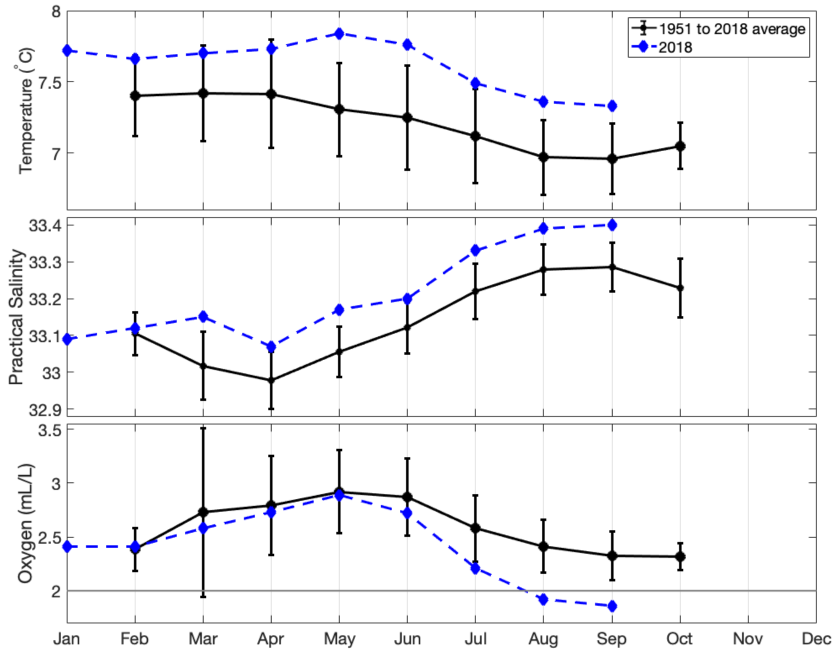

Figure 25-4. As in Figure 25-2 but for deep water, defined as water between the sill depth of 140 m and the bottom. The horizontal grey line in the bottom panel indicates 2 mL/L of oxygen, or hypoxic water.

25.4. Implications of those trends

Since 2015, the anomalously warm ocean conditions experienced on the coast of British Columbia were associated with an influx of southern copepod species and an abundance of other warm water taxa (Galbraith, section 16). The warm water associated zooplankton communities are known to be lipid poor and hence of poor quality as prey for juvenile salmon and forage fish. Therefore, the 2018 inlet conditions were likely associated with reduced salmon growth during the 2018 outmigration.

Deep water in the Strait of Georgia also had decreased oxygen (Chandler, section 26), suggesting that processes that brought low oxygen into Rivers Inlet influenced a large region of the BC coast. Research from Saanich Inlet (Grupe, section 36) showed that the biodiversity changed with different oxygen concentrations and this suggests that the hypoxic water observed in Rivers Inlet may have a significant impact on the local ecosystem. Biological and chemical data are collected monthly in Rivers Inlet and these data are being analyzed to determine how physical changes could have impacted the ecosystem.

25.5. References

Farmer, D.M. and Freeland, H.J. 1983. The physical oceanography of fjords. Progress in Oceanography: 12: 147-220.

Jackson, J.M., Johnson, G.C., Dosser, H.V., and Ross, T. 2018. Warming from recent marine heatwave lingers in deep British Columbia fjord. Geophysical Research Letters, 45: https://doi.org/10.1029/2018GL078971.

Pickard, G.L. 1961. Oceanographic features of inlets in the British Columbia mainland coast. J. Fish. Res. Bd. Canada 18(6): 907 – 999.

Tommasi, D., Hunt, B.P.V., Pakhomov, E.A., and Mackas, D.L. 2013. Mesozooplankton community seasonal succession and its drivers: Insights from a British Columbia, Canada fjord. Journal of Marine Systems, 115-116: 10-32.

Wolfe, A.M., Allen, S.E., Hodal, M., Pawlowicz, R., Hunt, B.P.V., and Tommasi, D. 2015. Impact of advection loss due to wind and estuarine circulation on the timing of the spring phytoplankton bloom in a fjord. ICES Journal of Marine Science, doi:10.1093/icesjms/fsv151.

26. TEMPERATURE AND SALINITY OBSERVATIONS IN THE STRAIT OF GEORGIA AND JUAN DE FUCA STRAIT IN 2018

Peter Chandler, Fisheries & Oceans Canada, Institute of Ocean Sciences, Sidney, B.C., Peter.Chandler@dfo-mpo.gc.ca

26.1. Highlights

- During the spring and summer surveys of 2018 temperature and salinity conditions were near-normal, but as the year progressed temperatures at all depths became warmer than normal.
- The fall and winter surveys showed widespread lower than normal oxygen levels with the exception of the deep Strait of Georgia.
- Nanoose CTDs showed depth averaged temperatures similar to conditions in 2017, with three warm water events extending to depths of 40 m. Although the long-term freshening trend continues conditions in 2018 were saltier than expected by this trend.
- There was an early, rapid and high volume Fraser River freshet. The mean annual discharge was near the 100 year average, but the median annual discharge occurred 16 days earlier than the long term average.

26.2. Description of the Time Series

Two sources of data are used to describe changes in the temperature and salinity conditions in the Strait of Georgia (between mainland British Columbia and Vancouver Island) and Juan de Fuca Strait (between Washington State and Vancouver Island). The first is profile data collected with a SeaBird 911 CTD during the Strait of Georgia water properties survey (Figure 26-1). In 2018 surveys were carried out in mid-April, mid-June, early October and mid-November. The second dataset is provided by the Department of National Defence from the 43 temperature and salinity profiles collected in 2018 with a SeaBird 19 CTD at its Maritime Experimental and Test Range (CFMETR) near Nanoose. Data from both sources collected since 1999 are used to calculate long-term averages and identify the 2018 anomalies from these average conditions.

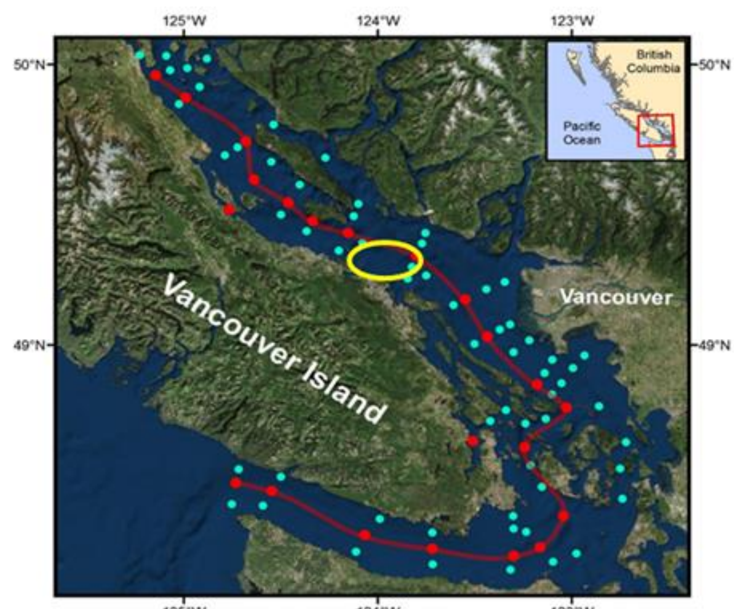

Figure 26-1. Dots show the locations of 79 stations sampled during the water properties surveys. The thalweg is shown as the red line joining the deepest stations along the centerline of the Straits. The yellow ellipse marks the area where depth profiles of temperature and salinity are collected at the Canadian Forces Maritime Experimental and Test Range (CFMETR).

26.3. Status and trends

Observations of temperature and oxygen made in 2018 are compared to the 1999-2018 averages and shown as anomalies in Figures 26-2 and 26-3. During the midpoint of the year the temperature throughout the system changed from near-neutral to above average.

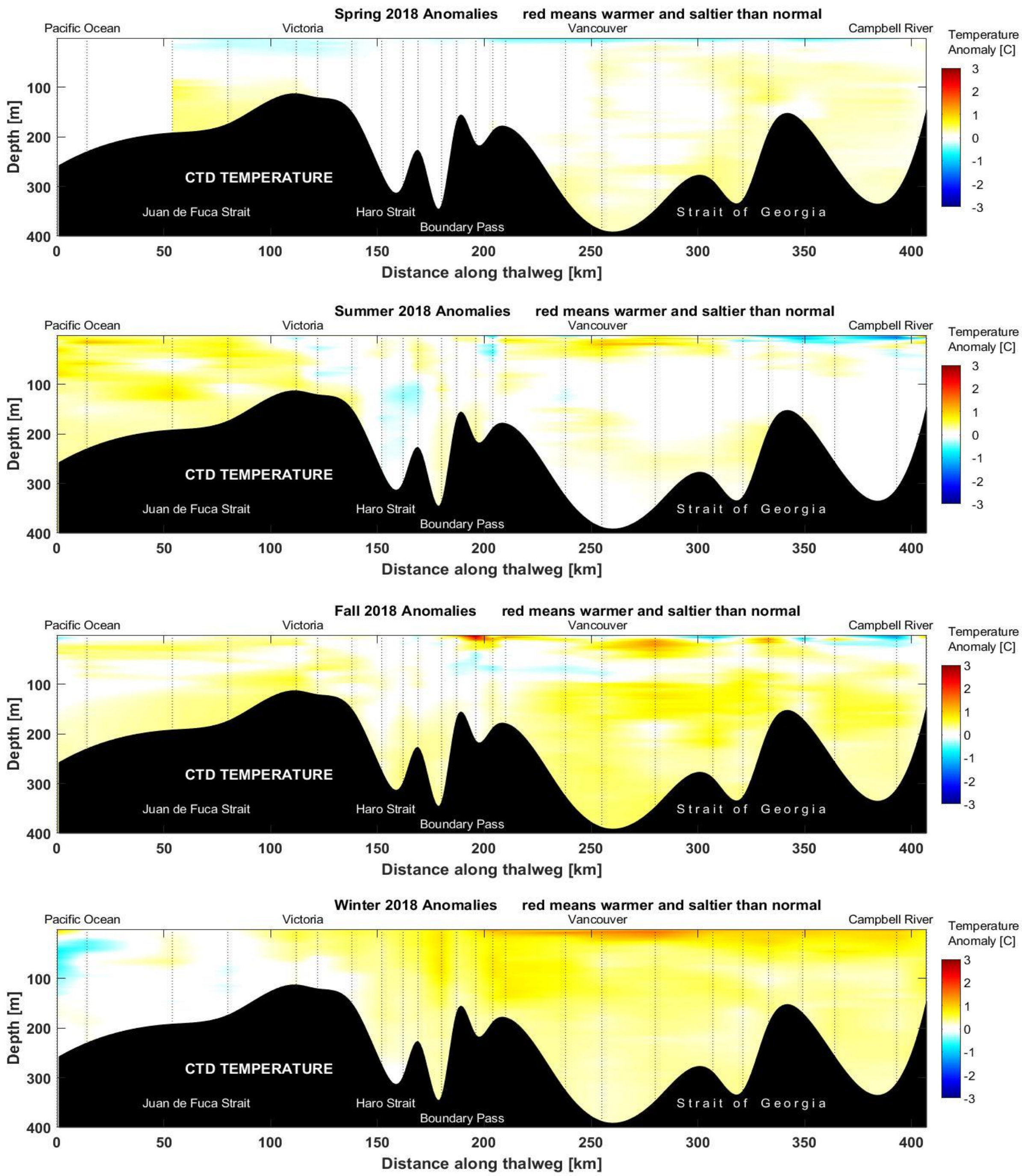

Figure 26-2. Temperature anomalies along the thalweg observed in spring, summer, autumn and winter in 2018.

For most of 2018 the waters of the Salish Sea showed normal levels of oxygen in the deeper waters of the Strait of Georgia, but reduced levels of oxygen for other regions, particularly in Juan de Fuca Strait during the winter survey.

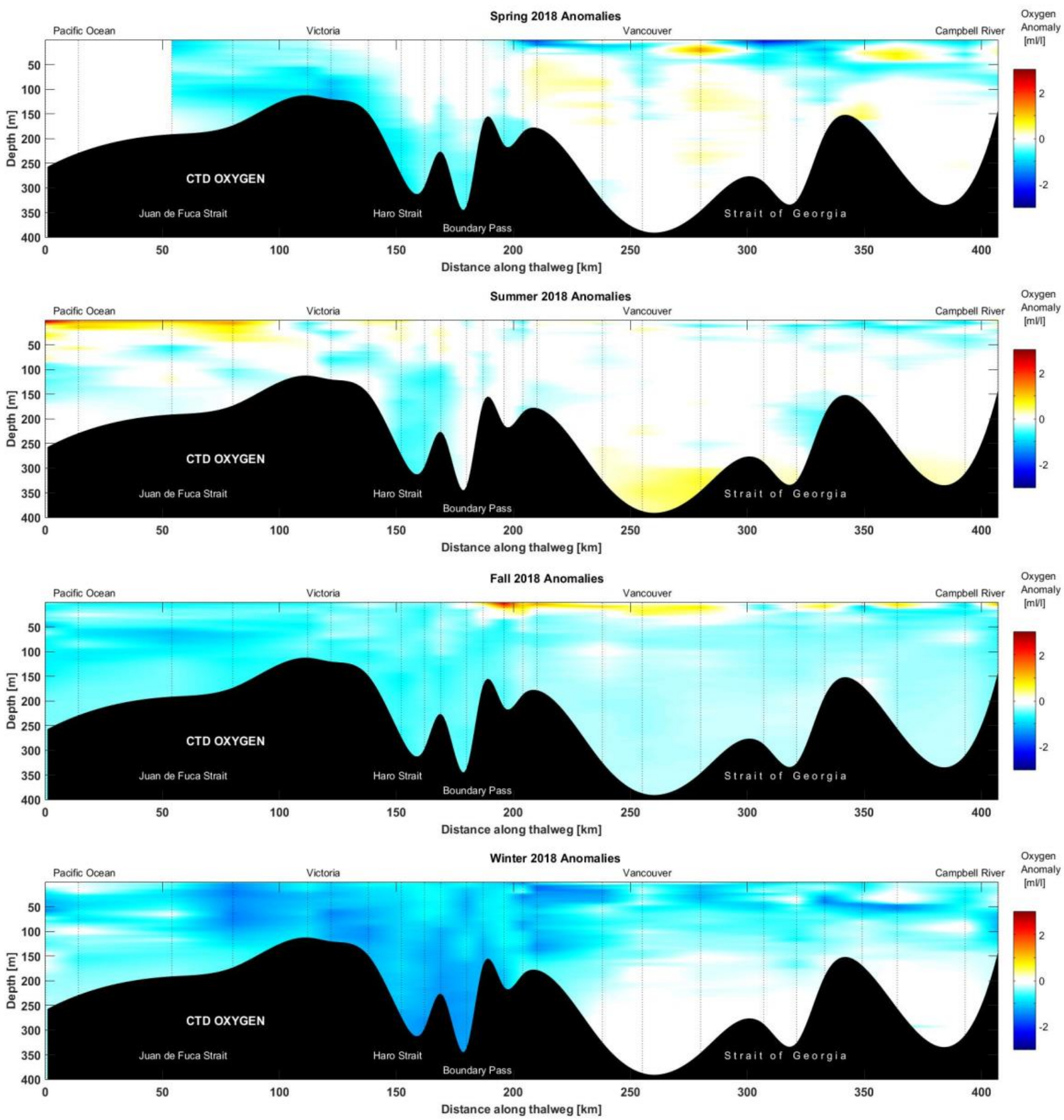

Figure 26-3. Oxygen anomalies along the thalweg observed in spring, summer, autumn and winter in 2018.

The interannual variations in the Nanoose temperature (Figure 26-4, upper panel) show depth averaged temperatures in 2018 at levels consistent with the long term average, and temperature with depth conditions very similar to those in 2017, and 2004-2006.

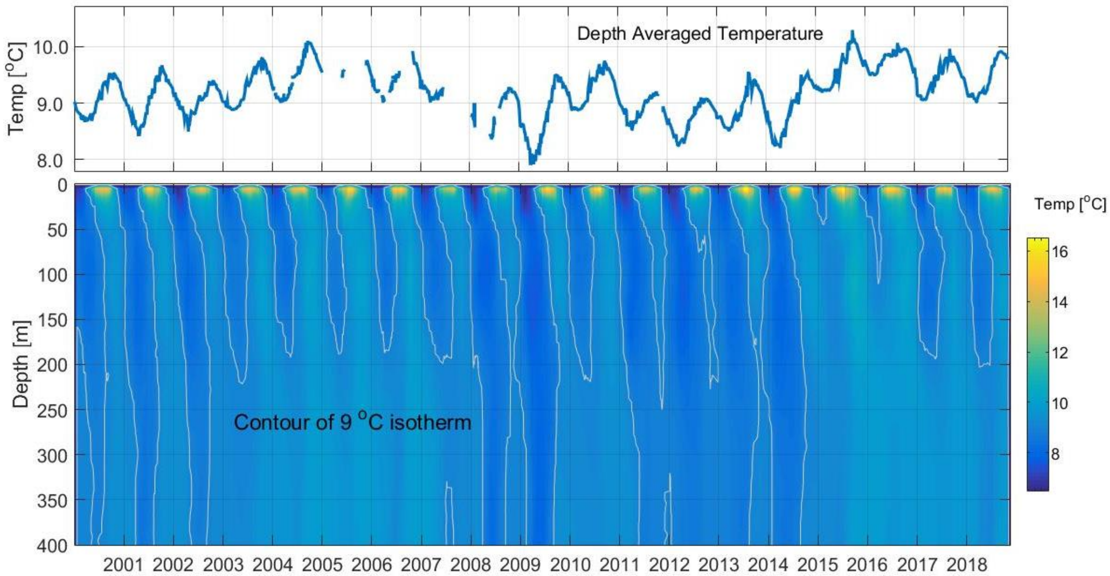

Figure 26-4. The time series of depth averaged temperature collected near Nanoose in the central Strait of Georgia (upper); the vertical distribution of these data (lower).

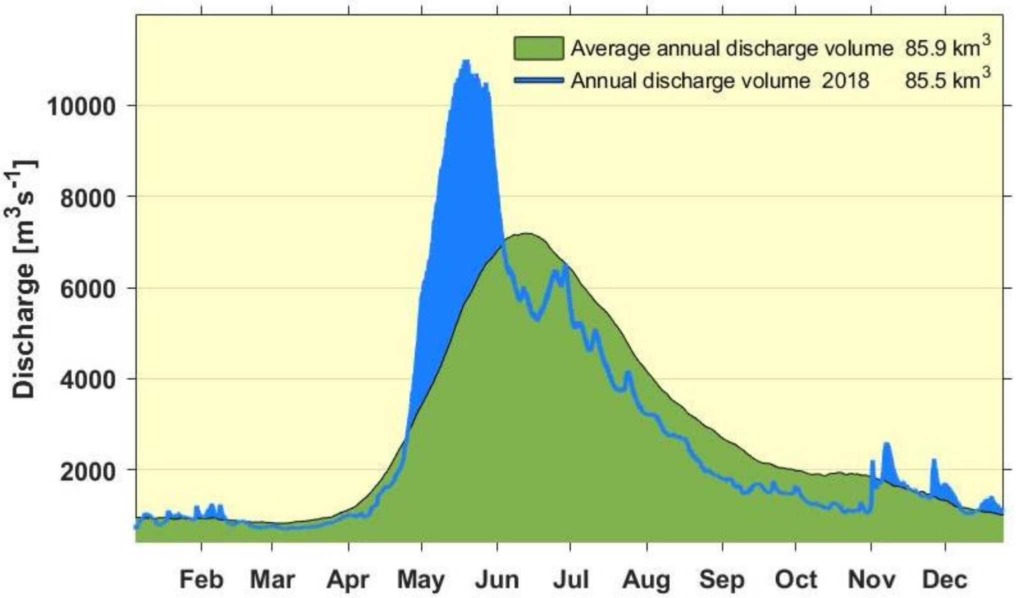

Figure 26-5. Fraser River discharge at Hope B.C.; 2017 (blue), 105 year average (green). Data source: The Water Survey of Canada).

The influence of the Fraser River discharge is particularly evident in the salinity of the surface waters of the central and southern Strait of Georgia. While the 2018 annual discharge of the Fraser River (as measured at Hope, BC, see Figure 26-5) was near the 100 year average there was a higher than average discharge early in the year and the median annual discharge occurred 16 days earlier than the long term average.

27. DEEP WATER AND SEA SURFACE PROPERTIES IN THE STRAIT OF GEORGIA DURING 2018: CABLED INSTRUMENTS AND FERRIES

Akash Sastri[1], Lu Guan[1], Richard Dewey[1], Steve Mihaly[1] and Rich Pawlowicz[2]

[1]Ocean Networks Canada, University of Victoria, Victoria, B.C. asastri@uvic.ca, lguan@uvic.ca, rdewey@uvic.ca, smihaly@uvic.ca

[2]Earth, Ocean, and Atmospheric Sciences, University of British Columbia, Vancouver, B.C., rich@eos.ubc.ca

27.1. Highlights

- Seasonal patterns of water temperature at the Ocean Networks Canada coastal sites: Folger Passage (98 m); Saanich Inlet (95 m); Strait of Georgia (SoG) East (170m); and SoG Central (300m), were generally cooler than 2014-2017 but still warmer than each time-series average.
- The 2018 SoG spring phytoplankton bloom started on March 9th and was the third earliest spring bloom relative to the ferry time series dating back to 2002, but comparable other long-term (1968-2010) observations (Allen et al., section 30).
- The first phytoplankton biomass peak occurred on March 14th. However, this first bloom peak was interrupted, and followed by a second peak of similar magnitude in early April.

27.2. Description of the time series

Here we report on temporal patterns of core seawater properties (temperature, salinity, density, and dissolved oxygen; 1 Hz) for four fixed-point cabled bottom moorings and surface monitoring of core seawater properties and chlorophyll fluorescence (0.1 – 1 Hz) by instrumented ferries in the Salish Sea (detailed methods for each deployment and real-time data are available at oceannetworks.ca).

i. *ONC Folger Deep*: 98 m cabled, fixed-point mooring (48° 48.8278' N, 125° 16.8573’ W). The instrument platform is located on the west coast of Vancouver Island shelf at the mouth of Barkley Sound, and the time series discussed here started on September 2, 2009. This time series is particularly useful for monitoring interannual variability of: i) the timing of upwelling and downwelling on the southern WCVI shelf; and ii) of water mass properties associated with upwelling and downwelling.

ii. *Strait of Georgia East Instrument Platform*: 170 m cabled fixed-point mooring (48° 48.8278' N, 123° 18.9986' W). The instrument platform is located in the southern Strait of Georgia at a ‘mid-basin’ depth on the seafloor and the time series reported here started on February 29, 2008. Inshore deep- and intermediate water properties in the Strait of Georgia (SoG) reflect seasonal patterns of increasing salinity and heating during the summer; due to the arrival of salty upwelled water on the shelf transiting through Juan de Fuca Strait and mixing with warm surface waters in Haro Strait (Mason 2002, Pawlowicz et al. 2007). Winter water properties are characterized by cooling and freshening associated with deep mixing of local surface waters in Haro Strait/Gulf Islands.

iii. *Strait of Georgia Central Instrument Platform*: 300 m cabled fixed-point mooring (49° 02.3850' N, 123° 25.5800' W). The instrument platform is located in the southern Strait of Georgia at a 'deep-basin' depth on the seafloor and the time series reported here started on September 24, 2008. See description above for the Strait of Georgia East instrument platform.

iv. *ONC-BC Ferries instrumented vessels*: Surface monitoring of water mass (temperature, salinity, density, dissolved oxygen) and biogeochemical (chlorophyll fluorescence, turbidity, coloured dissolved organic matter fluorescence, and pCO_2) properties in the central and southern Strait of Georgia. This surface monitoring program is useful for it broad spatio-temporal resolution for monitoring: i) water properties in the Strait of Georgia; ii) Fraser River plume dynamics; and iii) monitoring interannual patterns of the timing and magnitude of phytoplankton production. Instrumented ferries transit between:

a) M/V Queen of Oak Bay: Horseshoe Bay – Departure Bay. Started: July 2015 (single year of operations in 2003 as well).

b) M/V Queen of Alberni: Tsawwassen – Duke Point. Started: May 2012 (operated for 4 years 2003-2006 as well).

c) *M/V Spirit of Vancouver Island*: Tsawwassen – Swartz Bay. Started: December 2001 (out of service since Sep 2018).

27.3. Status and trends

27.3.1. ONC Folger Deep:

The transition to upwelling takes place in late spring and the downwelling period starts in late summer/early fall along the southern west coast of Vancouver Island. At ONC Folger Deep, the upwelling signal is characterized by cold, salty, less oxygenated waters whereas downwelling is signaled by relatively warm, fresh, and more oxygenated waters characteristic of summer surface waters in the Gulf of Alaska (Pawlowicz 2017). Cumulative upwelling calculated from the along-shore component of winds west of Cape of Flattery (48°N 125°W NOAA PFEL Buoy, Figure 27-1), indicate a typical seasonal pattern and magnitude with ~14 day early transitions to both upwelling and downwelling (time series means = April 25th and September 19th, respectively).

A strong storm event in early January 2018 compromised salinity, density, and oxygen data quality and resulted in a long data gap (January 18th to June 30th) at ONC Folger Deep. Temperature, however, was the only water mass property recorded for the entire year. Overall, 2018 was the fourth consecutive year characterized by above average temperatures (Figure 27-2), relative to the time series average. Note, however, that temperatures in 2018 were generally cooler relative to 2015, 2016, and 2017. With the exception of a cold event early in 2018, temperatures during early downwelling were above average. Temperatures during the upwelling phase in 2018 were warmer than the time series average followed by cooler than average temperatures during the late downwelling phase (Figure 27-1). During the fall transition, downwelling was associated with freshening and increased seawater temperature and oxygen; both temperature and oxygen were lower than average, but salinity was higher than averages for most of the downwelling period (Figure 27-2).

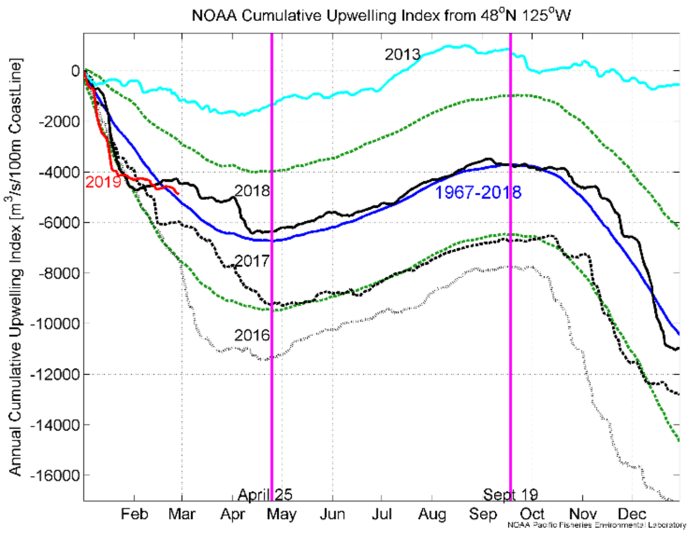

Figure 27-1. Cumulative Upwelling index from west of Vancouver Island (west of Cape Flattery, 48°N 125°W), as downloaded from NOAA's Pacific Fisheries Environmental Laboratory. Pink vertical lines represent time series average dates for the spring transition from downwelling to upwelling and the fall transition from upwelling to downwelling.

27.3.2. Strait of Georgia East:

Seawater properties for 2018 at SoG East includes a data gap for salinity, density and oxygen between April 3rd and October 1st due to an instrument plug. Fortunately, data quality for temperature was good for the entire year. Properties at the SoG East instrument platform (Figure 27-2) reflect, in part, mid-water renewal to the SoG: reflecting typical seasonal patterns, this water was cool and fresh in the early 2018 with frequent but moderate oscillations in salinity, density and dissolved oxygen. Water warmed up gradually over the summer due to the arrival and mixing of upwelled water from the shelf (Masson 2002, Pawlowicz et al. 2007). Then seasonal cooling, freshening and oxygenating followed over the winter due to local mixing with deep waters. The magnitudes of salinity maxima and oxygen minima later 2018 suggest relatively limited local water mixing. Similar to 2017, SoG East was still warmer than its time series average (to a lesser extent than the 2015-16 “Blob” period) for most of the year of 2018. Temperature patterns at SoG East reflect broader regional patterns with a continuation of the warm conditions starting in the late 2014.

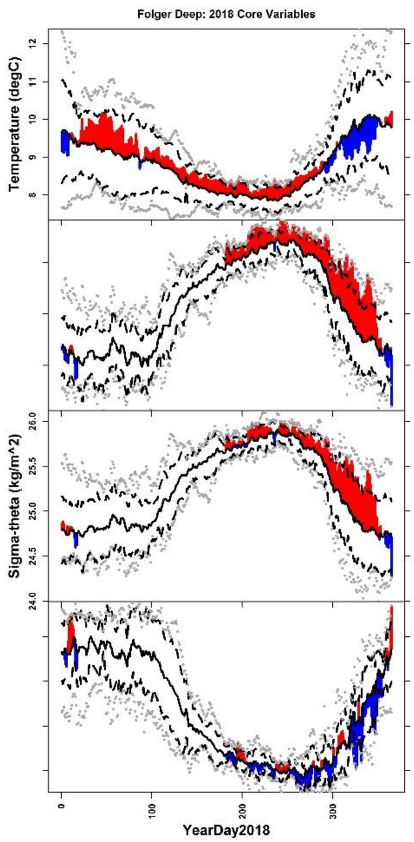

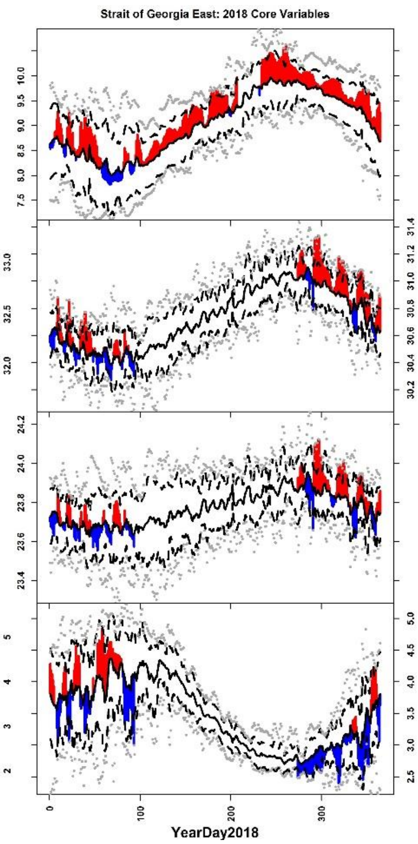

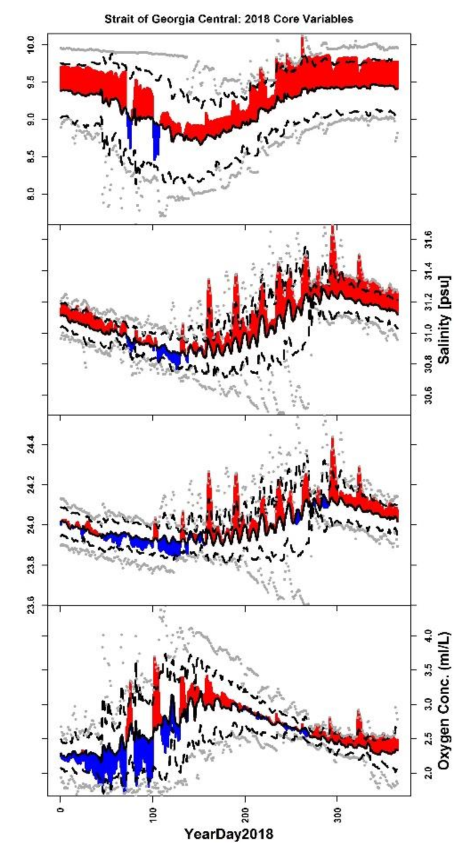

Figure 27-2. From top to bottom, mean daily temperature (°C), salinity (practical units), density (kg m-2), and dissolved oxygen concentration (ml L-1) for Folger Deep (left), SoG East (right), and SoG Central (bottom). Red/blue bars represent values greater/less than the time series mean (solid black line). The dashed black lines represent +/- 1 standard deviation about the mean, and grey symbols are the maximum and minimum daily values for each time series.

27.3.3. Strait of Georgia Central:

Similar to SoG East, seasonal patterns of water properties at SoG Central (Figure 27-2) were typically characterized by winter cooling/freshening due to top down flux and summer warming/increasing salinity due primarily to deep-water renewal events (Masson 2002). Compared with the previous three years (2015, 2016 and 2017), temperatures were still warm relative to the time series average during most of 2018, but to a lesser degree. Resumption of winter cooling was observed but associated with water warmer and saltier than average. Dissolved oxygen concentrations [DO] at 300m also followed a clear seasonal pattern: starting with values lower than the time series average during the 2017/18 winter and probably due to limited ventilation; increased rapidly with large fluctuations over spring, and gradually decreased through the summer, and then stabilized at anomalously high concentrations, with several oxygen maxima through the fall and winter of 2018.

27.3.4. Sea-Surface Water Properties Monitoring in the Strait of Georgia:

The start and development of the spring phytoplankton bloom in the central-southern SoG in 2018 was captured by high-resolution sea-surface measurements of chlorophyll fluorescence. The spring bloom occurred prior to the start of the Fraser River freshet. In 2018, the spring bloom was first detected along ferry route outside of the Fraser River plume on the March 9th followed by increased phytoplankton production inside the plume (Figure 27-3). The first chlorophyll fluorescence peak was recorded on March 14th which was ~1 week earlier than biomass peaks in 2016 and 2017 (March 22 and 21, respectively). However, this first bloom peak in 2018 was interrupted, and followed by a second peak of similar magnitude in early April. Timing of the spring phytoplankton bloom can vary by up to 6 weeks with a mean peak date of March 25th (Allen and Wolfe 2013). Thus, the 2018 spring bloom was relatively early, and was the third earliest (the earliest being late February of 2005 and the second earliest being early March of 2015) measured by ferry monitoring beginning in 2003. In terms of bloom magnitude, Chlorophyll fluorescence during the 2018 bloom was relatively low compared to the 2003-2018 time series of ferry-based measurements (Figure 27-4).

Inshore deep and intermediate water properties in the Strait of Georgia are strongly seasonal. The arrival of salty upwelled water on the shelf transiting through Juan de Fuca Strait and mixing with warm surface waters in Haro Strait cause the increasing temperature and salinity in summer water (Pawlowicz et al. 2007), while the deep mixing of local surface waters in Haro Strait/Gulf Islands cause the cooling and freshening in winter waters. Warmer than average temperatures were first observed at Folger Passage Deep in October of 2014 when the warm water anomaly (the “Blob”) arrived on the shelf with the onset of downwelling (Dewey et al. 2015). The anomalously warm water is thought to have transited through Juan de Fuca and mixed in Haro Strait before entering the Strait of Georgia basin. This very warm condition lasted throughout the strong El Niño years (2015-16), and was then followed by seasonal winter cooling at the start of 2017 and again in 2018 at Folger Passage Deep. The warm conditions for the deep- and intermediate-depth waters of the SoG continued in 2018 but to a lesser extent than 2016 and 2017 suggesting some but limited winter cooling.

(a)

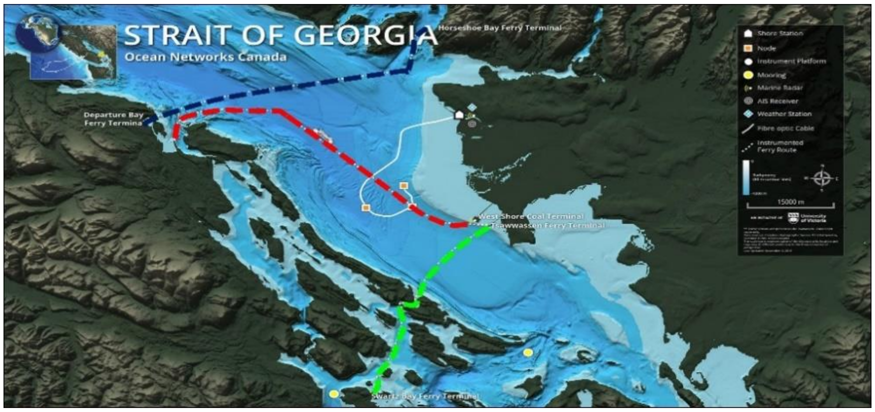

(b)

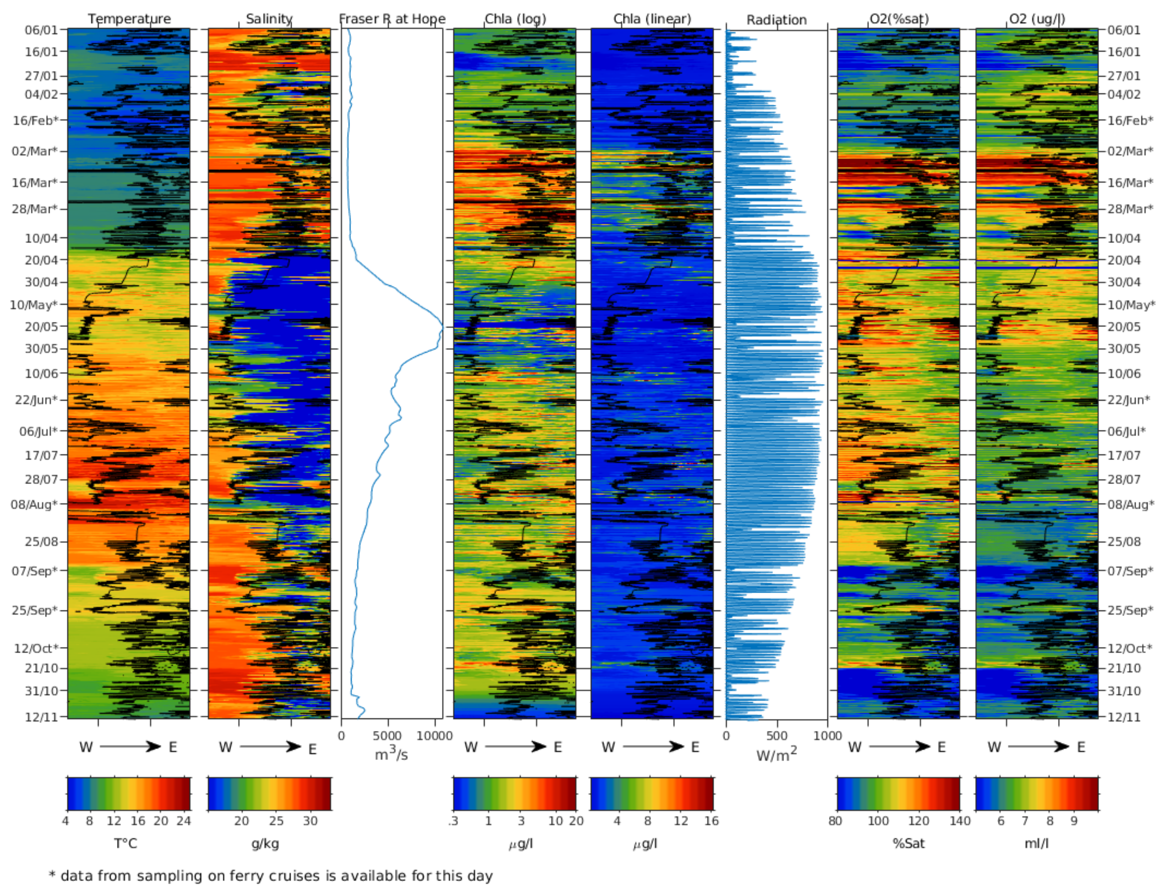

Figure 27-3. A summary of sea surface properties measured along the Tsawwassen-Duke Point ferry route in 2018: a) a map illustrating all three instrumented ferry routes; and b) contour and scalar plots with each subplot illustrating spatial and temporal variation. Observations track from Nanaimo (Duke Point; left) to Tsawwassen (right), and temporal variations along the vertical axis from top to bottom. Dates marked with'' indicate discrete water sampling events along the ferry route. Low-salinity waters from the Fraser River plume are seen on the right side of the salinity subplot; the boundaries of the plume are drawn in black on all other subplots. Phytoplankton biomass (mg Chl.m^{-3}) is shown on both a linear scale (which emphasizes the high values in the spring bloom), and a logarithmic scale which better illustrates summer variability. Dissolved oxygen is shown on both a percent saturation scale, which is relevant to air-sea gas exchange, and an absolute scale (mL L^{-1}) which is a better measure of biological production; they differ because of seawater temperature effects over the season and salinity effects inside and outside the Fraser River plume.*

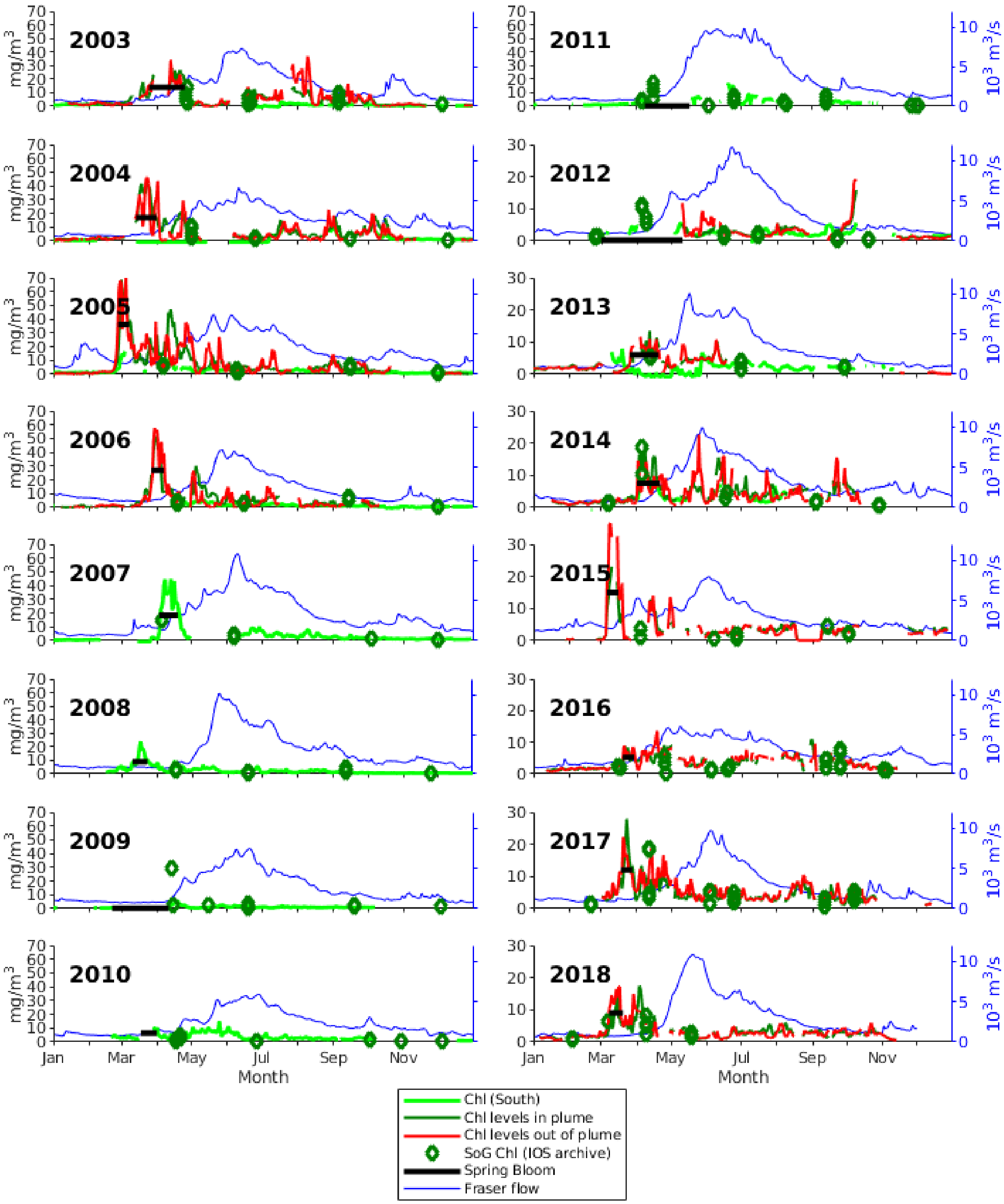

Figure 27-4. Time series of phytoplankton biomass (chlorophyll fluorescence) inside and outside of the Fraser River plume as measured from instrumented ferries transiting between Duke Point and Tsawwassen (dark green and red) and Swartz Bay and Tsawwassen (light green). Fraser River discharge (right-hand axis) is superimposed over the annual phytoplankton biomass time-series. Black lines show bloom timing (presumed in 2009, 2011 and 2012).

27.4. References

Allen, S.E., and Wolfe, M.A. 2013. Hindcast of the Timing of the Spring Phytoplankton Bloom in the Strait of Georgia, 1968-2010, Progress in Oceanography 115: 6- 13.

Dewey, R., Sastri, A., and Mihaly, S. 2015. The 2014 perspective from Ocean Networks Canada. In: Chandler, P.C., King, S.A., and Perry, R.I. (Eds.). State of the physical, biological and selected fishery resources of Pacific in 2014. Can. Tech. Rep. Fish. Aquat. Sci. 3131.

Masson, D., 2002. Deep Water Renewal in the Strait of Georgia. Estuarine, Coastal and Shelf Science 54: 115-126.

Pawlowicz, R., Riche, O., and Halverson, M. 2007. The circulation and residence time of the Strait of Georgia using a simple mixing-box approach. Atmosphere-Ocean 45 (2): 173-193.

Pawlowicz, R., 2017. Seasonal Cycles, Hypoxia, and Renewal in a Coastal Fjord (Barkley Sound, British Columbia), Atmosphere-Ocean, 55:4-5, 264-283.

Pawlowicz, R., Francois, R., Maldonado, M. 2018. Contaminant dispersion and removal in the Strait of Georgia (2018). Metro Vancouver Data Report, 256pp.

Sastri, A.R., Dewey, R., Mihaly, S. and Pawlowicz, R. 2017. Deep water and sea-surface properties in the Strait of Georgia during 2016: Ferries and cabled instruments. In: Chandler, P.C., King, S.A., and Boldt, J. (Eds.). State of the physical, biological and selected fishery resources of Pacific Canadian Marine Ecosystems in 2016. Can. Tech. Rep. Fish. Aquat. Sci. 3225.

28. 2018 COASTAL OCEAN CONDITIONS REVEALED BY THE HAKAI INSTITUTE'S CONTINUOUS CO_2 DATASETS

Wiley Evans, Hakai Institute, Heriot Bay, B.C., wiley.evans@hakai.org

28.1. Highlights

- 2018 surface CO_2 patterns consisted of ~mid-March initiation of seasonal seawater CO_2 drawdown, summertime high CO_2 events not seen in 2017, and a uniquely intense period of late season CO_2 drawdown.
- Seasonal CO_2 drawdown occurred ~1 week earlier in the Salish Sea than on the central and northern coasts.
- High CO_2 zone in Johnstone Strait and Queen Charlotte Strait separates regions of seasonal CO_2 uptake in the Salish Sea and central BC coast.
- This high CO_2 zone has seasonality with highest seawater pCO_2 during late summer and fall.
- High-resolution datasets revealed large near-shore bottom water (20 m) CO_2 system variability, as well as variability in Baynes Sound associated with neap tides.

28.2. Description of CO_2 Datasets

The Hakai Institute has been building a high-resolution dataset of surface water CO_2 partial pressure (pCO_2) measurements since December 18, 2014 at the Quadra Island Field Station (QIFS) in the northern Salish Sea (Figure 28-1). Previous analyses have reported on the seasonality in this record, its broad representativeness of the northern Salish Sea, and the occurrence of large variability during summer northwesterly wind events (Evans et al. 2019, Hare et al. 2017). During 2017 and 2018, new high-resolution datasets began to be collected by the Hakai Institute that provided additional information into CO_2 system variability along the British Columbia coast. These additions included: (1) underway measurements made from the Alaska Marine Highway System (AKMS) M/V *Columbia* (Figure 28-2), (2) surface measurements made from the KC (Kwakshua Channel) buoy (Figure 28-2), (3) bottom measurements made from a cabled Limpet platform deployed at 20 m depth offshore of the QIFS (Figure 28-3), and (4) measurements made at a shellfish facility (Fanny Bay Oysters) in Baynes Sound (Figure 28-4).

With the exception of data collected on the Limpet platform, all datasets consist of direct measurements of pCO_2, temperature, and salinity. The dataset from the Limpet platform consisted of direct measurements of seawater pH_T (pH reported on the total hydrogen scale), temperature, salinity, and dissolved oxygen. Seawater pH_T measurements made using a SeaFET were calibrated and handled as described in Evans et al. (2019).

28.3. Patterns in CO_2 Datasets

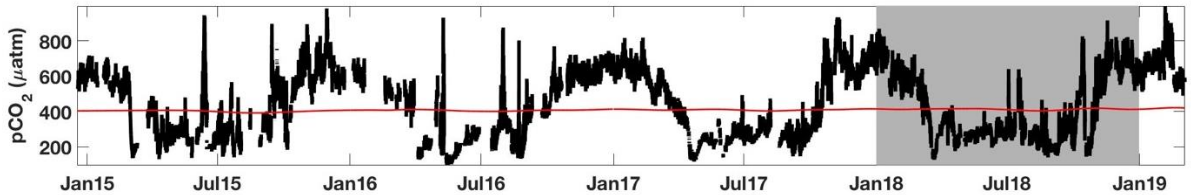

Figure 28-1. Long-term record of pCO_2 in the northern Salish Sea. Black is surface seawater pCO_2 from 1 m depth in Hyacinthe Bay adjacent to the Quadra Island Field Station (QIFS). Red is an atmospheric pCO_2 record from direct measurements made at the QIFS combined with the Earth System Research Laboratory Marine Boundary Layer product averaged between 45°N and 63°N. 2018 is highlighted in gray.

Our basis for understanding surface water CO_2 variability in the northern Salish Sea is the QIFS record (Figure 28-1). Surface pCO_2 data from 2018 revealed an earlier initiation of seasonal seawater CO_2 drawdown (driven by increased primary productivity and indicating spring bloom conditions) than was seen in 2017, more variable summer conditions, and a uniquely intense period of late season CO_2 drawdown associated with a fall phytoplankton bloom.

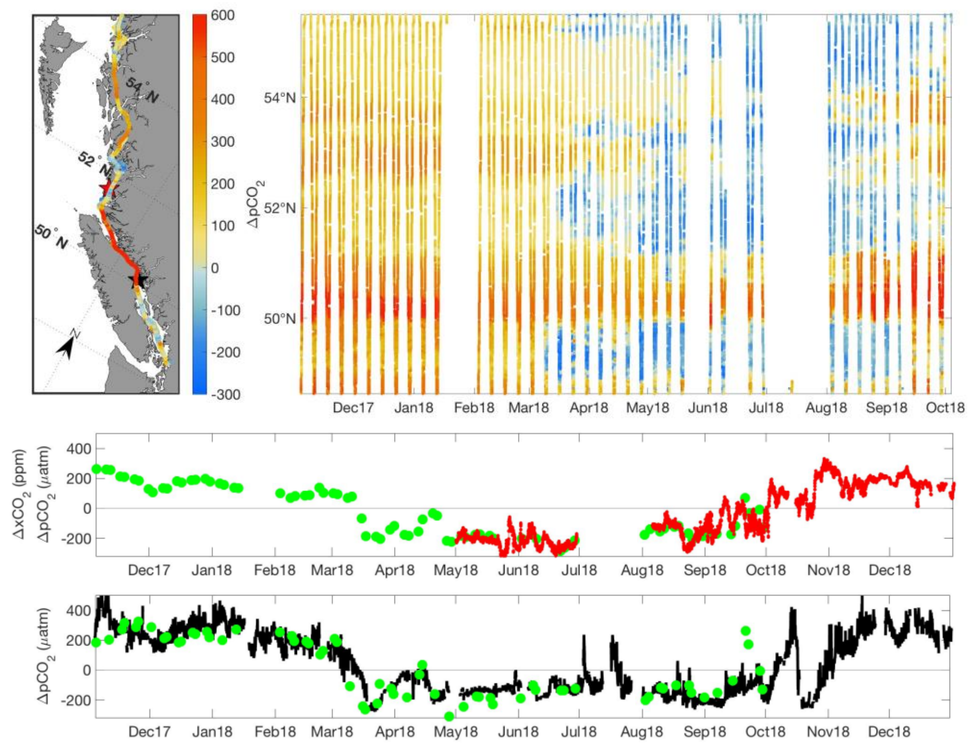

Figure 28-2. Surface CO_2 observations along the BC coast. Top panel shows a map and time series of observations of sea minus air pCO_2 (ΔpCO_2, µatm) made from the Alaska Marine Highway System (AMHS) M/V Columbia between November 2017 and October 2018. Positive ΔpCO_2 (warm colors) indicates a CO_2 source to the atmosphere, and negative ΔpCO_2 (cool colors) indicates a sink for atmospheric CO_2. Middle panel shows ΔpCO_2 and ΔxCO_2 data collected by the Columbia (green, data averaged over Fitz Hugh Sound) and the KC buoy (red star in map; 51.649°N, 127.967°W), respectively. ΔpCO_2 and ΔxCO_2 data are nominally the same within < 1%. The lower panel shows ΔpCO_2 data collected by the Columbia (green, data averaged over the northern Salish Sea) and at the QIFS (black star in map; 50.116°N, 125.222°W).

High-resolution data collected from the AKMS M/V *Columbia* and from the KC buoy provide important spatial and temporal information that builds upon the intelligence gained with the QIFS dataset (Figure 28-2). The Columbia transited the BC coast twice per week starting in November 2017, and the average of data collected in proximity to both the KC buoy and the QIFS agree well with the fixed station records, with a notable exception in the northern Salish Sea in September 2018. Both the fixed records and spatially-resolved *Columbia* data show seasonal CO_2 drawdown (negative ΔpCO_2) occurred ~1 week earlier in the Salish Sea than on the central and northern coasts of BC. By late June, CO_2 drawdown was widespread across the central and northern BC coast. A zone of high CO_2 in Johnstone Strait and Queen Charlotte Strait separated regions of CO_2 drawdown in the Salish Sea and central coast. This high CO_2 region has been documented previously (Evans et al. 2012, Nemcek et al. 2008, Tortell et al. 2012), but new data from the *Columbia* revealed seasonality in the region, with highest pCO_2 during late summer and fall (Figure 28-2).

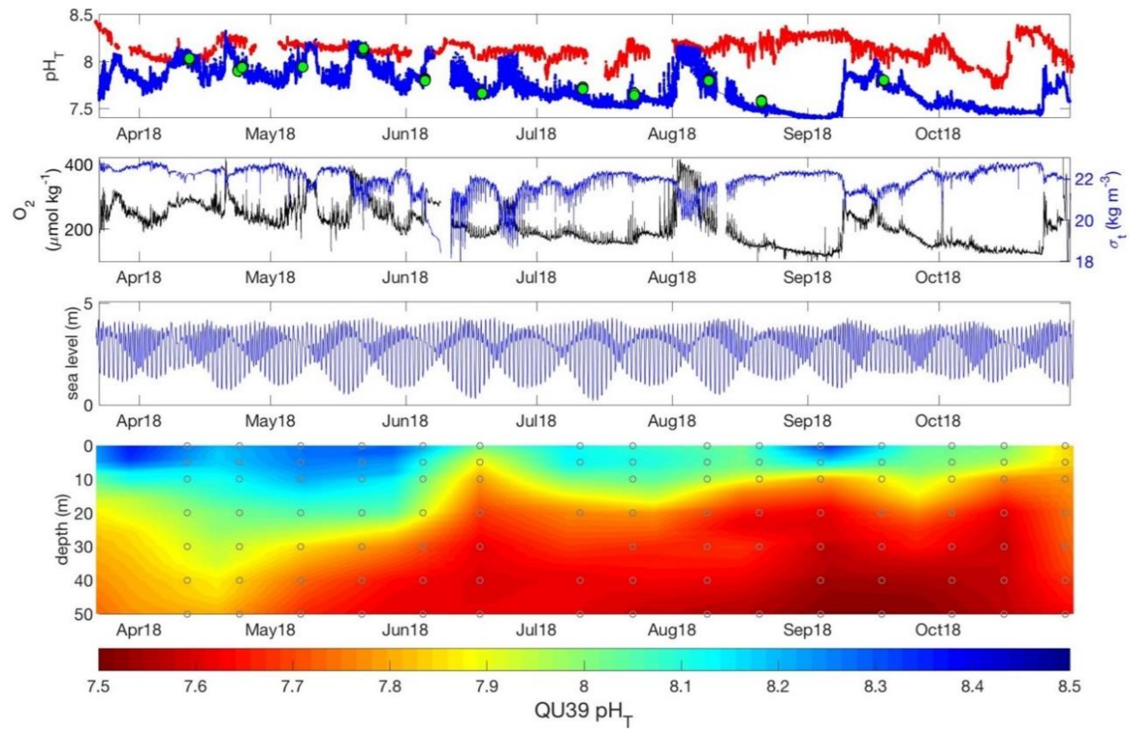

Figure 28-3. March to November 2018 water column pH_T observations in the northern Salish Sea. Top panel shows surface (1 m) and ~20 m pH_T (red is QIFS BoL, and blue is QIFS Limpet). Green dots are validation pH_T measurements made on seawater collected at 20 m adjacent to the Limpet. Second panel is 20 m dissolved oxygen (µmol kg^{-1}) and density anomaly (kg m^{-3}) data from the Limpet. Third panel is tide data from Campbell River (http://www.meds-sdmm.dfo-mpo.gc.ca/isdm-gdsi/twl-mne/inventory-inventaire/interval-intervalle-eng.asp?user=isdm-gdsi&region=PAC&tst=1&no=8074&ref=maps-cartes). Fourth panel is pH_T in the upper 50 m at hydrographic station QU39 (50.031°N, 125.099°W) in the northern Salish Sea.

New datasets collected in 2018 reveal large sub-surface variability that is important to consider within the context of our building understanding of CO_2 dynamics on the BC coast, and particularly in relation to organismal studies into ocean acidification impacts. Bottom water data collected from a cabled Limpet near-shore and proximal to the QIFS revealed a ~0.4-unit fortnightly signal in pH_T between April and July that exceeded the surface pH_T variability seen during that period (Figure 28-3). This signal decreased between July and October as 20 m pH_T decreased in the open northern Salish Sea. However, pH_T at the Limpet reached lower levels than was seen in the upper 50 m at the nearby hydrographic station, suggesting a benthic contribution to the observed low bottom water pH_T. Short-lived periods of increased pH_T during August and September 2018 occurred without concurrent decreases in pH_T at the surface and require further investigation.

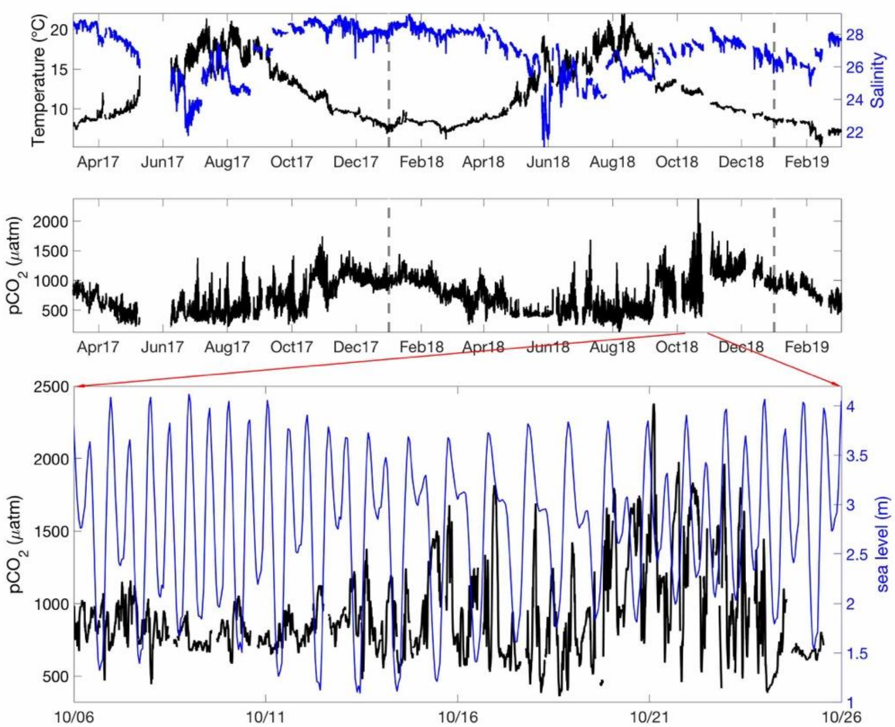

Figure 28-4. 2-year record of CO_2 observations in Baynes Sound. Top panel is the temperature and salinity of seawater drawn into Fanny Bay Oysters in Baynes Sound from a depth of ~ 5 m (varies from ~3 to ~6 depending on tide; 49.4716°N, 124.7928°W). Second panel is the pCO_2 of the incoming seawater. Third panel is seawater pCO_2 and tide data during a period of observed high pCO_2 variability in October 2018.

Seawater pCO_2 variability was most extreme in the new and growing dataset from Baynes Sound. A CO_2 system is configured within the Taylor Shellfish Fanny Bay Oysters facility and measuring incoming water from their seawater intake located at ~5 m depth. Seasonality is consistent with the pattern in the QIFS dataset, with high winter values and lower summer values, but variability is high between July and November in both 2017 and 2018 (Figure 28-4). The occurrence of high pCO_2 during this interval many times was in association with neap tides, suggesting a fortnightly change in flushing of the sound and buildup of CO_2. October 2018 was notable as the highest pCO_2 observed across all the Hakai Institute's high resolution datasets occurred during that time. pCO_2 increased with a decrease in daily tidal variance and the daily peak in pCO_2 followed the high tide, suggesting a tide-flat source of respiratory CO_2 being advected by the outgoing tide.

28.4. Implications of observed seawater CO_2 Patterns

Understanding dynamic CO_2 system variability in coastal settings is essential for detailing CO_2 "weather" patterns (Waldbusser and Salisbury 2014) and to assess how this variability may be changing due to climate change and anthropogenic CO_2 uptake (Fassbender et al. 2018). In addition, experimental work examining organismal response to anthropogenic forcings must consider inherent system variability (Gimenez et al. 2018), which is poorly constrained without highly-resolved records in coastal settings. The new datasets presented here provide some key examples of the inherent variability along the BC coast that build on the understanding generated by the longer QIFS dataset. Unfortunately, for each dataset presented here, trend detection is impaired by the short record lengths relative to the large inherent variability. Time-of-detection for the expected anthropogenic CO_2 signal, calculated following Carter et al. (2019), determined using the first year of observations from the M/V *Columbia*, ranged from 30 to 70 years across the BC coast. Given these long timeframes needed to resolve secular trends along the BC coast, estimates of anthropogenic CO_2 are therefore critical for understanding the changing marine CO_2 conditions. These estimates suggest anthropogenic CO_2 content in surface water ranging from 42 to 56 µmol kg^{-1}, with corresponding pH_T changes of 0.13 to 0.18 units. Note the estimated changes in pH along the entire BC coast exceeds the current global average decrease in surface water pH (Caldeira and Wickett 2003). Continuing to build and expand our high-resolution datasets of marine CO_2 chemistry along the BC coast is essential for observing, modeling, and understanding the impact of our changing marine seascape.

28.5. Data Availability and Acknowledgement

Final quality-controlled datasets are available at https://hecate.hakai.org. A number of people and agencies were involved in the collection of these datasets; including, Katie Pocock (Hakai Institute), Carrie Weeks (Hakai Institute), Alex Hare (Hakai Institute), Shawn Hateley (Hakai Institute), Jessy Barrette (Hakai Institute), Ray Brunsting (Hakai Institute), Jennifer Jackson (Hakai Institute), Christy Harrington (AKDOT), Geoff Lebon (NOAA PMEL/UW JISAO), Noah Lawrence-Slavas (NOAA PMEL), Darren Tuele (DFO-retired), Burke Hales (OSU), Jeremy Mathis (Georgetown University), Alaska Marine Highway System, Alaska Ocean Observing System, Alaska Coastal Rainforest Center, Northwest Association of Networked Ocean Observing Systems, BC Shellfish Growers' Association, Province of British Columbia, and the Tula Foundation.

28.6. References

Caldeira, K., and Wickett, M.E. 2003. Anthropogenic carbon and ocean pH. Nature 425: 365.

Carter, B.R., Williams, N.L., Evans, W., Fassbender, A.J., Barbero, L., and Sutton, A.J. 2019. Time-of-detection as a metric for prioritizing between climate observation quality, frequency, and duration. Geophysical Research Letters: doi:10.1029/2018GL080773.

Evans, W., Hales, B., Strutton, P.G., and Ianson, D. 2012. Sea-air CO2 fluxes in the western Canadian coastal ocean. Progress in Oceanography: doi: 10.1016/j.pocean.2012.1001.1003.

Evans, W., Pocock, K., Hare, A., Weekes, C., Hales, B., Jackson, J., Gurney-Smith, H., Mathis, J.T., Alin, S.R., and Feely, R.A. 2019. Marine CO2 Patterns in the Northern Salish Sea. Frontiers in Marine Science 5(536): doi: 10.3389/fmars.2018.00536.

Fassbender, A.J., Rodgers, K.B., Palevsky, H.I., and Sabine, C.L. 2018. Seasonal Asymmetry in the Evolution of Surface Ocean pCO2 and pH Thermodynamic Drivers and the Influence of Sea-Air CO2 Flux. Global Biogeochemical Cycles 32: 1476-1497.

Gimenez, I., Waldbusser, G.G., and Hales, B. 2018. Ocean acidification stress index for shellfish (OASIS): Linking Pacific oyster larval survival and exposure to variable carbonate chemistry regimes. Elementa: Science of the Anthropocene 6(51): doi.org/10.1525/elementa.1306.

Hare, A., Evans, W., and Pocock, K. 2017. Carbonate system time series of the northern Salish Sea. State of the Physical, Biological and Selected Fishery Resources of Pacific Canadian Marine Ecosystems in 2016. Canadian Technical Report of Fisheries and Aquatic Sciences 3225, Fisheries and Oceans Canada.

Nemcek, N., Ianson, D., and Tortell, P.D. 2008. A high-resolution survey of DMS, CO2, and O2/Ar distributions in productive coastal waters. Global Biogeochemical Cycles 22: GB2009, doi: 2010.1029/2006GB002879.

Tortell, P.D., Merzouk, A., Ianson, D., Pawlowicz, R., and Yelland, D.R. 2012. Influence of regional climate forcing on surface water pCO2, ΔO2/Ar and dimethylsulfide (DMS) along the southern British Columbia coast. Continental Shelf Research 47: 119-132.

Waldbusser, G.G., and Salisbury, J.E. 2014. Ocean acidification in the coastal zone from an organism's perspective: multiple system parameters, frequency domains, and habitats. Ann Rev Mar Sci 6: 221-247.

29. CHLOROPHYLL PHENOLOGY IN THE STRAIT OF GEORGIA: SPATIAL-TEMPORAL SATELLITE OBSERVATIONS

Maycira Costa[1]

[1]SPECTRAL Remote Sensing Laboratory, Department of Geography, University of Victoria, Victoria, B.C., *maycira@uvic.ca

29.1. Highlights

- Based on the satellite chlorophyll-a (chl-a) climatology (2003-2018) in the Strait of Georgia (SoG):
    - Spring bloom initiation occurs on average between March 22 and 30 in the Central SoG and between March 26 and April 6 in the Northern SoG.
- Spring bloom initiation occurred between March 6 to 12 for both Central and North SoG. This is similar to ferrybox observations (Sastri et al., section 27) and HPLC data (Nemcek et al., section 31).

29.2. Summary

Spatial and interannual variability of the surface chlorophyll in the SoG can be used as an indicator of phytoplankton biomass, and therefore to assess the impact of bottom-up forcing on fish populations. Data derived from satellite remote sensing offer an unparalleled tool for synoptic biomass sampling at high frequencies. This report provides an analysis of bloom initiation for the Central and Northern SoG based on MODIS-Aqua imagery from 2003-2018.

29.3. Description of the time series

MODIS-Aqua satellite data from February 2003 through November 2018 (Level 1a, 1 km^2 spatial resolution) were accessed from NASA's OceanColor web portal and atmospherically corrected using the method described in Carswell et al. (2017) and chlorophyll interpolated products described in Hilborn and Costa (2018).

The timing of the spring bloom was defined for the Central and Northern regions (Figure 29-1). The timing of bloom initiation was defined as the 8-day week where chl-a was greater than the annual median plus 5% (threshold value) and concentrations during one of the two following weeks were higher than 70% of the threshold value. These thresholds were defined annually based on regional statistics (Suchy et al., under review).

Ferrybox data was corrected according to the following steps (Travers-Smith, Costa, and Giannini, in prep.):

1) Apply a daily correction for sensor biofouling using the difference between measured fluorescence of a standard solution before and after sensor cleaning, assuming a linear increase or decrease in biofouling between cleaning dates.

2) Calculate PAR at a depth of ferry sampling using an estimated attenuation coefficient k_z. In this analysis, a regression between salinity and measured k_z obtained from CTD profiling data (Loss and Costa 2010) was used to calculate k_z for the entire ferry dataset.

3) Correct quenching using concurrent estimates of PAR_{2m} with the Davis et al., (2008) method, which removes the portion of the ferrybox measured fluorescence signal flChl-a, which is correlated with PAR_{2m}.

4) Calibrate quenching corrected qfChl-a to HPLC exChl-a (N=80) using log-log linear regression, accounting for the combined effects of sensor bias and CDOM contamination.

29.4. Status and trends

The time series analysis of the MODIS Aqua imagery shows that on average, the spring bloom initiation week (YW_{init}) is on the week of March 24 (±4 days) and on the week of March 30 (±4 days) for the Central and North Strait of Georgia, respectively. In 2018, bloom initiation happened during the week of March 9 (±4 days), for both Central and North region (Figure 29-2).

Overall, there was an excellent match-up between the regional Central SoG averages of MODIS derived chl-a andHPLC calibrated chlorophyll fluorescence ferrybox data collected between Duke Point to Tsawwassen Terminal acquired from 12:45 to 2:45 pm (time of satellite overpass and corrected for biofouling and quenching) on March 2018 (Figure 29-3). Both data showed low chl-a (<2.0 mg m^{-3}) on the first week of March, followed by concentration above 4 mg m^{-3} from March 6th to 13th defining the bloom initiation, averages concentrations decreased to values lower than 3 mg m^{-3} from March 14th to 21st, continued lower (averages < 2 mg m^{-3}) from March 22nd to 29th, and by the end of the March average concentrations are higher than 6 mg m^{-3}.

Spatially, March 2018 was a very interesting month (Figure 29-4).

- March 1-6: chl-a was low for both Central and North SOG, 2 mg m^{-3} and 1 mg m^{-3}, respectively.

- March 6-13: chl-a ranged from 4-10 mg m^{-3} for the Central region, and was around 10 mg m^{-3} for the North region, west of Texada Island, and values were around 4 mg $m^{-3}$to the north of Texada Island.

- March 22-29: Central region showed values ranging from 1-4 mg m^{-3}; North region values ranged from 1-5 mg m^{-3}.

March 30-April 6: Central region showed values ranging from 3-20 mg m^{-3}; East of Texada Island concentrations were around 20 mg m^{-3}, while the northern areas showed values from 1-3 mg m^{-3}.

29.5. References

Carswell, T., Costa, M., Young, E., Komick, N., Sweeting, R., Gower, J. 2017. Evaluation of MODIS-Aqua atmospheric correction and chlorophyll products of western North American costal waters based on 13 years of data. Remote Sensing. 9: 1063; doi:10.3390/rs9101063

Davis, R, E., Ohman, M.D., Rudnick, D.L., & Sherman, J.T. 2008. Glider surveillance of physics and biology on the Southern California Current System. Limnology and Oceanography, *53*(5,2), 2151-2168.

Hilborn, A., Costa, M. 2018. Applications of DINEOF to Satellite-Derived Chlorophyll-a from a Productive Coastal Region. Remote Sensing. 10: 1449.

Suchy, K., Hilborn, A., Costa, M., and Perry, I. (revisions submitted). Influence of environmental drivers on spatiotemporal dynamics of satellite-derived chlorophyll an in the Canadian waters of the Strait of Georgia. Progress in Oceanography. PROOCE_2018_243.

Travers-Smith, H., Costa, M., Giannini, F. (submitted) Estimating phytoplankton chlorophyll with a ferry-based instrument: correction methods. Limnology and Oceanography: methods.

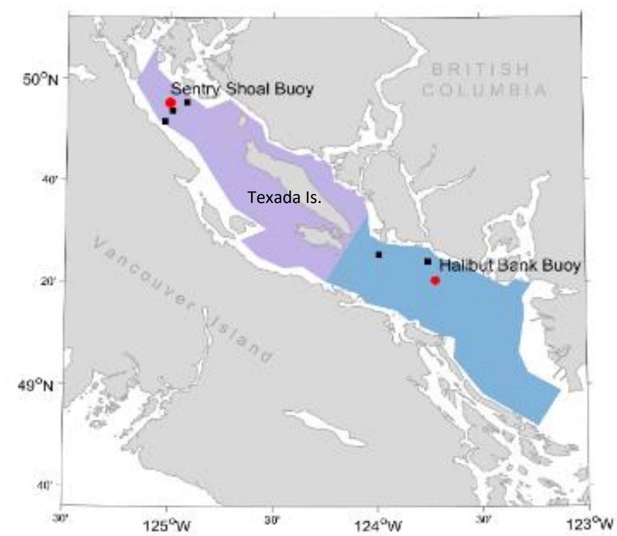

Figure 29-1. The Central (blue) and North (purple) regions of the SoG.

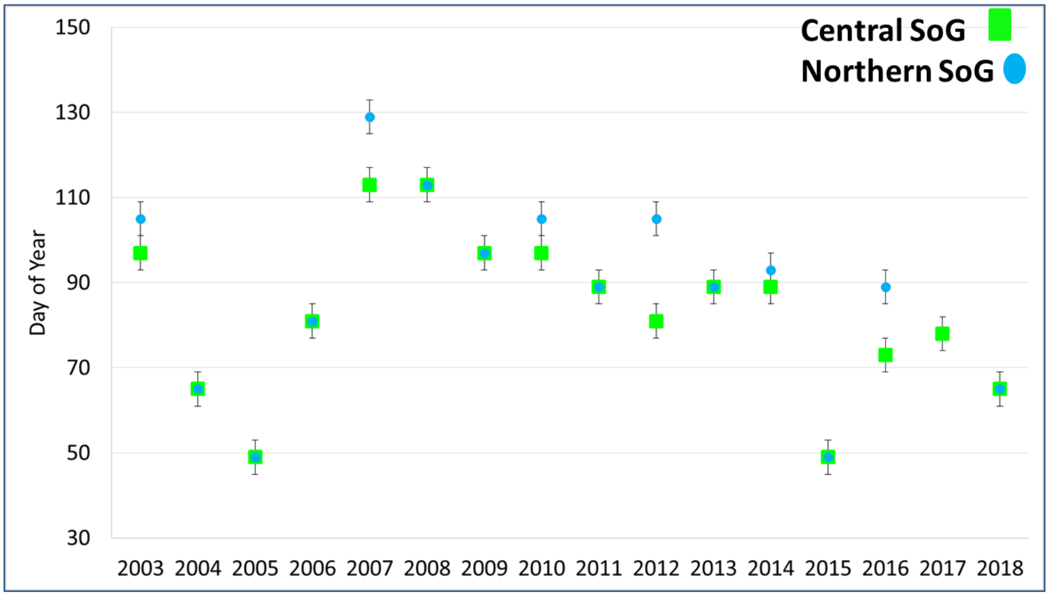

Figure 29-2. Week of bloom initiation for the Central (green) and North (blue) regions of the SoG.

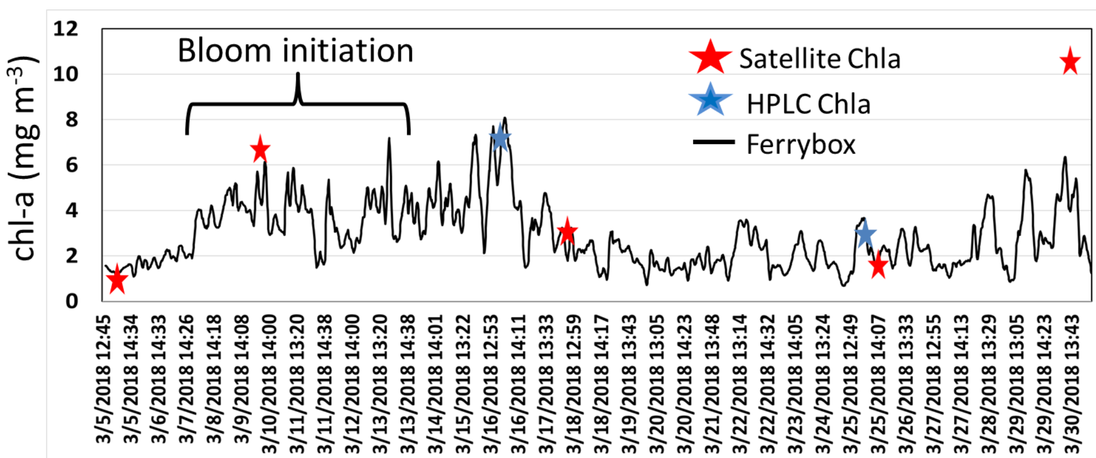

Figure 29-3. Chlorophyll time series (March 2018) for the Central Strait of Georgia from ferrybox fluorometer (black line), weekly average MODIS satellite data (red stars) and in situ measurements HPLC (blue stars). Ferrybox data corresponds to data acquired from 12:45 to 2:45 pm considering biofouling and quenching correction and calibrated to HPLC measurements.

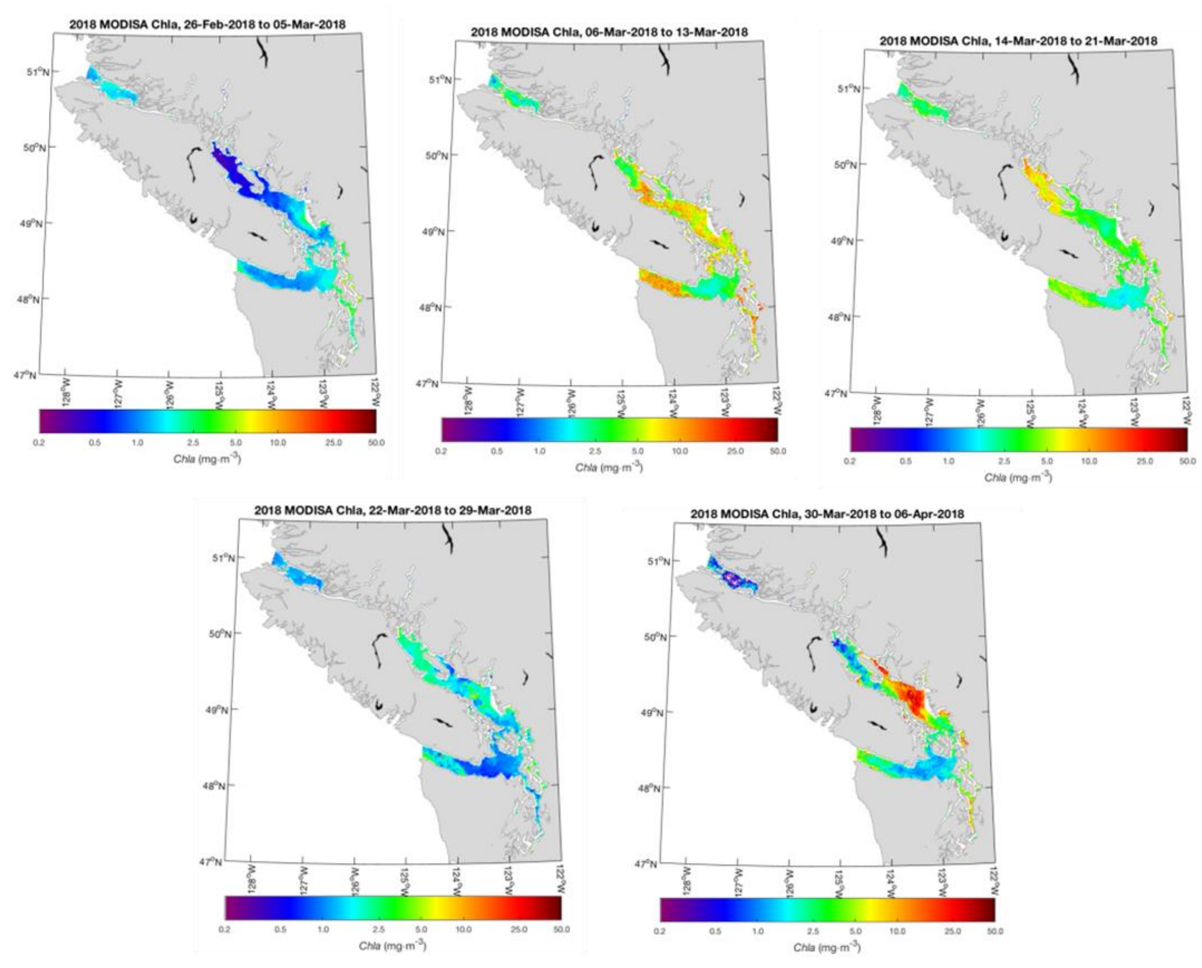

Figure 29-4. Spatiotemporal satellite derived weekly chla averages for the Salish Sea.

30. SPRING PHYTOPLANKTON BLOOM TIMING, INTERANNUAL SUMMER PRODUCTIVITY IN THE STRAIT OF GEORGIA

Susan Allen, Doug Latornell and Elise Olson, Earth, Ocean and Atmospheric Sciences, University of British Columbia, Vancouver, B.C., sallen@eoas.ubc.ca, dlatornell@eoas.ubc.ca, eolson@eoas.ubc.ca

30.1. Highlights

- The timing of the Spring Blooms in 2018 and 2019 was average.
- The spring bloom timing has changed little between consecutive years since 2006, unlike the previous 10 years.
- Mean summer productivity varies little between years in the SalishSeaCast model.

30.2. Description of the time series

Using the regions of the Strait of Georgia (SoG) defined by DFO plankton investigations based on hydrographic and plankton characteristics (unpublished, Perry and Galbraith, Fisheries and Oceans, Canada), the one-dimensional model results here pertain to the Central SoG. From the three dimensional model we show results from the Southern, Central and Northern SoG.

One-dimensional Biophysical Model: SOG: for Spring Bloom

SOG is a vertical one-dimensional physical mixing model coupled to a Nitrate-Diatom biological model (Collins et al. 2009). All two-dimensional oceanographic processes not resolved by the model are parameterized. The model location, station S3, is on the Tswwassen/Duke Point ferry route. The model is forced by winds measured at Sand Heads, clouds and temperature measured at YVR airport and river flow measurements at Hope (representing the snow melt dominated part of the Fraser River) and in the Englishman River (representing all other rivers and the rainfall dominated part of the Fraser River). Using these data sources we produced a time series of spring bloom time back to 1967 (Allen and Wolfe 2013).

Three-dimensional biophysical Model: SalishSeaCast: for Summer Productivity

SalishSeaCast is a three-dimensional coupled bio-physical model of the Salish Sea. The physical model is based on NEMO (Madec et al. 2012), with grid resolutions of about 500 m in the horizontal and 1-22 m in the vertical (Soontiens et al. 2016). Resolution is higher near the surface. It is forced by hourly realistic winds from Environment and Climate Change, Canada (2019), climatological rivers (Morrison et al. 2011) except for the Fraser River for which the flux at Hope is taken from observations. The biological model, SMELT, is based on the 3 nutrients, 3 phytoplankton, 2 zooplankton, 3 detritus model described by Moore-Maley et al. (2016).

Here we present the summer productivity as measured by 1) the biomass of the phytoplankton 2) the primary productivity and 3) the grazing by the mesozooplankton. Values are averaged over the summer (June 1 to August 31) and over the top 30-m depth, and only water with bottom depths deeper than 35-m is considered.

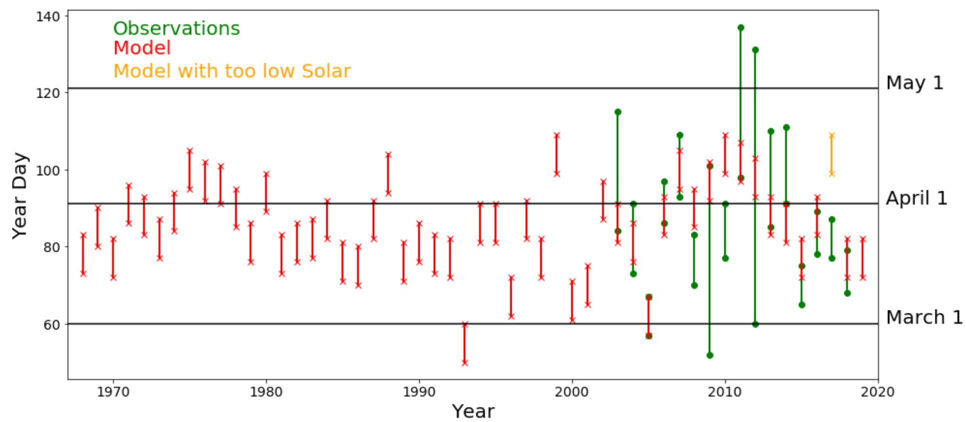

*Figure 30-1. Time series of the timing of the peak of the Spring Phytoplankton Bloom. **Green** - observations from ferry systems. **Red** – SOG model. **Orange** – SOG model with too little solar radiation (see Allen et al. 2018).*

30.3. Status and trends

Spring Bloom

The 2018 spring bloom happened between March 13 and March 23, 2018 according the SOG model (Figure 30-1). The ferry observations give ½ peak height to ½ peak height bloom timing of March 9 – March 20, 2018 (Figure 30-1). For details on the ferry observations see Sastri et al. section 27.

The 2019 spring bloom happened at the same time, according to the SOG model, between March 13 and March 23, 2019.

The mean of the SOG time series is March 26 with a standard deviation of 11 days. Of note, since 2011, the spring bloom timing has not varied strongly between years. This is similar to the time series before 1993 and very different from the large swings seen between 1993 and 2006.

Summer Productivity

In 2018, summer productivity (Figure 30-2) showed similar patterns whether measured by phytoplankton, primary productivity or mesozooplankton grazing. The northern and southern SoG are more productive than the central region.

Throughout the Strait, except in the extreme south, summer productivity in 2018 was lower than the four-year mean. The productivity was smaller than 2015 and 2016 but higher than 2017. Note that all these anomalies were small. Phytoplankton biomass, primary productivity and summer mesozoplankton grazing averaged over the domain and over the summer were 3%, 5% and 7%, respectively, which was lower than the four-year time series mean.

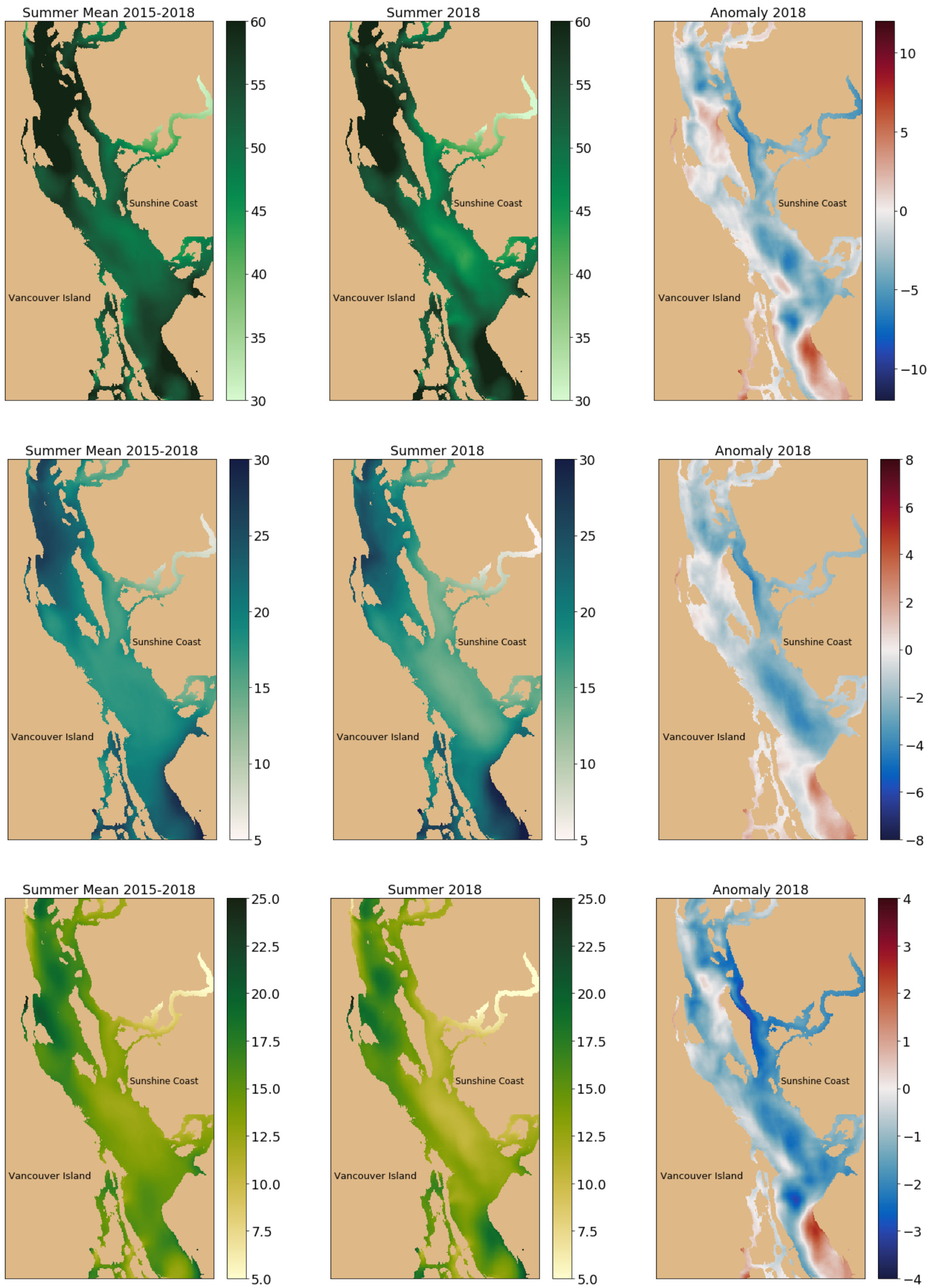

Figure 30-2. Summer productivity in the Strait of Georgia and its variation in 2018 compared to mean over 2015-2018. Values are averaged over June, July and August and integrated through the top 30-m of the water column. Only water depths greater than 35 m are shown. ***Top row****: sum of the primary producers in the model (in uM Nitrogen m^{-2}).* ***Middle row****: primary productivity in the model (in uMol Nitrogen m^{-2} day^{-1}).* ***Bottom row****: grazing by Mesozooplankton (in uMol Nitrogen m^{-2} day^{-1}).* ***Left column****: mean over four-years.* ***Middle column****: 2018.* ***Right column****: anomalies from the mean for 2018.*

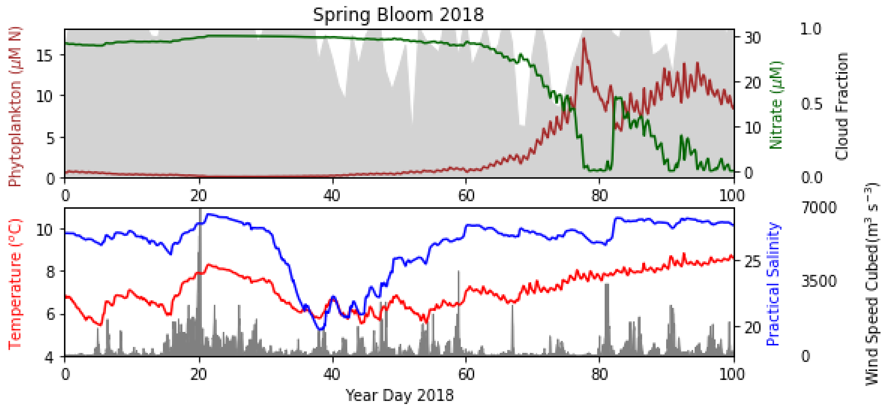

Figure 30-3. Hindcast of the 2018 spring bloom and related conditions in the Strait of Georgia. The lower panel shows temperature (in red) and salinity (in blue) averaged over the upper 3 m of the water column; in grey is the wind-speed cubed which is directly related to the strength of the mixing. The top panel shows phytoplankton biomass (in dark red) and nitrate (in green); in grey is the cloud fraction averaged over the day. The 2018 spring bloom was March 18 plus or minus 5 days. Plots span the period of January 1, 2018 to April 11, 2018.

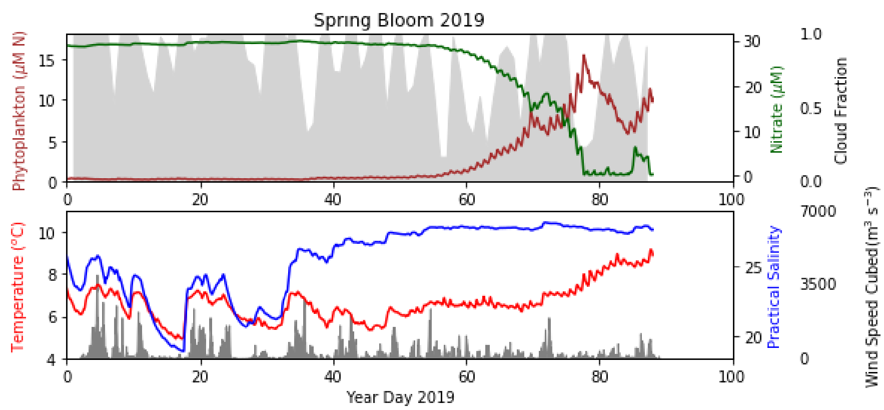

Figure 30-4. Hindcast of the 2019 spring bloom and related conditions in the Strait of Georgia. Format as for Figure 30-3. The 2019 spring bloom was March 18 plus or minus 5 days. Plots span the period of January 1, 2019 to April 1, 2019.

30.4. Factors influencing trends

Spring Bloom

According to the SOG model, the 2018 spring bloom commenced in early March after a stormy January and February (Figure 30-3). The weather improved and the clouds reduced. A single small storm delayed the bloom somewhat in early March but then the bloom happened quickly in mid March.

The 2019 spring bloom commenced a little earlier than the 2018 as winds were weaker and there was considerable more sun in January and February (Figure 30-4). The bloom was strongly interrupted by a storm in early March and then bloomed more slowly. The 2019 peak-bloom timing was the same as in 2018.

30.5. Implications of those trends

The timing of the spring phytoplankton bloom can impact herring recruitment, with recruitment being stronger for blooms with typical timing (Schweigert et al. 2013). Thus, the spring bloom timing in 2018 and 2019 was *good for herring recruitment.* Extreme shifts of timing have led to poor zooplankton growth (e.g. Sastri and Dower 2009). Consistent spring bloom timing seen in the 2010's should be *good for zooplankton such as copepods.*

The amount of phytoplankton biomass, primary productivity and mesozooplankton grazing should help define bottom-up food availability for higher trophic levels. Four years is a short time series and this is preliminary data but it appears that the gross food availability is fairly stable. It may be that the timing of that availability is more important.

30.6. References

Allen, S.E., Olson, E., Latornell, D.J., Pawlowicz, R., Do, V., Stankov, K. and Esenkulova, S. 2018. Spring phytoplankton bloom timing, interannual summer productivity. In: Chandler, P.C., King, S.A., and Boldt, J. (Eds.). State of the physical, biological and selected fishery resources of Pacific Canadian marine ecosystems in 2017. Can. Tech. Rep. Fish. Aquat. Sci. 3266.

Allen, S.E., and Wolfe, M.A. 2013. Hindcast of the timing of the spring phytoplankton bloom in the Strait of Georgia, 1968-2010. Prog. Oceanogr., 115: 6-13.

Collins, A.K., Allen, S.E., and Pawlowicz, R. 2009. The role of wind in determining the timing of the spring bloom in the Strait of Georgia. Can. J. Fish. Aquat. Sci., 66: 1597-1616.

Environment and Climate Change, Canada. 2019. HRDPS data in GRIB format [online]. weather.gc.ca/grib/grib2_HRDPS_HR_e.html

Madec, G. 2012. NEMO ocean engine. Note du Pôle de modélisation de l'Institut Pierre-Simon Laplace, No. 27, France.

Moore-Maley B., Allen, S.E. and Ianson, D. 2016. Locally driven interannual variability of near-surface pH and in the Strait of Georgia. J. Geophys. Res., 121: 1600-1625.

Morrison, J., Foreman, M., and Masson, D. 2011. A method for estimating monthly freshwater discharge affecting British Columbia coastal waters. Atmos.-Ocean., 50: 1–8.

Sastri, A.R. and Dower, J.F., 2009. Interannual variability in chitobiase-based production rates of the crustacean zooplankton community in the Strait of Georgia, British Columbia, Canada. Mar. Ecol. Prog. Ser., 288: 147-157.

Schweigert, J.F., Thompson, M., Fort, C., Hay, D.E., Therriault, T.W. and Brown, L.N. 2013. Factors linking Pacific herring (*Clupea pallasi*) productivity and the spring plankton bloom in the Strait of Georgia, British Columbia, Canada. Prog. Oceanogr., 115:103-110.

Soontiens, N., Allen, S.E., Latornell, D., Le Souef, K., Machuca, I., Paquin, J-P., Lu, Y., Thompson, K. and Korabel, V. 2016. Storm surges in the Strait of Georgia simulated with a regional model. Atmos.-Ocean, 54: 1-21.

31. SEASONAL DYNAMICS OF THE PHYTOPLANKTON COMMUNITY IN THE SALISH SEA FROM HPLC MEASUREMENTS 2015-2018

Nina Nemcek, Melissa Hennekes, and Ian Perry, Fisheries & Oceans Canada, Institute of Ocean Sciences, Sidney, B.C., Nina.Nemcek@dfo-mpo.gc.ca, Melissa.Hennekes@dfo-mpo.gc.ca, Ian.Perry@dfo-mpo.gc.ca

31.1. Highlights

- Centric diatoms dominated the spring bloom in all years with 2018 biomass levels in range of previous years. The spring bloom started ~ March 6th in the central Strait of Georgia (SoG).
- A very large *Heterosigma akashiwo* bloom was observed in the Strait of Juan de Fuca in mid-June. This harmful algal species could have negative impacts on outmigrating sockeye salmon smolts.
- Diatoms made up the bulk of the phytoplankton community in spring in the SoG, the community was composed of mixed flagellates the remainder of the year.

31.2. Description of the time series

Monitoring the seasonal and interannual variability in phytoplankton biomass and community composition is important for understanding ecosystem function, particularly as it relates to food availability for higher trophic levels (zooplankton and fish). While chlorophyll a (chl a) biomass gives an indication of the amount of available food, identifying the composition of the phytoplankton community is an important consideration for both food quality and food web structure. Fluorometric measurements of chl a have been taken on the SoG surveys since 1999 when the time series began; HPLC measurements for determining community composition were added in 2004 with a hiatus between 2012-2014. The time series was re-initiated in 2015.

Figure 31-1: Map of sampling locations in the Salish Sea with the thalweg highlighted.

Cruises take place on the *CCGS Vector* at least 3 times per year in April, June and Sept/Oct with water sampling occurring at stations along the thalweg (Figure 31-1). In 2018 we were able to capitalize on several other surveys in the area to get a more complete picture of the seasonal progression of the phytoplankton community. The biomass and composition of the phytoplankton community was determined from pigment concentrations measured by high performance liquid chromatography (HPLC) as described in Nemcek and Peña (2014). A factorization matrix program (CHEMTAX) was used to estimate the contribution of the various phytoplankton groups to total chl a (Mackey et al. 1996), and outputs were groundtruthed by comparison to microscopic analysis of Lugol's preserved samples.

31.3. Status and trends

The spring bloom in the SoG was well underway in all 4 years by the time of the April surveys with chl a biomass >10 mg m^{-3} (Figure 31-2). Centric diatoms dominated the spring bloom and comprised ~90-100% of the phytoplankton community in areas where biomass was highest. The spring phytoplankton community in 2018 was similar to that in previous years in the SoG both in terms of biomass and composition. In the Strait of Juan de Fuca, chl a was much lower in 2018 than in previous years likely due to stormy conditions during that survey that also prevented the sampling of several stations (Figure 31-2).

In June, biomass was usually much lower across the region than in spring especially in the northern SoG. In all 4 years the lowest summer biomass was observed in the north and this was also the region with the most diverse phytoplankton community (Figure 31-2). Diatoms virtually disappeared by June and smaller flagellates took over. In 2015 and 2016 haptophytes comprised ~50% of the community in the north and this could have set the stage for the significant, basin-wide coccolithophorid blooms witnessed throughout the SoG in July and August 2016. In 2017 and 2018, the community in the north was more mixed with a much larger proportion of prasinophytes and more diatoms than in the previous two years. This difference could be due to the more recent surveys capturing an earlier stage in the transition to summer conditions. In the previous 3 years in the central SoG and Juan de Fuca Strait although biomass was much lower than in spring, centric diatoms still made up a significant proportion of the phytoplankton community in summer likely due to continued nutrient inputs via the Fraser River and tidal mixing, respectively. However in 2018, diatom biomass in June was low throughout the region not exceeding 40% anywhere. The most prominent feature of the summer 2018 survey was the very large bloom of raphidophytes observed in the Strait of Juan de Fuca in June (Figure 31-2). Chl a biomass during this bloom was up to 3 times higher than the normal spring range over the last 4 years. Microscopy confirmed that this bloom was mostly composed of *Heterosigma akashiwo*, an ichthyo-toxic algae species. Smaller blooms of this raphidophyte were also observed 2 weeks prior in the central SoG and amongst the Gulf Islands (data not shown).

In September 2018, both phytoplankton biomass and community composition were comparable to the previous 3 years (Figure 31-2) Biomass levels in the SoG in fall were higher than in summer with smaller blooms compared to the spring. Diversity in the north SoG remained high and the community was generally mixed throughout the survey area. A rather unique pennate diatom bloom was observed in 2018 in the far north SoG. Microscopy revealed this was a *Pseudonitzschia sp.* bloom and was particularly unusual in that gametes were observed on the cell surfaces. Sexual reproduction in diatoms is less common that asexual cell division.

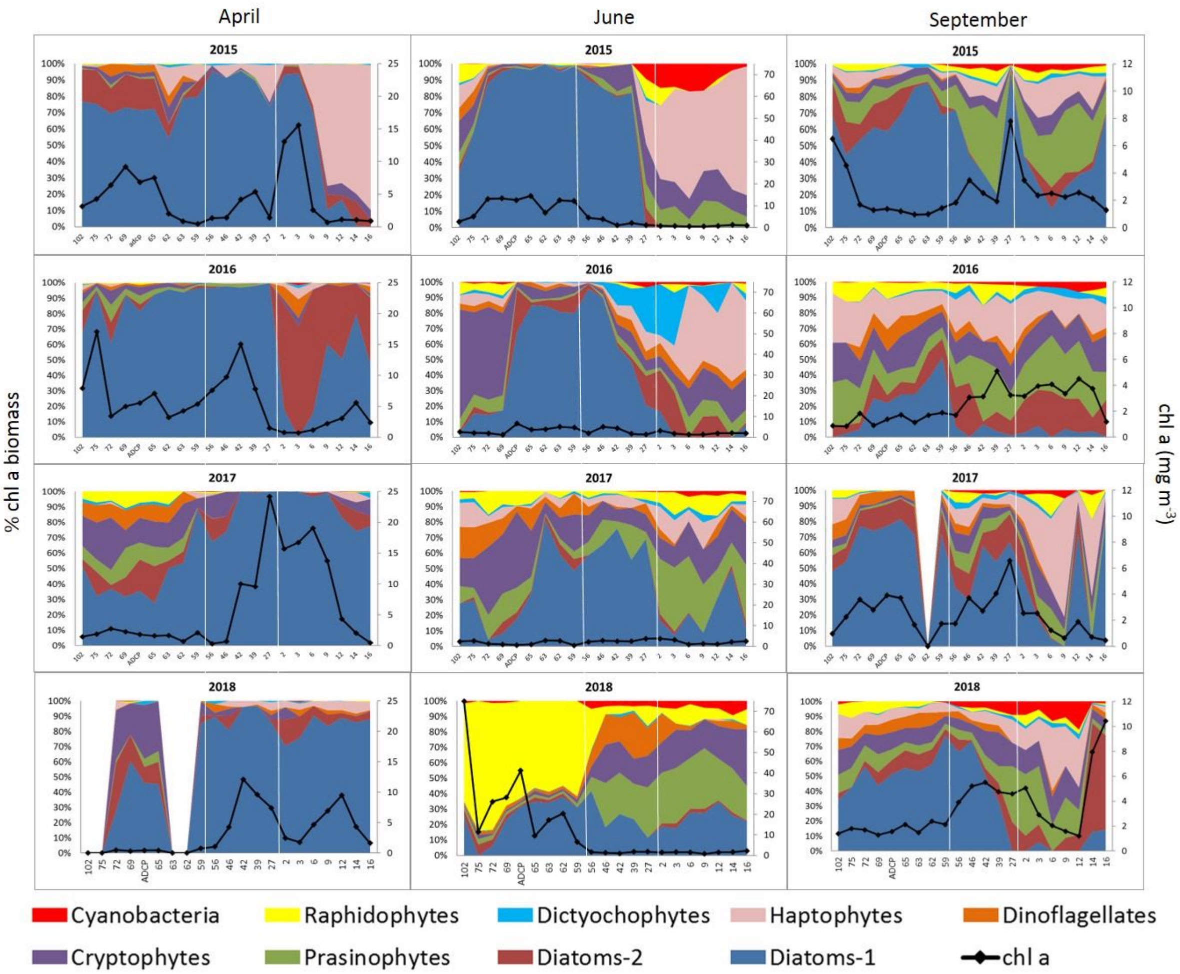

Figure 31-2: CHEMTAX outputs by station (see Figure 31-1) showing the relative contribution of each phytoplankton group to total chl a biomass (left axes) for each year and season. Absolute chl a values (black lines) are plotted on the right axes. Note the different scales for each season. White lines designate the approximate boundaries (left to right) of the Strait of Juan de Fuca, and central and northern SoG.

Supplementary sampling at select few stations in 2018 between the main spring, summer and fall surveys revealed interesting patterns in the seasonal changes in the phytoplankton community (Figure 31-3). During winter, biomass was low and nitrate levels were high everywhere. By early March in the central SoG chl a began increasing with a concomitant drawdown in nitrate. A tripling of the chl a biomass was observed over a 3 day interval between March 3-6th, indicating the start of the spring bloom (Figure 31-3a). A bloom date of ~March 6th is in close agreement with both the ONC ferry fluorescence data (Sastri et al., section 27) and satellite observations (Costa et al., section 29). In the north, the bloom likely started a week or more later and reached its peak later in April. Despite a later start, the spring diatom bloom in the north ended much more abruptly and by mid-May surface nitrate levels were depleted and the community shifted from diatoms to mixed flagellates (Figure 31-3b). In the central SoG surface nitrate depletion occurred almost a month later at which point the community also transitioned from diatoms to flagellates. In both areas of the SoG the flagellate community persisted even after bursts of nitrate were introduced in the early fall (Figure 31-3a-b). In contrast, in Haro and Juan de Fuca Straits, tidal mixing kept nitrate levels high throughout the year and centric diatoms were the main component of the phytoplankton community year round (Figure 31-3c).

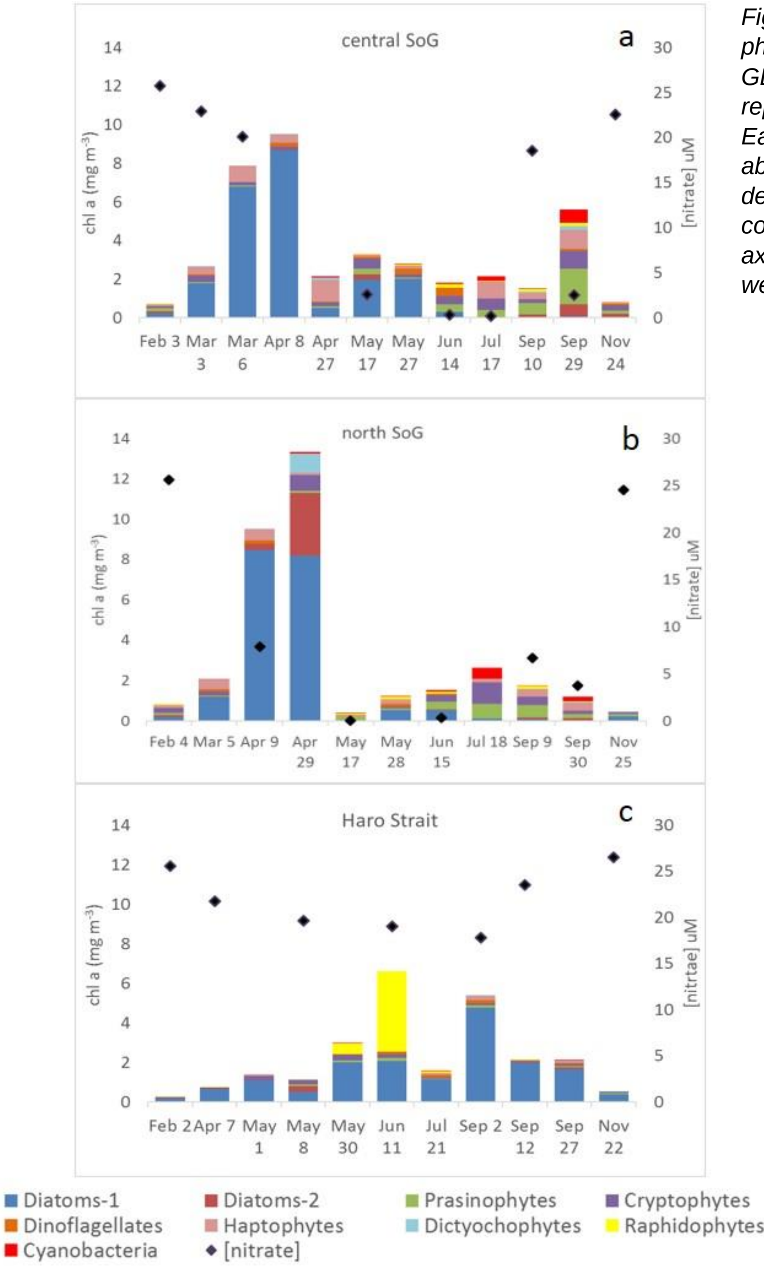

Figure 31-3. Seasonal changes in the phytoplankton community at 3 stations a) GEO1, b) stn 12 and c) stn 59 representing the 3 main survey regions. Each phytoplankton group is shown as absolute biomass equivalents of chl a as determined by CHEMTAX (left axes) with corresponding nitrate concentrations (right axes). Note that nitrate concentrations were not measured for all timepoints.

31.4. Factors influencing trends

A number of environmental factors control phytoplankton growth and community composition the two most important being nutrient and light availability. In the winter, nutrient concentrations are high but deep mixing and low irradiance prevents phytoplankton from thriving. Once the water column stabilizes the spring bloom can begin and nutrient drawdown follows. In the SoG we observed a dramatic shift in the phytoplankton community from diatoms to flagellates once surface nitrate was depleted (silicate concentrations were never limiting). Due to their larger surface area to volume ratios, the smaller flagellate cells have a competitive advantage compared to the much larger diatoms when nutrients are low. This shift happened earlier in the northern SoG presumably because the south was still receiving nutrient inputs via the Fraser River. A particularly early and large Fraser River freshet occurred in 2018 (Chandler, section 26) and was likely the driver for the large *Heterosigma* bloom which followed soon after as this species is known to thrive in low salinity waters (Rensel et al. 2010). Peak phytoplankton biomass in Juan de Fuca and Haro Straits occurred in June coincident with this bloom, not in spring like in the SoG.

31.5. Implications of those trends

Phytoplankton are the base of all marine food webs so their biomass and composition will determine both the quality and abundance of food available to higher trophic levels. Diatom based food chains are thought to be shorter with fewer trophic levels as energy is passed from phytoplankton to zooplankton to fish more efficiently, whereas flagellate based food webs rely on nutrient recycling and have more linkages and thus more losses as energy is passed to higher trophic levels. Furthermore, varying fatty acid profiles mean diatoms and flagellates have different nutritional value to their consumers. The Strait of Georgia and Strait of Juan de Fuca had very different phytoplankton community compositions. Large blooms of *Heterosigma akashiwo* have been devastating to finfish aquaculture operations but have also been linked to poor future returns of wild sockeye salmon (Rensel et al. 2010). The size and density of the summer *Heterosigma* bloom in the Strait of Juan de Fuca may thus have negatively impacted outmigrating salmon smolts which may be reflected in poor future salmon returns.

31.6. References

Mackey, M.D., Mackey, D.J., Higgins, H.W., and Wright, S.W. 1996. CHEMTAX-a program for estimating class abundance from chemical markers: application to HPLC measurements of phytoplankton. Mar. Ecol. Prog. Ser. 144: 265-283.

Nemcek, N. and Peña, M.A. 2014. Institute of Ocean Sciences Protocols for Phytoplankton Pigment Analysis by HPLC. Can. Tech. Rep. Fish. Aquat. Sci. 3117: x + 80 p.

Rensel, J.E.J., Haigh, N. and Tynan, T.J. 2010. Fraser River sockeye salmon marine survival decline and harmful blooms of *Heterosigma akashiwo*. Harmful Algae. 10: 98-115.

32. ZOOPLANKTON STATUS AND TRENDS IN THE CENTRAL AND NORTHERN STRAIT OF GEORGIA, 2018

Kelly Young[1], Moira Galbraith[1] and Ian Perry[2]

[1]Institute of Ocean Sciences, Fisheries and Oceans Canada, Sidney, B.C., Kelly.Young@dfo-mpo.gc.ca; Moira.Galbraith@dfo-mpo.gc.ca
[2]Institute of Ocean Sciences, Sidney, B.C. and Pacific Biological Station, Fisheries and Oceans Canada, Nanaimo, B.C., Ian.Perry@dfo-mpo.gc.ca

32.1. Highlights

- Little to no change in the total zooplankton biomass in 2018 compared to the last few years (preliminary).
- Zooplankton biomass in the Strait of Georgia peaks in the spring (North) or early summer (Central), based on bi-weekly surveys conducted in 2016 to 2018.
- Plankton that are not key prey for juvenile salmon (e.g. small copepods) dominated the Strait by numbers (abundance), but plankton which are preferred prey of juvenile salmon (euphausiids and amphipods) were more important by weight (biomass).
- Overall zooplankton biomass in the Strait had been trending up since 2005 until 2016. Biomass then decreased in 2017 with 2018 also low compared to previous years but having slightly higher than average biomass (preliminary).

32.2. Description of the time series

Historically, zooplankton sampling within the Strait of Georgia (SoG), has been sporadic with little coordination among short term sampling programs. Prior to 2014, zooplankton sampling did not follow consistent sampling protocols.

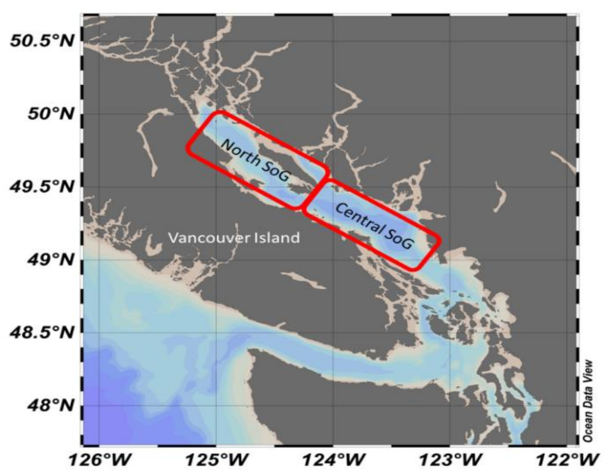

Figure 32-1. The central and northern Strait of Georgia (SoG) shown by the red boxes.

From 2015-2017 zooplankton samples were collected at approximately 20 standardized stations every 2-3 weeks from February to October as part of the Salish Sea Marine Survival of Salmon Program (supported in part by the Pacific Salmon Foundation). For 2018, the time-series was continued with monthly sampling at these same stations. The three main objectives of the zooplankton sampling program were to investigate: the seasonal and interannual patterns of the zooplankton community; the possible causes of any changes; and the potential consequences of those changes.

For this report, we address the first objective only and describe current trends of abundance (m^{-3}) and biomass (mg m^{-3} or g m^{-2}) as monthly averages of all samples collected in 2016-2018 in the deep (bottom depths greater than 80m, with at least 80% of the water column sampled) central and northern Strait of Georgia (Figure 32-1). Data were restricted to the central and northern regions as they have the most complete time series available at this time. Sample processing is ongoing to fill in the other regions.

For historical comparison, the seasonal variability in the zooplankton data was removed by calculating a regional, log-scale biomass anomaly for selected species for a given year. A multi-year (1996-2018) average seasonal cycle ("climatology") was calculated as a baseline to compare monthly conditions during any single year. Seasonal anomalies were then averaged within each year to give an annual anomaly (see Mackas et al. 2013).

32.3. Status and trends

The total zooplankton biomass in 2018 ranged from 2.5-129 g m^{-2}, with the lowest biomass occurring in the winter and peaking in the spring-early summer (May-June; Figure 32-2). Overall, total biomass was slightly above average in 2018 as shown by the annual biomass anomalies (Figure 32-3).

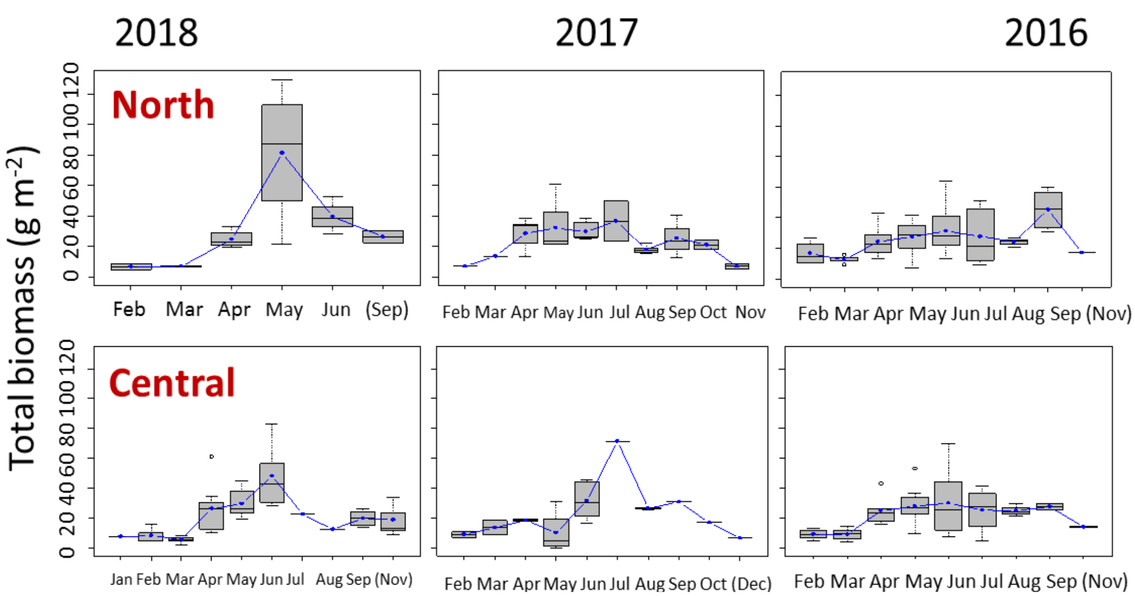

Figure 32-2. Average total biomass (g m^{-2}) of zooplankton by month in the north (top panels) and central (bottom panels) Strait of Georgia for 2016-2018.

Copepods, in particular calanoid copepods, dominated the zooplankton by abundance. Calanoid copepods and larger crustaceans (euphausiids and amphipods) dominated the biomass (Figure 32-4). Small copepods (such as *Pseudocalanus* spp. and cyclopoid-type copepods) were very abundant, but they contributed little to the overall biomass (Figure 32-5). Of the larger copepods, the copepod *Eucalanus bungii* made up the majority of the large copepod biomass in the Strait during the spring (Figure 32-5). This represents a change from the typical spring dominant large copepod *Neocalanus plumchrus*.

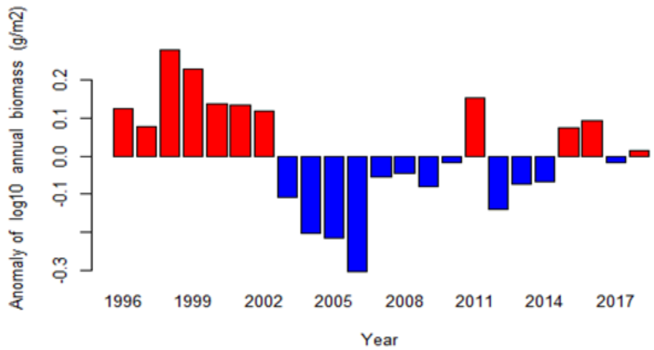

Figure 32-3. Annual biomass anomalies of total zooplankton biomass in the deep waters of the central and northern Strait of Georgia, 1996-2018.

The peak timing of the abundance and biomass of the zooplankton in the central SoG varied by species (Figure 32-4 to Figure 32-7). Within the crustacean groups considered as preferred food for juvenile salmon ('fish food'), euphausiid abundance peaked in spring. In comparison to 2017, their biomass did not peak in the fall of 2018. Decapod (mainly crab and shrimp) larval abundance also peaked in the spring, but their biomass dropped through the spring/summer as they transitioned from planktonic larvae to benthic adults. Amphipod abundance and biomass increased in the summer (Figure 32-6).

Within the ichthyoplankton, Gadiformes (mainly Hake, *Merluccius productus* in 2018) abundance and biomass peaked in the spring (Figure 32-7). Osmerid (smelts, mainly Northern Smoothtongue *Leuroglossus schmidti*) biomass increased slightly through the spring and peaked in the summer but was present in lower amounts compared to 2017. In 2018, Clupeiformes biomass increased in April, predominately Pacific Herring *Clupea pallasii* larvae (Figure 32-7, right). Clupeiformes abundance peaked in June, mainly due to the increased presence of Northern Anchovy (*Engraulis mordax*) eggs and larvae (Figure 32-7, left).

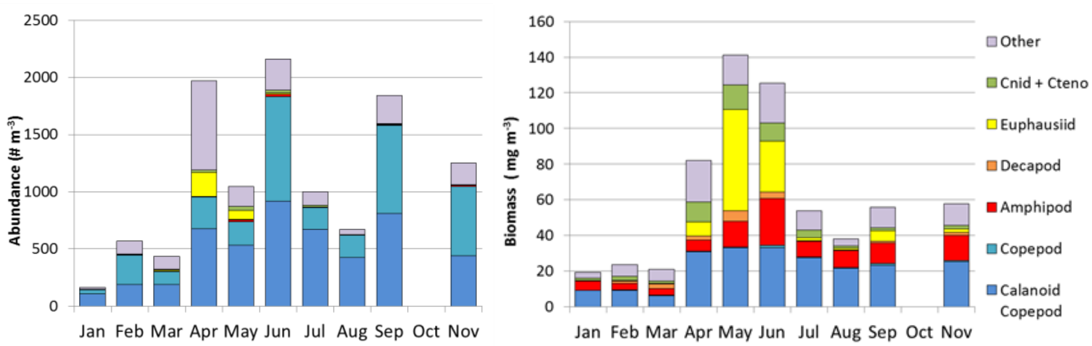

Figure 32-4. Taxonomic composition of zooplankton from northern and central Strait of Georgia in 2018, averaged by month. Left: abundance (m^{-3}); Right: biomass (mg m^{-3}). "Copepod" refers to non-calanoid copepods.

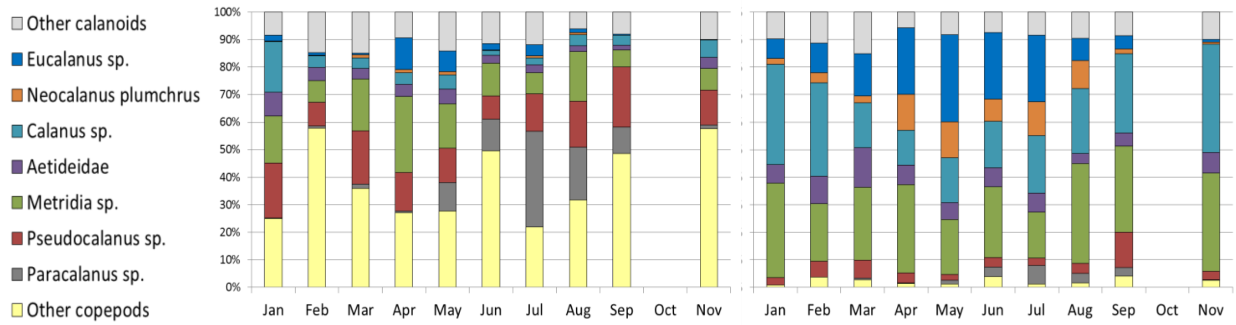

Figure 32-5. Relative abundance (left, m^{-3}) and relative biomass (right, mg m^{-3}) of all copepods collected from northern and central Strait of Georgia in 2018, averaged by month.

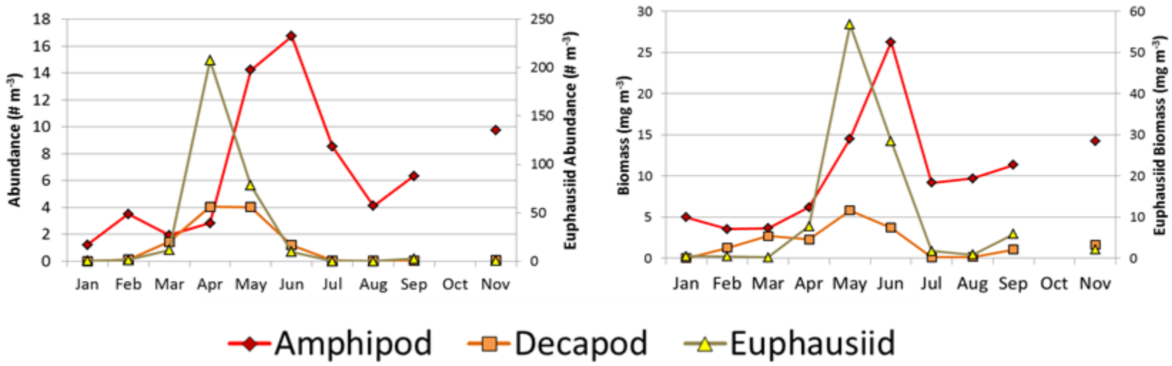

Figure 32-6. Abundance (left, m^{-3}) and biomass (right, mg m^{-3}) of 'fish food' crustaceans collected from northern and central Strait of Georgia in 2018, averaged by month. Euphausiids plotted on a secondary scale.

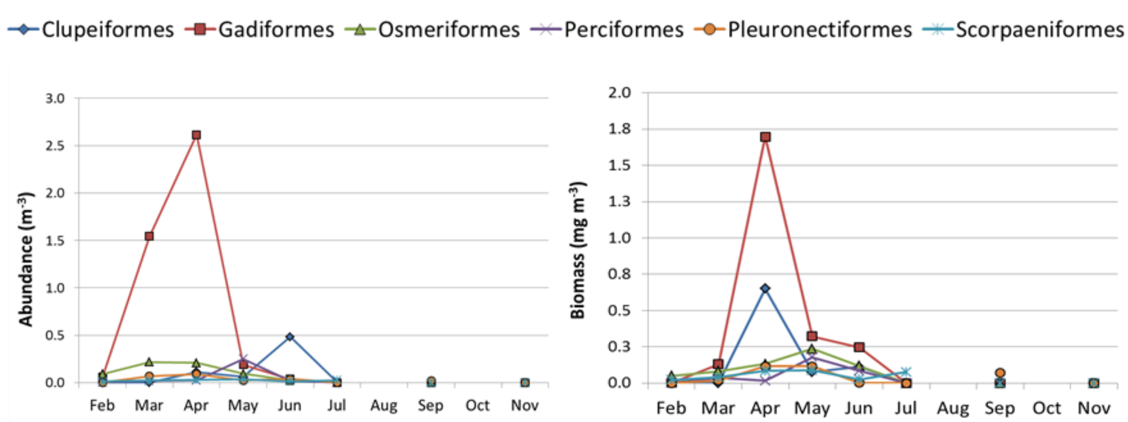

Figure 32-7. Abundance (left, m^{-3}) and biomass (right, mg m^{-3}) of ichthyoplankton collected northern and central Strait of Georgia in 2018, averaged by month.

32.4. Factors causing these trends

The factors causing these trends over time are being actively investigated as part of the Marine Survival of Salmon in the Salish Sea program, being led by the Pacific Salmon Foundation in Canada and Long Live the Kings in the United States. Research on trends between 1990 and 2010 of zooplankton biomass in the Strait of Georgia concluded that the dominant mode of variability (36% of the variance) was due to a low-frequency decadal fluctuation that declined from 1990 to 1995, increased to a maximum about 1999–2002, declined to a second minimum in 2005–2007, and then recovered to average levels by 2010. This zooplankton signal correlated positively with the North Pacific Gyre Oscillation (NPGO) climate index, negatively with temperature anomalies throughout the water column, and positively with survival anomalies of Strait of Georgia salmon and herring (Mackas et al. 2013). Current research is updating these analyses from 1995 to 2018.

32.5. Implications of these trends

Overall, the biomass of most zooplankton groups was slightly above-average for 2018. Biomass had been above average and increasing since the mid-2000's but the direction of the trend has reversed in 2017-2018 (Figure 32-3).

Sample processing is ongoing and results are preliminary. Work is ongoing to link the trends and patterns in the zooplankton to potential environmental drivers and potential impacts to higher trophic levels, including juvenile salmon survival. A consistent zooplankton monitoring program in the Salish Sea can assist with projections of future abundances of juvenile salmon.

32.6. References

Mackas, D.L, Galbraith, M., Faust, D., Masson, D., Young, K., Shaw, W., Romaine, S., Trudel, M., Dower, J., Campbell, R., Sastri, A., Bornhold Pechter, E.A., Pakhomov, E. and El-Sabaawi, R. 2013. Zooplankton time series from the Strait of Georgia: Results from year-round sampling at deep water locations, 1990–2010. Progr. Oceanogr. 115:129-159.

33. STRAIT OF GEORGIA JUVENILE HERRING SURVEY

Jennifer L. Boldt[1*], Matt Thompson[1], Matthew H. Grinnell[1], Jaclyn Cleary[1], Hilari Dennis-Bohm[1], Chris Rooper[1], Jake Schweigert[2], Terrance J. Quinn II[3], Doug Hay[2]

[1]Fisheries and Oceans Canada, Pacific Biological Station, B.C. [*]Jennifer.Boldt@dfo-mpo.gc.ca

[2]Emeritus, Fisheries and Oceans Canada, Pacific Biological Station, B.C.

[3]Juneau Center, School of Fisheries and Ocean Sciences, University of Alaska Fairbanks, U.S.A.

33.1. Highlights

- The age-0 herring index may be a leading indicator of the number of recruits joining the population 2.5 years later and the amount of prey available to herring predators in the SoG.
- In 2018, the age-0 herring index in the SoG was the 4th lowest recorded since 1992.
- In 2018, age-0 herring lengths and weights were higher than those measured in 2017 and their condition was above average.

33.2. Description of indices

The Strait of Georgia (SoG) juvenile (age-0) Pacific Herring and nearshore pelagic ecosystem survey, supported in part by the Pacific Salmon Foundation, is a monitoring program that samples the nearshore pelagic fish community, the zooplankton community, as well as the physical water column properties (e.g. temperature, salinity, oxygen). One goal of the survey is to provide an index of the relative biomass (abundance) of age-0 herring and relate it to the abundance of age-3 herring in the stock assessment model. This index may also represent trends in potential prey availability to Coho and Chinook Salmon and other predators. The methods of calculating an index of age-0 herring from the survey data collected to date are described in Boldt et al. (2015).

There are 10 core transects, each with three to five core stations (total 48 core stations), distributed at approximately equal intervals around the perimeter of the SoG that have been consistently sampled during the autumn since 1992 (except 1995; Thompson et al. 2013; see Thompson et al. 2003 for detailed survey design and methods; Figure 33-1). Sampling was conducted after dusk when herring were near the surface and, generally, one transect was sampled per night over the course of a four to seven hour period. The stations were sampled with “blind” (undirected) purse seine sets (sets were made at predetermined stations). Catch weights were estimated and all fish (or a subsample of fish) were retained for sampling in the laboratory, with the exception of large predator species (e.g. adult salmon and flatfish), which were individually measured in the field. In the laboratory, fish from each station were sorted to species and up to 100 individual age-0 herring were weighed, and measured. Herring were measured to standard length (nearest millimeter) and were between 54 and 125 mm long in all years sampled. The age-0 herring index was calculated using Thompson’s (1992) two-stage (transect, station) method and variance estimator to calculate the mean (and associated variance) of juvenile herring survey catch weight per-unit-effort (CPUE; for details see Boldt et al. 2015). In addition, herring condition was calculated as residuals from a double-log-transformed length-weight regression.

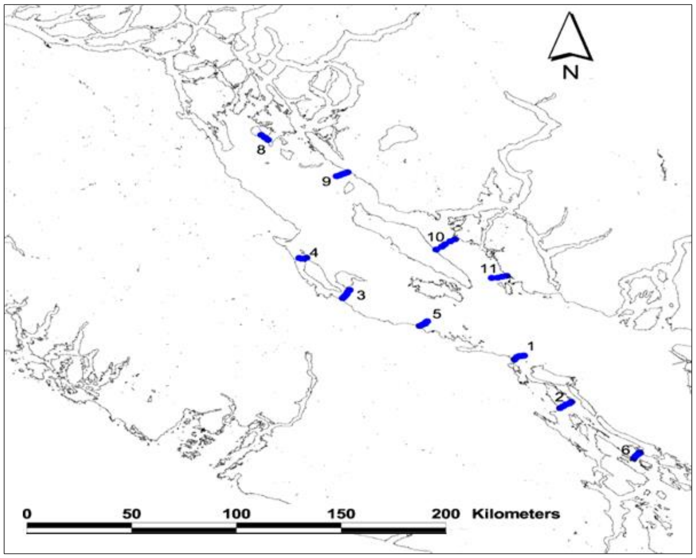

Figure 33-1. Core stations along the 10 core transects of the Strait of Georgia juvenile herring survey (there is no transect #7).

33.3. Status and trends

In 2018, 44 of the 48 core stations were sampled (1 station was not sampled due to a mechanical issue and 3 stations were not sampled due to weather). Age-0 herring were caught in all but 5 stations sampled (Figure 33-2). Estimates of age-0 catch weight CPUE (the index) varied annually, with no overall trend during 1992-2018 (Figure 33-3). The age-0 herring index tended to peak every two or three years, with the peaks occurring in even years during 2004-2012. During 2013-2018, the index was low compared to the peaks in the time series, and the 2018 index was the fourth lowest in the time series. High estimates of variability are associated with peak estimates; the survey coefficient of variation (CV) is 0.46. Age-0 herring length-weight residuals increased during 1997-2012, and were positive in 2005 and 2007-2018 (Figure 33-4). The proportion of catches that contained Northern Anchovy was still relatively high (not shown).

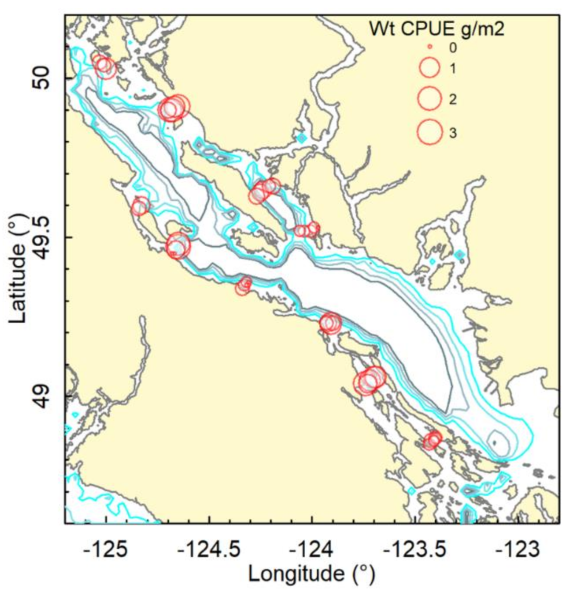

Figure 33-2. Catch weight per unit effort of age-0 herring sampled in the Strait of Georgia, 2018.

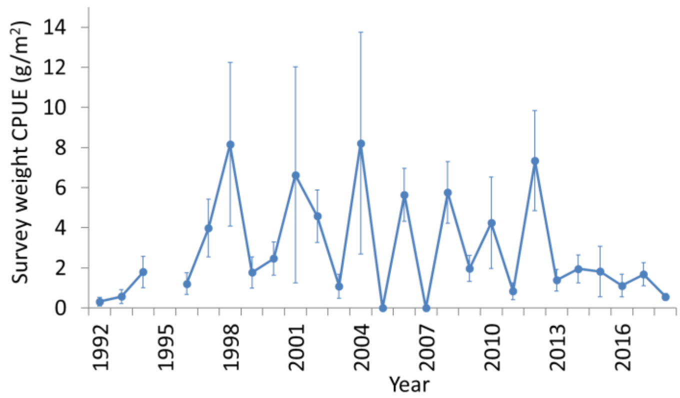

Figure 33-3. Mean catch weight per-unit-effort (CPUE) of age-0 Pacific Herring caught in the Strait of Georgia juvenile herring survey at core transects and stations during 1992-2018 (no survey in 1995; Boldt et al. 2015). Standard error bars are shown.

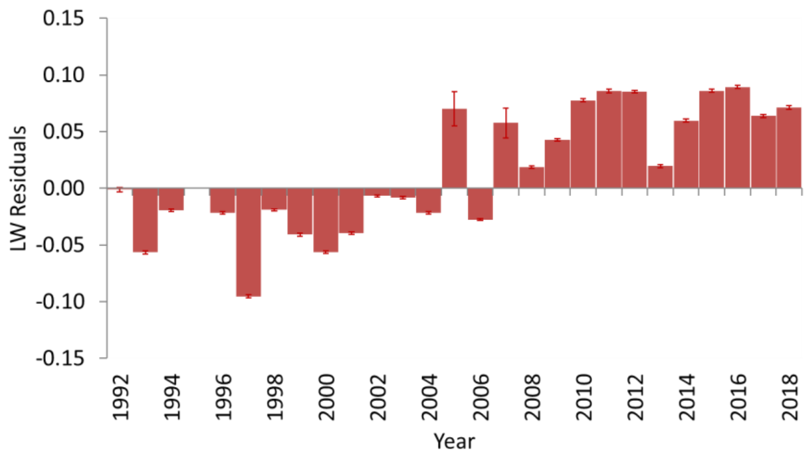

Figure 33-4. Mean age-0 Pacific Herring condition (residuals from a log-transformed length-weight regression) from the Strait of Georgia juvenile herring survey, 1992-2018 (no survey in 1995; Boldt et al. 2015). Standard error bars are shown.

33.4. Factors causing trends

Bottom-up processes (prey-driven) are the main factors affecting the interannual variability in age-0 herring abundance and condition (Boldt et al. 2018). Bottom-up factors include zooplankton prey availability, herring spawn biomass, temperatures and the date when most herring spawn relative to the spring bloom date. The timing or match-mismatch between herring and their prey appears to be important in determining abundance of age-0 herring in the fall (Schweigert et al. 2013, Boldt et al. 2018). No negative effects of the competitors or predators examined (i.e., juvenile salmon) were detected on age-0 herring abundance (Boldt et al. 2018), implying that when conditions are good for age-0 herring, they are also good for juvenile salmon species. There is some evidence that top-down (predator-driven; e.g., juvenile Coho and Chinook Salmon) processes may affect age-0 herring condition (but not age-0 herring abundance). Herring recruitment and survival has also been linked to water temperatures (Tester 1948, Ware 1991) and bottom-up control of production (Ware and Thompson 2005, Perry and Schweigert 2008, Schweigert et al. 2013).

33.5. Implications of trends

Analyses (Hay et al. 2003, Schweigert et al. 2009, Boldt et al. 2018) show that age-0 herring survey indices are correlated with the abundance of age-3 recruits (2.5 years later) as estimated by the age-structured stock assessment model (J. Cleary, DFO, pers. comm.). This correlation is heavily reliant on two years with both low age-0 and low age-3 recruit abundances (e.g. 2005 and 2007). The age-0 herring survey may therefore provide a leading indicator of low recruitment years.

Pacific Herring are prey for piscivorous fish, marine mammals, and seabirds and are important commercial species in British Columbia's coastal waters. Changes in herring abundance may affect availability to commercial fisheries as well as the survival of predators, such as Coho and Chinook Salmon. Boldt et al. (2015) state that increased age-0 herring condition indicates that "fish are heavier for a given length and may be more energy dense (Paul et al. 1998, Boldt and Rooper 2009). Fish that have a higher energy density have an improved chance at surviving reduced feeding opportunities during winter (Paul et al. 1998, Foy and Paul 1999) and present a more energy-rich prey for predators". Understanding trends in the populations of small pelagic fish species and factors that affect their abundance and condition requires long-term monitoring of the nearshore pelagic ecosystem.

33.6. References

Boldt, J.L., and Rooper, C.N. 2009. Abundance, condition, and diet of juvenile Pacific ocean perch (*Sebastes alutus*) in the Aleutian Islands. Fish. Bull. 107(3): 278-285.

Boldt, J.L., Thompson, M., Fort, C., Rooper, C.N., Schweigert, J., Quinn II, T.J., Hay, D., and Therriault, T.W. 2015. An index of relative biomass, abundance, and condition of juvenile Pacific Herring (*Clupea pallasi*) in the Strait of Georgia, British Columbia. Can. Manuscr. Rep. Fish. Aquat. Sci. 3081: x + 80 p.

Boldt, J.L, Thompson, M., Rooper, C.N., Hay, D.E., Schweigert, J.F., Quinn, T.J. II, Cleary, J.S., Neville, C.M. 2018. Bottom-up and top-down control of small pelagic forage fish: factors affecting age-0 herring in the Strait of Georgia, British Columbia. Mar. Ecol. Prog. Ser. https://doi.org/10.3354/meps12485.

Foy, R.J., and A.J. Paul. 1999. Winter feeding and changes in somatic energy content of age-0 Pacific Herring in Prince William Sound, Alaska. Trans. Am. Fish. Soc. 28: 1193-1200.

Hay, D.E., Schweigert, J.F., Thompson, M., Haegele, C.W., and Midgley, P. 2003. Analyses of juvenile surveys for recruitment prediction in the Strait of Georgia. Can. Sci. Advis. Sec. Res. Doc. 2003/107: 28 p.

Paul, A.J., Paul, J.M., and Brown, E.D. 1998. Fall and spring somatic energy content for Alaskan Pacific herring (*Clupea pallasi* Valenciennes 1847) relative to age, size and sex. J. Exper. Mar. Biol. and Ecol. 223: 133-142.

Perry, R. I., and Schweigert,J. F. 2008. Primary productivity and the carrying capacity of herring in NE Pacific marine ecosystems. Progress in Oceanography 77: 241–251.

Schweigert, J. F., Hay, D. E., Therriault, T. W., Thompson, M. and Haegele, C. W. 2009. Recruitment forecasting using indices of young-of-the-year Pacific herring (Clupea pallasi) abundance in the Strait of Georgia (BC). ICES Journal of Marine Science 66: 1681–1687.

Schweigert, J.F., Thompson, M., Fort, C., Hay, D.E., Therriault, T.W., and Brown, L.N. 2013. Factors linking Pacific herring (Clupea pallasi) productivity and the spring plankton bloom in the Strait of Georgia, British Columbia, Canada. Progress in Oceanography 115: 103-110.

Tester, A.L. 1948. The efficacy of catch limitation in regulating the British Columbia herring fishery. Transactions of the Royal Society of Canada, Vol. XLII: Series III: 135-163.

Thompson, S.K. 1992. Sampling. John Wiley and Sons, Inc. New York. 343 p.

Thompson, M., Hrabok, C. Hay, D.E., Schweigert, J. Haegele, C., and Armstrong, B. 2003. Juvenile herring surveys: methods and data base. Can. Manuscr. Rep. Fish. Aquat. Sci. 2651: 31 p.

Thompson, M., Fort, C., and Schweigert, J. 2013. Strait of Georgia juvenile herring survey, September 2011 and 2012. Can. Manuscr. Rep. Fish. Aquat. Sci. 3016: vi + 63 p.

Ware, D.M., 1991. Climate, predator and prey: behavior of a linked oscillating system, pp. 279–291. In: Kawasaki, T. (Ed.), Long-term Variability of Pelagic Fish Populations and their Environment. Pergamon Press, Tokyo.

Ware, D., and Thomson, R. 2005. Bottom-up ecosystem trophic dynamics determine fish production in the northeast Pacific. Science 308: 1280-1284.

34. HARMFUL ALGAL BLOOMS AROUND THE BC COAST IN 2018: DATA FROM THE HARMFUL ALGAE MONITORING PROGRAM

Nicola Haigh and Devan Johnson, Microthalassia Consultants Inc., Nanaimo, B.C., nicky@microthalassia.ca, devan.johnson@microthalassia.ca

34.1. Highlights

- *Heterosigma akashiwo* bloomed in 2018, in the Strait of Georgia and west coast Vancouver Island sites, after three years of lower than usual presence.
- Harmful *Chaetoceros* species were not seen in samples from the west coast of Vancouver Island, and levels were generally low on the east coast sites, except for a summer bloom of *C. convolutus* in the northern Strait of Georgia.
- No other HAB species were reported to cause mortalities to farmed salmon in 2018.

34.2. Summary

The Harmful Algae Monitoring Program (HAMP) works with the BC salmon aquaculture industry to monitor for harmful algal blooms (HABs). From spring to autumn, weekly samples are collected from sites around the BC coast and analyzed for the presence of algae species known or suspected to cause harm to farmed fish.

Heterosigma akashiwo (Raphidophyceae) is the most important harmful alga with respect to salmon aquaculture in BC. It is a frequent bloom-former, and responsible for more farmed fish kills in BC than any other HAB species (Table 34-1).

From 2015 to 2017 *H. akashiwo* blooms were less frequent than in most previous years, especially in the central Strait of Georgia. In 2018, *H. akashiwo* formed two large HABs: one in central Strait of Georgia from late May to late June, and one in Esperanza Inlet and Clayoquot Sound from mid-August to late September. The first bloom was responsible for a large mortality of farmed salmon in Jervis Inlet; mortalities were reported associated with the second bloom, but at a lower level.

Other HAB species that have been linked with farmed salmon mortalities in previous years were present in HAMP samples in 2018, but levels were generally low, and no fish-killing blooms were reported. *Chaetoceros* species that are known to cause mechanical damage to fish gills (*C. convolutus* and *C. concavicornis*) were present in samples from the eastern side of Vancouver Island, but not the western. Apart from a short-lived bloom of *C. convolutus* in the northern Strait of Georgia in late July, *Chaetoceros* cell counts were generally low. The dinoflagellates *Cochlodinium fulvescens* and *Alexandrium catenella* have caused fish kills at BC salmon farms, but although *A. catenella* was seen frequently in HAMP samples in 2018, it was never in bloom concentrations. *C. fulvescens* was seen in more samples than in recent years, however this species only formed one small bloom in Clayoquot Sound in early September. Both skeletal and non-skeletal forms of *Dictyocha*species (silicoflagellates) have been linked to farmed salmon mortalities at BC sites. From 2015 to 2017 summer blooms of non-skeletal *Dictyocha* were seen, especially in the Strait of Georgia, and some associated mortality was reported. In 2018, only low levels of*Dictyocha* were seen through the sampling season.

Other BC fish-killing HAB species were either not seen in HAMP samples in 2018, or were not reported to cause mortalities this year.

Table 34-1. HAB species causing farmed salmon mortalities in the period of 1999 – 2018, from HAMP data. Mortality levels are: LOW – 10s of fish killed; MOD – 100s to 1000s of fish killed; HIGH – tonnes of fish killed. Note: This data does not include all fish kills affecting farmed salmon in BC during this period, but only the ones that were reported to HAMP.

	MORTALITY LEVEL			
HAB Species	**LOW**	**MOD**	**HIGH**	**TOTAL**
Alexandrium catenella	1	1	1	3
Harmful *Chaetoceros*	13	8	9	30
Chattonella sp.	0	4	4	8
Chrysochromulina species	9	3	5	17
Cochlodinium fulvescens	1	0	1	2
Dictyocha species	3	2	2	7
Heterosigma akashiwo	23	22	21	66
Pseudochattonella verruculosa	0	2	3	5
Pseudopedinella pyriforme	1	0	0	1
TOTAL	**51**	**42**	**46**	**139**

34.3. Description of the time series

The Harmful Algae Monitoring Program (HAMP) is a 20-year program that has collected data on phytoplankton species prevalence and levels, with a focus on species that are harmful to fish, near salmon farm sites around the BC coast. The program is wholly funded by the BC salmon farming industry. Between 10 and 28 sites have been monitored each year, although the same sites are not monitored every year; in total 72 sites have been monitored (Figure 34-1a), with 10 sites monitored for 10 years or more, and 39 sites monitored for only one or two years. In 2018, 10 sites were monitored (Figure 34-1b). For the first time since the beginning of HAMP, Marine Harvest Canada (MOWI) did not contribute to HAMP in 2018, so there were no HAMP sites in Quatsino Sound or the Central Coast areas this year.

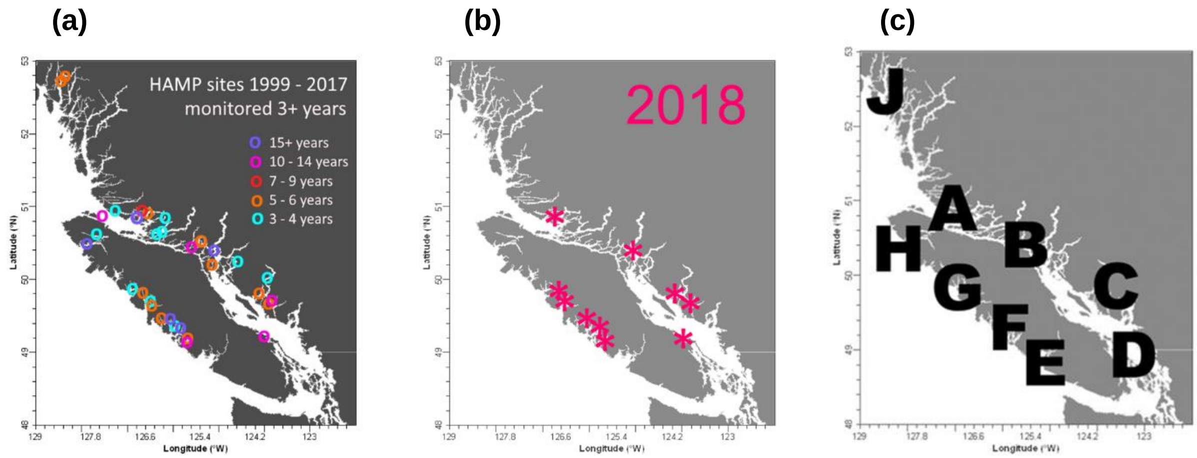

Figure 34-1. HAMP monitoring sites and areas: a) Sites monitored more than 3 years, from 1999 – 2017, b) Sites monitored in 2018, c) HAMP monitoring areas.

At the HAMP monitoring sites, discrete samples at 1-m, 5-m, and 10-m depths were taken weekly, preserved with Lugol's iodine solution, and sent to Nanaimo for analysis. Preserved samples were analysed in the Microthalassia laboratory. Analysis was done with a compound microscope using a Sedgewick-Rafter slide (Guillard 1978, LeGresley and McDermott 2010). All phytoplankton species were identified, to the lowest taxonomic level practicable, based on morphology (Hasle 1978). Algae species that are known or suspected to be harmful to finfish were enumerated, as was the dominant phytoplankton species or group (by biomass) in the sample.

Cell concentrations linked to harm to finfish vary between algae species. Certain algae species are seen at levels from 1 – 2 cells mL^{-1} to tens of thousands of cells mL^{-1}, so cell count data is ranked on a 3-point index, where 1 indicates the cells are present, but unlikely to cause harm, 2 indicates low to moderate amounts of the alga that may be at levels high enough to cause harm, and 3 indicates bloom conditions, with harmful effects very likely. Table 34-2 summarises the known harmful algae species in BC and the cell counts associated with these levels for each species.

Table 34-2. Algae species harmful to finfish in BC, with harmful index levels in cells mL^{-1}.

HAB Species	**1**	**2**	**3**
Alexandrium catenella	<10	10 – 299	300+
Harmful *Chaetoceros*	1 – 2	3 – 29	30+
Chattonella sp.	1 – 2	3 – 49	50+
Chrysochromulina species	<10	10 – 499	500+
Cochlodinium fulvescens	<10	10 – 499	500+
Dictyocha species	<10	10 – 299	300+
Heterosigma akashiwo	<10	10 – 499	500+
Pseudochattonella verruculosa	<5	5 – 99	100+

34.4. Status and trends

Heterosigma akashiwo is a common bloom former in BC, although peak levels differ in level and seasonality in the different HAMP areas around Vancouver Island and in the Central Coast (Figure 34-1c, Figure 34-2). *H. akashiwo* blooms in 2018 were fairly typical for the areas where they were observed, with highest levels in late spring in areas C and D and in August and September in areas F and G (Figure 34-3). However, peak *H. akashiwo* levels were seen 2 – 3 weeks earlier than average in areas C and D.

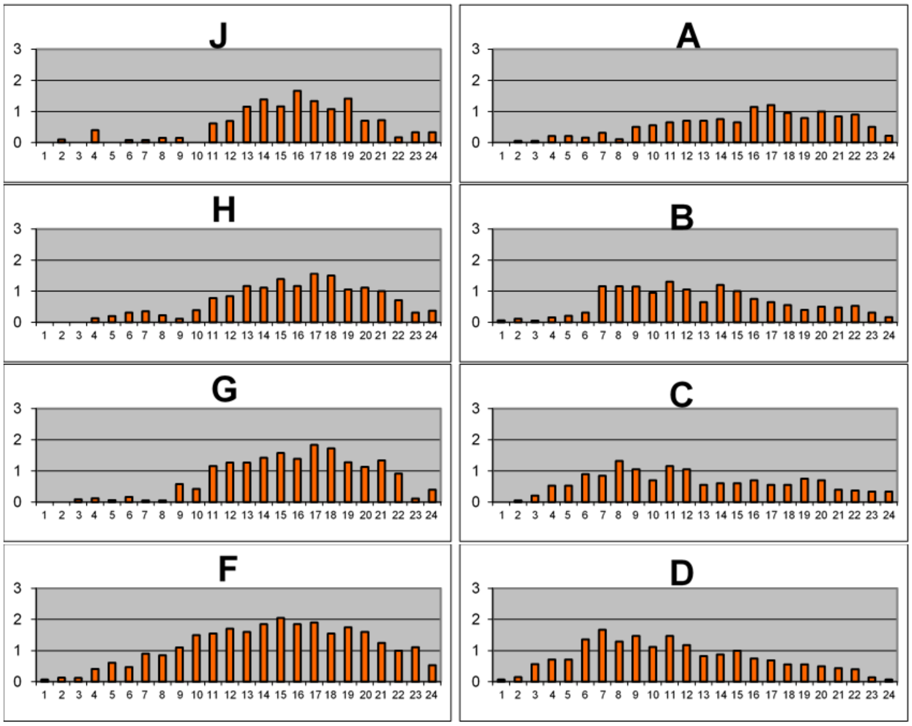

Figure 34-2. Mean weekly level of Heterosigma in HAMP areas from 1999 – 2018 data, for May 1st to October 31st. Mean is of the highest maximum level seen at all sites in that area for that week averaged over all years. Area E data is omitted, as the area was only monitored for two years.

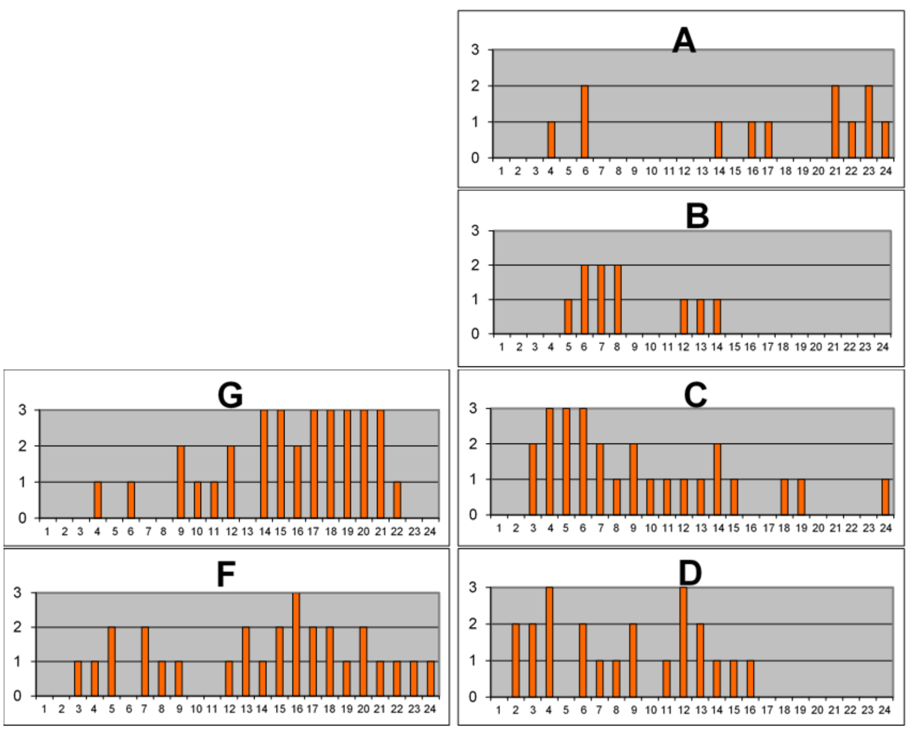

Figure 34-3. Maximum weekly H. akashiwo level at all sites in HAMP areas from May 1st to October 31st in 2018. Areas E, H, and J are omitted, as there were no HAMP sites in those areas in 2018.

34.5. Factors influencing trends

Early timing and high discharge of the Fraser River has been linked to *Heterosigma akashiwo* blooms in the Strait of Georgia (Rensel et al. 2010). The above average snow pack in the Fraser River watershed in the winter of 2017/2018, combined with record high temperatures in late April and May, caused an early and high peak in the Fraser River discharge in 2018 (Figure 34-4). This influx of fresh water, in combination with the high temperatures, contributed to the large *H. akashiwo* bloom in central Strait of Georgia this year.

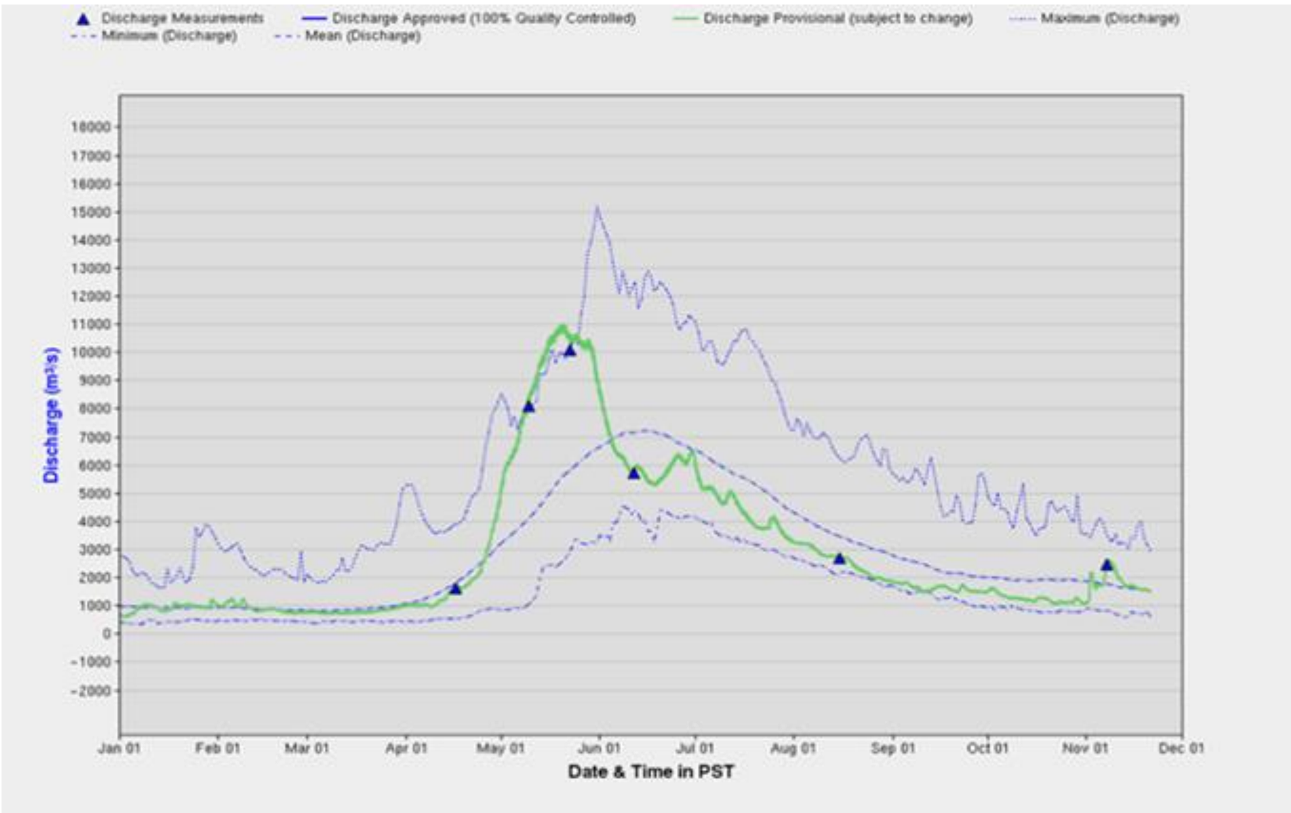

Figure 34-4. Fraser River discharge at Hope in 2018, with mean, maximum, and minimum for 1912 – 2018. From Environment Canada: http://www.wateroffice.ec.gc.ca

34.6. References

Guillard, R.R.L. 1978. Counting slides. In: Sournia, A. (Ed.), Phytoplankton Manual. Monographs on Oceanographic Methodology, vol. 6. UNESCO Publishing, pp. 182-189.

Hasle, G.R. 1978. Identification problems. General recommendations. In: Sournia, A. (Ed.), Phytoplankton Manual. Monographs on Oceanographic Methodology, vol. 6. UNESCO Publishing, pp. 125-128.

LeGresley, M., and McDermott, G. 2010. Counting chamber methods for quantitative phytoplankton analysis - haemocytometer, Palmer-Maloney cell and Sedgewick-Rafter cell. In: Karlson, B., Cusack, C., Bresnan, E. (Eds.), Microscopic and molecular methods for quantitative phytoplankton analysis. IOC Manuals and Guides, 55.UNESCO Publishing, pp. 25-30.

Rensel, J.J., Haigh, N. and Tynan, T.J. 2010. Fraser river sockeye salmon marine survival decline and harmful blooms of *Heterosigma akashiwo*, Harmful Algae, 10(1): 98-115.

35. HARMFUL ALGAL BLOOMS IN THE SALISH SEA 2018

Svetlana Esenkulova[1] and Isobel Pearsall[1]

[1]Pacific Salmon Foundation (PSF), Vancouver, B.C., svesen@uvic.ca, pearsalli@shaw.ca

35.1. Highlights

- Based on data collected as part of the Pacific Salmon Foundation (PSF) Citizen Science oceanography program, there were many prominent harmful algal blooms in the Strait of Georgia during the sampling season of 2018, in contrast to the years 2015, 2016, and 2017.
- There were widespread, highly-noticeable, bright orange *Noctiluca scintillans* blooms in April and May.
- There were significant, fish killing *Heterosigma akashiwo* blooms in June.
- There were blooms of *Gonyaulax* spp. in June/July and mixed blooms of *Rhizosolenia setigera* and *Pseudo-nitzschia* spp. in August.

35.2. Citizen Science Program

The Citizen Science Program was initially proposed by Dr. Eddy Carmack, DFO. He envisioned a 'mosquito fleet' of private boats collecting data for science everywhere in the Strait of Georgia at once. The Program was funded for 2015-2019 through the Pacific Salmon Foundation. Trained members of the local communities collected information in the Strait of Georgia 2 to 3 times a month between February and October at approximately 70 sites (Figure 35-1). Conductivity-temperature-depth (CTD) profiles were collected at all stations, nutrient samples at ~40 stations, phytoplankton samples at all stations, and zooplankton at three stations. Sample/measurement processing and analysis was done at the PSF, University of British Columbia (UBC), Ocean Networks Canada, Fisheries and Oceans Canada, and University of Victoria. The Citizen Science Program provided unique data for the entire Strait at a resolution that had not been possible before.

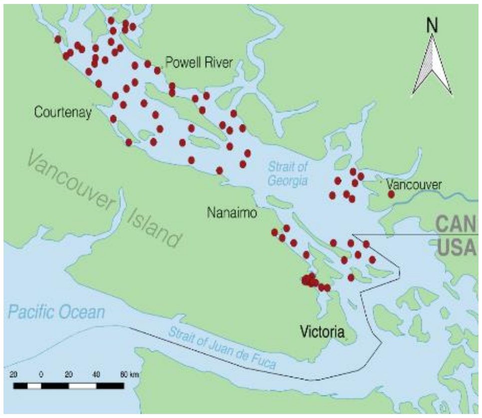

Figure 35-1. Map of the Strait of Georgia with Citizen Science Program sampling locations.

35.3. Description of the time series

Phytoplankton samples were collected 2 to 3 times a month between February and October 2015 – 2018; at the surface (0 m) at ~70 sites and depths (5, 10, and 20 m) at ~10 sites. Phytoplankton samples were analyzed on a Sedgewick-Rafter slide; the identification of specimens is done to the lowest taxonomic level possible; the enumeration (as cells mL-1) was performed for the species or group that is dominant in the sample and species that were known or suspected to have a negative effect on salmonids in B.C. (Haigh et al. 2004). This current report is based on over 1500 samples (about 75% of the total number of samples collected in 2018).

35.4. Status and trends

After the annual spring bloom (comprised mostly of *Thalassiosira, Skeletonema,* and *Chaetoceros*), there were numerous harmful algal blooms (HABs) throughout most of the sampling season. First notable HABs were caused by the dinoflagellate *Noctiluca Scintillans* (Figures 35-2 to 35-4). Blooms were first noticed in mid-April in the Northern parts of the Strait and were observed in most areas of the Strait in May. The most concentrated, vivid blooms were seen very close to the shore. The maximum concentration recorded was 3,000 cells per mL, which is extremely high considering the size of the cell *Noctiluca* (200-2000 µm).

Figure 35-2. Noctiluca Scintillans under microscope, Cowichan Bay sample, May 9, 2018. Phagocytic vacuoles with chains of Chaetoceros spp. inside can be seen. Image by S. Esenkulova.

Figure 35-3. Photo of the Noctiluca Scintillans bloom from the boat, Lund, April 18, 2018. Photo by E. Oldfield.

There were blooms of ichthyotoxic raphidophytes - *Heterosigma akashiwo* (Figure 35-5) with first cells occurring in early May samples and reaching concentrations of thousands cells per mL by the end of May and beginning of June. Most affected areas were Northern and Central SoG; the maximum cell concentration seen in analysed samples was 11,000 cells per mL, June 7. In some cases, there were mixed blooms of *Noctiluca* and *Heterosigma* (Figure 35-6).

Figure 35-4. Aerial photo of Noctiluca Scintillans bloom by the Salt Spring Island, May 2, 2018. Photo by M. Bahrey.

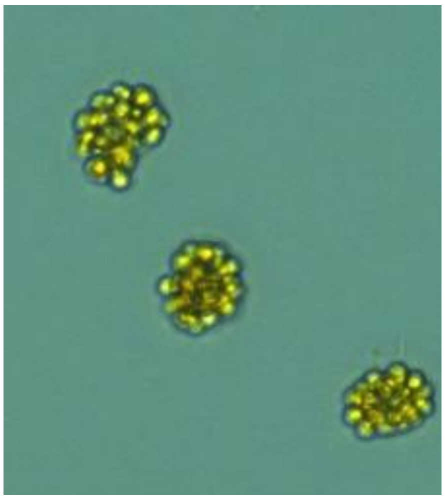

Figure 35-5. Cells of Heterosigma akashiwo, Citizen Science sample. Image by S. Esenkulova.

Figure 35-6. Aerial photo of mixed bloom of Heterosigma akashiwo and Noctiluca Scintillans, between Crofton and Kuper Island, May 22, 2018. Photo by M. Bahrey.

In the Southern SoG and Cowichan Bay, there were blooms of the small dinoflagellate *Gonyaulax* spp. (Figure 35-7) in June and the beginning of July. Samples were taken at the time when visible blooms were not present and the maximum concentrations seen were up to 200 cells per mL. Throughout August and the beginning of September, there were mixed blooms of diatoms *Rhizosolenia setigera* and *Pseudo-nitzschia* spp. Northern and Central parts of the Strait seemed to be the most affected with highest concentrations reaching 4,000 and 4,500 cell per mL respectively.

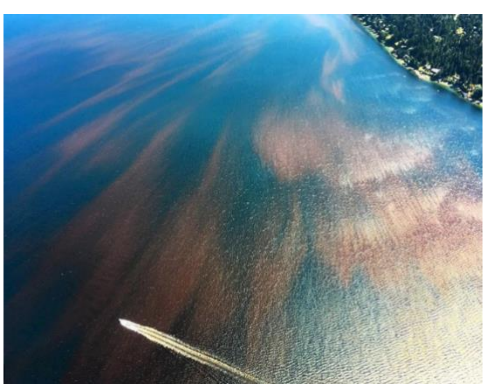

Figure 35-7. Aerial photo of Gonyaulax spp. bloom Mill Bay, June 16, 2018. Photo by M. Bahrey.

Significant blooms of these species (with the exception of *R. setigera*) were not observed in between 2015 and 2017 in the SoG, as seen in the Citizen Science samples (Table 35-1). There were no blooms of *Dictyocha* spp. in 2018 (max concentrations did not reach over 10 cell per mL) as opposed to 2016 and 2017 (where max concentrations were 450 and 400 cell per mL respectively). Our results show that the late spring and summer SoG HABs dynamics were drastically different in 2018 than for 2015-2017.

Table 35-1. The maximum cell concentrations (cell mL^{-1}) of select algae observed in the Citizen Science samples; number of samples for each year >1500.

Species	2015	2016	2017	2018
Heterosigma akashiwo	6	150	20	11,000
Noctiluca scintillans	1	2	2	3,000
Pseudo-nitzschia spp.	40	600	300	4,500
Rhizosolenia setigera	250	800	1,800	4,000

35.5. Factors influencing trends

Phytoplankton dynamics are directly governed by primary environmental factors – light, temperature, nutrients, stratification, etc. Preliminary results from CTD casts performed during the Citizen Science Program as analyzed by Dr. R. Pawlowicz showed that water temperatures of 2018 were more 'normal' (and close to 2017 values) but salinities were lower than in 2015-2017 (Figures 35-8, 35-9).

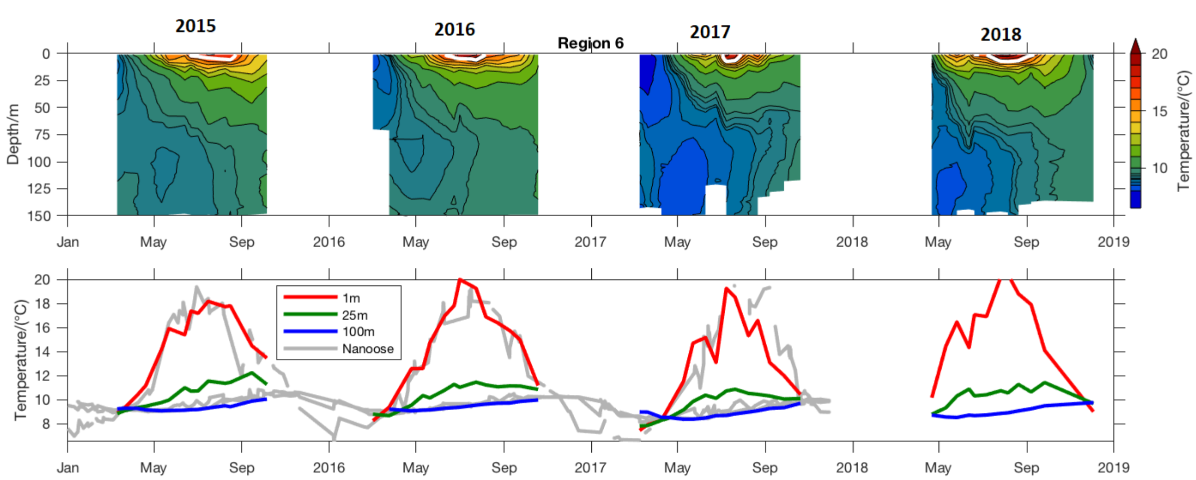

Figure 35-8. Seawater temperature at the Central Strait of Georgia (Citizen Science region 6) in 2015-2018.

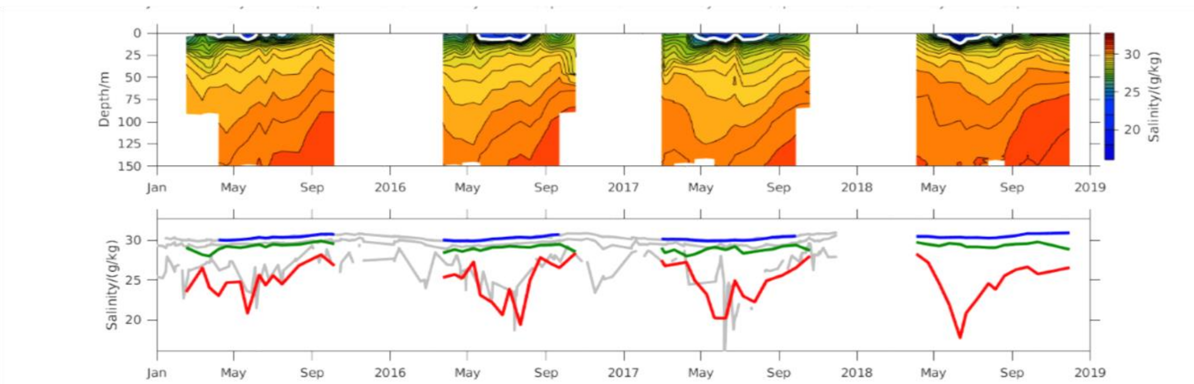

Figure 35-9. Seawater salinity at Malaspina Strait, Strait of Georgia in 2015-2018.

Lower seawater salinities and stratification are known to facilitate *Heterosigma* blooms in the SoG (Taylor and Haigh, 1993) but the relationships between other harmful algal species and environmental factors are less understood. Multiyear databases of harmful algae and environmental parameters (including nutrients) such as the PSF Citizen Science program, provide a foundation for analysis of the links between HABs and environmental characteristics in the Strait of Georgia.

35.6. Implications of those trends

Despite the common public belief that vivid blooms of *Noctiluca* are 'red tides' causing Paralytic shellfish Poisoning (PSP), this algae does not produce toxins and does not cause PSP. However, it can increase ammonia levels and cause hypoxia. This heterotrophic species is also known to disrupt classic diatom-based energy transfer. Effects of *Noctiluca* blooms on marine life in the Salish Sea are unknown.

Blooms of *Heterosigma* in the coastal waters of BC are the largest cause of direct farmed salmon losses (Haigh and Esenkulova 2014). In 2018, *Heterosigma* bloom in the Jervis Inlet killed 250,000 Atlantic salmon valued at ~$3.84 million CAD as reported by public news outlets (*e.g.* Vancouver Sun, Fishfarmingexpert). The link between marine survival of wild Chilko salmon and *Heterosigma* bloom timing in the SoG was reported (Rensel et al. 2010) and the impacts of *Heterosigma* blooms and other HABs on the wild salmon in BC must be further investigated.

Blooms of *Gonyaulax* spp. could be harmful depending on the species (some species produce toxins); however, blooms of this genus are not very common for the SoG and effects on SoG wildlife are unknown. Blooms of *R. setigera* can irritate fish gills while several *Pseudo-nitzschia* species produce toxins which cause Amnesic Shellfish Poisoning (ASP). Historic records by the Canadian Food Inspection Agency shows that levels of domoic acid (ASP toxin) almost never exceed regulatory limits in the SoG suggesting that the *Pseudo-nitzschia* blooms here have been generally nontoxic. Overall, the Citizen Science data illustrates the significant interannual variation of phytoplankton dynamics in the Strait, with 2018 being different from 2015-2017 and very eventful in terms of HABs.

35.7. References

Haigh, N., Whyte, J.N.C., and Sherry, K.L. 2004. Biological and oceanographic data from the harmful algae monitoring program associated with salmon farm sites on the west coast of Canada in 2003. Can. Data Rep. Fish. Aquat. Sci. 1158

Taylor, F.J.R., and Haigh, R., 1993. The ecology of fish-killing blooms of the chloromonad flagellate *Heterosigma* in the Strait of Georgia and adjacent waters. In: Smayda, T.J., Shimuzi, Y. (Eds.), Toxic phytoplankton blooms in the Sea, Elsevier pp. 705-710

Haigh, N., and Esenkulova, S. 2014. Economic losses to the British Columbia salmon aquaculture industry due to harmful algal blooms, 2009-2012. PICES Scientific Report. 47.

36. THE SAANICH INLET TRANSECT 2018: INCOMPLETE RECOVERY OF THE EPIBENTHIC COMMUNITY AFTER TWO YEARS OF SUSTAINED, SEVERE HYPOXIA

Jackson W. F. Chu[1], Benjamin M. Grupe[2], Janelle Curtis[3], Ryan Gasbarro[4], Jonathan M. Boschen-Rose[5], Verena Tunnicliffe[6]

[1]Memorial University of Newfoundland, St. John's, NL, jwfchu@gmail.com

[2]DFO, Institute of Ocean Sciences, Sidney, BC, ben.grupe@dfo-mpo.gc.ca

[3]DFO, Pacific Biological Station, Nanaimo, BC, Janelle.curtis@dfo-mpo.gc.ca

[4]Temple University, Philadelphia, PA, USA, rgasbarro1@gmail.com

[5]51 Matheson Road, Southampton, UK jonmrose@gmail.com

[6]University of Victoria, Victoria, BC, verenat@uvic.ca

36.1. Highlights

- In Saanich Inlet, oxygen conditions in 2018 recovered to the 2006-2013 benchmark period, as measured by the ONC VENUS array. However, the long-term trend of worsening oxygen conditions and increasing days below hypoxia thresholds continues.
- Commercial shrimp (e.g. spot prawn *Pandalus platyceros*) have recovered to the benchmark period.
- New (since 2016) species (*Armina californica* and *Pentamera* cf. *pseudocalcigera*) remain in the community, but are reduced in number.
- The sea whip (*Halipteris willemoesi*) population continues to decline; observed densities were less than 5% of the benchmark period and are at their lowest levels since the inception of this survey.

36.2. Description of the time series

Since 2006, remotely-operated vehicles (ROVs) outfitted with onboard dissolved oxygen (DO) sensors and high-definition video cameras have surveyed the same benthic transect (n=15) in Patricia Bay, Saanich Inlet, B.C (Chu and Tunnicliffe 2015, Gasbarro 2017). This near-annual survey (except for 2014-2015) is the longest-running benthic time-series in Canada designed using standardized ROV methods. The transect begins in the deep basin and runs from 180-40 m, transitioning through zones of low-to-high oxygen over a gradual slope covered in soft sediments. This survey results in imagery-based soft-bottom epifaunal counts with concomitant oxygen measurements made at 1 m above the seabed.

Also since 2006, Ocean Network Canada's (ONC) VENUS cabled observatory (96 m depth) has measured DO at one-minute intervals. Its position approximately mid-way between the start and end of the benthic transect characterizes temporal variability in the oxygen conditions of the system. Seasonal variability has been assessed at this site most recently with ROV surveys in the Spring, Summer, and Fall of 2013 (Chu and Tunnicliffe 2015) and 2016 (Gasbarro 2017, Gasbarro et al. 2017). A single survey was conducted each in 2017 (Spring) and 2018 (Fall).

Under the ecological context of this time series, hypoxia has been empirically defined by the oxygen requirements of key species present, which generally range from 0.3-1.0 ml L^{-1} (Chu and Gale 2017). The study design allows for direct comparisons of hypoxia-induced shifts in epibenthic animal distributions over time. Ten of the ~50 species that have been documented at this site have been observed in every survey from 2006-2013 (Chu and Tunnicliffe 2015, Chu 2016). Of these, we used the slender sole (*Lyopsetta exilis*) and squat lobster (*Munida quadrispina*) as indicator species of the hypoxia-tolerant community, spot prawn (*Pandalus platyceros*) as an indicator of the hypoxia-sensitive community, and the sea whip (*Halipteris willemoesi*) as an indicator of the sessile community. Because indicator species have high fidelity and specificity to their respective oxygen regimes, the relative depth of their occurrence can be useful in indicating the severity of hypoxia expansion events (Chu and Tunnicliffe 2015, Gasbarro et al. 2017).

Recently, a hypoxia-induced shift in the species assemblage occurred in Fall 2016, following the onset of a notable period of sustained oxygen deficiency (2015-2017: Gasbarro 2017, Gasbarro et al. 2017, Chu et al. 2018). Comparing survey results to the 2006-2013 benchmark period has revealed community-wide implications persisting for at least several years (Chu et al. 2018, Gasbarro et al. submitted). Most notable were the absence in Fall 2016 of spot prawn and other commercial shrimp species (*P. jordani* and *P. hyposintus*), the continued decline of sea whips and generally low populations of other epifauna (Gasbarro et al. 2017), and the occurrence of two 'new species' (the striped nudibranch *Armina californica* and the white sea cucumber *Pentamera* cf. *pseudocalcigera*) not observed in this system prior to 2016 (Gasbarro et al. submitted).

36.3. Status and trends

Annual oxygen levels in this habitat have declined by 0.05 ml L^{-1} $year^{-1}$ since the beginning of the ONC-VENUS monitoring program (Figure 36-1a, data from Feb 2006-Jan 2019). This decline accelerated to 0.07 ml L^{-1} after the 2015-2017 period of sustained hypoxia (0.88 ml L^{-1} threshold for the Eastern Pacific Ocean, Chu and Gale 2017; Figure 36-1b). To assess the vulnerability of ectotherms to climate-related stressors such as hypoxia, quantifying the severity and duration of exposure is important. The annual duration of hypoxia at this site has been increasing over time (Figure 36-1c). Since 2006, the number of days ONC-VENUS has measured oxygen conditions below the 0.88 ml L^{-1} and the 0.5 ml L^{-1} severe hypoxia thresholds has increased by a respective 9 and 8 days $year^{-1}$.

At the time of our survey on October 5, 2018, the habitat showed signs of recovering from the sustained oxygen depletion, with annual oxygen levels at ONC-VENUS having recovered just above the 0.88 ml L^{-1} severe hypoxia threshold. Despite the return of 'normal' seasonal patterns, however, oxygen was still far from recovering to 2006-2013 baseline levels, when the annual mean tended to be between 1.0-1.5 ml L^{-1}. The 2018-Fall ROV-measured oxygen profile appeared more similar to Fall profiles from the 2006-2013 benchmark period (Gasbarro et al. submitted), a recovery from the severe shoaling of hypoxic waters observed in 2016 (Figure 36-2).

The epibenthic community also showed signs of recovery. Hypoxia-tolerant species (slender sole and squat lobster) were distributed at typical depths and had normal abundances. Spot prawn returned to the system in relatively low abundances in 2017, and by 2018 had densities and depth distributions somewhat similar to 2013 (Figures 36-2, 36-3). The species that first appeared in the system in 2016 were still present in Fall 2018, though at reduced numbers (Figure 36-3). Notably, the number of sea whips observed (n=66) represents the lowest recorded abundance since this survey began, so this sessile species has continued to decline despite the improvement in oxygen conditions. Their abundance is now <5% what it was during the benchmark period.

36.4. Implications of these trends

Following the sustained period of hypoxia from 2015-2017, seafloor oxygen levels in Saanich Inlet have continued to measure above the severe hypoxia threshold for over a year. Based on abundance, most populations of key mobile fauna appear to have recovered from this extreme climatic event. Predictably, species that normally thrive in hypoxic waters (slender sole, squat lobsters) recovered first, followed by the mobile species with higher hypoxia sensitivity (e.g. pandalid shrimp), which recovered after about two years. The continued decline of the sea whip population along this transect highlights a key vulnerability for a slow-growing, sessile functional group. Pennatulacea corals are long-lived, slow-growing, and require relatively higher oxygen conditions (Chu and Tunnicliffe 2015, Neves et al. 2018), and are unable to move when hypoxic waters shoal. Post-recruitment recovery of a population would likely take several decades before community structure and function (e.g. adult biomass levels) resemble the benchmark period, which at one point peaked at >6,000 individuals in 2008. The added pressure of a new predator in the system (the striped nudibranch) could be playing a role in the continued decline of sea whips and will likely present an additional challenge to population recovery.

A novelty of this ROV monitoring program is that it controls for bottom-impact fishing activities, as commercial shrimpers generally avoid the site due to ONC infrastructure and the presence of the coast guard fleet. Thus, the decline and recovery in the benthic community can primarily be attributed to the effect of environmental stressors rather than cumulative effects of natural and anthropogenic factors. The continuation of this annual survey is critical for the ability to discern long-term trends of the effects of oxygen deficits and the potential for ecosystem persistence and resilience following sustained periods of deep-water hypoxia. There is no other benthic, ROV-based monitoring program in Canada that has a baseline existing prior to the extreme climate event.

36.5. Acknowledgements

Continuation of this time-series has been made possible by the continued support of ONC, the Canadian Healthy Oceans Network, and DFO. We are especially grateful to ONC for donating ship time with the ROV *Oceanic Explorer* in October 2018, as well as for the logistics, field, and technical expertise we received from Akash Sastri, Steve Mihaly, Paul Macoun, Ian Kulin, Reyna Jenkins, and Karen Douglas.

36.6. References

Chu, J.W.F. and Leys, S.P. 2010. High resolution mapping of community structure in three glass sponge reefs (Porifera, Hexactinellida). Mar. Ecol. Prog. Ser. 417: 97-113.

Chu, J.W.F. and Tunnicliffe, V. 2015a. Oxygen limitations on marine animal distributions and the collapse of epibenthic community structure during shoaling hypoxia. Global Change. Biol. 21: 2989-3004.

Chu, J.W.F. and Tunnicliffe, V. 2015b. Data from: Oxygen limitations on marine animal distributions and the collapse of epibenthic community structure during shoaling hypoxia. Dryad Digital Repository. https://doi.org/10.5061/dryad.1p55v

Chu, J.W.F. 2016. Influence of seasonally variable hypoxia on epibenthic communities in a coastal ecosystem, British Columbia, Canada. PhD Thesis. University of Victoria.

Chu, J.W.F. and Gale, K.S.P. 2017. Ecophysiological limits to aerobic metabolism in hypoxia determine epibenthic distributions and energy sequestration in the northeast Pacific ocean. Limnol. Oceanogr. 62: 59-74.

Chu J.W.F., Curkan, C., and Tunnicliffe V. 2018. Drivers of temporal beta diversity of a benthic community in a seasonally hypoxic fjord. R. Soc. Open sci. 5: 172284.

DFO. 2010. Pacific region cold-water coral and sponge conservation strategy 2010-2015.

DFO. 2012. Assessment of the impact of northern shrimp trawling on benthic habitats and communities in the Estuary and northern Gulf of St. Lawrence. DFO Canadian Science Advisory Secretariat. Science Advisory Report 2012/054.

Gasbarro, R. 2017. Benthic ecology in two British Columbian fjords: compositional and functional patterns. MSc Thesis. University of Victoria.

Gasbarro, R., Chu, J.W.F., and Tunnicliffe, V. 2017. Epibenthic community structure along a dissolved oxygen gradient. In: Chandler, P.C., King, S.A., and Perry, R.I. (Eds.). State of the physical, biological and selected fishery resources of Pacific in 2016. Can. Tech. Rep. Fish. Aquat. Sci. 3225.

Gasbarro, R., Chu, J.W.F., and Tunnicliffe, V. Disassembly of an epibenthic assemblage in a sustained, severely hypoxic event in a northeast Pacific basin (submitted).

Neves, B.M., Edinger, E., Wareham Hayes, V., Devine, B., Wheeland, L., and Layne, G. 2018. Size metrics, longevity, and growth rates in *Umbellula encrinus* (Cnidaria: Pennatulacea) from the eastern Canadian Arctic. Arctic Sci. 4: 722-749.

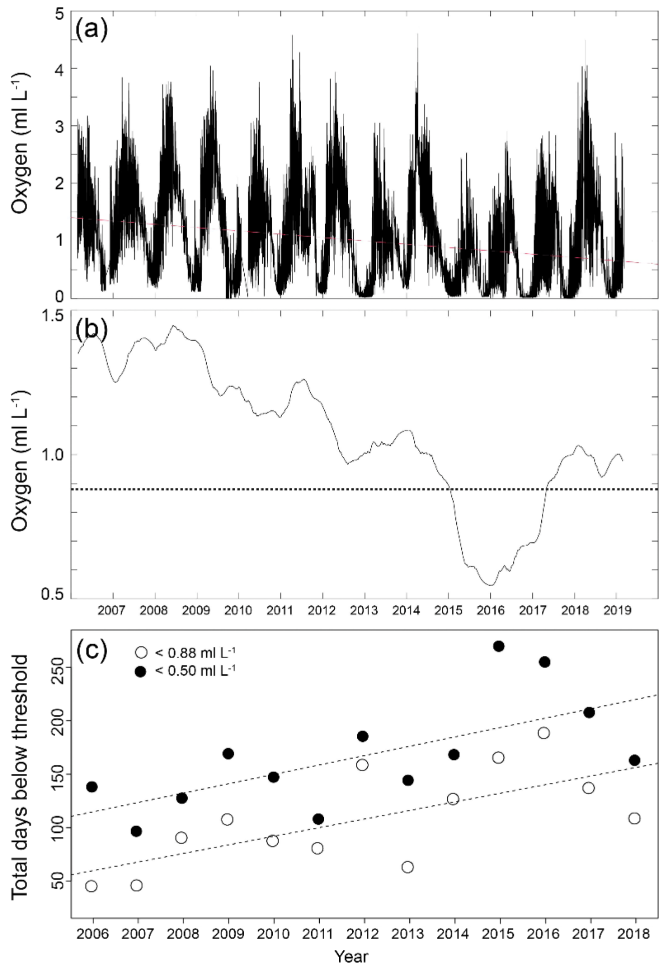

Figure 36-1. The 13-year continuous ONC-VENUS dissolved oxygen (DO) records measured per-minute at 96 m in Patricia Bay, Saanich Inlet. (a) Despite regular seasonal patterns, DO has decreased during the monitoring period (dashed line). (b) One-year running mean of the per-minute DO data illustrates the 2015-2017 sustained period hypoxia. Dashed line is the 0.88 ml L^{-1} East Pacific hypoxia threshold. (c) The cumulative annual days below hypoxia thresholds has increased over time.

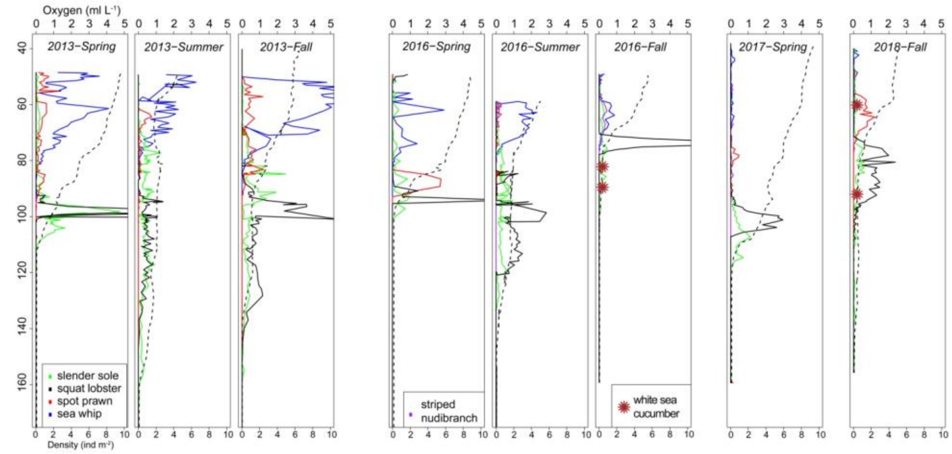

Figure 36-2. Surveys of key species depth-based densities in Patricia Bay, Saanich Inlet relative to DO gradient (dashed line) in 2013 (n=3), 2016 (n=3), 2017 (n=1), and 2018 (n=1). No surveys were conducted in 2014-2015. Note that spot prawn and two other commercial shrimp species were absent in the 2016-Fall survey, but have since recovered to benchmark period (2006-2013) numbers. Sea whip population abundance continued to decline in the 2018-Fall survey and is at its lowest recorded level since surveys began in 2006.

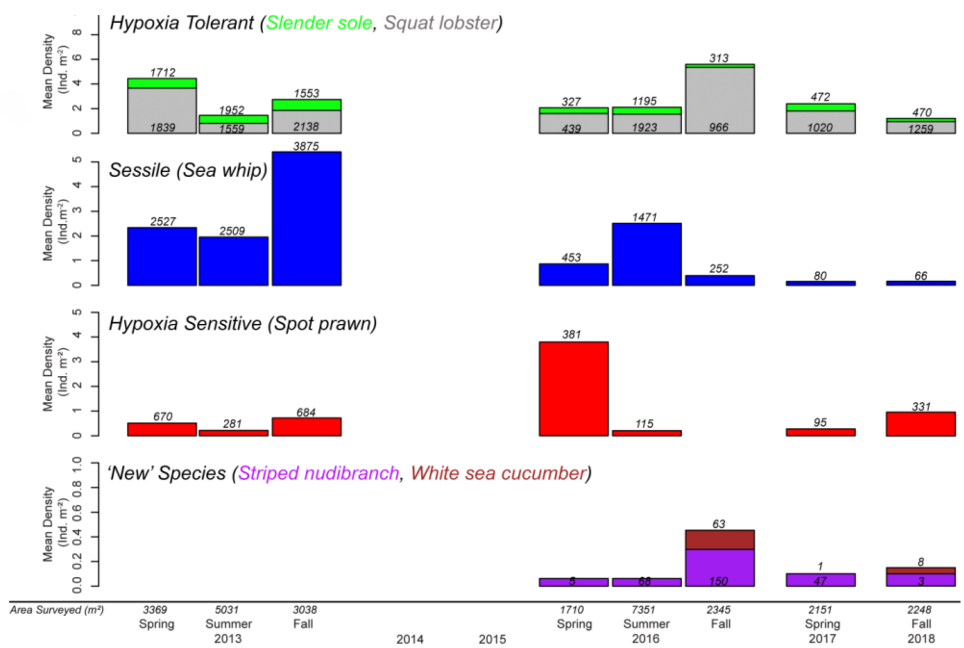

Figure 36-3. Average densities per survey for each key species presented and grouped by hypoxia tolerant (squat lobster, slender sole), sessile (seawhip), and hypoxia-sensitive (spot prawn) taxa. Total counts are indicated on each bar. Total area surveyed (m²) for each year is indicated on the x-axis. Differences in area surveyed among years is primarily attributable to truncation of the deeper portion of the transect and varying field performance among different ROV platforms [ROPOS: 2013 (Summer, Fall), 2016 (Summer); Oceanic Explorer: 2013 (Spring), 2016 (Spring, Fall), 2018 (Fall); Hercules: 2017 (Spring)]. No surveys were performed in 2014-2015. 'New species' (striped nudibranch, white sea cucumber) are taxa that were absent from 2006-2013 benchmark period. Average densities were calculated from abundances occurring in 20 m² sections along each transect where species occurred. 2013 data are from Chu and Tunnicliffe (2015a). 2016 data are from Gasbarro (2017). Earlier surveys (2006-2012) are not presented but are published in Chu and Tunnicliffe (2015b).

37. DFO SCIENCE DIVE SURVEYS - INVERTEBRATES AND NEARSHORE HABITATS

Joanne Lessard and Janet Lochead, Fisheries & Oceans Canada, Nanaimo, BC
Joanne.Lessard@dfo-mpo.gc.ca, Janet.Lochead@dfo-mpo.gc.ca

37.1. Highlights

- Most dive surveys to date have been species-specific surveys, targeting commercially important nearshore invertebrate species and are generally focused on density estimation for quota calculations – not the collection of representative data to assess stock status.
- Two methods have recently been developed to address some of the issues related to the lack of trend data as well as the lack of data on the distribution of nearshore habitats, which have hindered spatial planning.

37.2. Summary

This contribution summarizes seven of the most common ongoing dive surveys conducted in nearshore BC coastal waters by Fisheries & Oceans Canada (DFO), Marine Invertebrates Section (Stock Assessment & Research Division) and Marine Spatial Ecology and Analysis Section (Ecosystem Science Division). Many surveys are conducted in collaboration with the fishing industries as well as several First Nations. There are other types of dive surveys conducted by DFO in British Columbia (BC), notably herring spawn surveys and many experimental invertebrate surveys, which are not discussed. All surveys described here, focus on benthic habitats, specifically marine invertebrates and algae (for some). Survey designs, depths sampled, and data collected varied by survey; however, substrate data are collected on all surveys.

Most dive surveys to date have been species-specific surveys, targeting commercially important nearshore invertebrate species and are generally focused on density estimation for quota calculations – not the collection of representative data to assess stock status. As a result, there are no formal time-series survey programs to monitor stock trends over time for most benthic marine invertebrate fisheries, except for Northern Abalone and Green Sea Urchin which use index sites. Two methods have recently been developed to address some of the issues related to the lack of trend data as well as the lack of data on the distribution of nearshore habitats which have hindered spatial planning: Multispecies surveys and Benthic Habitat Mapping. These two methods take a broader ecosystem approach to surveys of nearshore benthic habitats.

*Figure 37-1. **Left**: divers collecting data along a transect with a 1 m long bar. **Right**: divers using a 1 m^2 quadrat to collect data.*

37.3. Description of dive surveys

37.3.1. Giant Red Sea Cucumber, *Apostichopus californicus*

Stock assessment surveys of the Giant Red Sea Cucumber populations in BC have been conducted annually since 1997. They are used to assess density and biomass in areas currently open to commercial harvesting or to assess areas not currently open to commercial harvesting where there is a desire to re-open the area in upcoming years.

Transect locations are determined by placing transects systematically every 1-2 km along the selected shoreline, usually most of the shoreline encompassed within a Pacific Fishery Management Area (PFMA). Transects are surveyed from 18 m to the surface, and transect length therefore depends on the slope of the sea floor. Sea Cucumbers are counted and recorded on both sides of the transect, every 5 m within 2 m of the transect (so that each quadrat is 2 x 5 m). For each quadrat, the following are recorded: number of adult and juvenile sea cucumbers; up to three dominant substrate types; and two dominant algae types. Relative abundance estimates of Geoducks, Green Sea Urchins and Red Sea Urchins are also recorded on the dive.

Duprey and Stanton (2018) described most recently published survey results for Sea Cucumber.

37.3.2. Geoduck, *Panope generosa*

Every year, four to five geoduck density dive surveys are conducted in various locations along the BC coast. These are specifically designed to estimate density for biomass calculation. Quota options for the Geoduck fishery are calculated on a by-bed basis.

In each survey, several Geoduck beds are surveyed. Within each randomly selected bed, transect positions are located randomly. Transects are marked at 5 m intervals and laid across the bed, extending from 3 m to 18 m chart-datum depth. Two SCUBA divers, one on either side of the transect, count visible geoduck shows (siphon) or dimples within 1 m of each side of the transect. At the end of each 5 m segment, divers record depth, total number of Geoducks and Horse Clams (*Tresus capax* and *T. nuttallii*), dominant algal species and the three most dominant substrate types. Depending on the length of transect, subsampling of quadrats within transects can take place.

Bureau et al. (2012), describes the assessment framework and has a brief description of the survey methods.

37.3.3. Green Sea Urchin, *Strongylocentrotus droebachiensis*

Fishery-independent dive surveys have been conducted at index sites in two areas of the South Coast: 1) PFMA12 in Northeast Vancouver Island, initiated in 1995; and 2) PFMA19 in Southeast Vancouver Island, initiated in 2008. Surveys were initially conducted annually, then biennially, and in recent years triennially. The main objectives of the surveys are to monitor trends in Green Urchin abundance in the areas that are open to commercial harvest, and to generate time series abundance indices that are used, along with CPUE, as indicators of stock status in the stock assessments.

Index sites have been selected in locations that were identified as productive sites by harvesters. At each index site, divers count or measure all species of urchins occurring within 1 m^2 quadrats along the length of each transect, following either a leadline or compass bearing. The transects run perpendicular to the shoreline and/or depth contours, from deep to shallow, from 10 m below Chart Datum to 0 m Chart Datum. Within each quadrat, other data are also collected: up to three dominant substrates, all algal species for each category of algae (canopy = >2 m tall, understory = 30 cm to 2 m tall/long, and turf = 0 to 30 cm tall/long) and the respective percent cover for each category, plus the percent cover for encrusting algae. Depending on the length of transect, subsampling of quadrats within transects can take place.

DFO (2018) described most recently published survey results for Green Urchin as well as the stock status in two regions of the coast.

37.3.4. Red Sea Urchin, *Mesocentrotus fransiscanus*

The Red Urchin fishery-independent surveys are designed to provide data that can be used to estimate density and biomass at the Subarea level of PFMA for the development of quota options for Fisheries Managers. Different Subareas have been surveyed each year and provide an annual snapshot of Red Urchin abundance and size in small areas of the coast.

Sites are selected using a random-systematic design that systematically places transects every 1-2 km along the shoreline within a Subarea, with a random start point. Transects are laid perpendicular to shore from shallow water to approximately 15 m gauge depth (chart datum depth plus tide height). Densities of Red Urchin are estimated within 1 m^2 quadrats along the transects. Test diameter is recorded for all Red Urchin as well as shell length for all Northern Abalone found within sampled quadrats. Within each quadrat, other data are also collected: up to three dominant substrates, all algal species for each category of algae (canopy, understory, and turf) and the respective percent cover for each category, plus the percent cover for encrusting algae. Depending on the length of transect, subsampling of quadrats within transects can take place.

Leus et al. (2014) described the assessment framework for Red Urchin as well as the results from multiple surveys.

37.3.5. Northern Abalone, *Haliotis kamtschatkana*

Northern Abalone has been monitored at index sites along the East Coast of Haida Gwaii and the Central Coast Regions of BC by DFO since 1978. In response to conservation concerns, surveys were expanded to include the West Coast of Vancouver Island Region in 2003, the Queen Charlotte Strait Region in 2004, and the West Coast of Haida Gwaii Region in 2008. Each Region is surveyed every five years.

At each site, divers place a 1 m^2 quadrat at the upper edge of Northern Abalone habitat, typically around 0 m chart datum, and sample 16 quadrats within a 7 x 16 m area (four transects separated by 4 m, each with four quadrats separated by 1 m) (Figure 37-1, right). In each quadrat, divers record the number and size of Northern Abalone, up to three dominant substrates, dominant algal species for each category of algae (canopy, understory, and turf) and the respective percent cover for each category plus encrusting, the number and relative size of any predator species present, and the number of Sea Urchins. Curtis and Zhang (2018) described most recently published survey results and stock status for Northern Abalone.

37.3.6. Multispecies

Quantitative stock assessment surveys for dive fisheries in BC have historically been conducted as single-species surveys. Since survey methods are similar for some species, it may be possible to gain efficiencies in the field by using a multispecies survey approach rather than the single-species approach historically used. Perhaps more importantly, moving to a multispecies survey design would help work towards an ecosystem based approach to stock assessment and an understanding of the interactions between species. For long term monitoring of population abundance and assessment of stock status, a new survey protocol is being developed where species of interest are assessed quantitatively (Table 37-1). The vision for the project is to set up a network of index sites in a number of regions throughout the BC coast and conduct multispecies surveys within each region on rotational basis. So far, three surveys have been conducted: 1) portions of Queen Charlotte Strait in 2016, 2) portions of the Gulf Islands in the Strait of Georgia in 2017, and 3) a re-survey of 2017 sites as well as additional sites in Queen Charlotte Strait in 2018.

The first time a region is surveyed, the survey locations are selected randomly. Transects are laid out from 2 m above chart datum to a depth of 12 m chart datum with a maximum length of 125 m. Divers record data within a 1 m^2 quadrat on one side of the transect. In each quadrat divers record depth, time, substrate with percentages for the three dominant substrates, algae species and the percent cover of algae in the following categories: canopy, understory, turf and encrusting. All Abalone, Sunflower Star (*Pycnopodia helianthoides*)*,* Red, Green and Purple Sea Urchins are measured. Geoducks and Sea Cucumbers are counted. In addition, relative abundance for the species measured and counted as well as two invasive species (*Ciona intestinalis* and *Botryllus schlosseri*) are estimated for the transect. Depending on the length of transect, subsampling of quadrats within transects can take place.

37.3.7. Benthic Habitat Mapping

Relatively little is known regarding shallow (0-20 m depth) benthic habitat types and associated marine benthic invertebrate and algae communities along the BC coast, most of the work having concentrated on species of commercial interest. The nearshore habitat types and community composition represents a data gap that needs to be addressed in order to provide scientific support to ongoing and future marine-use planning initiatives. A new visual survey design was developed in 2013 to help map the nearshore region. The data collected, when combined with some environmental data, will hopefully enable us to define several habitat types and map them (Table 37-1). Several surveys have been conducted in BC since 2013. The 2013-2015 survey results for eastern Haida Gwaii and north coast are described in Davies et al. (2018). In addition, portions of the southern Strait Georgia and Juan the Fuca Strait were surveyed in 2017 as well as portions of the west coast of Haida Gwaii and Queen Charlotte Strait in 2018.

Transect locations are randomly selected throughout the study area in order to encounter a variety of habitat types. The presence or absence of 102 invertebrate and 59 algae species or species groups is documented from as shallow as the conditions permit to a depth of 18 m (gauge depth). Divers recorded observations every 5 m within 1 m of the transect line (so quadrats are 1 x 5 m) (Figure 37-1, left). The diver on the left side of the transect recorded substrate (three most dominant and their percent cover) and all algae species as well as algal percent cover in the following categories: canopy, understory, turf and encrusting. The diver on the right looked for and recorded presence of all invertebrate species that were on the datasheet (therefore true absence are included). Relative abundance along the entire transect is also documented for 15 of the most commonly observed invertebrate species. Depending on the length of transect, subsampling of quadrats within transects can take place.

Table 37-1. Comparison between Multispecies and Habitat Mapping dive surveys.

	Benthic Habitat Mapping	Multispecies
Type of data	Qualitative • presence/absence - Quadrat • Relative abundance – Transect	Quantitative • Measure/count - Quadrat • Relative abundance – Transect
Objective	Define nearshore habitats & hopefully map them	Monitor trends in abundance and assess stock status of commercially important benthic invertebrates
Focus	Ecosystem/habitat	Sea Cucumber, Green & Red Urchins, Northern Abalone
Site selection	Random sites	Index sites (selected randomly on 1st survey)
Time series	Survey once throughout the BC coast Long-term plan is to use Multi-species and other surveys to ‘validate’ habitat type	Long-term monitoring of commercial important benthic invertebrates in fished and closed areas (MPA)

37.4. References

Bureau, D., Hand, C.M. and Hajas, W. 2012. Stock Assessment Framework for the British Columbia Geoduck Fishery, 2008. DFO Can. Sci. Advis. Sec. Res. Doc. 2011/121. viii + 79p.

Curtis, D.L. and Zhang, Z. 2018. Northern Abalone, *Haliotis kamtschatkana*, stock status and re-analysis of index site surveys in British Columbia, 2000-2016. Can. Man. Rep. Fish. Aquat. Sci 3162 vi + 161 p.

Davies, S.C., Bureau, D., Lessard, J., Taylor, S. and Gillespie, G.E. 2018. Benthic habitat mapping surveys of eastern Haida Gwaii and the North Coast of British Columbia, 2013-2015. Can. Tech. Rep. Fish. Aquat. Sci. 3278: vi + 24 p.

DFO. 2018. Stock Status Update for Green Sea Urchin (*Strongylocentrotus droebachiensis*) in British Columbia and Harvest Options for the Fishery in 2018 to 2021. DFO Can. Sci. Advis. Sec. Sci. Resp. 2018/054.

Duprey, N.M.T., and Stanton, L.M. 2018. Biomass estimates for sea cucumber (*Parastichopus californicus, Cucumaria miniata, C. pallida*) as determined through surveys conducted June 2013 to May 2014. Can. Manuscr. Rep. Fish. Aquat. Sci. 3112: x + 72 p.

Leus, D., Campbell, A., Merner, E., Hajas, W.C., and Barton, L.L. 2014. Framework for Estimating Quota Options for the Red Sea Urchin (*Strongylocentrotus franciscanus*) Fishery in British Columbia Using Shoreline Length and Linear Density Estimates. DFO Can. Sci. Advis. Sec. Res. Doc. 2013/094. vi + 68 p.

Individual reports on the special session

38. DFO'S STATE OF THE SALMON PROGRAM: SPECIAL SESSION ON SALMON

Sue C.H. Grant[1] & Bronwyn L. MacDonald[1]

[1]Fisheries and Oceans Canada, Pacific Biological Station, Nanaimo, B.C., Sue.Grant@dfo-mpo.gc.ca; Bronwyn.MacDonald@dfo-mpo.gc.ca

- The goal of DFO Science's State of the Salmon Program is to track and understand trends in Pacific Salmon. The Program achieves this goal by developing tools and processes to integrate our collective knowledge on salmon and their ecosystems.

- Land and ocean temperatures have increased globally over the past century, with the most recent five years representing the warmest on the planet. This is impacting the regional freshwater and marine ecosystems used by the Pacific Salmon stocks of BC and the Yukon. Interactions between regional drivers and local habitats create variability in freshwater and marine ecosystem responses to change, in some cases magnifying the effects.

- The Intergovernmental Panel for Climate Change (IPCC) projects further warming by 1-6°C over the next 30-80 years. Predicting how Pacific Salmon populations will be affected is one focus of DFO research.

- Salmon responses vary by species, latitude and population, and are further affected by variation in life-history, phenology, and physiology. Northern Sockeye, Chinook and Coho Salmon populations are generally doing better than historically compared to Southern populations. A number of Sockeye, Chinook, and Coho Salmon populations in the south are at imminent threat of extinction based on recent Committee on the Endangered Wildlife in Canada (COSEWIC) status assessments. Pink and Chum Salmon are generally doing better throughout their range. For all these general examples there are exceptions.

- DFO held the first State of the Salmon Workshop in May 2018 which brought together scientists working on salmon and ecosystems. The goal of this workshop was to integrate scientific knowledge to better understand current trends in salmon populations and ecosystem observations within the recent context of warming, exaggerated by the 2013-2016 marine heatwave.

- A second State of the Salmon Workshop (March 2019) built upon knowledge shared in the first workshop, to begin to develop a framework for predicting salmon responses to future climate change. This work is necessary to support the adaptation of current salmon recovery, habitat restoration, salmon enhancement, and fisheries management efforts to future, not past, salmon biodiversity.

- A series of presentations in the special State of the Pacific Ocean (SOPO) session focussed on Pacific Salmon, and formed a foundation for the second State of the Salmon workshop, convened during the week after the SOPO meeting subsequent week.

39. FRASER RIVER SOCKEYE 2018 UPDATE: ABUNDANCE AND PRODUCTIVITY TRENDS

Sue C.H. Grant[1], Bronwyn L. MacDonald[1], Keri Benner[1], Catherine G.J. Michielsens[2] and Steve Latham[2]

[1]Fisheries and Oceans Canada, Pacific Biological Station, Nanaimo, B.C., Sue.Grant@dfo-mpo.gc.ca, Bronwyn.MacDonald@dfo-mpo.gc.ca, Keri.Benner@dfo-mpo.gc.ca

[2]Pacific Salmon Commission, Vancouver, B.C., Michielsens@psc.org, Latham@psc.org

39.1. Highlights

- Fraser River Sockeye Salmon (*Oncorhynchus nerka*) productivity and returns for the aggregate have declined since the mid-1990s.
- This trend was interrupted for a brief period from 2010 to 2013, when productivity and returns improved to average.
- Fraser Sockeye that returned in 2015 to 2018 generally exhibited lower productivity and returns. These Sockeye spent most of their lives in above average to exceptionally warm freshwater and marine conditions that began in 2013.
- Examination of disaggregated data on 19 individual Fraser sockeye stocks shows that most trends were synchronous across stocks in the early period of this decline, suggesting broad-scale regional factors were affecting returns.
- In recent years, productivity estimates displayed greater asynchrony indicating that local drivers or unique stock-specific factors have contributed to the observed trends.

39.2. Description of the time series

Fraser River Sockeye Salmon returns, productivity (recruits-per-spawner), and Chilko Sockeye Salmon freshwater and marine survival are presented in the current report. Methods associated with analyses of these data are described in Grant et al. (2011). Details on the annual recruitment data quality are presented in Ogden et al. (2015).

Fraser Sockeye Salmon typically return to freshwater to spawn as four year old fish, after spending their first two winters in freshwater, and their last two winters in the ocean. Therefore, total Fraser Sockeye Salmon survival is influenced by both the freshwater and marine ecosystems.

Fraser Sockeye Salmon use different freshwater and marine habitats throughout their life. Specifically, after their second winter in freshwater, most smolts leave their rearing lakes and migrate down the Fraser River to the Strait of Georgia. Most Fraser Sockeye migrate north through the Strait of Georgia in approximately 40 days (Preikshot et al. 2012, Neville et al. 2016) and exit this system via the Johnstone Strait. Fraser Sockeye juveniles continue their northward migration along the continental shelf, and move into the Gulf of Alaska by their first winter at sea (Tucker et al. 2009). They subsequently spend one more winter in the marine environment before they return to their natal freshwater spawning grounds as adults.

39.3. Status and trends

Total Fraser Sockeye returns have declined since the mid-1990's, with the exception of returns on the 2018 cycle (Figure 39-1A). Sockeye returns in 2010 and 2014 were particularly high with 30 and 20 million fish, respectively.

Declines in Fraser Sockeye returns have coincided with declines in their aggregate productivity (Figure 39-1B). This productivity pattern was interrupted by improved productivities in 2010 to 2013 (Figure 39-1B), influencing the improved returns observed during this period (Figure 39-1A). The 2014 return, though large, exhibited lower than average productivity, which continued in subsequent years.

Trends in total Fraser Sockeye returns and productivity are largely determined by the populations that comprise the greatest proportion of the total abundance in each year, namely the Summer Run (e.g. Chilko), and Late Run populations (e.g. Late Shuswap on dominant cycle years). Across the individual Fraser Sockeye populations there has been considerable variability in productivity (recruits-per-spawner) (Figure 39-2).

Although most populations, such as Chilko and Stellako, have exhibited declining trends since the 1990's, some populations, such as Late Shuswap, have not exhibited any persistent trends, and the Harrison River population that increased in productivity during this period (Figure 39-2). Particular stock characteristics may explain why some stocks deviate in terms of trends in productivity.

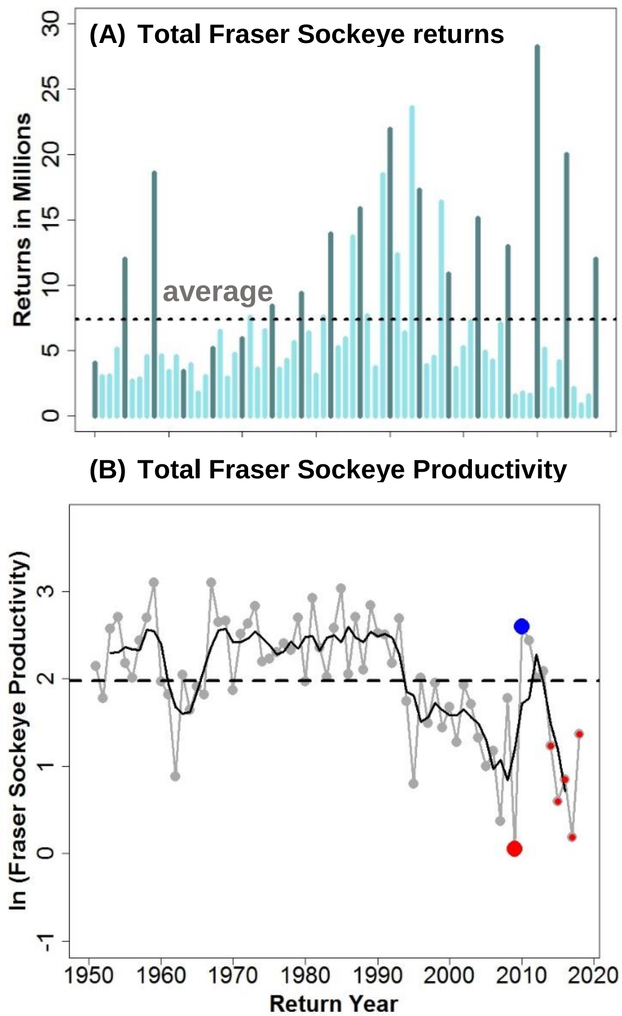

Figure 39-1. (A) Total Fraser Sockeye annual returns (dark blue vertical bars for the 2018 cycle and light blue vertical bars for the three other cycles). Recent returns from 2016 to 2018 are preliminary, and 2018 (the last data point) is an in-season estimate only. (B) Total Fraser Sockeye productivity (log_e (returns/total spawner)) is presented up to the 2018 return year. The grey dots and lines represent annual productivity estimates and the black line represents the smoothed four year running average. For both figures, the dashed line is the time series average.

Late Shuswap is a unique stock that displays considerable variability in abundances on four-year cycles, with one large dominant return year, followed by a smaller subdominant year, and two weaker years, making it harder to detect changes in productivity across cycle lines. Harrison Sockeye are unique in that, unlike other Fraser Sockeye stocks, they do not rear in freshwater as juveniles, but move into the ocean shortly after they emerge from their spawning gravel.

While there has been considerably more asynchrony in productivity across stocks in the past decade compared to previous years, survival was consistently below average across most populations in the 2005, 2013, and 2014 brood years (2009, 2017 and 2018 return years).

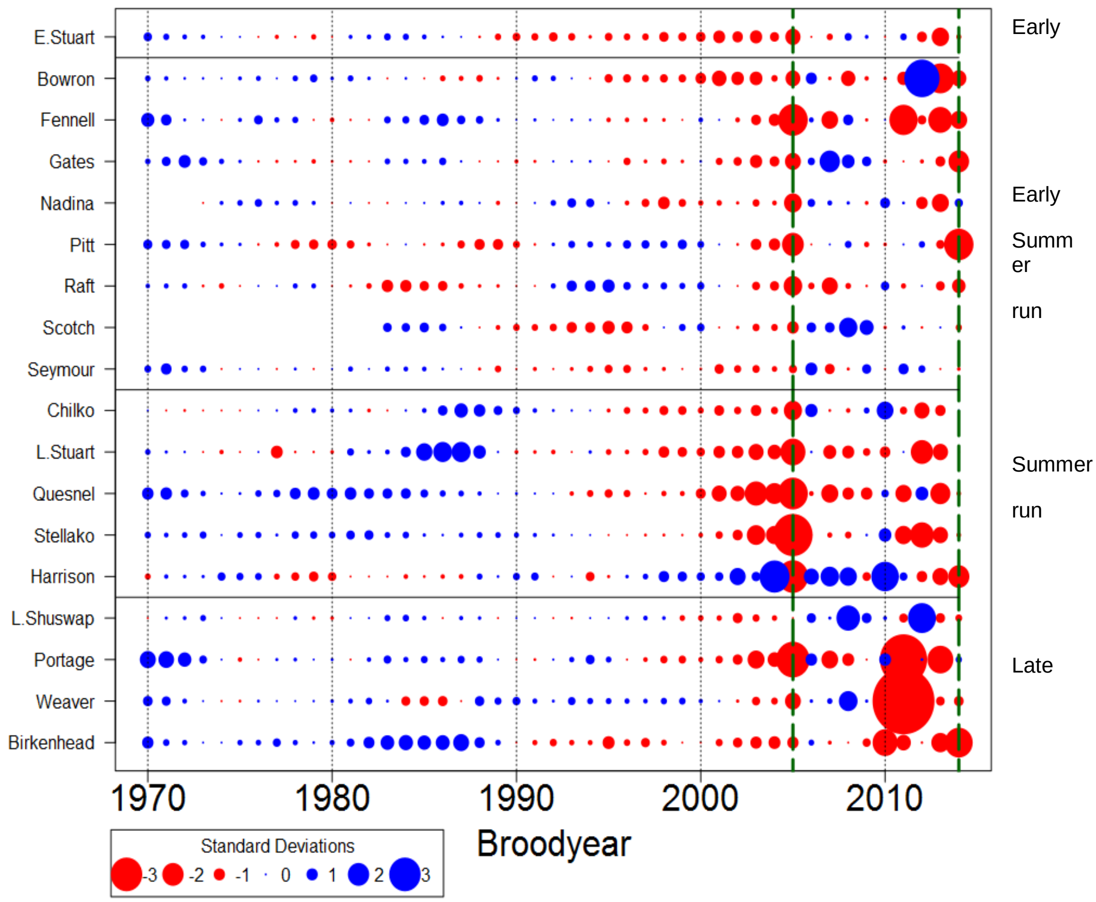

Figure 39-2. Fraser Sockeye productivity (Ricker model residuals for all populations except Scotch, Seymour and Late Shuswap, which are Larkin residuals) up to the 2014 brood year (2018 return year) across 18 different stocks and 4 different management groups (Early Stuart, Early Summer run, Summer run and Late run, named based on the migration timing of adults returning to their spawning grounds). Prior to the 2005 brood year, 4 year moving averages are plotted while annual estimates are provided for the more recent years. For the 2012 to 2014 brood years (2016 to 2018 return years), preliminary estimates of recruits by age are not yet available; preliminary in-season returns divided into stock group using escapement proportions were applied to estimate recruits for each stock. Both freshwater and marine factors contribute to the observed productivities. Red dots indicate below average productivity and blue dots indicate above average productivity. The smallest dots represent average annual productivity and the larger the diameter, the greater the deviation from average. The 2005 and 2014 brood years (2009 and 2018 return years) have been highlighted using a broken vertical green line.

39.4. Factors influencing trends

Chilko is the only Fraser Sockeye population with a long and complete time series of freshwater and ‘marine’ survival and contributes a large proportion to the total annual Fraser Sockeye returns. The overall survival trends of this population can therefore help evaluate the influence of freshwater or marine survival to the overall survival trend of the aggregate Fraser Sockeye returns. For Chilko Sockeye, freshwater survival has generally improved in recent years (Figure 39-3). ‘Marine’ survival data for Chilko (Figure 39-3) is similar to the aggregated Fraser Sockeye total survival trend (Figure 39-1B). Chilko exhibited declines in ‘marine’ survival in the 1990’s, which culminated in the lowest survival on record in the 2005 brood year (2009 return year). Although Chilko ‘marine’ survival improved for the 2006 to 2010 brood years (2010 to 2014 return years), in recent years marine survival has been poor.

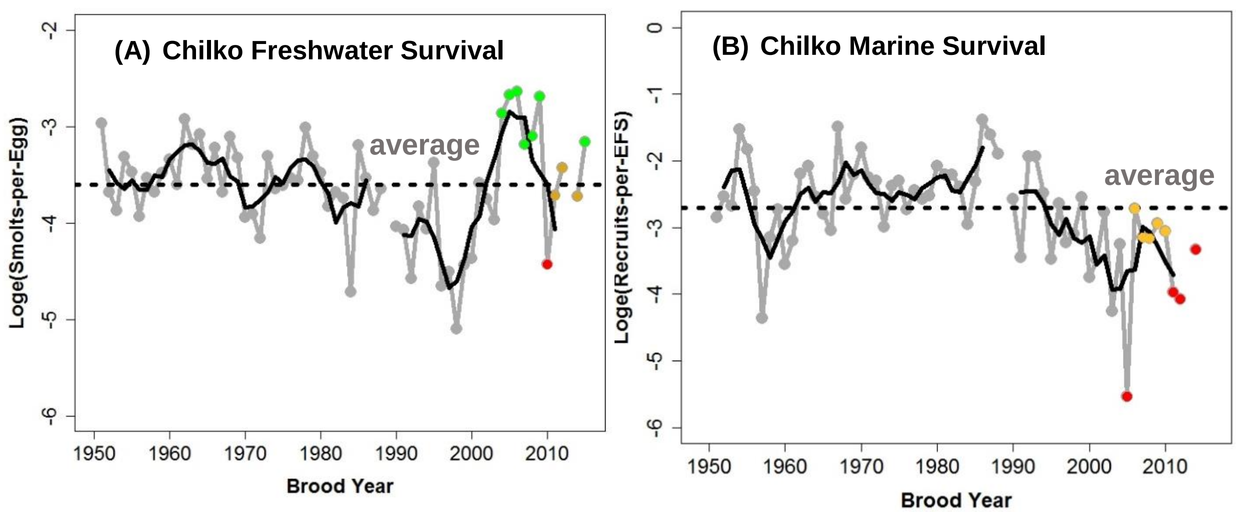

Figure 39-3. (A) Chilko River Sockeye freshwater survival ($\log_e$ smolts-per-egg) and (B) ‘marine’ ($\log_e$ recruits-per-smolt) annual survival. The filled grey circles and grey lines are annual values and the black line is the smoothed four-year running average survival. Freshwater survival has generally increased in the past decade, with the notable exception of 2010, when poor survival was associated with density-dependent factors caused by the large escapements in this brood year. Marine survival has generally been below average for the past decade, and particularly low in the 2005 and last three brood years: 2011 2012 and 2014 (2013 is a gap in the time series). Note: Chilko ‘marine’ survival includes a freshwater period during their downstream migration as smolts from the outlet of Chilko Lake to the Strait of Georgia, and their entire marine residence period. The horizontal dashed line indicates average survival.*

**Note: High water levels prevented accurate counting of smolts in 2015, therefore freshwater and marine survival estimates are unavailable for the 2013 brood year (2017 return year).*

Although it is unknown what factors drive the observed patterns in survival, some of the variability observed in recent years may be associated with specific events affecting particular populations. Birkenhead and Weaver Sockeye experienced a major landslide upstream of their freshwater rearing habitat, which coincided with exceptionally poor survival in recent years. A mine breach (Mount Polley) in the Quesnel system dumped mine tailings into the west arm of Quesnel Lake, the effect of which is currently unclear with regards to the productivity of Quesnel Sockeye. Populations that rear in the Shuswap Lake complex (Scotch, Seymour and Late Shuswap) appear to have experienced lagged density-dependent effects in recent years, due to the high density of juvenile sockeye in this lake from the large 2010 brood year. Overall, warming conditions starting in 2013, also have likely contributed to poorer survival in the most recent years across stocks (2017 and 2018 return years).

39.5. Implications of the observed trends

Understanding factors that contribute to Fraser Sockeye Salmon return trends can increase the certainty associated with the pre-season return forecasts (DFO 2017). These return forecasts are used pre-season to provide a preview of potential fishing opportunities to stakeholders, and they are used in-season to manage fisheries until sufficient in-season test-fishery data become available to update expectations. Currently, these forecasts are associated with high uncertainty (Grant et al. 2010).

To improve our understanding of Fraser Sockeye Salmon population dynamics, a supplemental Canadian Science Advisory Secretariat paper was prepared as part of the 2018 forecast process (MacDonald et al. 2018). This supplement provided additional information on the condition and abundance of various populations from the 2014 brood year escapement through to 2017 jack returns. It also provided information on the freshwater and marine conditions Fraser Sockeye populations experienced throughout their life-history, from the brood year as eggs in the gravel, up to the return year.

39.6. References

DFO. 2017. Pre-season run size forecasts for Fraser River Sockeye (*Oncorhynchus nerka*) and Pink (*O. gorbuscha*) salmon in 2017. DFO Can. Sci. Advis. Sec. Sci. Resp. 2017/016.

Grant, S.C.H., MacDonald, B.L., Cone, T.E., Holt, C.A., Cass, A., Porszt, E.J., Hume, J.M.B., and Pon, L.B. 2011. Evaluation of uncertainty in Fraser Sockeye (*Oncorhynchus nerka*) Wild Salmon Policy status using abundance and trends in abundance metrics. Can. Sci. Advis. Sec. Res. Doc. 2011/087: viii + 183.

Grant, S.C.H., Michielsens, C.G.J., Porszt, E.J., and Cass, A.J. 2010. Pre-season run size forecasts for Fraser River Sockeye salmon (*Oncorhynchus nerka*) in 2010. Can. Sci. Advis. Sec. Res. Doc. 2010/042: vi + 125.

MacDonald, B.L., Grant, S.C.H., Patterson, D.A., Robinson, K.A., Boldt, J.L., Benner, K., Neville, C.M., Pon, L., Tadey, J.A., Selbie, D.T., and Winston, M.L. 2018. State of the Salmon: Informing the survival of Fraser Sockeye returning in 2018 through life cycle observations. In Canadian Technical Report of Fisheries and Aquatic Sciences 3271. p. v + 53.

Neville, C.-E., Johnson, S., Beacham, T., Whitehouse, T., Tadey, J., and Trudel, M. 2016. Initial estimates from an integrated study examining the residence period and migration timing of juvenile sockeye salmon from the Fraser River through coastal waters of British Columbia. N. Pac. Anadrom. Fish. Comm. Bull. 6: 45–60.

Ogden, A.D., Irvine, J.R., English, K.K., Grant, S., Hyatt, K.D., Godbout, L., and Holt, C.A. 2015. Productivity (recruits-per-spawner) data for Sockeye, pink and chum salmon from British Columbia. Can. Tech. Report. Fish. Aquat. Sci. 3130: iv + 57.

Preikshot, D., Beamish, R.J., Sweeting, R.M., Neville, C.M., and Beacham, T.D. 2012. The residence time of juvenile Fraser River Sockeye salmon in the Strait of Georgia. Marine and Coastal Fisheries: Dynamics, Management, and Ecosystem Science 4: 438-449.

Tucker, S., Trudel, M., Welch, D.W., Candy, J.R., Morris, J.F.T., Thiess, M.E., and Wallace, C. 2009. Seasonal population-specific migrations of juvenile Sockeye salmon along the West Coast of North America: implications for growth. Trans. Am. Fish. Soc. 138: 1458-1480.

40. UPPER ALBERNI INLET WATER QUALITY DATA FROM THE DISSOLVED OXYGEN MONITORING PROGRAM

Howard Stiff* and Kim Hyatt, Regional Ecosystem Effects on Fish and Fisheries, Ecosystem Science Division, Fisheries and Oceans, Nanaimo, BC, V9R 6N7 Howard.Stiff@dfo-mpo.gc.ca.

40.1. Highlights

- Port Alberni paper mill Dissolved Oxygen Monitoring Program (DOMP) data provide a CTD time-series spanning nearly 30 years at multiple stations in Alberni Harbour and upper Alberni Inlet (1990-2018).
- The relatively high-resolution (weekly) time-series identify within- and between-year fluctuations in Temperature, Salinity and Oxygen (TSO) water properties affecting salmon pooling in the holding zone (HZ) of upper Alberni Inlet.
- Weekly DOMP data can be used to monitor how HZ conditions in upper Alberni Inlet are taking shape prior to- and during salmon migration(s). Managers can use DOMP data to inform decision-making regarding fishery openings, especially early in the season.

40.2. Description of the DOMP Time-Series

The Dissolved Oxygen Monitoring Program (DOMP) is a water quality monitoring program managed by the paper mill in Port Alberni for the purpose of monitoring the potential impacts of mill effluent on Alberni Inlet water quality and biota. The program commenced in the early 1990s with implementation of the nation-wide Environmental Effluent Management Program for industrial pulp & paper mills (Hatfield 2018). Mill staff collect, record, and report physical-chemical data using CTD equipment[1] during daylight hours (Monday to Friday, 08:00-16:00) at weekly (June-October) or tri-monthly (November-May) intervals. Data are submitted to Environment Canada on a monthly basis as per Schedule VII of the Pulp and Paper Effluent Regulations (SOR/92-269) under Canada's *Fisheries Act.*

DOMP data currently collected include station, date, time, depth, water temperature (°C), salinity (ppt), dissolved oxygen (DO) in mg/L and percent saturation[2] for the Somass River station and four upper inlet stations, from the effluent Outfall station (adjacent to the mill) in the estuary, to the 5km point down-inlet (Figure 40-1)[3]. All variables are measured at depths of 0 (surface), 1-10, 12, 15, 20, 25, 30, 35, 40, and 50 m (where these depths exist), and at bottom, for each monitoring station (e.g. Figure 40-2). The original data are recorded in spreadsheets by mill staff, and have been provided to Fisheries and Oceans Canada (DFO). The DFO copy of

[1] Via surface vessel using a *Eureka Manta Water Quality* multi-probe with a 60 m cable.

[2] Temperature, salinity, and pH probes are routinely calibrated as per instrument specifications (Hatfield 2018). Salinity is calibrated monthly, at a minimum, and typically twice per month. Calibration of the DO probe occurred prior to each survey using air calibration according to manufacturer's instructions. In addition, a grab sample is taken once per sampling day at one station at multiple depths for laboratory analysis using the Winkler DO analysis method (Hatfield 2018). Though not required for the DO monitoring program, acid/base (pH) concentration was sampled for most years until February 2016.

[3] Stations are located along the 124°49'W longitude from 49°11′N to 49°15′N. Another station at the 10 km point (49°09′N) was routinely sampled in the 1990s but has been discontinued. The HI3 station at Hohm Island was considered redundant and discontinued in 1999.

the data is currently housed in an MS-Access® database. Survey method changes, data issues, and handling of anomalous data are documented in a data report (Stiff et al. 2019).

40.3. Status and Trends

Annual time-depth contour plots indicate relatively moderate conditions during the adult Sockeye migration period in 2018 (Figure 40-3). Above-average precipitation in January, and a strong pulse in April, freshened surface layers with well-oxygenated waters. Sub-halocline salinity increased through May (to 32 ppt at 5-10 m depth). Though surface temperatures (0-3 m) exceeded 18°C by late June, moderate temperatures (12-15°C) were available below 5 m. However, the 10°C isotherm[4] descended to 15-20 m during Jul-Aug, where DO was sub-optimal[5] (range: 2-3 mg/L) for holding salmon (Figure 40-4). Migration delays were not reported.

Mean sub-halocline DO concentration (e.g. at 10 m) is a metric of interest during peak adult Sockeye migration (July), as fish will hold and seek cooler temperatures (9-10°C) if Somass River temperatures exceed 20°C. Mean summer DO levels at 10 m (and below) have been, *on average*, sub-optimal for salmon (~2-3 mg/L), but trending upward since 1990 *overall* ($r = 0.50$; $P = 0.03$; $n = 28$). However, the positive linear trend is characterized by strong inter-annual oscillations (±2.5 mg/L). No trends in sub-halocline water temperature or salinity were evident over the same time period, though in 2015, July-August temperatures at 10 m exceeded the long-term mean (~10.5°C) by almost two standard deviations (~1.5°C), and topped previous high means of 1996-1998 (11-12°C), before returning gradually to average conditions by 2018. The coolest summer water temperatures in the time-series occurred in 2014.

40.4. Factors Influencing Trends

The water in Alberni Inlet is stratified with a freshwater upper layer largely influenced by freshwater inputs from the Somass River, and a denser, saline lower layer, affected by influxes of marine water (inlet 'renewal') and vertical mixing mechanisms (Sullivan 1978).

Industrial factors affecting annual variation in upper Alberni Inlet DO and water temperature include effluent volume, total suspended solids (TSS), and biochemical oxygen demand (BOD). By 1990, summer sub-halocline DO declined ~4 mg/L due to industrial BOD loadings (40-50 t/d at peak) since mill operations commenced in the 1940s (Birtwell et al. 2014). However, since 1994, effluent volumes have been significantly reduced (~0.5 t/d) due to improvements in mill operations and waste management[6], and summer sub-halocline DO concentration has displayed a positive linear trend of +1 mg/L over the past three decades.

Freshwater factors affecting upper Alberni Inlet DO include Somass River discharge and oxygen content ($r > 0$), and Somass temperature ($r < 0$). These are in turn controlled by climate conditions and weather, including precipitation and winds (Farmer and Osborn 1976). Other factors affecting oxygen content include biological processes (photosynthesis, respiration), and decomposition from natural and other anthropogenic BOD in the inlet (e.g., log boom debris, municipal wastewater effluent; Siedlecki et al. 2015) or along the shelf (Connolly et al. 2010).

[4] When forced to hold in Alberni Inlet due to elevated Somass River temperatures (>20°C), Sockeye prefer DO concentrations >4 mg/L and temperatures of 9-10°C (Hyatt et al. 2015).
[5] Below the instantaneous minimum DO water quality guideline of 5 mg/L for aquatic life (ww2.gov.bc.ca).
[6] Annual production of effluents reduced to <5% of peak outputs in the 1960s and 1970s (Hatfield 2018).

Wind-driven coastal upwelling processes initiate annual Alberni Inlet ‘renewal’ with the influx of dense, saline waters in late spring (Picard 1963, Bell 1976, Stucchi 1982). The oxygen content of renewal waters depend on the source waters (Peterson et al. 2013, Meinvielle and Johnson 2013), which in turn depend on the magnitude and persistence of upwelling-favourable equator-ward winds (Hickey et al. 2006, Pawlowicz 2017), depth of source waters (Whitney et al. 2007, Thomson and Krassovski 2010, 2015), and whether buoyancy currents (Bianucci et al. 2011, Thomson et al. 2017) or the Juan de Fuca Eddy (Freeland and Denman 1982, Foreman et al. 2008) may be ‘blocking’ upwelling processes on the shelf. Renewal of upper inlet waters may also be mediated by the interaction between source water density and submarine sills which restrict the ventilation of deep coastal fjords (Pickard 1963, Thomson et al. 2017).

Large-scale ocean climate dynamics also play a role (Mantua et al. 1997, Peterson et al. 2013). Warm, dry summers characteristic of warm phase PDO/El Niño tend to be associated with extended periods of elevated surface water temperatures and sub-optimal DO conditions at depth, while cool, wet summers associated with cool phase PDO/La Niña correspond to moderate surface conditions and adequate oxygen levels in the sub-halocline (Chhak and DiLorenzo 2007, Birtwell et al. 2014).

40.5. Implications of Trends

Adult Sockeye halt upstream migration when Somass River temperatures exceed 19-20°C (Hyatt et al. 2015) and congregate in the holding zone (HZ) if drought conditions (low flow, high temperatures) persist (unpub. acoustic survey data). However, low DO levels (< 4 mg/L) frequently occur in the harbour and HZ during the migration period (June-August), and can be a source of additional stress on the fish, and lead to significant enroute mortalities[7] (Birtwell et al. 1994, 2014).

Historically, low DO levels in the HZ have been largely attributed to industrial BOD sedimentation from mill effluent discharged into the surface waters, despite strong stratification of the water column (e.g., Stucchi 1992, Birtwell et al. 2014). Notwithstanding significant reductions in industrial BOD, and an overall positive trend in sub-halocline DO levels, water quality in the HZ tends to oscillate annually between “good” (DO > 4 mg/L) and “poor” (DO < 4 mg/L) conditions, most likely related to the oxygen content of annual inlet renewal events driven by coastal upwelling processes.

DOMP data support other findings (e.g. Bell 1976, Stucchi 1983, Pawlowicz 2017) indicating that upper inlet renewal occurs annually one or more times beginning in March, and that summer DO conditions in the HZ are generally configured by May-June. This information can be used in conjunction with weather forecasts and river conditions to inform managers about whether valuable Sockeye salmon fisheries are at risk if the fish are unable to ascend the Somass River for extended periods of time.

Climate-induced rising temperatures and declining oxygen levels in the northeast Pacific (Crawford and Peña 2013, Keeling et al. 2010), combined with upwelling-favourable winds during warm phase ocean climate cycles (Thomson and Krassovski 2015), may increase the frequency of poor oxygen conditions in the HZ in upper Alberni Inlet, increase the risk of mortality to Sockeye Salmon and alter the sustainability of associated fisheries.

[7] Contributing to 100,000 - 200,000 adult Sockeye mortalities in 1990 (Stucchi 1992).

40.6. References

Bell, W.H. 1976. The exchange of deep water in Alberni Inlet. Pac. Mar. Sci. Rep. 76-22: 19 pp.

Bianucci, L., K. L. Denman, and D. Ianson. 2011. Low oxygen and high inorganic carbon on the Vancouver Island Shelf, J. Geophys. Res. 116: C07011 doi:10.1029/2010JC006720.

Birtwell, I.K., K.D. Hyatt, J.S. Korstrom, G.M. Kruzynski, C.M. Langton, G.E. Piercey, and S. Spohn. 1994. Behaviour and physiological responses of adult Sockeye (*Oncorhynchus nerka*) salmon to simulated estuarine conditions and salt water hypoxia. *In* High Performance Fish. *Edited by* Mackinley, D.D. Proceedings of an International Fish Physiology Symposium, University of British Columbia, Vancouver. American Fisheries Society and Fish Physiology Association. pp. 243-245.

Birtwell, I.K., M.E. Wright, and P. Edgell. 2014. Aquatic habitat in the Somass River estuary: a selective review and implications to Chinook salmon. Prepared for Fisheries and Oceans Canada, Nanaimo; Alberni Valley Enhancement Association, BC. DFO CATNO 352934. 151 p.

Chhak, K., and E. Di Lorenzo. 2007. Decadal variations in the California Current upwelling cells. Geophys. Res. Lett. 34: L14604, doi:10.1029/2007GL030203.

Connolly, T. P., B. M. Hickey, S. L. Geier, and W. P. Cochlan. 2010. Processes influencing seasonal hypoxia in the northern California Current System. J. Geophys. Res. 115: C03021 doi:10.1029/2009JC005283.

Crawford, W. R., & M. A. Peña. 2013. Declining oxygen on the British Columbia continental shelf. Atmosphere-Ocean 51: 88–103.

Farmer, D.M. and T.R. Osborne. 1976. The influence of wind on the surface layer of a stratified inlet. J. Phys. Oceanogr. 6: 931-940.

Foreman, M. G. G., Callendar, W., MacFadyen, A., Hickey, B. M., Thomson, R. E., and Di Lorenzo, E. 2008. Modeling the generation of the Juan de Fuca Eddy, *J. Geophys. Res.* 113: C03006, doi:10.1029/2006JC004082.

Freeland, H.J. and K.L. Denman. 1982. A topographically-controlled upwelling centre off southern Vancouver Island. J. Mar. Res. 40(4): 1069-1093.

Hatfield Consultants Ltd. 2018. Port Alberni Dissolved Oxygen Monitoring Program Interpretive Report (2017). Prepared for Catalyst Paper Corporation, Port Alberni Division, by Hatfield Consultants Ltd., March 2018.

Hickey, B., A. MacFadyen, W. Cochlan, R. Kudela, K. Bruland, and C. Trick. 2006, Evolution of chemical, biological, and physical water properties in the northern California Current in 2005: Remote or local wind forcing? Geophys. Res. Lett. 33: L22S02 doi:10.1029/2006GL026782.

Hyatt, K.D., Stiff, H.W., Stockwell, M.M., Luedke, W., Rankin, D.P., Dobson, D., and Till, J. 2015. A synthesis of adult Sockeye salmon migration and environmental observations for the Somass watershed 1974-2012. Can. Tech. Rep. Fish. Aquat. Sci. 3115: 199 pp.

Keeling, R.F., A. Körtzinger and N. Gruber. 2010. Ocean Deoxygenation in a Warming World. Annual Review of Marine Science 2: 199-229.

Mantua, N. J., S. R. Hare, U. Zhang, J. M. Wallace, and R. C. Francis. 1997. A Pacific interdecadal climate oscillation with impacts on salmon production. Bull. Amer. Meteor. Soc. 78: 1069-1079.

Meinvielle, M. and G.C. Johnson. 2013. Decadal water-property trends in the California Undercurrent, with implications for ocean acidification. J. Geophys. Res: Oceans 118. doi:10.1002/2013JC009299.

Pawlowicz, R. 2017. Seasonal Cycles, Hypoxia, and Renewal in a Coastal Fjord (Barkley Sound, British Columbia), Atmosphere-Ocean 2017: 1–20 Canadian Meteorological and Oceanographic Society https://doi.org/10.1080/07055900.2017.1374240.

Peterson, J.O., C.A. Morgan, W.T. Peterson and E. Di Lorenzo. 2013. Seasonal and interannual variation in the extent of hypoxia in the northern California Current from 1998–2012. Limnol. Oceanogr. 58(6): 2279–2292. doi:10.4319/lo.2013.58.6.2279

Pickard, G.L. 1963. Oceanographic Characteristics of Inlets of Vancouver Island, British Columbia. J. Fish. Res. Bd. Can. 20: 1109-1144.

Siedlecki, S. A., N. S. Banas, K. A. Davis, S. Giddings, B. M. Hickey, P. MacCready, T. Connolly, and S. Geier. 2015. Seasonal and interannual oxygen variability on the Washington and Oregon continental shelves. J. Geophys. Res. Oceans: 120 doi:10.1002/2014JC010254.

Stiff, H. W., K. D. Hyatt, and L. Cross. 2019. Database of physical-chemical water properties in Alberni Inlet, 1934-2018. Can. Data Rep. Fish. Aquat. Sci. 1290: iv + 147 pp.

Stucchi, D.J. 1982. Shelf-fjord exchange on the west coast of Vancouver Island. In: Coastal Oceanography (eds: H.G. Gade, A. Edwards). NATO Conf. Series IV: Marine Sciences: 439-450.

Stucchi, D.J. 1992. Management of water quality and salmon fisheries in a Vancouver Island fjord. In: Intergovernmental Oceanographic Commission (IOC) Workshop on Coastal Oceanography in Relation to Integrated Coastal Zone Management Report 85: 11-20.

Sullivan, D. L. 1978. The effects of pulp mill discharges on phytoplankton productivity in Alberni Inlet, 1974-1976. West Vancouver, B.C.; Environmental Protection Service Canada. Environmental Protection Service. Pacific Region.

Thomson, R. E. and M. V. Krassovski. 2010. Poleward reach of the California Undercurrent extension. J. Geophysical Research 115: C09027. doi.org/10.1029/2010JC006280.

Thomson, R. E. and M. V. Krassovski. 2015. Remote alongshore winds drive variability of the California Undercurrent off the British Columbia-Washington coast. J. Geophys. Res. Oceans 120: 8151–8176. doi:10.1002/2015JC011306.

Thomson, R. E., D. J. Spear, M. V. Krassovski, R. A. S. Hourston, T. A. Juhasz, and S. F. Mihaly. 2017. Buoyancy-driven coastal current blocks ventilation of an anoxic fjord on the Pacific coast of Canada. J. Geophys. Res. Oceans 122: doi:10.1002/2016JC012512.

Whitney, F.A. H.J. Freeland and M. Robert. 2007. Persistently declining oxygen levels in the interior waters of the eastern subarctic Pacific. Progress in Oceanography 75: 179-99.

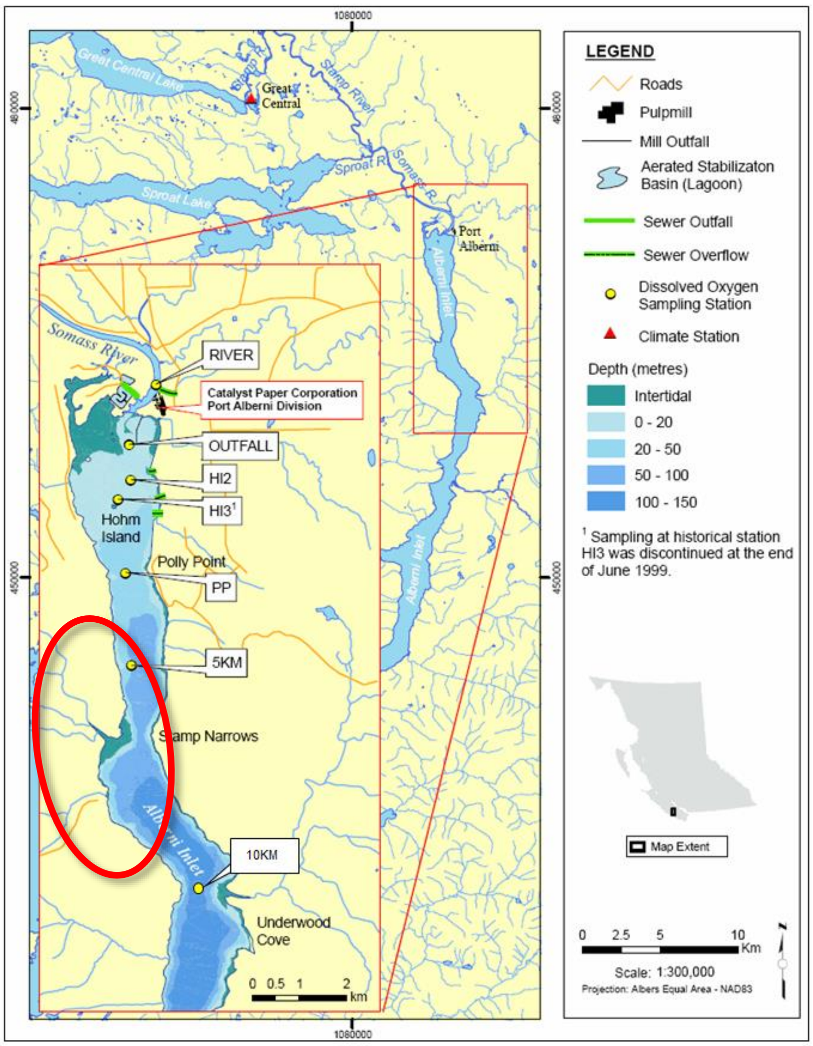

Figure 40-1. Mill location, DOMP survey stations, and Sockeye salmon "holding zone" (red ellipse) in upper Alberni Inlet, 1990-2018. Stations HI3 and 10km discontinued in 1999. (Adapted from Hatfield Consultants 2018).

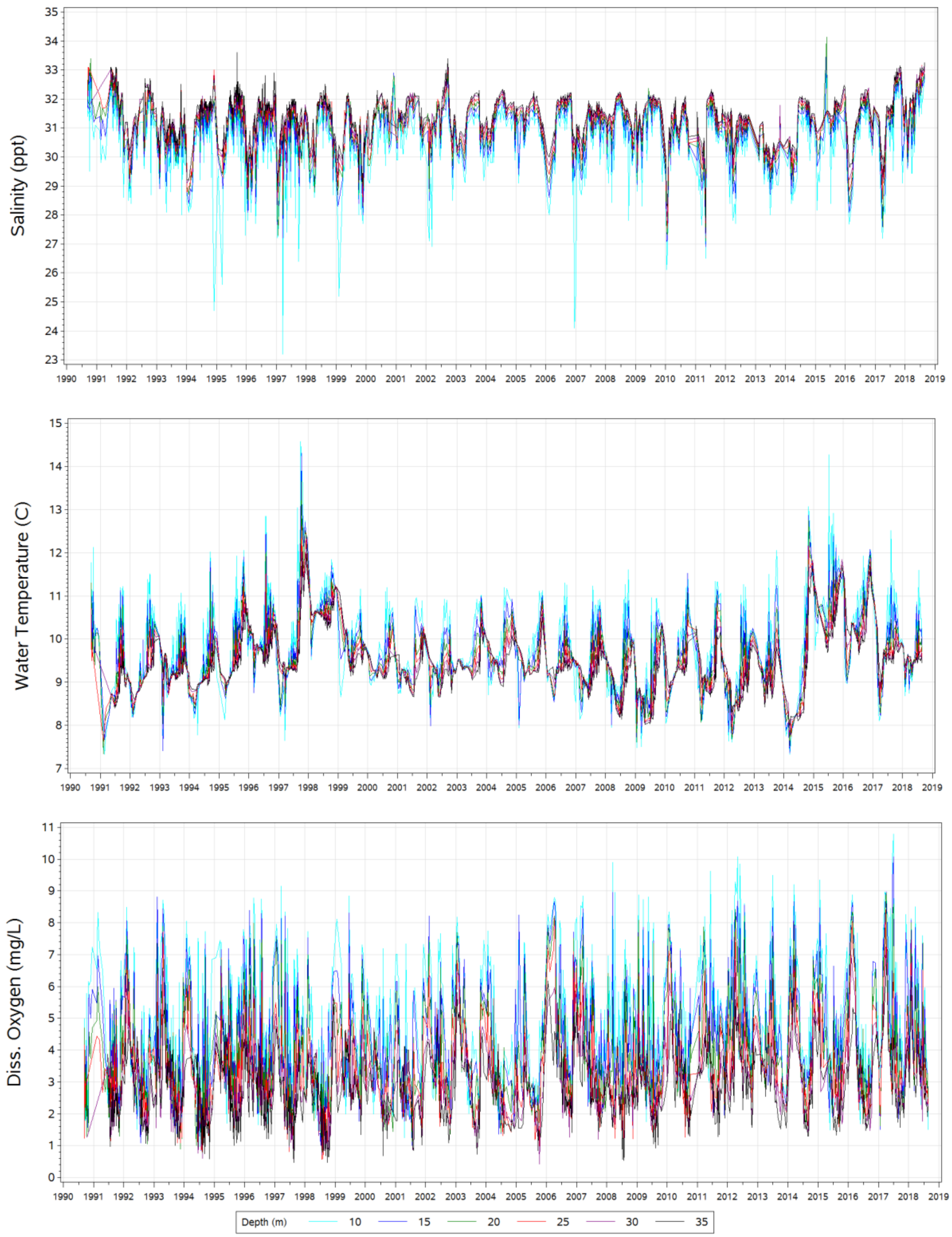

Figure 40-2. Time-series of salinity (ppt), water temperature (°C), and DO (mg/L) at Station 5km, 1990-2018.

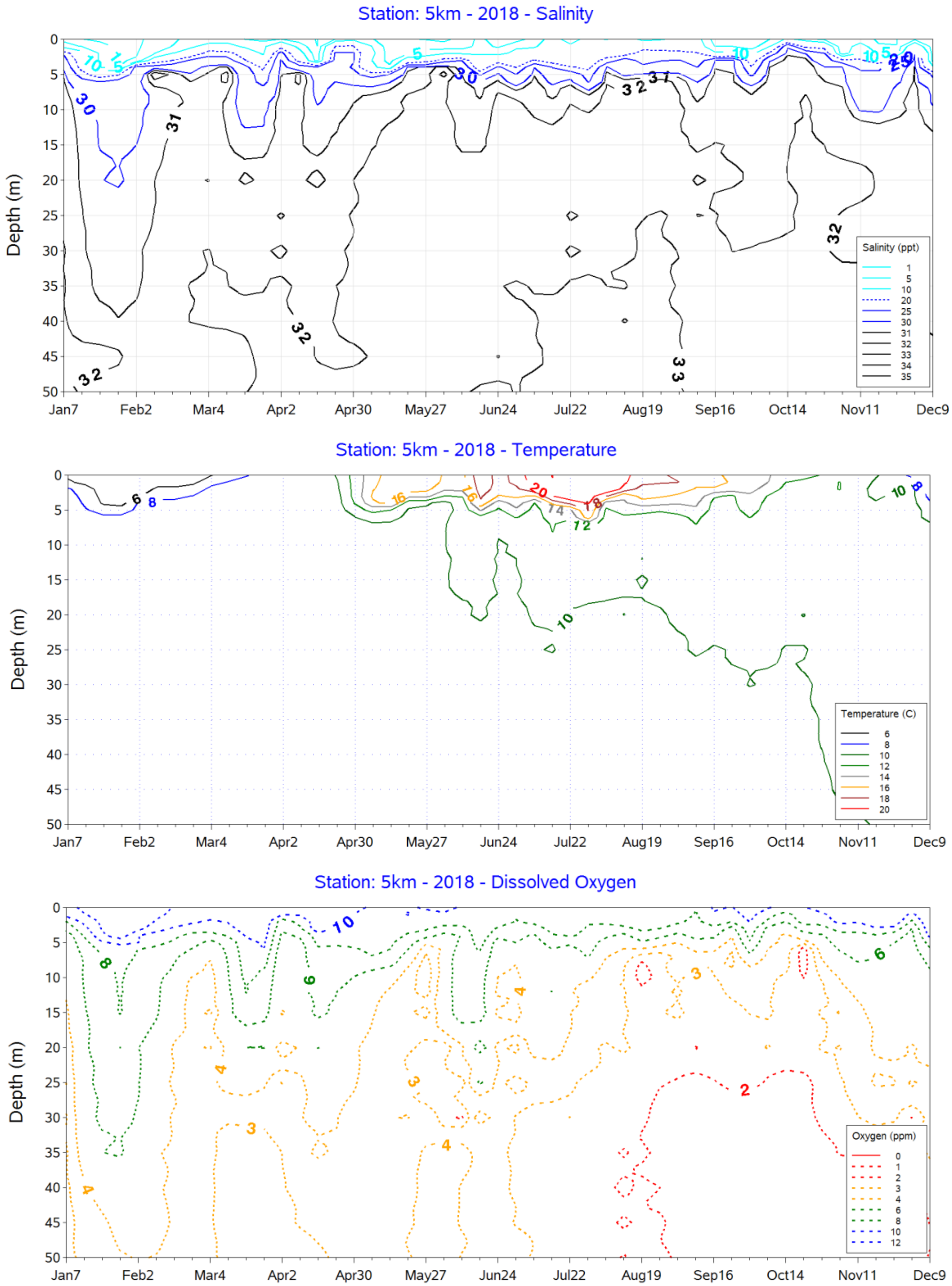

Figure 40-3. 2018 TSO chronograph at Station 5km. From top: Salinity (ppt), Temperature (°C), and DO (mg/L).

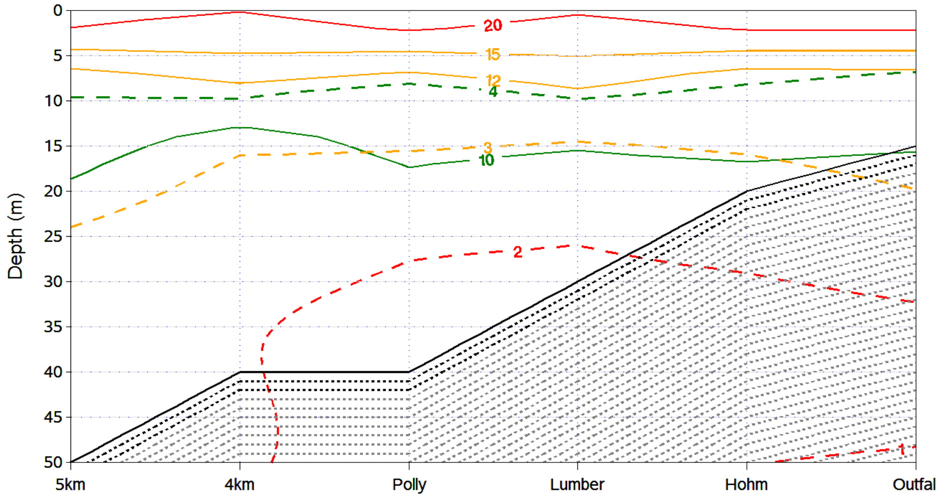

Figure 40-4. Key isotherms (mean temperature °C; solid lines) and isopleths (mean DO mg/L; dashed lines) for Sockeye in the Holding Zone and Harbour, July-August 2018.

41. COAST-WIDE SOCKEYE SALMON PERFORMANCE INDICATORS, REGIONAL OVERVIEW OF TRENDS, 2018 RETURNS AND 2019-2020 OUTLOOK

Kim Hyatt*, Howard Stiff, Margot Stockwell, and Athena Ogden, Fisheries and Oceans Canada, Pacific Biological Station, Nanaimo, B.C., *Kim.Hyatt@dfo-mpo.gc.ca

41.1. Highlights

- Warm ocean temperatures in 2014-2016 (“Blob”, El Niño) resulted in unfavourable survival for B.C.’s Sockeye Salmon ‘index stocks’ returning in 2016-2018.
- Freshwater conditions (high temperatures, early freshets, and summer drought) likely negatively impacted rearing fry and subsequent smolt production in 2015 with impacts on adult returns in 2017 and 2018.
- Returns of B.C.’s Transboundary, North Coast and Central Coast Sockeye index stocks in 2017 and 2018 were either close to or well below their all-year average returns. Returns of Chilko Sockeye (Fraser River) were well below their historic average and far below pre-season forecasts (i.e. closer to the 25 percentile than the median of the forecast range). Returns of WCVI and Columbia (Okanagan) index stocks continued a multi-year decline from record returns in 2014-2015.

41.2. Time Series – Annual Returns of Coast-wide Sockeye “Indicator Stocks”

Comparisons of annual forecasts and observed returns of Sockeye Salmon for major rivers and fisheries in B.C. have been completed annually by DFO for decades. Many Sockeye Salmon populations in Washington State and Alaska are also monitored annually and form a *de facto* international network of coast-wide Sockeye Salmon performance indicators (Figure 41-1) from which inferences about trends in geographic patterns of abundance and biological traits may be inferred. Total Sockeye returns in all cases are comprised of estimates of total annual harvest from all fishery sectors plus total ‘escapement’ to spawning grounds based on standard site-specific methods (e.g. counting weirs, electronic counters, mark-recapture, etc.). Historical returns and pre-season forecasts are generally available from DFO and Alaska Department of Fish and Game regional Fisheries Management Plans, infilled where necessary with unpublished summaries from resource managers.

Production trends of “data-rich” Sockeye populations or stock aggregates (i.e. “indicator stocks”) are assumed to represent other populations sharing the same marine domains that characterize the critical first weeks of early marine life (see Hyatt et al. 2016 for additional details of rationale behind “indicators”). Representative domains (with associated stocks) are loosely defined by sea-entry points in Figure 41-1 spanning 2,400 km of the west coast from western Alaska in the north to the Oregon border in the south.

41.3. Status and Trends Exhibited by Coast-wide Sockeye Indicators

Trend comparisons among Sockeye indicator stocks permit the following generalizations:

- Return variations are large, with the maximum at 10 to 90 times the minimum return.
- Despite wide variation in abundances between stocks, multi-year productivity correlations exist, especially for proximal stocks such as Tahltan and Meziadin, or Somass and Okanagan. Chilko Sockeye returns co-vary the least with other stocks.
- In 2018, all BC indicator stock returns were either close to or well below average returns observed over the most recent 12 years (i.e. roughly 3 Sockeye generations).
- Declining returns to BC systems in 2017 and 2018 were generally anticipated (compare forecasts to observed in Figure 41-2) given that environmental conditions in freshwater and marine ecosystems for the past 3-4 years have favoured reduced survival at multiple life stages (Hyatt et al 2018, MacDonald et al. 2018).
- Of special note in 2018, returns of Sockeye to the Bristol Bay stock aggregate far to the north reached 121% of the pre-season forecast and set a new record return of 62.3 million adult Sockeye.
- Exceptional returns to Bristol Bay in 2018 confirmed the multi-year persistence of the previously noted (Hyatt et al. 2017) south-to-north inverse production pattern for Sockeye stocks along the eastern rim of the Pacific Ocean.
- Stocks returning to southeast to southcentral Alaska exhibited total numbers well below expectation (e.g. Copper River, Prince William Sound Sockeye returned at less than 50% of the pre-season forecast of 1.9 million fish which resulted in the closure of fisheries there).
- Sockeye stocks (returning in 2018) from Bristol Bay through to northern B.C. all exhibited exceptional declines in average size due to either earlier maturation ages or reduced size-at-age. Sockeye returning to Barkley Sound and the Somass River in the South, however, were well within the range of size-at-age variations observed over the past 15 years (Figure 41-3).

41.4. Factors Influencing Trends in Numbers and Biological Traits of Sockeye

Freshwater and coastal marine conditions along the continental shelf during winter 2014, spring 2015 and 2016 likely drove 2017 and 2018 declines in adult salmon returns. In the freshwater environment, above-average air temperatures in the winter to early spring of 2014/15 and 2015/16 resulted in early snowmelt and rapid run-off (Anslow et al. 2016). High winter to early spring flows for southern BC Sockeye stocks may have scoured spawning grounds, potentially reducing fry survival from brood year 2014 and adult returns in 2018. High discharge events for southern BC rivers (i.e. 1 in 200 year flood events, Shaun Reimer pers. comm.) in the spring of 2017 may have facilitated rapid migration of Sockeye smolts and higher riverine survival to sea-entry. Adult returns in 2019 will reflect any significant impacts of exceptional discharges on smolt migration success in spring 2017.

For any successful seaward migrants in 2015-2016, biophysical conditions over much of the eastern Pacific were not favourable for survival in the marine environment. During ocean entry in 2015 and 2016, above average temperature anomalies due to multi-year impacts of the marine heat wave (i.e. the 2014-2016 "Blob") and a strong El Nino in 2015-2016 were still in effect. Although these phenomena started to dissipate in the latter half of 2016 (Ross 2017), Pacific Ocean temperatures remained much warmer than average over these years, resulting in northward transport of less nutritious, low-lipid zooplankton prey, predators 'foreign' to juvenile salmon, and competitive invertebrate populations (e.g. jellyfish, salps, etc.; Galbraith and Young 2017). These factors are believed to contribute to slow growth and high mortality for juvenile Sockeye; thus SST at ocean entry is a reasonable predictor of marine survival of Sockeye stocks and especially those that directly enter the northern California Current System (CCS) (Hyatt et al. 2016, 2017, 2018) and possibly the Salish Sea (MacDonald et al. 2018).

Alignment of El Niño and La Niña events from the Ocean Nino Index with annual B.C. Sockeye Salmon indicator stock returns indicated that:

- Large returns in the 1990s occurred for all Sockeye index stocks from the North Coast to the Fraser in association with a powerful 1989 La Niña event 2-3 years earlier. Similarly, moderate La Niñas in 1999, 2000, 2008 and 2011 were followed by above-average returns two years later, with near-record returns in 2010 and 2015 for several stocks.
- Warm ocean conditions linked to moderate El Niños through the 1990s were associated with sub-average returns late in the decade for stocks entering most directly into the CCS. A powerful El Niño event in 1997/98 likely depressed all stocks' returns in the early 2000s. Weaker El Niños in 2002/03 and 2009/10 were associated with sub-average returns for most southern and central stocks, and an El Niño event in 2015/16 – equivalent in amplitude to the 1997/98 event – was also followed by declines in the majority of BC-origin Sockeye stocks to below average returns in 2017 and 2018.
- Relatively warm atmospheric and ocean conditions are known to induce a host of freshwater and marine conditions that reduce production of Sockeye stocks on the southern end of their range (e.g. in Washington State and southern British Columbia) but favour production in the northern end of their range.
- The 2018 record breaking abundance of Bristol Bay Sockeye rearing in waters of the Bering Sea and Gulf of Alaska may have induced reduced growth for themselves as well as for northern BC and southeast Alaska stocks that shared these waters during 2016 and 2017 (Figure 41-3).
- Despite observations of a broadly shared suppression of growth among many Sockeye stocks returning in 2018 (Figure 41-3), the divergence in return numbers and implicit juvenile survival rates among Bristol Bay versus other coast-wide Sockeye Indicators suggests their survival patterns were not determined through density dependent interactions in the Gulf of Alaska.

41.5. Implications and Outlook

The onset of a weak La Niña in 2016-2017 has been associated with a return of B.C. outer coast temperatures (but not the Salish Sea) close to the climatological mean in 2018 (Chandler

2018) and mixed signals with respect to food-web structure in B.C. shelf waters (e.g. increase in subarctic zooplankton but persistence of subtropical forms, Galbraith et al., section 16). Above-average snow pack in southern B.C. and Fraser watersheds in 2017[8] should improve egg-to-smolt survival for the 2016 brood (ocean entry year 2018, return year 2020). Similarly, high discharge conditions in southern river systems during the main interval for Sockeye smolt migration in 2017 and 2018 (BC River Forecast Centre) should contribute to reduced mortality between lake-exit and sea-entry by smolts. Adding to this, development of a weak La Niña through the 2016/17 and 2017/18 winters anticipates a positive change in the quality of the forage base and in juvenile Sockeye marine survival on the southern end of their range for 2017 and 2018 sea entry years. Taken together, these factors signal a modest boost in marine survival for 2017 and 2018 sea entry years and thus for adult Sockeye returns to British Columbia in 2019 and especially 2020.

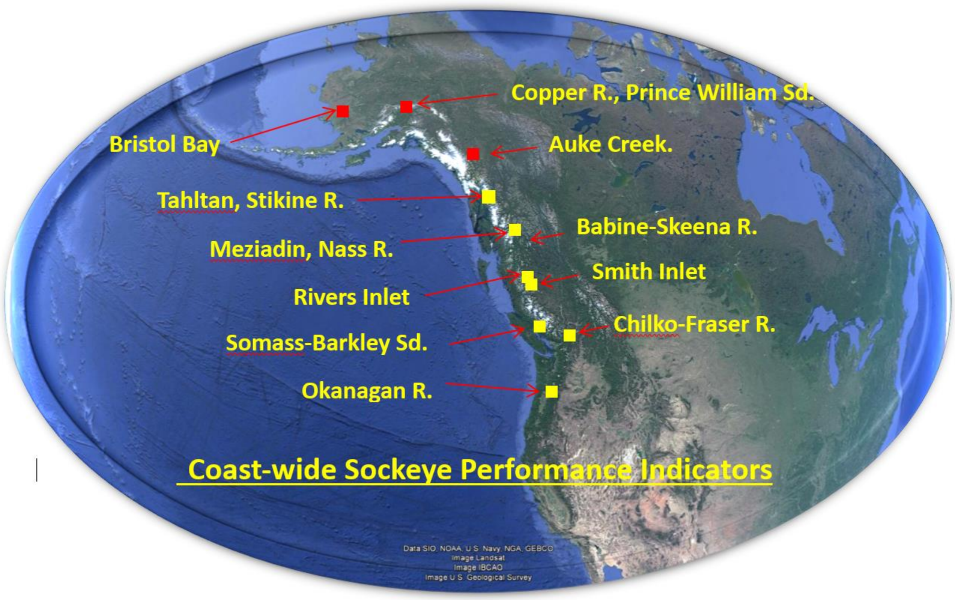

Figure 41-1. Approximate points of sea entry for a network of relatively data-rich Sockeye stocks monitored by DFO (yellow) and ADF&G (red) on an annual basis for biological traits (age-at-return, size-at-return, return timing etc.) and total returns (catch plus escapement) relative to predicted returns.

[8] B.C. Min. Forests, Lands and Natural Resources Operations River Forecast Centre – Basin Snow Water Index map (http://bcrfc.env.gov.bc.ca/bulletins/watersupply/SnowIndexMap.htm).

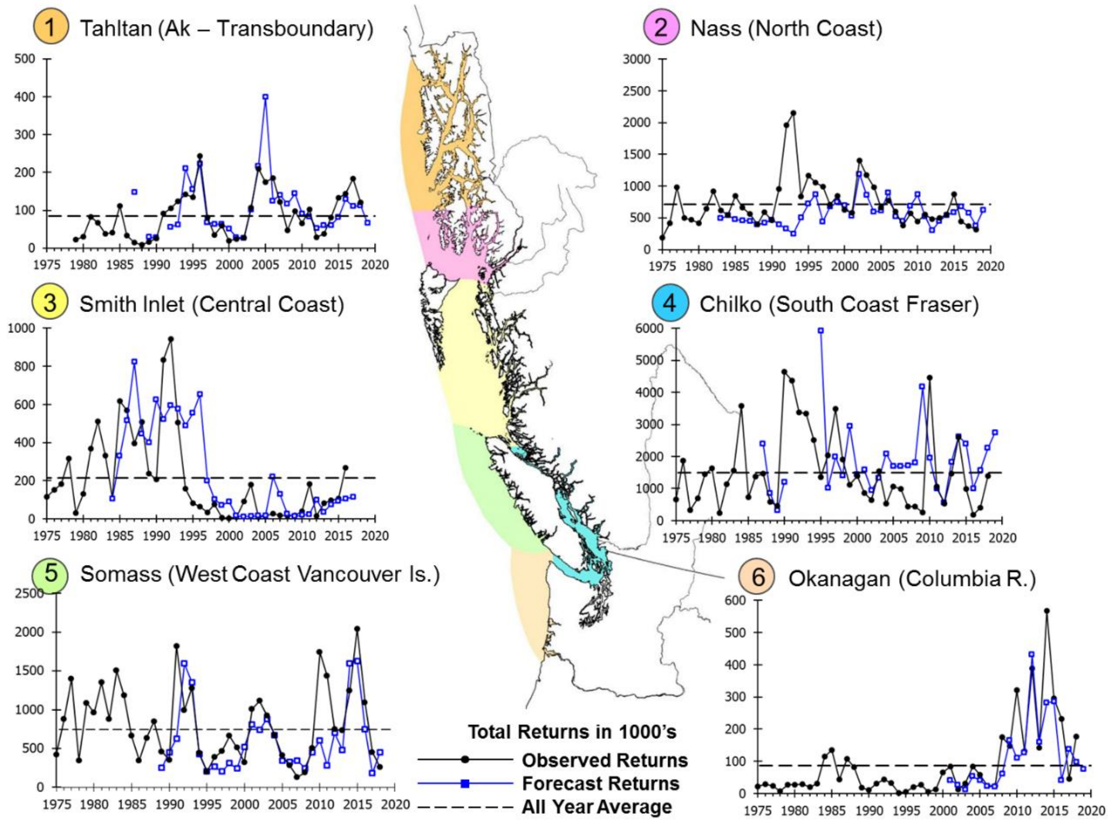

Figure 41-2. Trends in the total returns (black line) and resource manager forecasts (blue dashed line) for a set of British Columbia Sockeye index stocks including: (1) Stikine – Tahltan; (2) Nass – Meziadin; (3) Smith Inlet – Long; (4) Fraser – Chilko; (5) Barkley Sound – Somass; and (6) Columbia – Okanagan. Y-axis represents returns in thousands of fish.

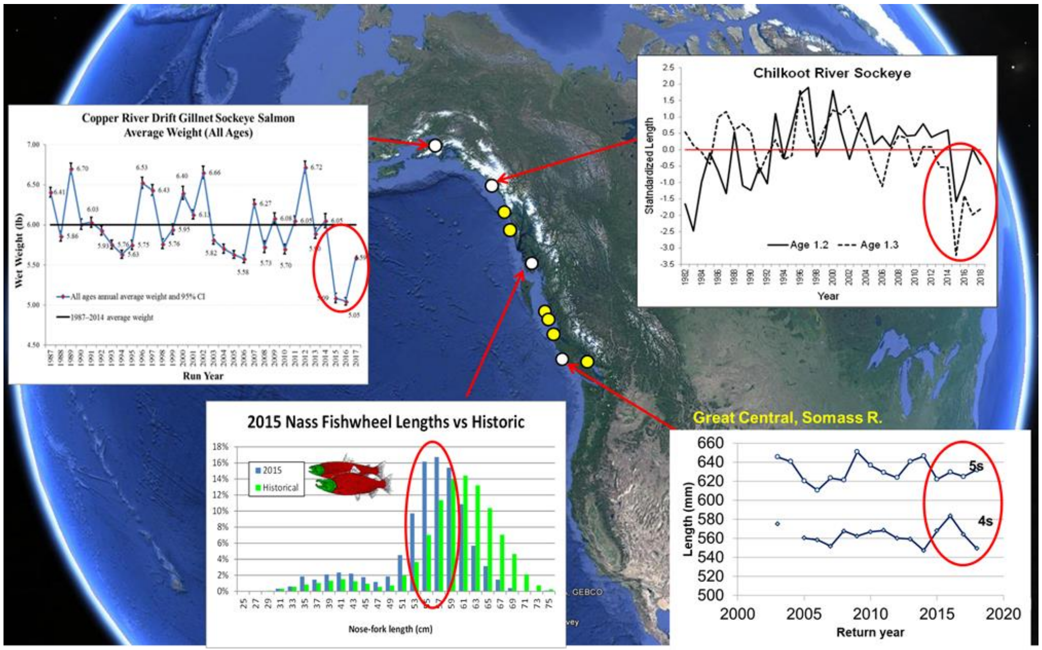

Figure 41-3. Evidence for reduced size of adult Sockeye Salmon returning to south central Alaska (average weight of Copper River fish and length of Chilkoot) and northern B.C. (length of NassRiver fish) during years from 2015-2018 relative to earlier years. Sockeye returning to Great Central Lake (Somass River) have not exhibited the extremes of low size-at-return observed for northern stocks. Red ovals highlight anomalously low size-at-return observations relative to all-year average size. Data for Copper River (Andrew Munro, ADF&G), Chilkoot River (Leon Shaul, ADF&G),Nass River (Steve Cox-Rogers, DFO) and Great Central –Somass (Erin Porszt, DFO).

41.6. References

Anslow, F. S. 2017. Hydrological patterns in B.C. in 2016. In: Chandler, P.C., King, S.A., and Boldt, J. (Eds.). 2017. State of the physical, biological and selected fishery resources of Pacific Canadian marine ecosystems in 2016. Can. Tech. Rep. Fish. Aquat. Sci. 3225: vi + 243 p.

Anslow, F. S., M. Schnorbus and D. Campbell. 2016. Hydrological patterns in B.C. in 2015. In: Chandler, P.C., King, S.A., and Perry, R.I. (Eds.). 2016. State of the physical, biological and selected fishery resources of Pacific Canadian marine ecosystems in 2015. Can. Tech. Rep. Fish. Aquat. Sci. 3179: viii + 230 p.

Chandler, P.C., King, S.A., and Boldt, J. (Eds.). 2018. State of the physical, biological and selected fishery resources of Pacific Canadian marine ecosystems in 2017. Can. Tech. Rep. Fish. Aquat. Sci. 3266: viii + 245 p.

Beamish R. J., C. Mahnken, and C. M. Neville. 2004. Evidence that reduced early marine growth is associated with lower marine survival of Coho salmon. Trans. Am. Fish. Soc. 133: 26-33.

Galbraith, M. and K. Young. 2017. Zooplankton along the B.C. continental margin in 2016. In: Chandler, P.C., King, S.A., and Boldt, J. (Eds.). 2017. State of the physical, biological and selected fishery resources of Pacific Canadian marine ecosystems in 2016. Can. Tech. Rep. Fish. Aquat. Sci. 3225: vi + 243 p.

Hannah, C., N. Bolingbroke and W. Crawford. 2017. Patterns of SST variability along the west coast of North America. In: Chandler, P.C., King, S.A., and Boldt, J. (Eds.). 2017. State of the physical, biological & selected fishery resources of Pacific Canadian marine ecosystems in 2016. Can. Tech. Rep. Fish. Aquat. Sci. 3225: vi + 243 p.

Hyatt, K., Stockwell, M., and Stiff, H. 2016. Salmon responses to hydroclimatological conditions in British Columbia in 2015. In: Chandler, P.C., King, S.A., and Perry, R.I. (Eds.). State of the Physical, Biological and Selected Fishery Resources of Pacific Canadian Marine Ecosystems in 2015. Can. Tech. Rep. Fish. Aquat. Sci. 3179: viii + 230 p.

Hyatt, K. D., Stockwell, M. M., Ogden, A., and Stiff, H. 2017. Sockeye Salmon indicator stocks – Regional overview of trends, 2016 returns, and 2017-2018 outlook. In: Chandler, P.C., King, S.A., and Boldt, J. (Eds.). State of the physical, biological and selected fishery resources of Pacific Canadian marine ecosystems in 2016. Can. Tech. Rep. Fish. Aquat. Sci. 3225: vi + 243 p.

Hyatt, K. D., Stockwell, M. M., Ogden, A., and Stiff, H. 2018. Sockeye Salmon indicator stocks – Regional overview of trends, 2017 returns, and 2018-2019 outlook. In: Chandler, P.C., King, S.A., and Boldt, J. (Eds.). State of the physical, biological and selected fishery resources of Pacific Canadian marine ecosystems in 2017. Can. Tech. Rep. Fish. Aquat. Sci. 3266: vi + 245 p.

MacDonald, B. L., S. C. H. Grant, D. A. Patterson, K. A. Robinson, J. L. Boldt, K. Benner, C. M. Neville, L. Pon, J. A. Tadey, D. T. Selbie, and M. L. Winston. 2018. State of the Salmon: Informing the survival of Fraser Sockeye returning in 2018 through life cycle observations. Can. Tech. rep. Fish. Aquat. Sci. 3271. 52 p + Appendix.

Ross, T. 2016. El Niño, the Blob, and another warmest year. In: Chandler, P.C., King, S.A., and Perry, R.I. (Eds.). 2016. State of the physical, biological and selected fishery resources of Pacific Canadian marine ecosystems in 2015. Can. Tech. Rep. Fish. Aquat. Sci. 3179: viii + 230 p.

Ross, T. 2017. La Niña, the Blob, and another warmest year. In: Chandler, P.C., King, S.A., and Boldt, J. (Eds.). 2017. State of the physical, biological and selected fishery resources of Pacific Canadian marine ecosystems in 2016. Can. Tech. Rep. Fish. Aquat. Sci. 3225: vi + 243 p.

Scheuerell, M. D., Zabel, R. W. and Sandford, B. P. 2009. Relating juvenile migration timing and survival to adulthood in two species of threatened Pacific salmon. Journal of Applied Ecology 46: 983–990. doi:10.1111/j.1365-2664.2009.01693.

42. 2018 JUVENILE SALMON SURVEYS ON THE CONTINENTAL SHELF OF VANCOUVER ISLAND

Jackie King, Erika Anderson, Jennifer Boldt, Tyler Zubkowski and Hilari Dennis-Bohm

Fisheries and Oceans Canada, Pacific Biological Station, Nanaimo, B.C., Jackie.King@dfo-mpo.gc.ca, Erika.Anderson@dfo-mpo.gc.ca, Jennifer.Boldt@dfo-mpo.gc.ca, Tyler.Zubkowski@dfo-mpo.gc.ca, Hilari.Dennis-Bohm@dfo-mpo.gc.ca

42.1. Highlights

- Catch rates of juvenile Sockeye Salmon in June throughout the northern migratory corridor for Fraser River Sockeye Salmon were below average. Catch rates of juvenile Sockeye Salmon in July on the whole continental shelf of Vancouver Island were also below average. These fish are typically from stocks along the west coast of Vancouver Island. Juvenile Sockeye Salmon will return as adults mainly in 2020.
- Catch rates of juvenile Chinook and Coho Salmon in July on the continental shelf of Vancouver Island were below average. These are fish mainly from Columbia River, Puget Sound and west coast of Vancouver Island. Chinook Salmon juveniles will return as adults mainly in 2020 (stream-type) and 2021 (ocean-type); Coho Salmon juveniles will return as adults in 2019.
- Catch rates of juvenile Chum and Pink Salmon in July on the continental shelf of Vancouver Island were below average. Chum Salmon juveniles will return as adults mainly in 2021; Pink Salmon juveniles will return as adults in 2019.

42.2. Description of the time series

Fraser River Sockeye Salmon Migratory Corridor Survey

Juvenile salmon surveys have been conducted in the northern migratory corridor for Fraser River Sockeye Salmon, which includes Johnstone Strait, Queen Charlotte Strait and the southeastern continental shelf of Queen Charlotte Sound, since 1998. These surveys have occurred intermittently, dependent on funding and vessel availability, in early summer (June) and fall (October) and catches are dominated by Chilko (summer) or Harrison (fall) Sockeye Salmon stocks of the Fraser River. In 2018 this survey was conducted in summer only, June 9-15, along standard transects at headrope depths of surface and 15m, using a LFS 7742 mid-water trawl net.

Integrated Pelagic Ecosystem Survey on the continental shelf of Vancouver Island

Since 1998, juvenile salmon surveys have been conducted on the continental shelf of the northern and western coast of Vancouver Island (WCVI) during summer, typically late-June to early-August. For 1998-2016 surveys, tows were conducted at headrope depths of surface, 15m or 30m using mid-water trawl gear (CanTrawl 250) along standard transects that sometimes extended beyond the shelf-break and into coastal inlets. In 2017, the survey design was switched to a stratified, random design (King et al. 2019b) which continued in 2018 (July 5-29). The survey area was portioned into 8 strata based on depth contours (50-100m; 100-200m) and known biological communities. Each stratum was gridded into 4 x 4km blocks from which a random set of blocks were selected in proportion to the relative area of each strata to the whole survey area. Fishing was conducted with the same historical trawl gear in 2017 and with a replacement mid-water trawl net (LFS 7742) in 2018. In 2017-2018, trawling was limited to headrope depths of surface and 15m. Gear calibration between the historic CanTrawl 250 and the replacement LFS 7742 nets indicate that catch-per-unit effort (CPUE) calculated with swept volume (km^3) are comparable (Anderson et al. 2019). In order to minimize differences between 1998-2016 and 2017-2018 survey designs, we selected trawls conducted 1998-2016 with headrope depths of surface and 15m, that were conducted within waters with depths 50 – 200m, i.e. excluding any historic fishing events that occurred on the slope or within inlets.

For both surveys length and weight data were used to estimate species-specific length-weight regressions across years, with annual weight residuals presented to represent condition.

42.3. Status and trends

Relative abundance

Generally, Chum and Pink Salmon are the dominate species of Pacific salmon caught on the continental shelf of Vancouver Island (Figure 42-1). The 2018 summer CPUE estimates for all juvenile salmon were below the mean of the 1998-2018 time series (Figure 42-1). For Sockeye and Chinook Salmon this continues the below average abundance estimates observed in the last five years. For Coho Salmon, the last five years have exhibited average and below average juvenile abundance. For Chum Salmon, abundance estimates in the last five years have varied from above average and below average estimates. The Pink Salmon CPUE data reflect the cyclical pattern in run size, with dominant odd year runs (adults) corresponding to abundant juveniles in even years. The 2018 Pink Salmon CPUE is well below the 2014 estimate (no survey in 2016) and is well below the long-term mean observed in even years.

Condition

The 2018 summer median and quartile ranges of weight residuals for Chinook and Coho Salmon were above average (Figure 42-2). The median weight residuals for Chum Salmon were also above average, but the lower quartile range marginally includes zero (Figure 42-2). Conversely, the median for Sockeye Salmon captured in the migratory corridor survey was below average and the upper quartile range marginally includes zero. The weight residual medians and quartiles for Sockeye Salmon (continental shelf of Vancouver Island) and Pink Salmon indicate average condition (Figure 42-2).

42.4. Factors influencing trends

The relative abundance of juvenile salmon in coastal regions reflects cumulative impacts, including but not limited to, spawner-egg-fry productivity in freshwater, in-river mortality for out-migrating smolts and ocean conditions coupled with trophic impacts (prey quality and availability, predation) in the first few months in the ocean. Basin-wide climate and ocean patterns (e.g. Pacific Decadal Oscillation and North Pacific Gyre Oscillation) have been linked through coastal processes, to coherency in broad-scale patterns in Pacific salmon marine survival (Malick et al., 2017). Adding to this complexity is the occurrence of recent extreme ocean warming events, i.e. marine heatwaves, which are exhibiting spatial variability (see

Hannah et al., section 9). King et al. (2019a) recently examined catch rate anomalies from eight regional-scale juvenile salmon trawl surveys conducted throughout the northeastern Pacific and the Bering Sea. They reported that the 2015 marine heat wave event was associated with the most coherent response in juvenile salmon catch rates across regions. However, in 2017 and 2018 they observed the largest year to year difference in survey catch rates in 20 years, indicating highly variable responses of the Pacific Salmon community in different regions post-2015.

42.5. Implications of those trends

Below average relative indices of abundance (CPUE) suggests below average returns for the stocks typically examined in these surveys. The majority of Sockeye Salmon encountered in the migratory corridor and the continental shelf of northern Vancouver Island originate from the Fraser River, and those on the WCVI originate from stocks on the west coast, most notably Barkley Sound. The majority of Chinook and Coho Salmon captured along the Vancouver Island continental shelf originate from Columbia River, Puget Sound and west coast Vancouver Island stocks in order of dominance. Genetic stock identification for Chum and Pink Salmon are not available for these surveys. The juvenile Pacific salmon encountered in these surveys will return to spawn at varying times, but generally these catch rates apply to Sockeye Salmon returning in 2020, stream-type Chinook Salmon returning in 2020, ocean-type Chinook Salmon returning in 2020, Coho Salmon returning in 2019, Chum Salmon returning in 2021 and Pink Salmon returning in 2019.

Preliminary 2018 energy density proxy data for Chinook and Coho Salmon (whole fish dry weight ratio as per Trudel et al. (2005) compared to available historic data (1998-2006) suggest that the above average weight residuals observed in 2018 (Figure 42-2) do not correspond to above average caloric content in juvenile salmon (King, unpub. data), i.e. do not reflect above average condition. Alternate hypotheses include storage of water or muscle build-up in lieu of lipid storage or size-selective mortality.

42.6. References

Anderson, E., Zubkowski, T. and King, K. 2019. Comparison of juvenile salmon catch in Cantrawl 250 and LFS 7742 mid-water trawl nets. Can. Tech. Rep. Fish. Aquat. Sci. *In press*.

King, J., Boldt, J., Burke, B., Greene, C., Moss, J. and Neville, C. 2019a. Northeast Pacific Juvenile Salmon Summer Surveys in 2018. PICES Press Vol 27(1): 19-26. https://meetings.pices.int/publications/pices-press/volume27/PPJan2019.pdf

King, J., Boldt, J., Dennis-Bohm, H., Zubkowski, T., Flostrand L. and Tucker, S. 2019b. Integrative Pelagic Ecosystem Surveys on the Vancouver Island Continental Shelf, July 7 - August 2, 2017 and July 5 - July 29, 2018. Can. Tech. Rep. Fish. Aquat. Sci. *In press*.

Malick, M.J., Cox, S.P., Mueter, F.J., Dorner, B. and Peterman, R.M. 2017. Effects of the North Pacific Current on the productivity of 163 Pacific salmon stocks. Fisheries oceanography, 26(3): pp.268-281.

Trudel, M., Tucker, S., Morris, J.F.T., Higgs, D.A. and Welch, D.W. 2005. Indicators of energetic status in juvenile Coho Salmon and Chinook salmon. North American Journal of Fisheries Management, 25(1), pp.374-390.

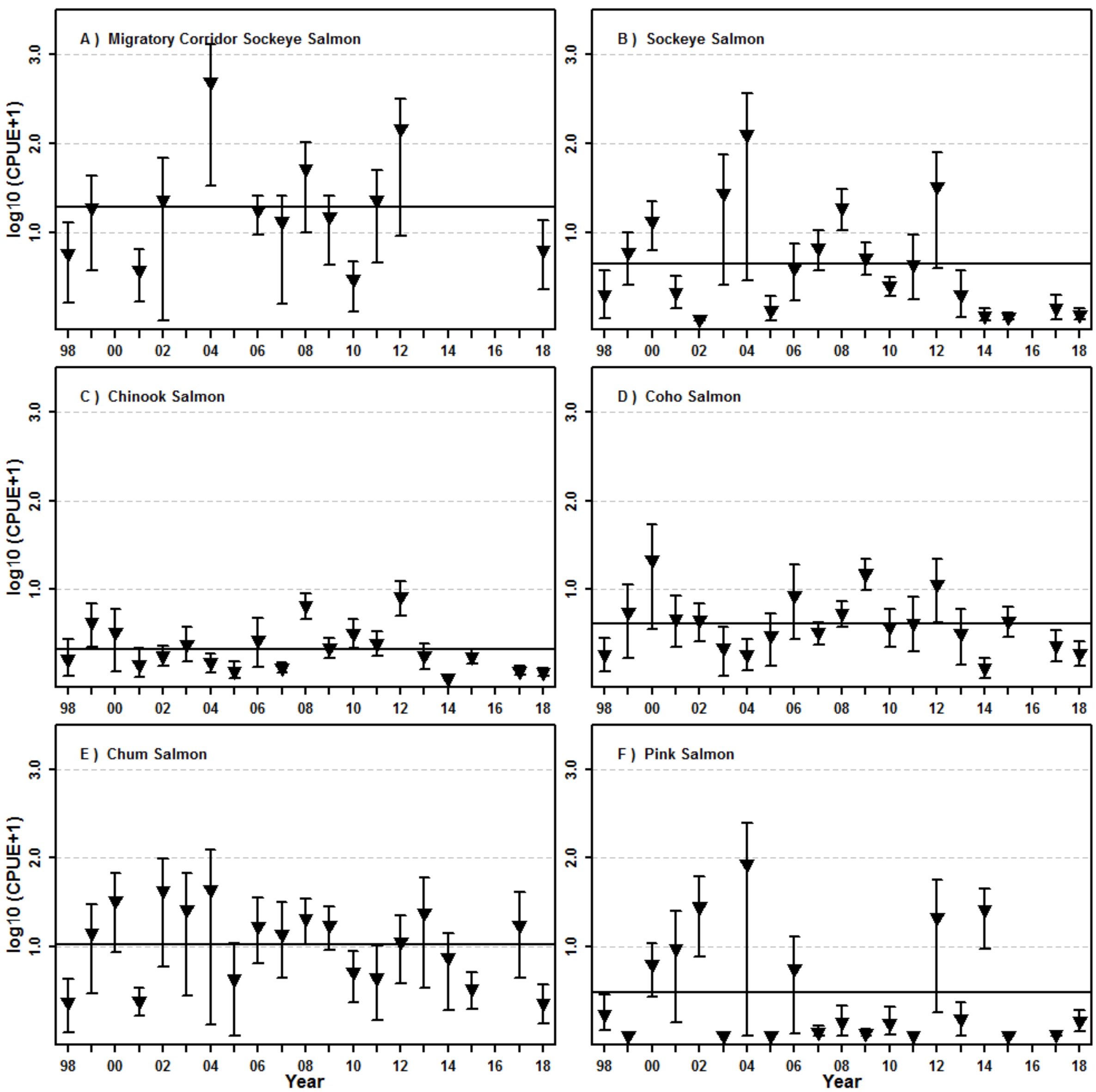

Figure 42-1. Annual catch per unit effort (CPUE; fish per swept volume [km^3]) estimates for juvenile A) Sockeye Salmon caught in the migratory corridor survey (Johnstone Strait, Queen Charlotte Strait, southern Queen Charlotte Sound) in June, B) Sockeye, C) Chinook, D) Coho, E) Chum and F) Pink Salmon caught on the Vancouver Island continental shelf in summer (late-June to early-August). Annual values (triangles) and error bars denote mean of median CPUE and 95% confidence intervals respectively, both obtained from bootstrap approximations. Black lines denote long-term mean CPUE values.

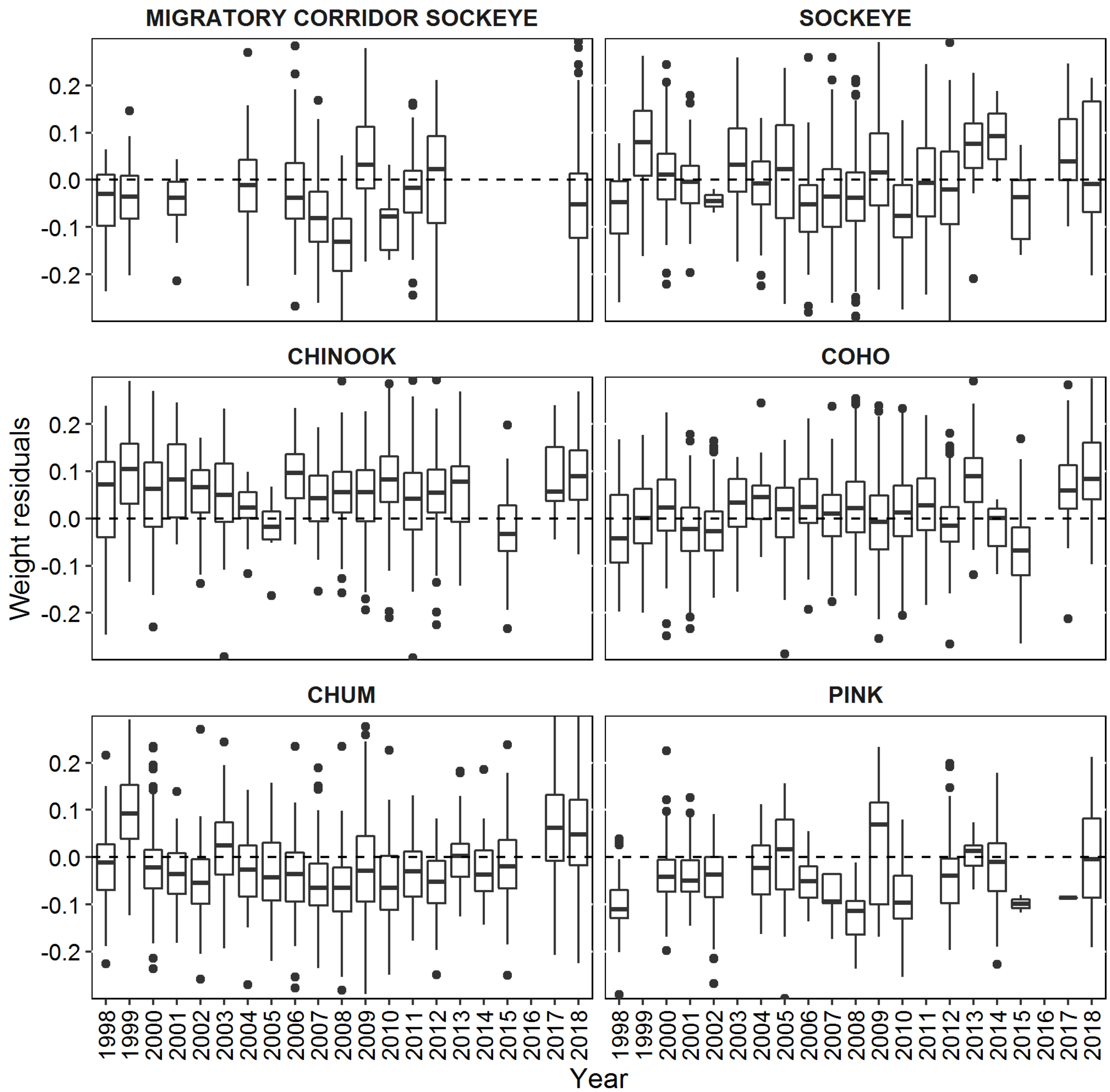

Figure 42-2. Box plots of weight residuals calculated from species-specific length-weight regressions (all years combined): estimates for juvenile Sockeye Salmon caught in the migratory corridor survey (Johnstone Strait, Queen Charlotte Strait, southern Queen Charlotte Sound) in June; estimates for juvenile Sockeye, Chinook, Coho, Chum and Pink Salmon caught on the Vancouver Island continental shelf in summer (late-June to early-August). Boxes denote lower and upper quartile range, solid lines denote median, and whiskers denote 95% confidence intervals.

43. JUVENILE SALMON IN THE STRAIT OF GEORGIA 2018

Chrys Neville, Fisheries and Oceans Canada, Pacific Biological Station, Nanaimo, BC, chrys.neville@dfo-mpo.gc.ca

43.1. Highlights

- The highest CPUEs were observed for Coho Salmon in both the early summer and fall 2018 surveys. Additionally, juveniles were large suggesting strong early marine growth.
- Strong catch rates for Chinook Salmon in September surveys suggests good condition for late ocean entrants that represented 73% of the juveniles encountered.
- In 2018, Northern Anchovy remained abundant in survey catches in the SOG.

43.2. Introduction

Juvenile salmon generally enter the Strait of Georgia (SoG) from April to June and many remain and rear in the SoG until the fall. Trawl surveys are designed to sample juvenile salmon throughout the SoG during this first ocean summer and fall. In 2018 juvenile salmon were sampled during two trawl surveys (June 21 – July 4 and September 11 – 28). The Canadian Coast Guard research vessel W.E. Ricker that has conducted most of the surveys over the past 20 years was retired from service. In its place, DFO chartered the commercial trawl vessel FV Sea Crest to conduct the surveys in 2018. Surveys were conducted within the time frame required and sets on the standard track lines that have been fished since 1998 following the protocol in Beamish et al. (2000) and Sweeting et al. (2003) were completed. In addition, some sets were completed in Desolation Sound, Discovery Islands, Gulf Islands and Juan de Fuca Strait.

The relationship between the abundance of juvenile Coho Salmon in the September survey and subsequent returns the following years was described in Beamish et al. (2010). This work indicated that brood year strength for Coho Salmon from the Strait of Georgia was determined during their first summer in the ocean and within the Strait of Georgia region. In this report we examine this relationship for the 2018 catch year. We also examine the catch rates and distribution of other species of juvenile salmon and size and condition of individuals in 2018 in comparison to catch levels and condition from 1998-2017.

43.3. Description of the time series

Catch-per-unit-effort (CPUE) for each survey is calculated using sets conducted on the standard track line (sets in red in Figure 43-1) and for specified habitat depths (Chinook Salmon 0-60 m, Coho Salmon 0-45 m, Pink, Chum and Sockeye Salmon 0-30 m) (Beamish et al. 2000, Sweeting et al. 2003). For the given sets, the total catch and area surveyed is used to calculate average catch per hour. Distribution catch maps include sets both on and off the standard track line. Although there was not consistent sampling in some of the associated areas, general patterns in overall distribution are used to provide insight.

Time series of average length included salmon < 300 mm in summer survey and < 350mm in September survey in the analysis. This 20 year time series demonstrates that changes in the abundance, distribution, and condition of juvenile salmon have occurred over the past 20 years.

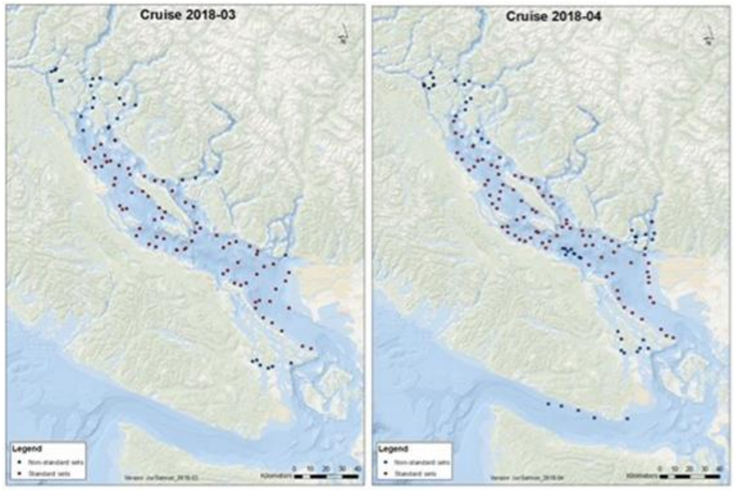

Figure 43-1. Location of sets in survey 2018-03 (June 21 – July 4, 2018; left panel) and survey 2018-04 (September 11-28, 2018; right panel).

43.4. Status and trends

The CPUE of Coho and Chinook Salmon was above average in the summer and fall survey (Figure 43-2). During both surveys, Coho Salmon CPUE was the highest in the time series. The CPUE of Chinook Salmon was similar in the summer to observations over the past 10 years and CPUE in the fall were one of the highest observed in the time series. The CPUE of other salmon species remained similar to observations over the past decade. Chum Salmon CPUE was average and remained similar to the past four years in the summer and past decade in the fall. The CPUE of Sockeye Salmon in the summer was average but above levels observed for cycle year in 2014, 2010, 2006 and 2002. However, the CPUE of Sockeye Salmon in the fall was one of the lowest observed. The fall survey typically represents the ocean type Sockeye Salmon from the Harrison River system. Pink Salmon catches were average for both surveys. During the 2018 summer survey, the distribution of juvenile salmon was generally consistent with distribution patterns observed over the time series. This included the distribution and migration timing of juvenile sockeye salmon into the Discovery Island and Strait of Georgia regions. In 2018, with supplemental information from purse seine surveys, this timing was similar to observations in 2010 – 2014 with migrations occurring in early to mid-June (Neville et al. 2013, 2015). The size of the juvenile salmon captured in both surveys was above average for the time series. Northern Anchovy continued to be caught in large numbers in 2018 and were a common diet item of Coho and Chinook sub-adult and adult salmon caught in the southern Strait of Georgia.

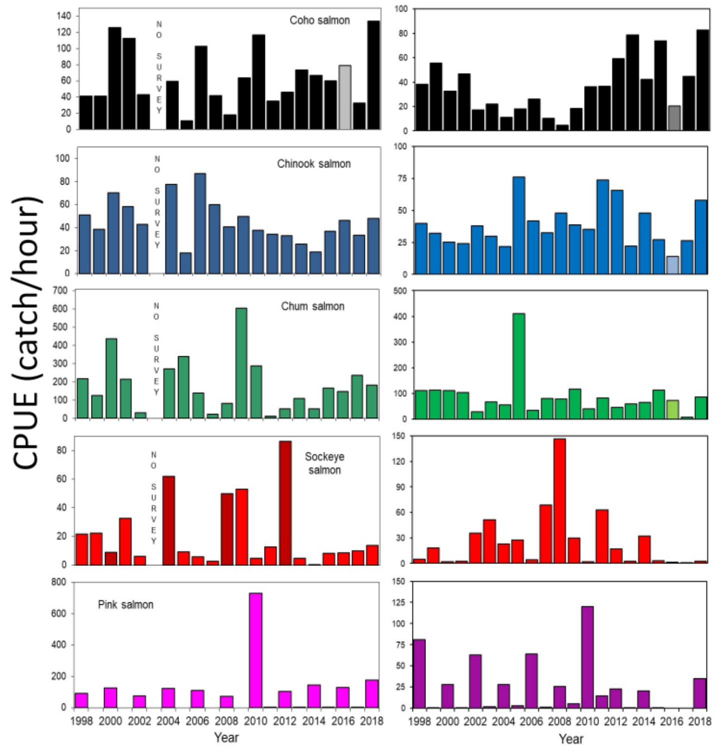

Figure 43-2. Juvenile salmon catch per unit effort (CPUE) in the spring (left panel) and fall (right panel) Strait of Georgia juvenile salmon surveys, 1998-2018.

43.5. Factors influencing trends

Consideration must be given to a change in fishing vessel in 2017. However, with experience the charter vessels were towing the net with more consistent speed and less variation in depth. The increase in size of juvenile salmon, especially Coho Salmon, suggests good early marine growth within the Strait of Georgia. This increase in size may be expected to reduce catchability of the juveniles, however catch rates were high and is a good indication that the net and gear were fishing effectively.

43.6. Implications of those trends

Improved towing speed and consistency between sets increased confidence in the catch numbers for surveys in 2018 compared to those in 2017. The high catch numbers and size of the juvenile Coho Salmon in the September survey is a good indication of strong returns in 2019. The early marine survival index (Beamish et al. 2010) indicates that the returns of Coho Salmon in 2019 should be average to above average. Stock ID is not yet available to determine if this would be expected for specific stocks however. The average catch of Chinook Salmon in June/July and the high catch of Chinook Salmon in September suggests average to above average conditions for this species. DNA results are not yet available but will be required to determine if this trend is driven by specific stocks. Sockeye Salmon catches were low they were above average for this run cycle and pink and chum catches in the summer were average or above average. Overall, the early marine conditions for juvenile salmon in the Strait of Georgia in 2018 were good and suggest high early marine growth and condition. If Coho and Pink

Salmon returns are strong in 2019 this would suggest good returns for the other species in subsequent years.

43.7. References

Beamish, R.J., McCaughran, D., King, J.R., Sweeting, R.M., and McFarlane, G.A. 2000. Estimating the abundance of juvenile coho salmon in the Strait of Georgia by means of surface trawls. North American Journal of Fisheries Management 20: 369-375.

Beamish, R.J., Sweeting, R.M., Lange, K.L., Noakes, D.J., Preikshot, D., and Neville, C.M. 2010. Early marine survival of coho salmon in the Strait of Georgia declines to very low levels. Marine and Coastal Fisheries: Dynamics, Management, and Ecosystem Science 2: 424-439.

Neville, C.M., Trudel, M., Beamish, R.J., and Johnson. S.C. 2013. The early marine distribution of juvenile Sockeye Salmon produced from the extreme low return in 2009 and the extreme high return in 2010. North Pacific Anadromous Fish Commission Technical Report 9:65-68.

Neville, C.M., Beamish, R.J., and Chittenden, C.M. . 2015. Poor Survival of Acoustically-Tagged Juvenile Chinook Salmon in the Strait of Georgia, British Columbia, Canada. Transactions of the American Fisheries Society 144(1): 25-33.

Sweeting, R.M., Beamish, R.J., Noakes, D.J., and Neville, C.M. 2003. Replacement of wild coho salmon by hatchery-reared coho salmon in the Strait of Georgia over the past three decades. North American Journal of Fisheries Management 23: 492-502.

44. HOW FRASER SOCKEYE SALMON RECRUITMENT WAS AFFECTED BY CLIMATE CHANGE: A MODEL STUDY

Yi Xu[1], Mike Hawkshaw[1], David Patterson[2], Roy Hourston[3], Peter Chandler[3]

[1]Fraser and Interior Area 3, Fisheries and Oceans Canada, Delta, B.C., Yi.Xu2@dfo-mpo.gc.ca; Mike.Hawkshaw@dfo-mpo.gc.ca

[2]School of Resource and Environmental Management, Simon Fraser University, Burnaby, B.C., David.Patterson@dfo-mpo.gc.ca

[3]Institute of Ocean Sciences, Fisheries and Oceans Canada, Sidney, B.C., Roy.Hourston@dfo-mpo.gc.ca, Peter.Chandler@dfo-mpo.gc.ca

44.1. Highlights

- Boosted regression trees models (BRT) have been developed to study the association between Fraser River sockeye recruitment and multiple environmental variables.
- The BRT model explained over 50% of the variation of Early Stuart and Chilko stocks.
- The top environmental contributors varied among stocks but included both freshwater and marine variables.
- Additional forecasts by stock can be provided to managers to inform planning for the coming fishing season.

44.2. Description of the time series

Fisheries Data The Fraser sockeye salmon (*Oncorhynchus nerka*) recruitment time series (1948-2011) were provided by Pacific Salmon Commission (PSC) for 19 major stocks. For this model study, we examined the Early Stuart and Chilko stocks. Time series of effective spawners (for Early Stuart) and juveniles (for Chilko) for the same period were collected by DFO. The details of these data were described in Grant et al. (2011).

Environmental Data The current suite of forecast models incorporate time series of Pacific Decadal Oscillation (PDO), sea surface temperature (SST) from Pine Island and Entrance Island (lighthouse stations), and Fraser River discharge at Hope as environmental co-variants. For the new model we added oceanographic variables and climate indices as candidate co-variants. The time series of these additional variables spans 1950-2013 (offset to account for juvenile outmigration year). The physical variables included: the averaged SST of the Gulf of Alaska from the COBE model (Ishii et al. 2005); sea surface salinity from Amphitrite and Race Rocks lighthouse stations; and regional upwelling and downwelling-favored wind stress (Kistler et al. 2001). The climate indices considered are: the seasonal and annual North Pacific Gyre Oscillation (NPGO, Di Lorenzo et al. 2008); the Multivariate El Nino and Southern Oscillation Index (Wolter and Timlin 1998); the Northern Oscillation Index (Schwing et al. 2002); the Aleutian Low Pressure Index (Surry and King 2015); and the North Pacific Current Bifurcation Index (Cummins and Freeland 2007).

A tree-based model (boosted regression trees, Elith, et al. 2008) was developed to study the association between sockeye recruitment and multiple environmental co-variants. This model has three advantages: 1) it can fit complex nonlinear relationships easily with multiple predictors; 2) it is not sensitive to outliers and transformation; 3) it is able to handle missing data. The BRT model was developed using packages of "gbm" and "dismo" using R (R Developmental Core Team 2019).

44.3. Status and trends

In recent years, the Early Stuart sockeye has had low recruitment (since late 1990s, Figure 44-1A). In general, the BRT model prediction was able to explain a high proportion of the variability in recruitment (R^2=0.99). Using the BRT model we made an additional forecast of 38,000 sockeye for the 2019 Early Stuart return. This suggests that the return will be lower than the median of the current pre-season forecast (41,000). Chilko sockeye return shows a strong interannual variation over the last half century (Figure 44-1B), and a large proportion of the variation was captured by BRT model (R^2=0.89). Again, using the BRT an additional return forecast can be made for 2019 of 1.2 million, less than half of current pre-season median forecast (2.75 million).

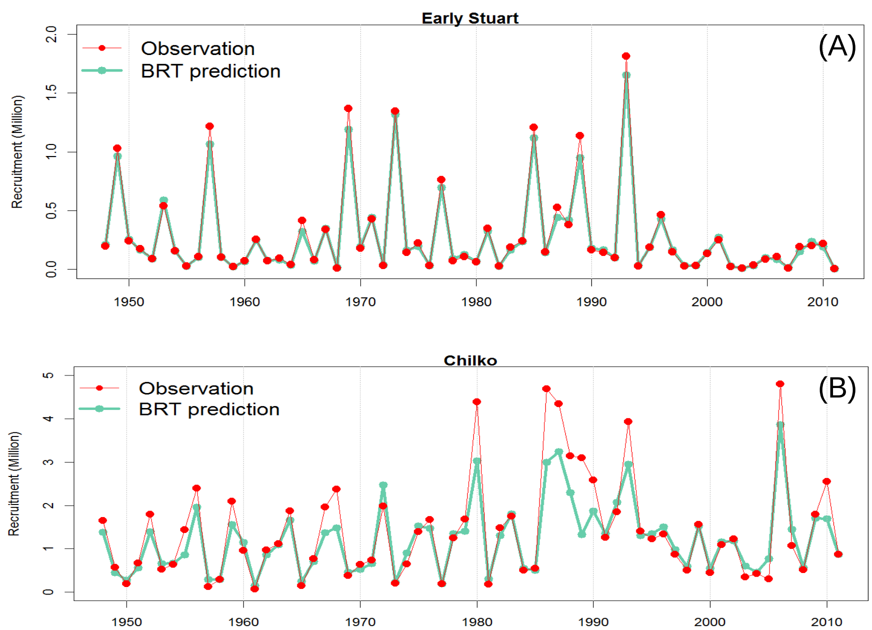

Figure 44-1. Fraser sockeye salmon recruitment observations (red dots) and BRT model results (green dots) for (A)Early Stuart and (B)Chilko stock from 1948-2011.

44.4. Factors influencing trends

The relative contribution of each predictor was calculated using the BRT model. For Early Stuart sockeye, the most important predictor was effective spawners which explained 66.3% of the total variance in recruitment (Figure 44-2A). The two strongest environmental variables that were associated with recruitment variation were identified to be April Fraser River discharge and coastal upwelling favorable wind stress, which contributed 6% and 5.7%, respectively (Figure 44-2B&C). The fitted function of BRT model shows a typical spawner-recruitment curve, a negative non-linear step-wise relationship associated with April river discharge, and a positive non-linear relationship associated with upwelling wind stress. For Chilko sockeye, their juvenile abundance was the most important predictor (51.8%, Figure 44-2D), followed by summer ocean SST in the Gulf of Alaska (6.8%, Figure 44-2E) and the PDO (4%, Figure 44-2F). Both SST and PDO showed a negative non-linear step-wise relationship with sockeye recruitment.

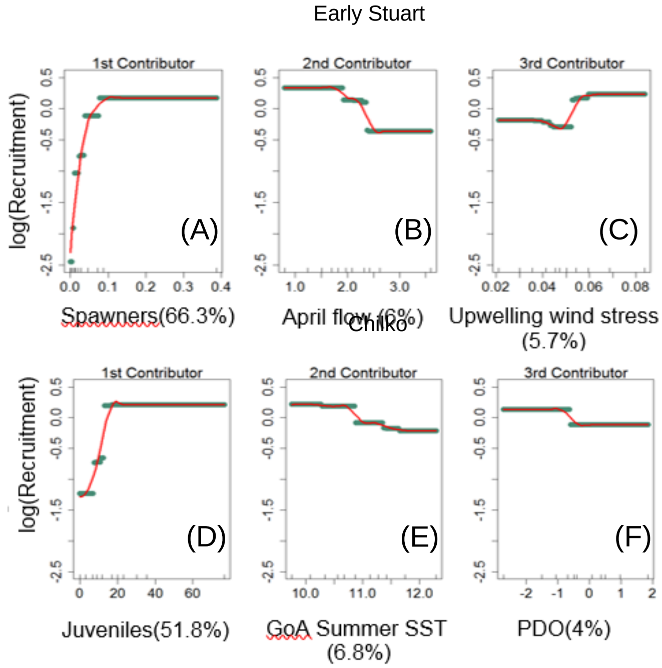

Figure 44-2. Fitted functions of top three predictors from Boosted Regression Tree models (BRT).

44.5. Implications of these trends

Understanding the effects of climate change on sockeye recruitment may help reduce uncertainties in forecast models. The development of a BRT model provides a unique way to evaluate the relative importance of population dynamics and multiple environmental effects on recruitment. Introducing candidate environmental predictors allows us to identify riverine and/or marine life history stages where strong environmental variability has an impact on recruitment. This will improve our understanding of Fraser River Watershed and North Pacific ecosystems and their impact on sockeye salmon. Application of the BRT model forecast in 2019 provides additional information to guide pre-season decisions.

44.6. References

Cummins, P.F., and Freeland, H.J. 2007. Variability of the North Pacific Current and its bifurcation. Progress in Oceanography, 75: 253-265.

Di Lorenzo, E., Schneider, N., Cobb, K.M., Chhak, K, Franks, P.J.S., Miller, A.J., McWilliams, J.C., Bograd, S.J., Arango, H., Curchister, E., Powell, T.M., and Rivere, P. 2008: North Pacific Gyre Oscillation links ocean climate and ecosystem change. Geophysical Research Letters, 35: L08607.

Elith, J., Leathwick, J.R., and Hastie, T. 2008. A working guide to boosted regression trees. Journal of Animal Ecology, 77: 802-813.

Grant, S.C.H., MacDonald, B.L., Cone, T.E., Holt, C.A., Cass, A., Porszt, E.J., Hume, J.M.B., and Pon, L.B. 2011. Evaluation of uncertainty in Fraser Sockeye (*Oncorhynchus nerka*) Wild Salmon Policy status using abundance and trends in abundance metrics. Can. Sci. Advis. Sec. Res. Doc. 2011/087: viii+183.

Ishii, M., Shouji, A., Sugimoto, S., and Matsumoto, T. 2005. Objective Analyses of Sea-Surface Temperature and marine meteorological variables for the 20th century using ICOADS and the Kobe collection. Int. J. Climatol., 25, 865-879.

Kistler, R., Kalnay, E., Collins, W., Saha, S., White, G., Woollen, J., Chelliah, M., Ebisuzaki, W., Kanamitsu, M., Kousky, V., van den Dool, H., Jenne, R., and Fiorino, M. 2001: The NCEP–NCAR 50-year reanalysis: Monthly means CD-ROM and documentation. Bulletin of American Meteorological Society, 82: 247–268.

R Core Team. 2019. R: A language and environment for statistical computing. R Foundation for Statistical Computing, Vienna, Austria. URL https://www.R-project.org/.

Schwing, F.B., Murphree, T., and Green, P.M. 2002. A climate index for the northeast Pacific. Progress in Oceanography, 53: 115-139.

Surry, A.M., and King, J.R. 2005. A new method for calculating ALPI: the Aleutian Low Pressure Index. Can. Tech. Rep. of Fish. Aquat. Sci. 3135. 16pp.

Wolter, K., and Timlin, M. S. 1998. Measuring the strength of ENSO events - how does 1997/98 rank? Weather, 53: 315-324.

45. PATTERNS IN FRASER SOCKEYE PRODUCTIVITY

Ann-Marie Huang, Fisheries & Oceans Canada, Pacific Biological Station, Salmon Assessment Section, Delta, B.C., Ann-Marie.Huang@dfo-mpo.gc.ca

45.1. Highlights

- Fraser Sockeye Salmon run size and productivity trends are:
  - not consistent across stocks and,
  - difficult to forecast out into the time period needed for recovery potential assessments required by Species at Risk Act (10+ years) and other forward simulation projects.
- Multi-generational run size projections for all salmon species could benefit from incorporating cross-disciplinary sources of information outside of the traditional stock-recruit time series.

45.2. Description of the time series

The Fraser River Sockeye Salmon stock (effective female spawners) and recruits-per-spawner time series were used to estimate a time-varying Ricker model alpha parameter that represents historical stock-specific productivity trends. Data was available up to the 2011 brood year except for Harrison which was available up to the 2012 brood year. Cultus Lake Sockeye Salmon were excluded, due to high levels of hatchery influence. The time series is detailed in DFO (2018).

45.3. Status and trends

The historical trends and current (up to and including 2016 run size returns) status of the time-varying Ricker alpha estimates for forecasted Fraser River Sockeye stocks (excluding Cultus Lake) is presented in Figure 45-1 (blue dots), with the long term average productivity shown by the red horizontal line.

Some interesting trends:

- steady decline starting at least since the 1970s: Bowron, Fennell, Portage
- steeper decline starting in 1980s/1990s: Quesnel, Late Stuart, Birkenhead, Stellako
- mostly stable productivity: Gates, Nadina, Late Shuswap
- increasing productivity: Harrison
  - Harrison is the only large Fraser stock that migrates to sea during the year of emergence from the gravel instead of overwintering in a lake. (DFO 2016)
- Note that these trends only cover up to the 2016 return year.

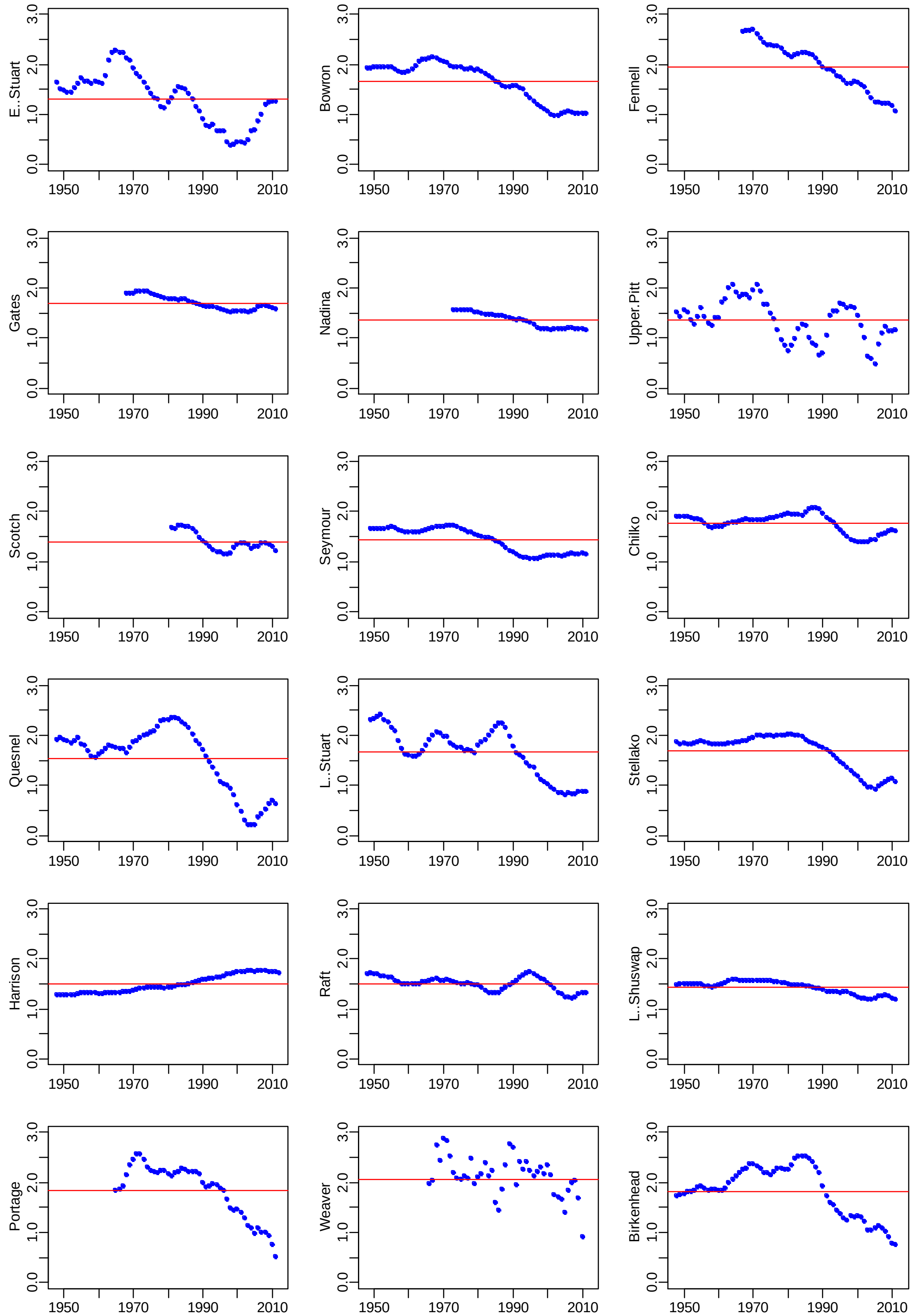

Figure 45-1. Productivity trends for forecasted Fraser Sockeye stocks (excluding Cultus Lake Sockeye).

45.4. Factors influencing trends

It is unknown what factors are influencing the trends in Fraser Sockeye Salmon productivity. However, many of the "usual suspects" are associated with the effects of increased temperatures at all life history stages, e.g.:

- adult return: stress during in-river migration associated with increased en-route mortalities and potential to pass along impacts to offspring (MacDonald et al. 2018)
- eggs: increased temperatures negatively affect fertilization success and egg survival (Whitney et al. 2014 cited in MacDonald et al. 2018)
- juveniles: decreased prey quality and quantity is associated with increased temperatures (MacDonald et al. 2018)

45.5. Implications of those trends

The productivity trends exhibited by Fraser Sockeye differ by stock and while most can be categorized into "stable" or "decreasing" *at the moment*, the ability to project the trends several sockeye generations into the future is problematic, given current information and methods.

Multi-generation projections of salmon populations are required for the recovery potential assessment after a stock is listed by COSEWIC and the recovery strategy phase of the SARA listing process, along with longer term assessments such as management strategy evaluations. With the increasing uncertainty that comes with climate change and the likelihood that it will affect different stocks of salmon in different ways, it becomes important for traditional stock-recruit modellers to expand their toolkit and the time series used to project salmon populations into the future. Working with oceanographers and other State of the Pacific Ocean participants is of particular interest.

Improved longer term projections of Pacific salmon productivity trends would allow the creation of a more robust and resilient fisheries management system. Actions that could improve understanding include, for example: begin collecting stock-recruit data on a future salmon "winners"; begin regulatory changes / biological analysis / decision processes needed for fisheries on salmon "winners"; incorporating future productivity trends into multi-year decision support tools (e.g. management strategy evaluation).

45.6. References

DFO. 2016. Supplement to the pre-season run size forecasts for Fraser River Sockeye Salmon (Oncorhynchus nerka) in 2016. DFO Can. Sci. Advis. Sec. Sci. Resp. 2016/047.

DFO. 2018. Pre-season run size forecasts for Fraser River Sockeye (*Oncorhynchus nerka)* salmon in 2018. DFO Can. Sci. Advis. Sec. Sci. Resp. 2018/034.

MacDonald, B.L., Grant, S.C.H., Patterson, D.A., Robinson, K.A., Boldt, J.L., Benner, K., Neville, C.M., Pon, L., Tadey, J.A., Selbie, D.T. and Winston, M.L. 2018. State of the Salmon: Informing the survival of Fraser Sockeye returning in 2018 through life cycle observations. Can. Tech. Rep. Fish. Aquat. Sci. 3271: 53 + v pp.

Whitney, C.K., Hinch, S.G., and Patterson, D.A. 2014. Population origin and water temperature affect development timing in embryonic sockeye salmon. Trans. Am. Fish. Soc. 143(5): 1316–1329. doi:10.1080/00028487.2014.935481.

Appendix 1 - Poster Session Abstracts

46. FILLING IN CRITICAL GAPS IN SPECIES DISTRIBUTION USING HABITAT SUITABILITY MODELS

J. Finney[1], E. Gregr[2], J. Nephin[3], C. St. Germain[1], C. Fields[1]

[1]Fisheries and Oceans Canada, Institute of Ocean Sciences, Sidney, BC, Jessica.Finney@dfo-mpo.gc.ca
[2]SciTech Environmental Consulting, Vancouver, BC
[3]Fisheries and Oceans Canada, Pacific Biological Station, Nanaimo, BC

As part of the Regional Response Plan program on the Pacific coast, Fisheries and Oceans Canada Science developed habitat suitability models (HSMs) to fill in critical data gaps on the distribution of 12 species that are highly vulnerable to oil. HSMs use algorithms to relate known presence and absence of species to background environmental variables, and can be used to create maps of habitat suitability throughout a study area. The resulting habitat suitability maps can be used in a variety of applications, including identification of critical habitat, marine spatial planning, oil spill preparedness and response, fisheries management, and risk assessments. We developed and tested models using data from the North Central Coast and the Strait of Georgia using three methods: habitat suitability index, generalized linear models, and boosted regression trees (Nephin et al. *in prep*). In addition to developing models, we are producing a workbook to provide a standardized best practices approach to habitat suitability modelling. The workbook will include recommendations for data requirements, modelling approaches, strategies for dealing with modelling challenges, as well as interpretation and application of results. Along with the workbook, we will make publicly available the code for our three HSM methods to make it easier for others to develop HSMs. The habitat suitability modelling workbook, code, and model predictions provide scientists and managers with a valuable suite of tools to fill in critical data gaps for a number of marine spatial planning applications.

46.1. References

Nephin, J., Gregr, E.J., St. Germain, C., Fields, C., Finney, J.L. *In prep*. Development and Application of a Species Distribution Modelling Framework to a Collection of Species on Canada's Pacific Coast. DFO Can. Sci. Advis. Sec. Res. Doc.

47. DYNAMIC OCEAN ACIDIFICATION MANIPULATION EXPERIMENTAL SYSTEM (DOAMES) V. 2.0 AT HAKAI

DECOUPLING CARBONATE VARIABLES AND SIMULATING NATURAL VARIABILITY IN FLOW-THROUGH EXPERIMENTS

Iria Gimenez Calvo[1,2], George G. Waldbusser[3], Burke Hales[3], Wiley Evans[1]

[1]Hakai Institute, BC, CA
[2]Department of Zoology, University of British Columbia, BC, CA
[3]College of Earth, Ocean and Atmospheric Sciences (CEOAS), Oregon State University, OR, USA, iria.gimenez@hakai.org

PCO_2, pH, and saturation state (Ω) decouple in dynamic coastal margins and estuarine waters. The individual effects of these parameters on organismal physiology, populations, and biogeochemical processes are poorly understood. Yet, traditional chemical manipulation techniques prevent the empirical identification of the carbonate parameter driving organismal sensitivity.

Building on our prototype Dynamic Ocean Acidification Manipulation Experimental System (DOAMES), we present an improved feed-forward, flow-through carbonate chemistry control system capable of decoupling PCO_2, pH or Ω and producing dynamic experimental treatments by independently manipulating total alkalinity (TAlk) and total inorganic carbon (TCO_2). In January 2019, this experimental system was installed in the Hakai Institute Marna Laboratory, located in Quadra Island, BC.

The results of the validation of the proof-of-concept prototype demonstrate that:

1. the flow-through experimental system automatically decouples carbonate chemistry parameters and produces long-term, stable carbonate chemistry treatments,
2. responds to source seawater variability in temperature, salinity and carbonate chemistry conditions, and can produce stable, dynamic and off-set carbonate chemistry targets in simultaneous manipulation channels; and,
3. is suitable for organismal studies after bivalve embryos developed successfully in water manipulated through DOAMES.

The new version of the experimental system installed at Hakai resolves observed mechanical issues in the prototype, improves software control over reagent pumps, and has a built-in alarm system to alert on mechanical failures. After validation is completed, planned experiments include assessment of responses to decoupled carbonate chemistry parameters, dynamic conditions and multi-environmental stressors.

48. A COMPILATION AND META-ANALYSIS OF SALMON DIET DATA IN THE NORTH PACIFIC OCEAN

Caroline Graham[1,2], Evgeny A. Pakhomov[1,2] and Brian P.V. Hunt[1,2,3]

[1]Institute for Oceans and Fisheries, University of British Columbia, Vancouver, BC, Canada, c.graham@oceans.ubc.ca
[2]Earth Ocean and Atmospheric Sciences Department, University of British Columbia, Vancouver BC, Canada, epakhomov@eoas.ubc.ca
[3]Hakai Institute, Campbell River, BC, Canada, b.hunt@oceans.ubc.ca

Although the freshwater phase of the salmon life cycle has been studied in depth, there is much less information available on the marine phase, even though Pacific salmon can spend anywhere from 1 to 7 years of their life in the ocean. With rapidly changing ocean conditions, it is important to understand this phase of the salmon life cycle. One of the most significant factors for the survival of salmon is the presence and abundance of nutritious prey. Although it is difficult to measure prey occurrence across the scale of the Pacific Ocean basin, information on prey presence and abundance can be obtained by studying salmon diets. Diet data can give insight into food webs, niche overlap between species/stocks, potential competition, health, and changing ocean conditions. Over the past century, there has been sporadic research on salmon diets in the ocean, and inconsistent methods have been used to quantify this information. There is an urgent need to consolidate available data in a useful way to understand salmon habitat, identify knowledge gaps, and project future changes. We are constructing a database that will include all historic salmon diet information for salmon in the North Pacific Ocean, starting with stomach content data, in order to characterize the feeding biology of Pacific salmon and to model salmon diet based on historic data and environmental conditions. A product of this research will be a comprehensive, open-access database, containing available diet information that can be used as a research tool to address a variety of questions related to salmon marine survival. As changes in salmon abundance become increasingly unpredictable, it is critical to further our understanding of the ocean phase of the salmon life cycle.

49. CARBONATE SYSTEM DYNAMICS IN TWO CONTRASTING B.C. FJORD SYSTEMS

Alex Hare, Wiley Evans, Katie Pocock, Carrie Weekes, Hakai Institute, Heriot Bay, B.C., alex.hare@hakai.org, wiley.evans@hakai.org, katie.pocock@hakai.org, carrie.weekes@hakai.org

49.1. Highlights

- A new and unique ~2.5-year time-series of near-monthly carbonate system measurements was produced for the Rivers and Bute Inlet systems.
- Carbonate parameters were similar across years within systems, but distinct between Bute and Rivers Inlets.
- Calcite undersaturation was measured throughout the water column in the Bute system in late 2016 but not in 2017 or 2018, and not at all in the Rivers Inlet time-series.
- A model derived from the time series estimates historical and projected carbonate system parameters across the Anthropocene from 1765 C.E. to 2100 C.E.

49.2. Description of the time series

This time-series is composed of TCO_2 (µmol · kg^{-1}) and pCO_2 (µatm) measurements from bottle samples collected at 12 depths at weekly to monthly intervals at one location each in Rivers Inlet (51.5210 N -127.5588 E) and Calm Channel (50.3393 N, -125.1177 E). Derived carbonate system parameters (pH, aragonite saturation state) were computed from the directly measured parameters, along with conductivity, pressure, depth, and nutrient (silicate and phosphate) measurements collected concurrently with TCO_2 and pCO_2. The time series cover the period May 2016 to September 2018 in Rivers Inlet and June 2016 to January 2019 in Calm Channel, exclusive of several winter months during which bottle samples were not collected. TCO_2 and pCO_2 were measured as described in Evans et al. (2019).

This time-series is useful for understanding climate change impacts because it contains sub-seasonal level measurements that can provide a means to determine carbonate system change during the Anthropocene when used with an appropriate modelling approach (e.g. the C* method, Gruber et al. 1996). This approach provides insight into historical trends where directly measured carbonate system data are not available.

We applied the ΔTCO_2 variation of the C* method (Pacella et al. 2018) using the RCP6 atmospheric pCO_2 trajectory (Masui et al. 2011) to these time series. This approach provides estimates of the historical trends and future trajectory of the carbonate system in these fjord environments from the onset of the Anthropocene, here estimated at 1765 C.E., to the year 2100 C.E.

49.3. Status and trends

Directly measured carbonate data are not available in these fjords systems prior to the start of this study in 2016 and interannual trends are not identifiable in the directly measured 2.5-yr time series. Historical trends are available only as estimates from model outputs based on this time-series. These estimates indicate increasing (TCO_2, pCO_2) and decreasing (pH, saturation states) trends over the Anthropocene, with higher rates of change in the latter half of the 20th century (i.e., 1950 C.E. onwards). Currently, we estimate between 40 and 48 µmol · kg^{-1} of carbon from anthropogenic activities is present in Rivers Inlet, and between 37 and 47 µmol · kg^{-1} in Calm Channel, for the year 2017.

The time series of direct carbonate system measurements was suspended in Calm Channel at the end of January, 2019 and is currently continuing in Rivers Inlet.

49.4. Factors influencing trends

The increase in TCO_2 and pCO_2 is most likely caused by increasing atmospheric pCO_2 concentration, which is driven by anthropogenic carbon emissions to the atmosphere. Other processes that may cause increasing seawater TCO_2 and pCO_2 are unlikely the cause because these processes have not changed substantially throughout the Anthropocene. For instance, evidence suggests that neither total alkalinity in the north Pacific nor productivity in the Strait of Georgia have changed substantially over the past several decades (Cross et al. 2016, Sutton et al. 2013). Industrial and agricultural practices are localized contributors to declining pH in the Puget Sound area of the southern Salish Sea (Feely et al. 2010) but are unlikely to influence the sampling areas of this study (> 300 - 500 km away). In contrast, both historical trends and mechanistic links connecting anthropogenic carbon emissions and increasing marine TCO_2 and pCO_2 have become well-established (e.g. Caldiera and Wickett 2003, Sabine et al. 2004, Zeebe et al. 2008, Doney et al. 2009). Model results are also influenced by circulation patterns and as such trends are sensitive to the assumption that current circulation patterns along the coast remain relatively unchanged throughout the Anthropocene.

49.5. Implications of trends

The model time series trends imply that the mean annual aragonite saturation state will become < 1 in the years 2034 and 2064 in the surface layer of Calm Channel and Rivers Inlet respectively, and remain < 1 throughout the projection to 2100. These trends also imply that TCO_2 and pCO_2 concentrations will continue to increase and pH will continue to decrease until 2100.

49.6. References

Caldeira, K. and Wickett, M.E. 2003. Anthropogenic carbon and ocean pH. Nature 425(6956): 365-365.

Cross, J.N., Carter B.R., Siedlecki, S.A., Alin, S.R., Dickson, A.G., Feely, R.A., Mathis, J.T., Wanninhkof, R.H., Macdonald, A.M., Mecking, S. and Talley, L.D. 2016. Ocean acidification and Decadal Alkalinity Variability in the North Pacific. 4th International Symposium on the Ocean in a High-CO2 World. 3-6 May 2016, Hobart, Australia.

Doney, S. C., Fabry, V.J., et al. 2009. Ocean Acidification: The Other CO2 Problem. Annual Review of Marine Sciences 1: 169-192.

Evans, W., Pocock, K., Hare, A., Weekes, C., Burke, H., Jackson, J., Gurney-Smith, H., Mathis, J.T., Alin, S.R., Feely, R.A. 2019. Marine CO2 patters in the Northern Salish Sea. Frontiers in marine Science, 5:536. doi: 10.3389/fmars.2018.00536, January 2019.

Feely, R. A., Sabine, C.L., et al. 2008. Evidence for upwelling of corrosive "acidified" water onto the continental shelf. Science 320(5882): 1490-1492.

Gruber, N., Sarmiento, J.L., Stocker, T.F. 1996. An improved method for detecting anthropogenic CO2 in the oceans. Global Biogeochemical Cycles 10(4):809-837.

Masui, T., Matsumoto, K., Hijioka, Y., Kinoshita, T., Nozawa, T., Ishiwatari, S., Kato E., Shukla, P.R., Yamagata, Y. and Kainuma, M. An emission pathway for stabilization at 6 Wm^{-2} radiative forcing. 2011. Climatic Change 109:59-76.

Pacella, S.R., Brown, C.A., Waldbusser, G.G., Labiosa, R.G., Hales, B. 2018. Seagrass habitat metabolism increases short-term extremes and long-term offset of CO2 under future ocean acidification. Proc. Natl. Acad. Sci. USA. 115(15):3870-3875.

Sabine, C. L., Feely, R.A., et al. 2004. The oceanic sink for anthropogenic CO2. Science 305(5682): 367-371.

Sutton, J.N., Johannessen, S.C., Macdonald, R.W. 2013. A nitrogen budget for the Strait of Georgia, British Columbia, with emphasis on particulate nitrogen and dissolved inorganic nitrogen. Biogeosciences 10:7179-7194.

Zeebe, R.E., Zachos, J.C., Caldeira, K., Tyrrell, T. 2008. Carbon Emissions and Acidification. Science 321(5885) 51:52.

50. A REGIONALLY-DEFINED EMPIRICAL ALGORITHM FOR ESTIMATING NET COMMUNITY PRODUCTION IN THE SUBARCTIC NE PACIFIC

Robert Izett and Philippe Tortell

Department of Earth, Ocean & Atmospheric Sciences, University of British Columbia, Vancouver, BC, rizett@eoas.ubc.ca, ptortell@eoas.ubc.ca

50.1. Abstract

Net community production (NCP) defines the balance between gross primary production and total aerobic respiration. As such, it is an important ecological metric that sets upper limits on regional fisheries production and the capacity for carbon export from marine surface waters. A common approach to estimating mixed layer-integrated NCP involves continuous O_2 sampling, where underway measurements can be obtained using ship-board sensors. This provides high-resolution coverage along a ship's cruise track, but the spatial and temporal extent of NCP estimates remains limited. For example, underway O_2 measurements are not common on all research cruises, such that the resultant NCP dataset, even following years of repeat surveying, is sparse with respect to the potential coverage provided by satellites or from a variety of ship-based surveys. We present a regionally-derived, empirical algorithm for estimating NCP in the Subarctic NE Pacific from commonly measured oceanographic variables. The model was derived using data collected from Line P and La Perouse cruises between 2015 and 2018 (17 datasets to-date). Using a multiple linear regression approach forced with a variety of physical, chemical and biological variables, we obtained a model predicting NCP from chlorophyll *a* and the mixed layer depth. This model out-performed an existing algorithm that was derived using a global dataset (Figure 50-1). The next step will be to derive a more robust algorithm using non-linear statistical approaches (e.g. neural networks). We will ultimately combine observations from ship-based surveys, remote sensing, Argo floats, and gridded products (e.g. climatologies, atlases, and reanalyses products) to reconstruct NCP time-series in the NE Pacific over the past several decades (e.g. Figure 50-2). This work holds significant promise for describing spatial and temporal variability in NCP over synoptic scales, and for understanding its role in regulating key ecosystem services such as fish production and C-export.

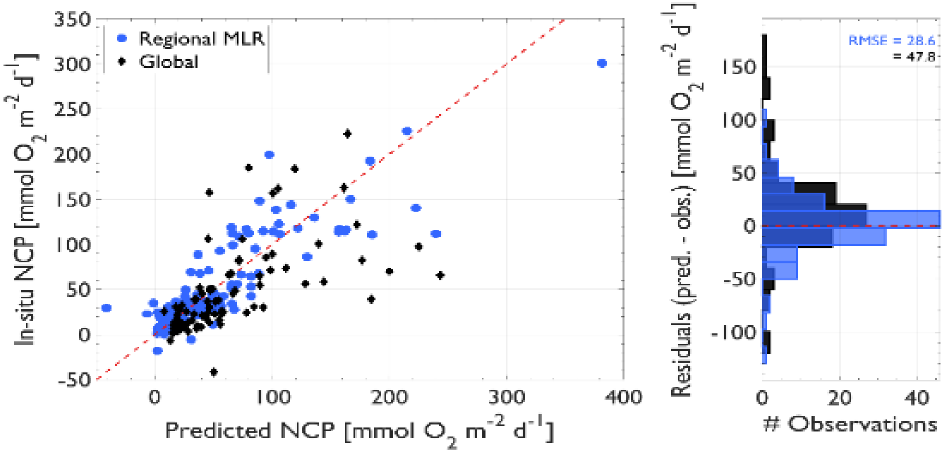

Figure 50-1. Left: Observed (in-situ) vs. modeled (predicted) NCP derived from a regionally-defined (blue) and a globally-calibrated (black) model. The dashed red line represents the 1:1 fit. Right: The histogram shows the distribution of residual errors for the two models. Our regional model performed better than the global model.

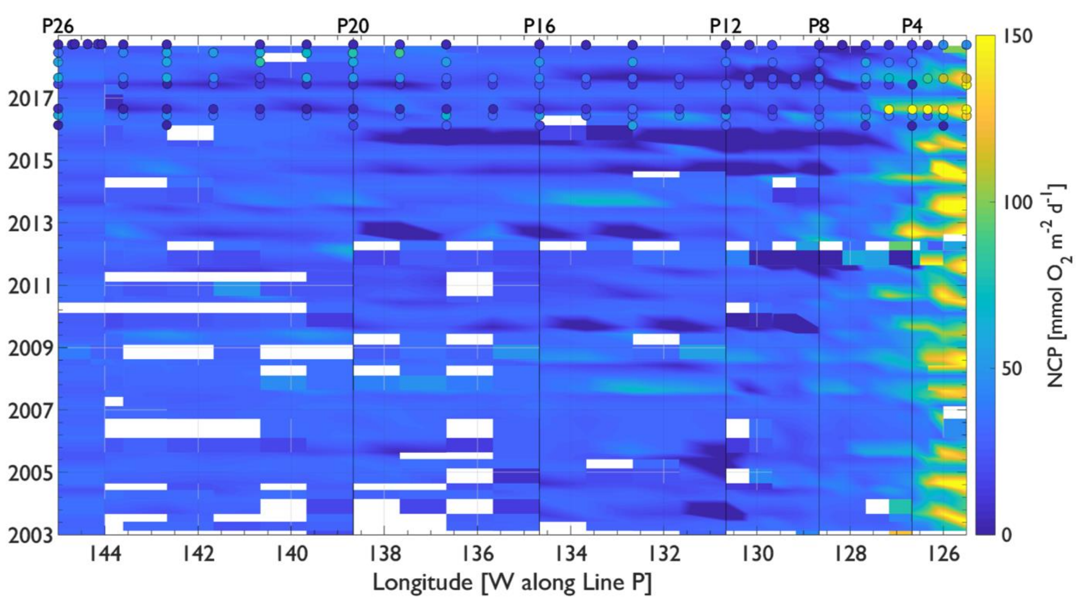

Figure 50-2. A re-constructed time-series of NCP along the Line P transect (Ocean Station Papa, P26, at left edge; continental shelf and West Coast of Vancouver Island at right edge) based on Line P observations of chlorophyll a concentration and mixed layer depth from 2003-2018. Gaps represent locations where Line P observations were not obtained. Markers represent the in-situ data that were used to derive the algorithm. The time-series identifies low NCP during "Blob" years (2014-2016), and considerable variability in the near-shore region.

51. HAKAI INSTITUTE JUVENILE SALMON PROGRAM

Brett Johnson[1] and Brian Hunt[1,2,3]

[1]Hakai Institute, Quadra Island, BC, Brett.Johnson@hakai.org
[2]Institute for the Oceans and Fisheries, UBC, Vancouver, BC, B.Hunt@oceans.ubc.ca
[3]Department of Earth, Ocean and Atmospheric Sciences, UBC, Vancouver

51.1. Highlights

- In 2018 sockeye, pink, and chum migrations through the Discovery Islands and Johnstone Strait were the earliest observed in our 2015–2018 time series.
- In May and June 2018, we observed the warmest 30 m depth integrated mean temperature in our time series.
- In 2018 the majority of juvenile sockeye salmon exited the north Strait of Georgia (SoG) in a pulse on May 23 (+/- 5 days) through the Discovery Islands.

51.2. Description of the time series

The Hakai Institute Juvenile Salmon Program was launched in 2015 in collaboration with the University of British Columbia, Fisheries and Oceans Canada, Pacific Salmon Foundation, Simon Fraser University, Salmon Coast Field Station, and the University of Toronto (Hunt et al. 2018). The program collects annual observations and samples of juvenile salmon as they migrate north from the Strait of Georgia through the Discovery Islands. In addition, the program monitors juvenile salmon migrations at the western end of Johnstone Strait at the interface with Queen Charlotte Strait based out of the Salmon Coast Field Station.

51.3. Status and trends

May and June ocean temperatures in 2018 were the warmest of the 2015-2018 observation period (Figure 51-1). Between 2015–2018 British Columbia experienced anomalous atmospheric and oceanic conditions (Chandler et al. 2018) and it is important to keep this in mind when observing our study-period variability. The peak sockeye migration date through the Discovery islands in 2018 was May 23, the same peak timing as 2015 when the B. C. coast was experiencing a marine heatwave. This peak date was one to two weeks earlier than 2014 (Neville et al. 2016), and appears to be the earliest peak migration date reported for sockeye salmon in the Strait of Georgia. Pink and chum migrations between 2015 and 2018 were a week earlier than migration observations from Levings and Kotyk (1983). Pink salmon comprised 52% of total catch in 2018, followed by chum (33%) and sockeye (13.1%). Sockeye fork lengths in 2018 were 117 mm, 8 mm longer than our time series average ($p < 0.0001$, 95% CI 5.5–11.2), while pink were 10 mm shorter ($p < 0.0001$, 95% CI 11.8–7.2) and chum were 8 mm shorter than average ($p < 0.0001$, 95% CI 9.9–5.8). Sea-louse abundance in 2018 was the lowest observed in our time series.

51.4. References

Chandler, P.C., King, S.A. and Boldt, J. (Eds.). 2018. State of the Physical, Biological and Selected Fishery Resources of Pacific Canadian Marine Ecosystems in 2017. Can. Tech. Rep. Fish. Aquat. Sci. 3266: viii + 245 p.

Hunt, B.P.V., Johnson, B.T., Godwin, S.C., Krkošek, M., Pakhomov, E.A., and Rogers, L.A. 2018. The Hakai Institute Juvenile Salmon Program: Early Life History Drivers of Marine Survival in Sockeye, Pink and Chum Salmon in British Columbia. Institute for the Oceans; Fisheries; Department of Earth, Ocean; Atmospheric Sciences, University of British Columbia, Hakai Institute, Earth to Ocean Research Group, Simon Fraser University, Department of Ecology; Evolutionary Biology, University of Toronto.

Levings, C.D., and Kotyk, M. 1983. Results of Two Boat Trawling for Juvenile Salmonids and Nearby Channels, Northern Strait of Georgia. Canadian Manuscript Report of Fisheries and Aquatic Sciences: 1730, iv +55 p..

Neville, C., Johnson, S., Beacham, T., Whitehouse, T., Tadey, J., and Trudel, M. 2016. Initial Estimates from an Integrated Study Examining the Residence Period and Migration Timing of Juvenile Sockeye Salmon from the Fraser River through Coastal Waters of British Columbia. North Pacific Anadromous Fish Commission Bulletin 6 (1): 45–60. (https://doi.org/10.23849/npafcb6/45.60).

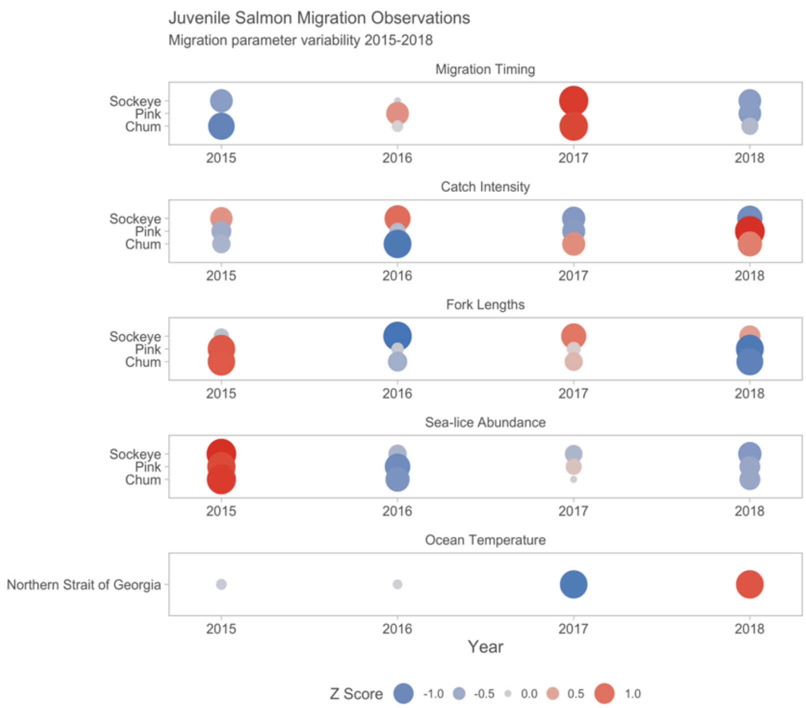

Figure 51-1. The number of standard deviations (z score) from the study-period average (2015-2018) for relevant salmon migration parameters. Size and colour saturation of circles indicates the magnitude of the anomaly. Blue colour indicates less than average; grey indicates average; red indicates greater than average. Peak migration date is based on the median date of fish capture in the Discovery Islands. Length is based on the average fork length from the Discovery Islands and Johnstone Strait combined. Parasite load is the average abundance of all sea-louse species in their motile life stages for both the Discovery Islands and Johnstone Strait regions. Ocean temperature describes the mean ocean temperature in the top 30 m at station QU39 in the northern Strait of Georgia in May and June.

52. ASSESSING OCEAN HABITAT FOR SEABIRDS – SCOTT ISLANDS MARINE NATIONAL WILDLIFE AREA

Greg Jones and Charles Hannah, Fisheries and Oceans Canada, Sidney, BC,
reshook@shaw.ca, Charles.Hannah@dfo-mpo.gc.ca

52.1. Highlights

- GPS drifters, carried by surface currents, demonstrated the Scott Islands marine National Wildlife Area (NWA) is part of the larger marine ecosystem, the potential for substance releases to be transported long distances in relatively short time periods, and consistency with information showing westward movement of nutrients into the NWA (Borstad et al. 2011).
- Zooplankton data showed an increase in gelatinous species (squishies) and a decrease in northern copepod species beyond the shelf break in recent years (Galbraith et al., section 16). Gelatinous species are poor-quality forage compared to northern copepods for seabirds to feed their chicks in the breeding season.
- Data from sub-surface moorings in the NWA demonstrated variations in dissolved oxygen, resulting from mixing of various depths, such as a substantial decline in February 2018.

52.2. Description

- The Scott Islands NWA was established by the Government of Canada in 2018 (Figure 52-1). The NWA provides for conservation and research on migratory seabirds, and the ocean foraging habitats essential to support their breeding and productivity. About 40% of seabirds breeding in Canada's Pacific Ocean breed on the Scott Islands, including about ½ of the worlds Cassin's Auklet (*Ptychoramphus aleuticus*).
- Seabirds are marine wildlife:
  - All their food comes from the ocean.
  - Ocean conditions influence seabird breeding through effects on forage species.
  - Seabirds are affected by ocean dynamics similar to other marine predators such as fish and marine mammals.
- In 2015, Canadian Wildlife Service of Environment and Climate Change Canada and Ocean Sciences Division of Department of Fisheries and Oceans developed a Collaborative Agreement running to end of fiscal 2018 – 2019. The purpose of the Agreement was to build on past success by expanding use of oceanography to assess seabird habitats. All work under the Agreement was conducted on an ocean ecosystem basis, not the legal boundary of the NWA. The most important projects implemented in the NWA were:

- Continuation of La Perouse oceanographic surveys in the NWA as part of the coast network, with particular emphasis on analysis of zooplankton due to importance as forage species (Figure 52-1 and Galbraith et al., section 16).
- Placing of 2 sub-surface oceanographic moorings, as part of a coast wide network to continuously record ocean characteristics at various depths (Figures 52-1 and 52-2). Data collected during 2017-2018 showed seasonal variability in dissolved oxygen at 100m due to vertical mixing. The cause of the dramatic decline in oxygen at 100m in February 2018 is under investigation. Further work is needed to assess potential implications of oxygen levels on marine life including forage species.
- Ocean surveys and moorings in the NWA resulted in 307 sample events producing thousands of data points.
- GPS drifters were released in the NWA, and drifters released elsewhere were carried by currents into it (Figure 52-1).
- Use of satellite data, for example provided via NASA Giovanni.

52.3. References

Borstad, G., Crawford, W., Hipfner, J.M., Thomson, R. and Hyatt, K. 2011. Environmental control of the breeding success of rhinoceros auklets at Triangle Island, British Columbia. Mar. Ecol. Prog. Ser. 424: 285-302.

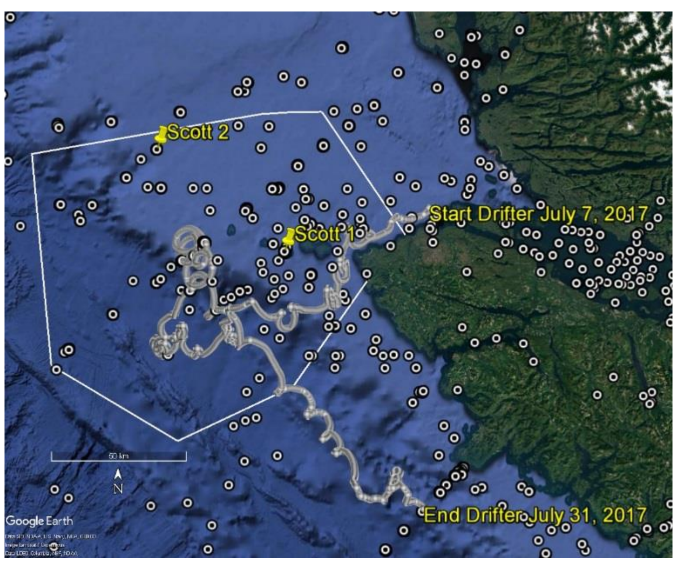

Figure 52-1. Scott Islands marine National Wildlife Area boundary (white line). 2015 – 2018 La Perouse sample sites - dots. Sub-surface moorings – yellow icons. Example of GPS drifter – yellow start and end points, grey route carried by currents. Drifter data provided by Roy Hourston, DFO.

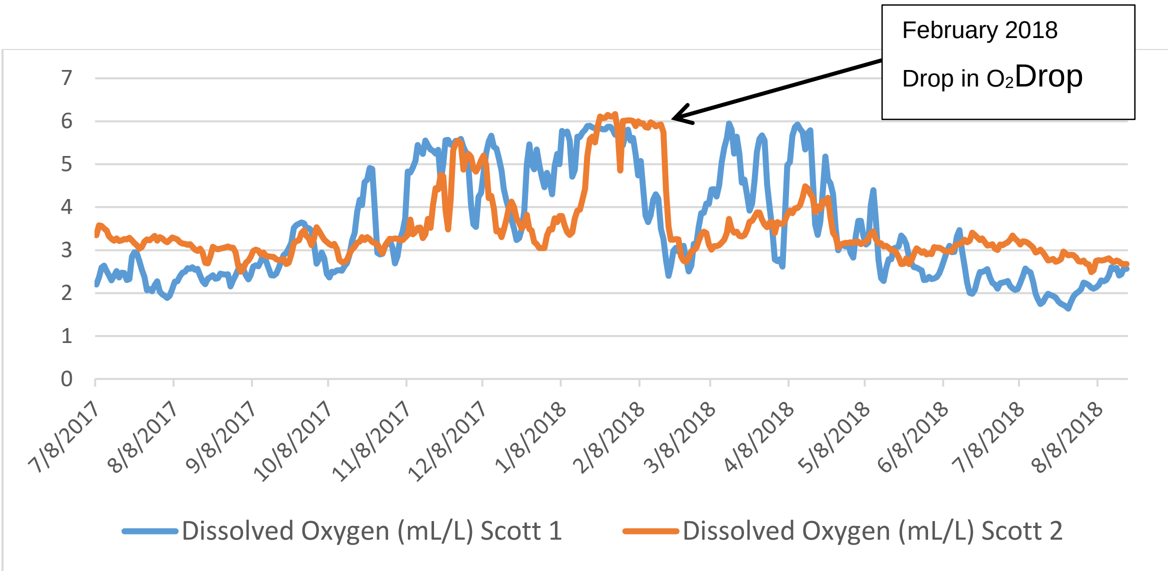

Figure 52-2. Dissolved Oxygen at 100m depth, sub-surface moorings at Scott1 and Scott2 in the Scott Islands marine National Wildlife Area, July 2017 to August 2018. Data provided by Stephen Page, DFO.

53. OCEAN MONITORING OF GWAII HAANAS NATIONAL PARK RESERVE, NATIONAL MARINE CONSERVATION AREA RESERVE, AND HAIDA HERITAGE SITE

Stephen Page[1], Charles Hannah[1], Lynn Lee[2], David Spear[1], Cindy Wright[1], Moira Galbraith[1]

[1]Fisheries and Oceans Canada, Sidney, BC, Stephen.Page@dfo-mpo.gc.ca
[2]Gwaii Haanas National Park Reserve, National Marine Conservation Area Reserve, and Haida Heritage Site, Parks Canada Agency, Skidegate, BC, Lynn.Lee2@canada.ca

53.1. Highlights

- An oceanographic instrumented subsurface mooring was installed in Juan Perez Sound in 2017.
- New ship-based oceanographic surveys occurred in Juan Perez Sound and surrounding areas on the eastern side of Gwaii Haanas.

53.2. Description of the time series

Gwaii Haanas management partners - Fisheries and Oceans Canada, Parks Canada Agency and Council of the Haida Nation - have been collaboratively conducting oceanographic monitoring in Gwaii Haanas since 2016. An oceanographic instrumented subsurface mooring was installed in Juan Perez Sound in 2017 and outfitted to measure temperature, salinity, dissolved oxygen and water currents (Figure 53-1). The mooring provided insights into the oceanographic conditions in Juan Perez Sound over time. Ship-based oceanographic operations occurred in Juan Perez Sound, through Darwin Sound and around Lyell Island, which provided a cross-section of oceanographic conditions spatially in the study area but over a short time frame.

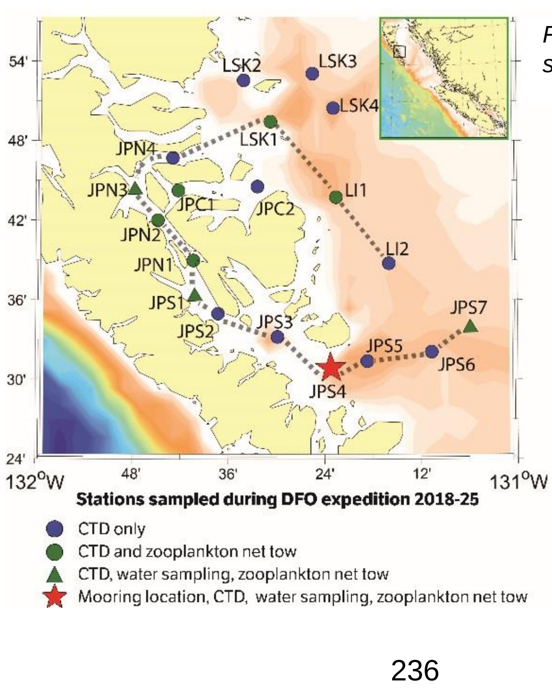

Figure 53-1. Oceanographic monitoring stations sampled in August 2018.

53.3. Status and trends

Juan Perez Sound is well stratified for temperature and salinity, while Darwin Sound is weakly stratified, likely as a result of tidal mixing (Figure 53-2). The high dissolved oxygen and fluorescence near the sill between the two basins was a result of an active plankton bloom.

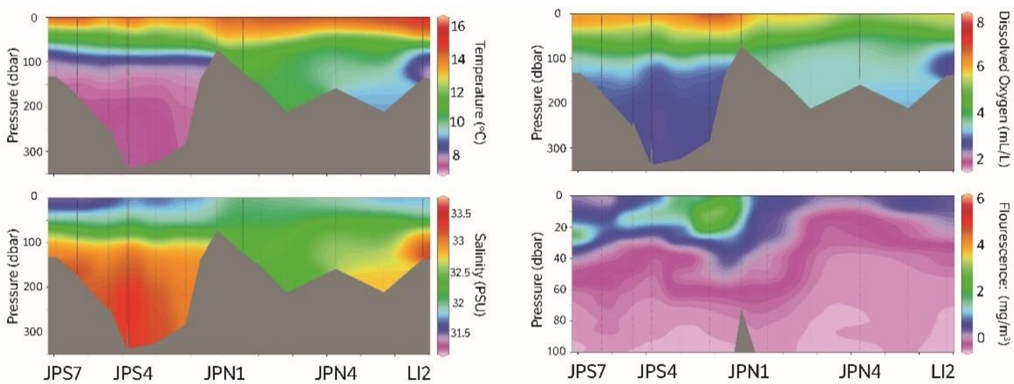

Figure 53-2. Cross-section plots of temperature, salinity, oxygen and fluorescence along route shown in Figure 53-1.

Because the mooring is a subsurface mooring, instrument data is only downloaded when the mooring is recovered, a year after deployment. Data for the time period of July, 2017 to August, 2018 show that through the winter months the entire water column is well mixed (Figure 53-3). Seasonal trends follow very closely to what is seen at the south end of Hecate Strait.

Zooplankton analysis revealed that the study area is dominated by copepods, primarily *Pseudocalanus minimus* and *Pseudocalanus newmani* (Figure 53-4).

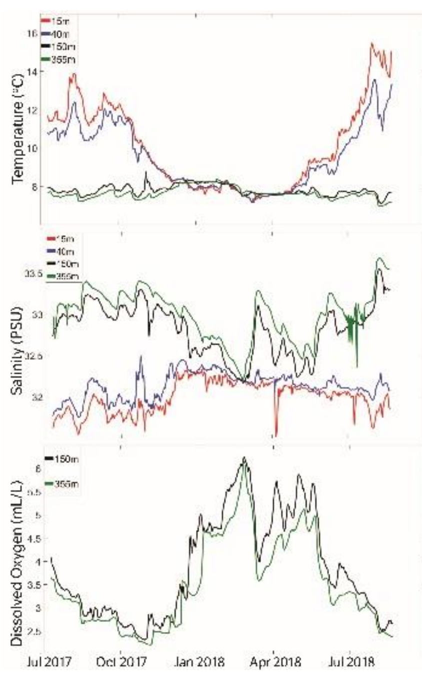

Figure 53-3. Time series of temperature, salinity, and oxygen (July 2017-August 2018) at several depths recorded at the mooring position shown in Figure 53-1.

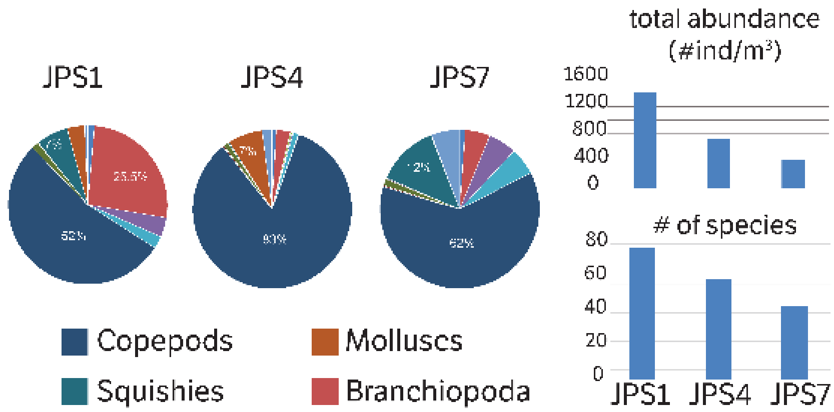

Figure 53-4. Abundance of zooplankton at three locations, shown in Figure 53-1, in July 2017.

53.4. Factors influencing trends

This was the first year of data in this region and we saw similar seasonal trends in the water properties of Juan Perez Sound as we did at other central and north coast mooring sites that have multi-year records. We expect the recent increase in ocean temperatures as seen at other mooring sites to be reflected here in subsequent years.

54. OPEN GOVERNMENT: THE APPROACH TO OPEN GOVERNMENT FROM SCIENCE IN DFO'S PACIFIC REGION

Jason Parsley[1]

[1]Fisheries and Oceans Canada, Nanaimo, BC, Jason.Parsley@dfo-mpo.gc.ca

Technology has provided the capability to distribute large amounts of data and information through many different platforms on a vast array of subjects. The Government of Canada believes it is important to provide Canadians with access to the data that is produced, collected, and used by departments and agencies across the federal government. Open Government is a culture that fosters greater openness and accountability, enhances citizen participation in policymaking and service design, facilitates innovation, and creates a more cost-effective, efficient and responsive government.

The Treasury Board Secretariat of Canada (TBS) released the Open Government Directive in 2014 mandating open government as a requirement for all departments and agencies across the government of Canada. DFO Pacific Region Science initiated their Open Government program in the fall of 2016. Initially, through communication and collaboration with the region's scientists, a data inventory was created. The inventory was used as a starting point to target datasets that were easily and rapidly publishable to Open Government.

Since 2016 the goals of the program have evolved. Now, more complex, multi-layered spatial datasets that are in demand by the public are being targeted for publication to Open Government. As of the 2019 State of the Pacific Ocean meetings DFO Pacific Region Science has published 52 of their datasets to Open Government.

Proactively providing data that is relevant to Canadians reduces the amount of access to information requests, e-mail campaigns and media inquiries. This greatly reduces the administrative cost and work load associated with responding to such data inquiries and provides scientists and researchers more time to continue the work they are deeply passionate about: studying our ocean.

55. THE STRAIT OF GEORGIA DATA CENTRE

http://sogDataCentre.ca
An excellent source of information for the Strait of Georgia
- extending to the Salish Sea, the Pacific Ocean and beyond

Isobel Pearsall[1], Terry Curran, Ben Skinner and Brian Riddell

[1]Pacific Salmon Foundation, Vancouver, BC, pearsalli@psf.ca

55.1. Founding Objectives

The Strait of Georgia Data Centre is a collaborative program between the Pacific Salmon Foundation (PSF) and the Institute for the Oceans and Fisheries (IOF UBC), to build a secure data archive for marine ecosystem information on the Strait of Georgia. The Centre is housed at UBC, and funded through the Sitka Foundation and PSF. The goal of the Data Centre is to serve as a central data repository, to protect and collate marine ecosystem information for the Strait and to allow for data sharing and integration in a comprehensive manner.

55.2. Underlying Design

The data archive is fully compliant with all the international standards for data sharing and embraces the open source data management tools and techniques for low cost maintenance and utmost compatibility. The applications used are GeoNetwork for metadata management and online mapping, Geoserver for creation of data layers for downloading and geospatial information system (GIS) access, and a reliable PostgreSQL spatial database cluster to hold metadata and data. Data is securely held wholly within Canada in the cloud at the University of British Columbia. A basic principle is no data duplication and that data should be managed closest to origin, if the data is freely available elsewhere. Sometimes datasets are not instantly share-able, and in these cases the PSF is required to host a copy.

55.3. Pillars of the Strait of Georgia Data Centre

1. Metadata
2. Data Layers
3. Online mapping
4. Story maps
5. Interactive maps
6. List of Salish Sea researchers
7. List of Publications
8. Data summaries by spreadsheet

55.4. Metadata, managed by GeoNetwork

There are more than 500 metadata records held within the sogDataCentre. Almost all of these are linked to datasets, which can be very large federal holdings like the DFO IOS Archive of physical and chemical measurements, the large and growing DFO biological datasets, datasets provided by non-governmental organizations, citizen scientists, post-secondary institutions and municipal governments.

All of the metadata is compliant with ISO-19115/19139, and where possible includes lineage describing what has been done to the data from acquisition to presentation.

Data is categorized by the 15 international groups, as follows:

- Biota - 177
- Oceans - 150
- Economy - 45
- Environment - 27
- Inland waters - 22
- Climatology and meteorology - 19
- Elevation-16
- Boundaries -10
- Farming - 5
- Transportation - 4
- Location - 2
- Health -1

Data is searchable by date, provider, topic, keywords, data formats, status, etc. In practice, one or two search words are sufficient to instantly find desired records.

Datasets (like Excel spreadsheets) can be accessed as a 'blob', stored in the database cluster, or both.

55.5. Data Layers, managed by GeoServer

Modern data access uses GIS techniques to access data. GeoServer sits between the database cluster and the user to perform on-the-fly format conversion and re-projection to thousands of different coordinate systems.

55.6. Online Mapping, within GeoNetwork

Data layers can be instantly acquired from anywhere in the world that adheres to the international standards (not just the sogDataCentre), and combined to create and output a quality map or illustration including topography and bathymetry, with one or more layers of other data.

55.7. Story Maps

This is a recent innovation. It was recognized that information needed to be presented in a context that would serve the needs of those beyond the data specialists – data needed to be interpreted and placed in context. This can incorporate videos and in-depth discussion of data and data collection techniques, for instance. It invites a discussion with the audience.

55.8. Interactive Map Catalogue

Very frequently, there is a need to present four-dimensional data – data in the three spatial coordinates and the evolution over time, or to create maps of a pre-selected subset of layers. The PSF have created many animated maps.

One very important dataset is the ShoreZone dataset collected by Coastal and Ocean Resources Inc. It contains about a hundred layers of foreshore data, primarily in the geological and biological categories. These layers are individually switchable on/off.

55.9. List of Salish Sea researchers

Searchable lists of approximately 150 researchers are listed, with a brief bio and email contact information.

55.10. List of Publications

A searchable list of publications back to 1930 is available. It contains approximately 12,000 entries.

56. SMOLT PRODUCTION AS A MEANS OF SETTING ENVIRONMENTAL FLOWS

Thomas Smith[1,4], Jordan Rosenfeld[1,2] and Brian P.V. Hunt[1,3,4]

[1]Institute for Oceans and Fisheries, University of British Columbia, Vancouver, BC, Canada, t.smith@oceans.ubc.ca;
[2] BC Ministry of Environment, Vancouver, BC, Canada
[3] Hakai Institute, Pruth Harbour, Calvert Island, BC
[4] University of British Columbia, Department of Earth, Ocean and Atmospheric Sciences, Vancouver, BC, Canada

In stream environments, low water flow often leads to negative implications in regards to ecosystem function and biological productivity. Additionally, human water needs often result in increasing pressure on these systems. With exponential growth in the global human population and increasingly observed environmental impacts of climate change, the need to establish minimum flow requirements is becoming increasingly important. Previous research on instream flow modelling has focused on the physical habitat as opposed to biological response, and these models have rarely been validated. However, by analyzing co-variation in smolt recruitment and stream discharge, low flow thresholds to production can be more accurately identified. With data obtained from primary and grey literature, a meta-analysis investigating this relationship across the Pacific Northwest will be conducted. Through providing empirical evidence to regional managers to make better informed decisions in setting low flow requirements, this project will increase protection of habitat vital to the freshwater stages of Pacific salmon.

Appendix 2 - Meeting Agenda

		SOPO DAY 1
P#	**Name**	**Title**
		Settling in
	Chandler/Boldt	Introduction
	Chief Jimmy	Tseycum Chief Tanya Jimmy
	Kim Houston	Welcome from DFO
1	Faron Anslow	Land temperature and hydrological conditions in 2018
2	Tetjana Ross	Temperature, salinity and density of the NEP using Argo, satellite and Line P data
3	Charles Hannah	Ocean Surface Temperatures in 2018 – another marine heat wave?
4	Roy Hourston	Wind-driven upwelling along the Northwest coast of North America: timing and magnitude.
5	Peter Chandler	Sea surface temperature and salinity on the BC Coast
6	Bill Crawford	Changes in Oxygen Concentration in BC shelf and deep-sea waters
7	Jim Gower	Satellite observations of BC waters
8	Anne Ballantyne	Water level observations on the BC coast
9	Jennifer Jackson	Interdecadal oceanographic trends in Rivers Inlet, BC
	Lunch	
10	Angelica Pena	Results from phytoplankton monitoring at Line P and the west coast of Vancouver Island
11	Moira Galbraith	West coast zooplankton: annual anomaly time series
12	Sonia Batten	An update on oceanic and west coast shelf/slope plankton populations from the CPR survey
13	Ian Perry	West Coast of Vancouver Island small mesh multispecies bottom trawl survey (target species: smooth pink shrimp) – 2018 update
14	Jennifer Boldt and Jaclyn Cleary	Pelagic fish: an update on Pacific Herring status and trends
15	Jennifer Boldt	Eulachon update: Fraser River Egg and Larval Survey and West Coast of Vancouver Island Small Mesh Bottom Trawl survey
16	Greg Workman	A review of groundfish surveys in 2018 and an introduction to the groundfish data synopsis report.
	Break	
17	Wiley Evans	2018 Coastal Ocean Conditions Revealed by the Hakai Institute's Continuous CO2 Datasets
18	Mark Hipfner	Seabird observations on the BC Coast
19	Joanne Lessard	DFO dive surveys
20	Svein Vagle	Acoustics monitoring for Southern Resident Killer Whales
21	Jessica Heke	Canadian Hydrographic Service Pacific: activities and results
22	Matthais Herborg	Oil spills in BC waters
23	Hauke Blanken	A snapshot of 2018 NE Pacific conditions from ECCC's new CIOPS-W forecasting system
	Chandler/Boldt	Discussion
	Poster Session	

		SOPO DAY 2
	Chandler/Boldt	Reflections and highlights on day 1
1	Peter Chandler	The 2018 Strait of Georgia Water Properties Surveys
2	Akash Sastri	Deep water and sea surface properties in the Strait of Georgia during 2018: Cabled instruments and ferries.
3	Susan Allen	Spring bloom and interannual variations in primary productivity in the Strait of Georgia
4	Nina Nemcek	Seasonal dynamics of the phytoplankton community in the Strait of Georgia
5	Kelly Young	Zooplankton status and trends in the central Strait of Georgia, 2018
	Break	
6	Svetlana Esenkulova	The phytoplankton community and harmful algae in the Salish Sea
7	Nicky Haigh	Harmful Algal Blooms around the BC coast in 2018; data from the Harmful Algae Monitoring Program
8	Ben Grupe	An update on the annual benthic ROV survey in Saanich Inlet
9	Maycira Costa	Chlorophyll phenology in the Strait of Georgia: Spatial-temporal satellite observations
10	Sue Grant	The State of the Salmon initiative
11	Sue Grant	Fraser River Sockeye: abundance and productivity trends
	Lunch	
12	Howard Stiff	Inter-Annual Fluctuations in Upper Alberni Inlet Sub-Halocline Oxygen Conditions
13	Kim Hyatt	Sockeye salmon recruitment variations, ocean state changes, year 2018 performance and 2019 "outlook"
14	David Welch	A Survey of the Coast-wide Collapse in Northeast Pacific Chinook and Steelhead Survival: Looming Problems for Set Piece Solutions
15	Jackie King	2018 Juvenile Salmon Surveys on the Vancouver Island Continental Shelf
16	Chrys Neville	Juvenile salmon in the Strait of Georgia
17	Chrys Neville	The joint international survey looking at salmon and ocean conditions in the NE Pacific during winter
	Break	
18	Scott Akenhead	The International Salmon Data Laboratory
19	Mike Hawkshaw	Best Practices for incorporating environmental variables to sockeye salmon forecasting
20	Yi Xu	How Fraser sockeye salmon recruitment was affected under climate changes? A model study
21	Ann-Marie Huang	Modeling future salmon productivity in the looming spectre of climate change
	Chandler/Boldt	Wrap up

Appendix 3 - Meeting Participants

Participant	Affiliation
Akash Sastri	University of Victoria
Alex Hare	Hakai Institute
Alyssa Gerick	Fisheries and Oceans Canada
Amanda Tillerman	University of Victoria
Ana C. Franco	University of British Columbia
Andrew McMillan	Fisheries and Oceans Canada
Angelica Pena	Fisheries and Oceans Canada
Anne Ballantyne	Fisheries and Oceans Canada
Ann-Marie Huang	Fisheries and Oceans Canada
Aroha Miller	Oceanwise
Ashu Bhudia	University of British Columbia
Athena Ogden	Fisheries and Oceans Canada
Ben Grupe	Fisheries and Oceans Canada
Bill Crawford	Fisheries and Oceans Canada
Brett Johnson	Hakai Institute
Brian Hunt	UBC Hakai
Bruce Patten	Fisheries and Oceans Canada
Chuanbo Guo	Natural Sciences and Engineering Research Council of Canada
Caitlin O'Neill	Fisheries and Oceans Canada
Candice St. Germain	Fisheries and Oceans Canada
Caroline Graham	University of British Columbia
Caroline Wells	Fisheries and Oceans Canada
Carrie Robb	Fisheries and Oceans Canada
Caterina Rodriguez Giner	University of British Columbia
Cecilia Wong	Environment Canada
Chad Ormond	
Charles Hannah	Fisheries and Oceans Canada
Charlotte Houston	
Charmaine Carr-Harris	Fisheries and Oceans Canada
Chelsea Stanley	Fisheries and Oceans Canada
Colleen Kellogg	Hakai Institute
Dave Argue	
David Spear	Fisheries and Oceans Canada
David Welch	Kintama Research Services
Deb Ianson	Fisheries and Oceans Canada
Deirdre Finn	Fisheries and Oceans Canada
Dennis Chalmers	Fisheries and Oceans Canada, retired
Don Noakes	Thompson Rivers University
Doug Bertram	Environment and Climate Change Canada
Doug Latornell	University of British Columbia
Doug Moore	Continuous Plankton Recorder (CPR) Survey at the Marine Biological Association
Elise Olson	University of British Columbia
Emily Rubidge	Fisheries and Oceans Canada
Erika Anderson	Fisheries and Oceans Canada
Faron Anslow	University of Victoria
Fiona Francis	Oceanwise
Germaine Gatien	Fisheries and Oceans Canada
Greg Jones	Fisheries and Oceans Canada

Participant	Affiliation
Greig Oldford	Fisheries and Oceans Canada
Hal Batchelder	North Pacific Marine Science Organization (PICES)
Hauke Blanken	Fisheries and Oceans Canada
Hayleigh Rados	Fisheries and Oceans Canada
Hayley Dosser	Hakai Institute
Hilari Dennis-Bohm	Fisheries and Oceans Canada
Howard Stiff	Fisheries and Oceans Canada
Ian Perry	Fisheries and Oceans Canada
Iria Gimenez	Hakai Institute
Jackie King	Fisheries and Oceans Canada
Jaclyn Cleary	Fisheries and Oceans Canada
Jacqueline Belzile	Fisheries and Oceans Canada
Jacqueline Maud	University of British Columbia
Jan Buermals	ASL Environmental Sciences
Jasmine Wietzke	Fisheries and Oceans Canada
Jason Parsley	Fisheries and Oceans Canada
Jason Scher	Prince Rupert Port Authority
Jay Pudota	Marine Harvest
Jeff Marliave	Coastal Ocean Research Institute, Ocean Wise
Jennifer Jackson	Hakai Institute
Jenny Smith	Hakai Institute
Jessica Finney	Fisheries and Oceans Canada
Jessica Heke	Fisheries and Oceans Canada
Jessica Nephin	Fisheries and Oceans Canada
Jim Gower	Fisheries and Oceans Canada
Joanne Lessard	Fisheries and Oceans Canada
Jocelyn Nelson	Fisheries and Oceans Canada
Jon Chamberlain	Fisheries and Oceans Canada
Karyn Suchy	Pacific Salmon Foundation
Katie Gale	Fisheries and Oceans Canada
Kelly Young	Fisheries and Oceans Canada
Ken Morgan	Environment Canada
Kieran Forge	Fisheries and Oceans Canada
Kim Houston	Fisheries and Oceans Canada
Kim Hyatt	Fisheries and Oceans Canada
Kyle Simpson	Fisheries and Oceans Canada
Kyra St Pierre	University of British Columbia
Laura Bianucci	Fisheries and Oceans Canada
Lu Guan	Ocean Networks Canada and University of Victoria
Lynn Lee	Parks Canada
Margot Stockwell	Fisheries and Oceans Canada
Marie Robert	Fisheries and Oceans Canada
Mark Hipfner	Environment and Climate Change Canada
Marlene Jeffries	Fisheries and Oceans Canada
Matt Grinnell	Fisheries and Oceans Canada
Matt Miller	University of Victoria
Matthais Herborg	Fisheries and Oceans Canada
Maycira Costa	Fisheries and Oceans Canada
Melissa Hennekes	Fisheries and Oceans Canada
Micah Quindazzi	University of Victoria
Michael Dunphy	Fisheries and Oceans Canada
Michael Folkes	Fisheries and Oceans Canada

Participant	Affiliation
Michelle Biggs	Fisheries and Oceans Canada
Mike Hawkshaw	Fisheries and Oceans Canada
Moira Galbraith	Fisheries and Oceans Canada
Natalie Mahara	University of British Columbia
Natasha Salter	Fisheries and Oceans Canada
Nicholas Ens	Fisheries and Oceans Canada
Nick Bolingbroke	Fisheries and Oceans Canada
Nicky Haigh	Microthalassia Consultants Inc.
Nina Nemcek	Fisheries and Oceans Canada
Pandora Gibb	University of Victoria
Patrick Cummins	Fisheries and Oceans Canada
Paul Covert	Fisheries and Oceans Canada
Rachael Mueller	University of British Columbia
Rhona Govender	Fisheries and Oceans Canada
Robert Izett	University of British Columbia
Roger Kanno	Fisheries and Oceans Canada
Roy Hourston	Fisheries and Oceans Canada
Sandy Argue	
Sarah Cook	
Sarah-Ann Quesnel	Fisheries and Oceans Canada
Scott Akenhead	Fisheries and Oceans Canada
Sean Anderson	Fisheries and Oceans Canada
Sean Cheesman	BC Ministry of Agriculture
Sean MacConnachie	Fisheries and Oceans Canada
Skip McKinnell	Salmoforsk International Environmental Consulting
Sonia Batten	Continuous Plankton Recorder (CPR) Survey at the Marine Biological Association
Stephanie King	Pentair Aquatic Ecosystems
Stephen Ban	
Stephen Page	Fisheries and Oceans Canada
Stephen Wischniowski	Fisheries and Oceans Canada
Steve Gormican	Camosun College
Steve Latham	Pacific Salmon Commission
Steve Schut	Fisheries and Oceans Canada
Stuart Crawford	Haida Oceans Technical Team
Sue Grant	Fisheries and Oceans Canada
Susan Allen	University of British Columbia
Svein Vagle	Fisheries and Oceans Canada
Tamara Fraser	Fisheries and Oceans Canada
Tanya Jimmy	Tseycum First Nation
Tereza Jarnikova	University of British Columbia
Terry Curran	Pacific Salmon Foundation
Tetjana Ross	Fisheries and Oceans Canada
Thomas Smith	University of British Columbia
Todd Mudge	ASL Environmental Sciences
Wendy Callendar	Fisheries and Oceans Canada and University of Victoria
Wiley Evans	Hakai Institute
Yi Xu	Fisheries and Oceans Canada